

POLITECNICO DI TORINO

Collegio di Ingegneria Meccanica, Aerospaziale, dell'Autoveicolo e della
Produzione

**Corso di Laurea Magistrale
in Ingegneria dell'Autoveicolo**

Tesi di Laurea Magistrale

Impact of the V2G ancillary services on the vehicle's battery and power electronics



Relatore/i

prof. Tenconi Alberto (DENERG)
prof. Vaschetto Silvio (DENERG)

Candidato

Gentilini Maurizio

Luglio 2018

Riassunto in italiano

Il primo obiettivo di questa tesi è stato quello di analizzare lo stato dell'arte nel campo della mobilità elettrica, sia per quanto riguarda i componenti On-Board di veicoli BEVs/PHEVs, sia per quanto riguarda le strutture Off-board necessarie per la ricarica delle batterie.

Successivamente, dopo aver caratterizzato i principali servizi Vehicle-to-Grid (in particolare i cosiddetti servizi ancillari), con le loro peculiarità, caratteristiche e i relativi vantaggi/svantaggi, è stato possibile identificare quali gap tecnologici è necessario colmare per poter implementare tali servizi in maniera efficace ed efficiente.

Partendo dall'elettronica di potenza, sono state individuate delle configurazioni adatte, in termini di hardware, strategie di controllo e taglie di potenza, tenendo presente la duplice funzione di carica del veicolo e supporto della rete elettrica.

Un'ulteriore analisi ha focalizzato l'attenzione sul sistema che maggiormente potrebbe limitare la diffusione dei veicoli elettrici e dei servizi V2G: è stata perciò inserita un'ampia descrizione delle batterie adatte ad un utilizzo nel settore dei trasporti (sia a livello di celle che a livello di moduli), con particolare attenzione alla tecnologia agli ioni di litio, permettendo di caratterizzare tali sistemi, i relativi componenti ausiliari (Battery Management System, Thermal Management System...) e le logiche di controllo al loro interno.

Continuando su questo tema è stato necessario assicurare che le applicazioni V2G riducessero al minimo (idealmente a zero) l'impatto sul pacco batterie che, in particolare su veicoli BEVs è già sottoposto a condizioni operative che determinano una riduzione marcata di performance e vita utile.

Per questo motivo è stata condotta una ricerca bibliografica che ha permesso di selezionare i principali fattori che influenzano l'invecchiamento delle batterie agli ioni di litio, e di determinare sia le condizioni di stoccaggio che quelle operative in maniera da minimizzare l'eventuale deterioramento aggiuntivo causato dall'utilizzo nelle applicazioni V2G.

Table of contents

1. INTRODUCTION.....	1
1.1 V2G description.....	1
1.2 Thesis structure	1
1.3 Targets	2
2. STATE OF ART	3
2.1 Grid requirements and targets	3
2.1.1 Grid description and support necessity.....	3
2.1.2 Smart-grid concept.....	6
2.2 EVs/PHEVs characterization	9
2.2.1 Electric power-train classification.....	9
2.2.2 Market analysis.....	11
2.2.3 Trends and technological evolution	14
2.3 Toward V2G: scale effect and deployment issues	19
3. V2G POTENTIALITIES, HARDWARE AND ARCHITECTURES	22
3.1 V2G applications	22
3.1.1 Peak shaving and Load levelling.....	24
3.1.2 Frequency regulation.....	27
3.1.3 Reactive power compensation and Voltage control	35
3.1.4 THD control	40
3.1.5 Conclusion.....	44
3.2 EVs/PHEVs chargers: common topologies and standards.....	45
3.2.1 AC/DC and DC/DC converters	45
3.2.2 On-Board vs Off-Board solutions	52
3.2.3 AC vs DC charge procedures	57
3.2.4 New scenarios: Integrated and Wireless chargers	61
3.2.5 Conclusion.....	68

4. BATTERIES: EVOLUTION IN THE AUTOMOTIVE SCENARIO.....	69
4.1 Characterization and classification	69
4.1.1 Figures of merit	70
4.1.2 Batteries in the automotive market and future developments.....	73
4.1.3 Conclusion.....	82
4.2 Li-Ion batteries: present and future	84
4.2.1 Classification	84
4.2.2 Main degradation modes	94
4.2.3 BMS and On-Board control strategies.....	98
4.2.4 Economic and Geo-politic considerations	113
5. MINIMIZATION OF V2G IMPACT ON THE STORAGE SYSTEM... 134	
5.1 Test procedures from USABC manual	134
5.1.1 Introduction	134
5.1.2 Core Performance Testing.....	135
5.1.3 Life Cycle Tests	139
5.1.4 Safety/Abuse tests	143
5.1.5 Other Performance Tests	144
5.2 Synthetization of the experiments in literature	146
5.2.1 Introduction	146
5.2.2 Description of the experiments	151
5.2.3 Conditions to minimize the degradation during V2G operations.....	161
6. CONCLUSION AND FUTURE WORKS	165
List of figures	168
References	173

1. Introduction

In the automotive global scenario, the need to concentrate efforts and investments towards a technological step (mainly focused on mass electrification of vehicles) allowed to bring to the attention the peculiarities of "Vehicle-To-Grid" technology in coordination with the evolution of electric generation and distribution networks.

Through a wide bibliographic research, have been collected and summarized information about the achievements so far obtained, the future perspectives and the feasible alternatives to proceed in this direction: from the results of this thesis could be possible to get some directives useful to test a prototype V2G application.

Starting from the analysis and the detailed description of the of BEVs/PHEVs it was essential to provide a characterization of the main components/systems (vehicle and network sides) of their limits and possible evolutions; more precisely, hardware components such as on/off-board chargers, inverters, connectors, and especially the battery pack have been deeply analysed obtaining a complete review on the state of art of these systems and the possibilities for future developments.

The last part of the work tried to match, at the same time, the requirements of V2G services with the constraints relative to the battery pack and its performance: from the tests in literature has been obtained an ideal set of operating conditions with the purpose to minimize the ageing phenomena.

1.1) V2G description

The basis of the "V2G" concept is the evolution of the relationship between a vehicle equipped with a plug-in electric powertrain (BEVs / PHEVs / PFCEVs), and the network.

The fundamental technology behind the development of a similar interconnection is the communication system that binds the two active players: through the exchange of information it is possible to control energy flows through advanced strategies while, in conventional applications, an electric vehicle is seen by the network as a simple load.

Therefore, in V2G systems, the vehicle takes an active role thanks to the features that allow it to participate actively in the management of the system. In the most rudimentary applications, the possibilities of the vehicle are limited to the role of "intelligent load", limiting the absorption of energy in case of network necessity (adjusting the recharging phase according to the requests of the grid).

The most advanced V2G systems allow the management of bi-directional energy flows, admitting the possibility of supplying services to the network thanks to connections and conversions of energy from the network to the vehicle and vice versa: the possible functionalities range from the injection of active power into the grid, in case overloaded network, up to filtering and reactive power compensation functions.

This innovative scenario lies in the middle of enormous technological developments, between the development of the new "Smart Grid" paradigm and the diffusion of renewable energy sources distributed unevenly along the distribution line with the emergence of quality, reliability and efficiency problems in the whole system.

The listed motivations, together with the push towards electric mobility, bring to the attention the need to study and verify potential and limits of V2G technology in order to support the electric network and the electrification of the vehicles itself.

1.2) Thesis structure

In the thesis it's possible to highlight several key steps in the overall structure: the first is the description of the environment in which the electric mobility and the V2G services would be developed, including the alternatives that may direct the evolution of these fields in a direction rather than the others.

After this introduction to the boundary conditions, the work has been focused on the components of infrastructures and electric/hybrid powertrains, individuating criticalities and drawbacks that could mine the feasibility of the system.

Going into details, the work is introduced describing the state of art of the two main actors: the electricity grid, with its developments towards the new concept of "Smart-grid" and the integration of renewable energy sources, and the electrified vehicles, with a description of the electrification levels, the related technical and economic characteristics and with a conclusive analysis on the barriers that could negatively influence the diffusion of V2G-enabled vehicles.

Moreover, the V2G services have been described with their peculiarities and affinity with BEVs/PHEVs, together with the different hardware solutions (vehicle and network sides) that directly influence the performance and future possibilities of these services.

Subsequently, focusing on the On-Board battery pack, mounted on the clear majority of purely electric and hybrid electric vehicles, a bibliographic research was carried out on today's technologies and on future alternatives that could go beyond the enormous limits that curb modern applications. Attention has been given to the classification of the main degradation mechanisms/modes and, above all, to the possibility of improving the system of analysis and control of the energy storage system (on board), with specific in-situ methodologies that allow the identification of aging phenomena and the sudden intervention in order to maximize the useful life of the component.

Still in this direction, the main methodologies used in the experimental field to test battery performance have been reported and described; these procedures, described in detail in the USABC manual of the United States Council for Automotive Research, are widely used in research activities and are at the base of almost all the battery experiments found in literature.

Finally, the last step was to summarize the experimental data, obtained from the existing scientific literature, to derive optimal operating conditions that minimize the negative effects, during V2G operations to support the network, identifying which of the possible applications can be adapted to the fixed boundary conditions.

1.3) Targets

Vehicle-to-Grid services would be a feasible solution to support the electric power grid just if they would not reduce the performance of the vehicle, or in case they could be profitable for the owner who chooses to share the functionalities of his vehicle with the network operator.

Among the key points, studied in this thesis to enhance the diffusion of both electric vehicles and Vehicle to Grid services, there is the identification and the analysis of several major targets that, in the future, should be necessary achieved and some indications on the most promising alternatives, in particular:

- Description of the design of infrastructures and vehicles to adequately manage the bi-directional power flows and the exchange of information through the implementation of an "Aggregator" in order to coordinate many vehicles in a single "smart load/source".
- Review of In-situ diagnostic procedures, to analyse in real-time the evolution of the main degradation modes evolving in the cells of the battery pack, in order to increase the lifespan of the energy storage system.
- Definition of a set of "safe" boundary conditions that should be respected to supply ancillary services preserving the Battery pack performance (Li-Ion batteries), with a proper design of the control algorithms of chargers and Battery Management Systems.

Therefore, a main target of the thesis is to suggest a baseline for further studies, in particular through indications about working and storage conditions of the Li-Ion batteries to avoid misuse of V2G services (with a worsening of the vehicle performance) and, at the same time, highlighting critical aspects (both hardware and software) that, if not faced, would negatively affect the evolution of the analysed technologies.

2. State of Art

2.1) Grid requirements and targets

2.1.1.) Grid description and support necessity

The electric power system is an infrastructure based on the continuous matching between the power generated and consumed, this due to the absence of storage devices; this structure has not changed in the years (at least this base concept) and real-time balancing is one of the most important features required to get a stable service. Among the services to guarantee the operational requirements of the power grid there are spinning reserves and frequency regulation (also called ancillary services) and voltage control/reactive power compensation at distribution level.

As shown in figure 2.1, the rising renewable sources (i.e. photovoltaic and wind-generation technologies) will cover, in 2050, 10% of the electric power request [1], differently from the conventional powerplants, the interface will be at distribution level and the network will include many different input points to compensate their stochastic behaviour. This diffusion put under stress the grid that, in the past, was designed to manage power flows from higher voltage levels to lower voltage levers and then, a change in this paradigm creates concerns on the power quality, reliability and stability [2].

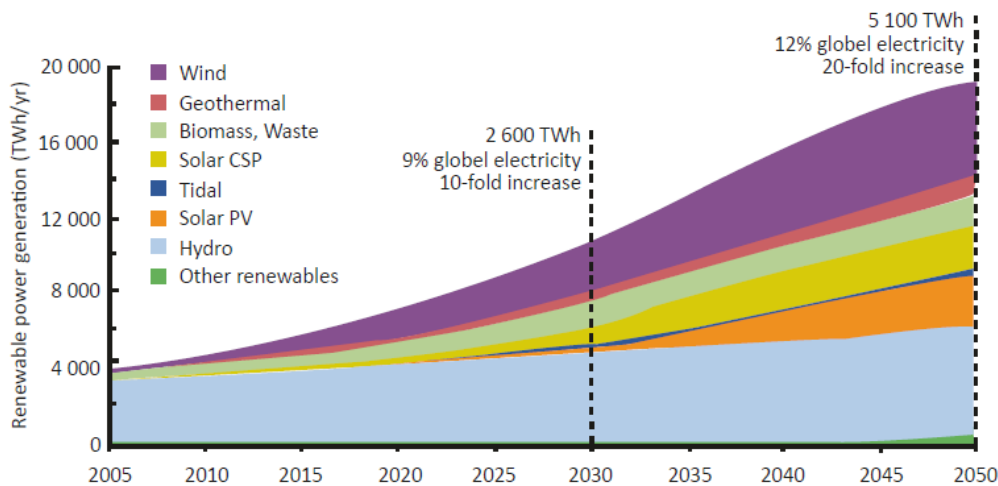


Figure 2.1: Evolution of different forms of renewable sources [1]

Analysing a nation like Denmark, in which both energy demand and renewable sources are expected to rapidly increase in the future (electricity demand from 35 TWh in 2001 to 45 TWh in 2020, installed capacity of wind power from 2440 MW to 5700 MW in 2020); V2G technology seems a promising possibility to enhance the integration of these sources (mitigating their oscillating output) and to deeply modify the oil-based transport system toward concepts like e-mobility and e-economy [3].

The growing interest in electric vehicles, witnessed by governments, customers and manufacturers in order to reduce the bond with fossil fuels, could be a detrimental event for the already stressed national electric systems.

In [17] is studied the effect of a large implementation of BEVs on the U.S. power grid (similar considerations can be used for the European power grid).

The penetration of BEVs, together with the increasing demand in ultra-fast charge (with charging power over 50 kW), will easily put under critic conditions the whole system.

The characterization of the impact on the grid of different scenarios can be done considering:

- 1) Uni-directional or Bi-directional chargers
- 2) Number of vehicles charging in the same area of interest
- 3) Geographic localization
- 4) Charging levels
- 5) SoC of batteries and specifications
- 6) Charging times and duration
- 7) Charging strategies

If these factors are not studied tuned and coordinated, the sustainability of the system is not guaranteed and both the diffusion of renewable sources and electric vehicles cannot be achieved.

In figure 2.2 the focus is on the necessary number of BEVs connected to the grid to store a fraction of the energy generated by wind turbines and then to stabilize the output of this source: just with a very large penetration there would be the possibility to play a significant role in this service.

	E(wind) 50 %	E(wind) 70 %	E(wind) 100 %
	Numbers of V2G [millions]		
Germany	~11	~15	~24
Europe	~50	~70	~97
North America	~70	~96	~136
Central & South America	~20	~17	~25
Eurasia	~18	~25	~36
Middle East	~9	~12	~17
Africa	~7	~11	~15
Asia & Oceania	~97	~115	165

Figure 2.2: Vehicles necessary to store a percentage of the energy produced by wind turbines [1]

In [3] the behaviour of a low-voltage power grid has been analysed, the oscillations in voltage have been studied to understand their main causes:

- DERs connection and disconnection
- Lack of a master controller leading to unbalanced loads
- Fast power electronic non-linear dynamic and saturation limits cause high frequency oscillations

Here comes the request to support the integration of renewable energy sources but, at the same time, to keep a high level of reliability and stability: traditional layouts, based on Automatic Generation Control (AGC), were used to balance the deviations caused by unpredictable demand peaks [4].

This “quasi-static approach” uses, as feedback signal, the Area Control Error (ACE generated by each balancing authority) sent to the fast-responding powerplants to correct the error within tens of minutes.

$$ACE = -\Delta P_{tie} - B\Delta f$$

In actual networks, many degrees of freedom have been introduced, this lead to a rethinking in regulation services and in [4] the concept of Enhanced Automatic Generation Control (e-AGC) is introduced. European concept of “smart grid” is presented in the chapter 1.1.2 of [1]; 6 points are identified as basis steps to integrate new technologies and strategies in the existing architecture:

- 1) Enabling fast and easy deploying of DERs in existing grids avoiding conflicts with voltage and frequency regulation, power-flow capacity...
- 2) Design of new types of automatic controls (e-AGC)
- 3) Harmonization of economical regimentations in Europe and definition of cross-border trading strategies
- 4) Creation and consolidation of widely shared technical standards and protocols
- 5) Enlarging of services and features, exploiting new ICT technologies, enhancing the consumers possibilities

These steps describe two main trends in the power system development:

- Liberalization of the energy market causing a congestion of the transmission capacity.
- Increased amount of energy directly generated at the distribution level and complex management of bi-directional power flows.

The definition of a completely new conceptual framework, to reach the targets in flexibility and efficiency, it's a key step in the development of V2G [5]: a master aggregator, as represented in figure 2.3, must be projected to coordinate many BEVs (ideally all the electric vehicles should be managed as a single load/source) optimizing both grid and vehicle/customer requirements.

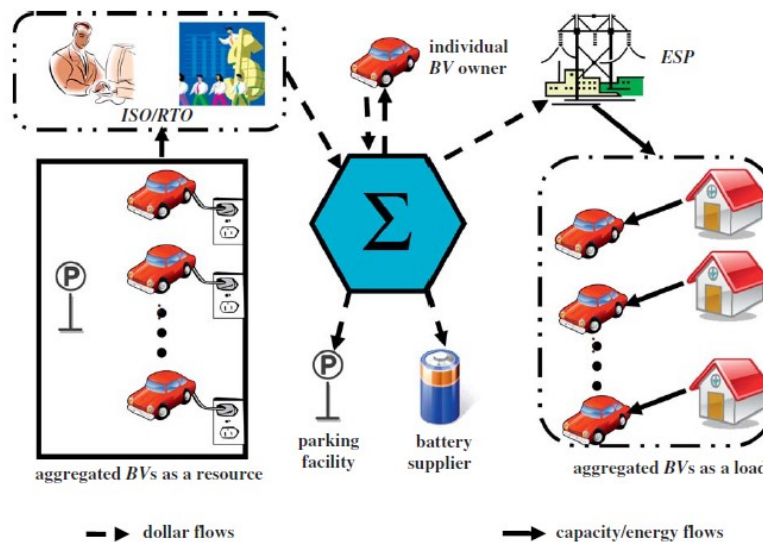


Figure 2.3: Role of the master aggregator in V2G concept [5]

The bi-directional connection of BEVs and PHEVs with exchange of active power is the best solution to enhance the possibilities of V2G technologies.

After more than 15 years of studies this concept has been expanded with many different services and in [6] the most promising features are listed and described with a particular interest on the achievable benefits and the effects resulting on vehicle/grid.

	Situation	Power Flow and Switches	Power Level	Control	Cost	Battery Effect	Distribution system	Requirements and Challenges	Benefits
Unidirectional Power Flow	Available	One-way electrical energy flow, basic battery charge (G2V) Diode Bridge + Unidirectional converter	Levels 1, 2 and 3	Simple. Active control of charging current. Basic control can be managed with time-sensitive energy-pricing.	Low price, no additional cost	No discharging degradation	No update or investment. With high penetration of PEVs: meets most utility objectives	Power connection to the grid	-Simplifies interconnection issues -Simple control and easy management -Provides services based on reactive power and dynamic adjustment of charge rates, even without reversal -Supplies or absorbs reactive power, without having to discharge a battery, by means of current phase-angle control -Voltage and frequency control
Bidirectional Power Flow	Not available	Two-way electrical energy flow and communication, charge/discharge (V2G) MOSFET (low power) IGBT (Medium power) GTO (High power level)	Expected only for Level 2	Complex. Extra drive control circuits. Extensive measures.	High price	Extra degradation due to frequent cycling	Necessary updates and investment costs	-Two-way power connection and communication -Suitable smart metering/sensors -Substantial information exchange -Extra investment and cost -Energy losses -Device stress	-Ancillary services -Active power regulation and stabilization Voltage regulation Frequency regulation (down-up) -Spinning reserves -Reactive power support -Peak shaving -Valley filling -Load following -Energy balance -Current harmonic filtering -Tracking the output of renewable energy sources

Figure 2.4: Characterization of Uni/Bi-directional V2G services, requirements and targets [6]

In this review, a lot of valuable information that can be used to understand important characteristics of these different approaches: the unidirectional power flow seems to be easily available with the actual technologies, nevertheless there are developments that can lead to a more complex configuration, such as the bidirectional one, in order to obtain a wider range of services with higher degrees of freedom and then higher flexibility.

2.1.2.) Smart-Grid concept

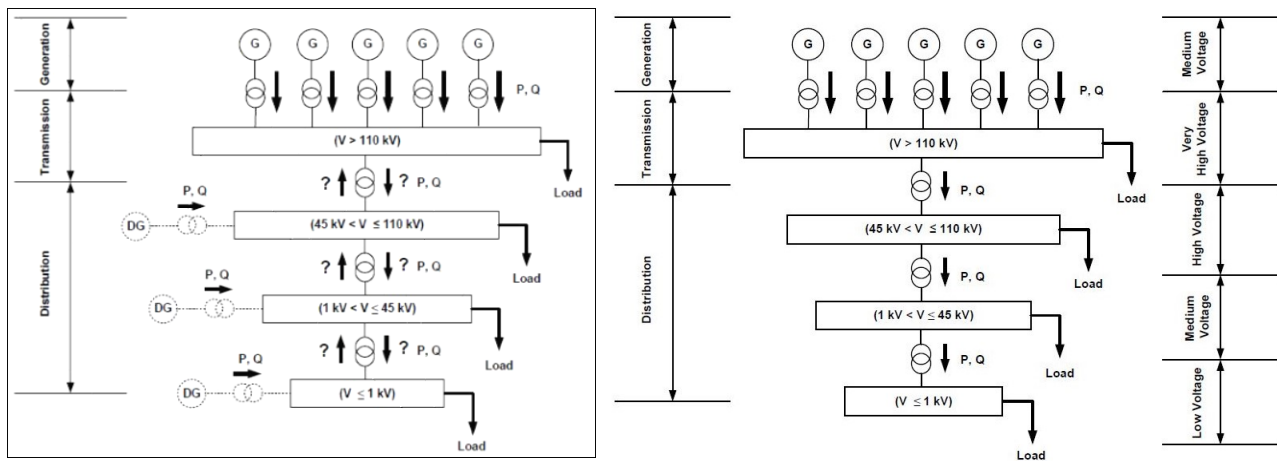


Figure 2.5: Comparison between conventional power system layout and new paradigm [7]

The shift toward “electric mobility” is an evolving challenge, technological improvements and a global focus on the problems to be solved, together with the rising attention of customers, media and governments, makes interesting and appealing, for all the major players in the automotive scenario, a strong effort in terms of

investment and research. The necessity to include new paradigms, such as the idea of “smart grid”, defined from the European Commission as “electricity network that can intelligently integrate and coordinate the actions of generators/consumers in the most efficient way”, comes from the rapid diffusion of “decentralized energy resources” (DERs as represented in figure 2.5) and the consequent quality degradation of the distribution service due to the architecture of the actual distribution system, not designed for a bi-directional energy flow and an intermittent power output operation of these kinds of sources. In classic architectures the design was based on the studied deterministic power flows, considering the worst-case scenario, in order to assure the adequate grid stability/safety; in this concept the control efforts are reduced to a minimum but the efficiency of the system is not optimized and can be easily destabilized by the new power flows from DERs. Combining intelligent monitoring, advanced control strategies and information/communication technologies (ICT), it’s possible to get new features and services:

- Satisfying new users requirements
- Enabling the inter-connection of different types of generators
- Allowing consumer to play a role in the grid optimization
- Enlarging the ways to receive electricity supplies based on dynamic tariffs, network state
- Finally enhancing reliability, quality, efficiency of the whole distribution system
- Implementation of active loads, with a set of control strategies based on the grid status and/or on prices based algorithms

Thanks to this approach, a distributed generation system (composed by DERs) can be optimized to reduce the need of expansion of the distribution grid and, displacing the generation near to the consumers, could enhance the performance increasing the efficiency, reliability and providing ancillary services.

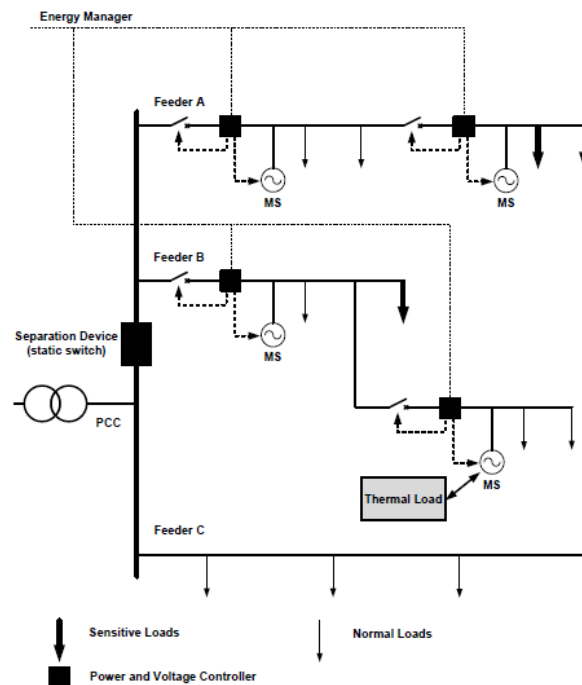


Figure 2.6: Integration of sensitive loads and energy manager in the power grid [7]

With “sensitive loads”, as in figure 2.6, distributed along the grid it’s possible to minimize the delay among loads and operators, moreover, local regulation services could be implemented (through Energy Manager Systems) to optimize the behaviour of the larger power plants and to enhance the penetration of alternative generators.

Storage systems could become fundamental players inside this scheme, being able to compensate the intermittent behaviour of most DERs, allowing to obtain an almost constant output power; The Battery Electric

Vehicles (BEVs) if not just considered as loads, could participate to those services if integrated in an advanced management and control system.

This idea seems appealing considering that the daily usage of an electric vehicle represents just a very small fraction of the available time, in which the vehicle could be connected to the grid (at home/work), and that could be profitable for the owner compensating the higher initial investment and the cost related to the battery wear [8].

There are other storage devices that should be considered, with different operational characteristics and performance:

- Supercapacitors
- Flywheels
- Compressed gas systems
- Hydraulic reservoirs

The choice among the alternatives should take into account the requirements in terms of energy exchange, power levels, lifespan and costs and reliability.

Integration and evolution of the actual power grid faces many obstacles that could slow down the increasing demand in “green energy” and “e-mobility”: i.e. legislative barriers and technical limits that will be described in this work.

Just with effort in advanced planning, complex strategies and strong R&D campaigns it's foreseeable an adequate step forward.

There are several factors that lead to the necessity to study new ways in the development of a new power grid paradigm:

- Rapid evolution and penetration of DERs
- Higher targets in efficiency, reliability and safety
- Different market opportunities for new players

This is a quite established scenario and V2G is just one of the alternatives to support this process.

Much more efforts are required to investigate the feasibility, profitability and constraints using BEVs for such purposes.

2.2) EVs/PHEVs characterization

2.2.1) Electric power-train classification

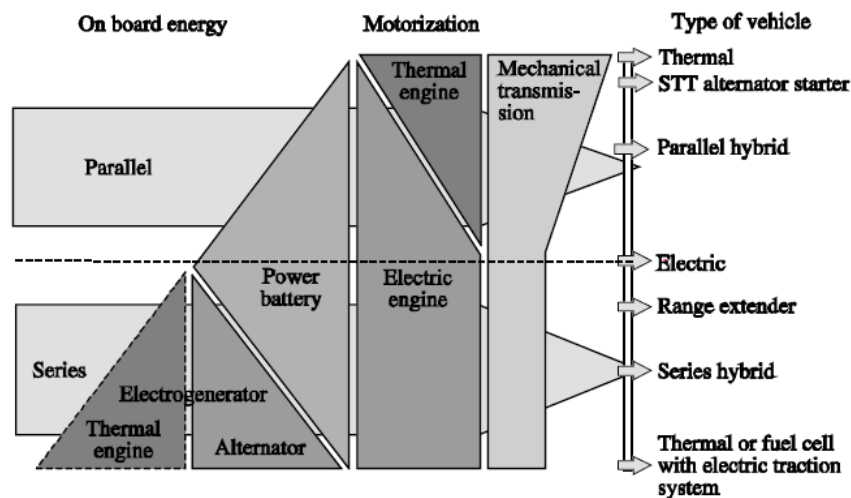


Figure 2.7: Classification of electrified vehicles [9]

The proposed classification from [9] allows to effectively characterize:

- All types of hybrid vehicles
- Single and multi-source propulsion systems
- Simple and complex hybrid

Being able to correctly classify the different architectures of electrified vehicle (then speaking of thermal-electric hybrid vehicles) in the market is essential to understand the requirements and the constraints that deeply influence the performance, not only of the vehicle and its on-board devices (battery pack, converters, BMS...) but also the off-board devices to charge and control the vehicle connected to the grid.

Each hybrid traction system it's obtained connecting two or more elementary traction systems; each elementary traction system is the sum of two main subsystems: Powertrain and On-Board storage system (figure 2.8).

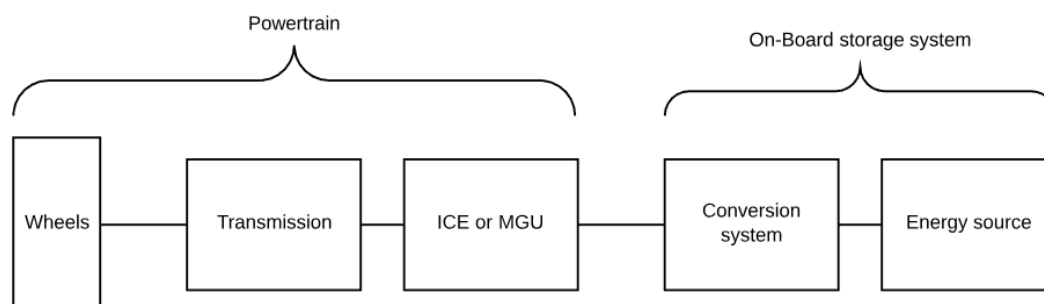


Figure 2.8: elementary traction system building blocks

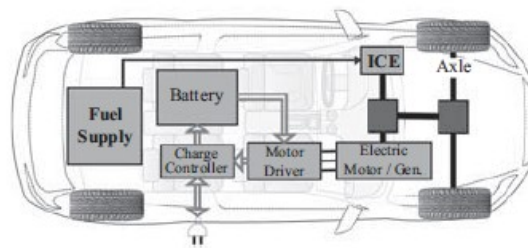
In the ICE elementary traction system, the fuel tank is the on-board storage system and the internal combustion engine is the core traction system in the powertrain while in the pure BEV elementary traction system we have the battery as energy source, the power electronic in the conversion block and finally the motor-generator unit that replaces the ICE.

It's important to clarify the classification between simple/complex and series/parallel hybrid traction systems: simple thermal-electric hybrid traction systems are realised through the connection of one ICE elementary layout with one electric elementary layout.

Considering the type of connection between these blocks it's possible to obtain a further classification:

- Parallel Simple Thermal-Electric hybrids: the connection is at powertrain level and there are two mechanical actuators (ICE and MGU).

Parallel-hybrid

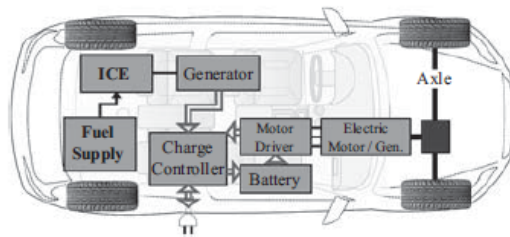


- Dual drive options through electric motors and ICE
- Battery energy supply with grid tie options. Liquid hydrocarbon fuel for higher velocity driving

Figure 2.9: Parallel-hybrid layout and main characteristics [10]

- Series Simple Thermal-Electric hybrids: where the connection is at energy source level and there is just one mechanical actuator (the MGU).

Series-hybrid



- Electric drive through an electric motor
- Battery energy supply with grid tie options. Liquid hydrocarbon fuel and generator to extend range

Figure 2.10: Series-hybrid layout and main characteristics [10]

- Series-parallel Thermal-Electric hybrids: where both the previously introduced configurations are available with dual drive options.

Series-parallel hybrid

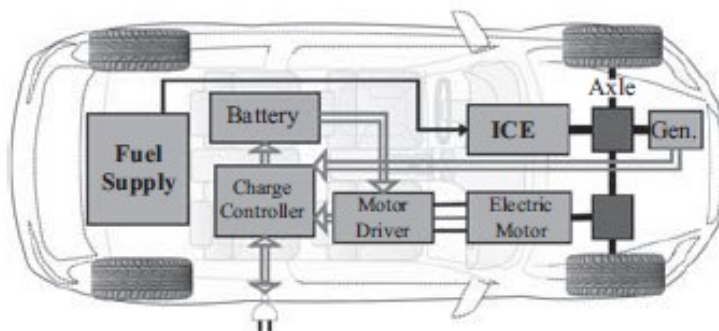


Figure 2.11: Series&Parallel-hybrid layouts [10]

Looking again at figure 2.7 it's possible to see how there are different degrees of hybridisation between the conventional ICE based powertrain, the pure electric vehicle and a vehicle with an electric transmission (respectively the top, in the middle and in the bottom of the bar on the right).

In order to classify each level of hybridisation for both simple series/parallel hybrids, it's possible to use the "Hybridisation Ratio" introduced by F. Badin. In parallel configuration the ratio considers the power of the conventional ICE over the sum of both ICE and MGU powers: $R=1$ corresponds to a conventional ICE based powertrain and $R=0$ to a pure electric vehicle.

$$R_{h \text{ paral.}} = P_{ICE} / (P_{ICE} + P_{elt})$$

In series configuration the index is evaluated from the ratio between the electric generator and the electric motor power: $R=0$ corresponds to a pure electric vehicle while $R=1$ corresponds to a vehicle with an electric transmission.

$$R_{h \text{ series}} = P_{g_elt} / P_{m_elt}$$

Complex hybrids derive from the more linking components or more than two elementary traction systems; three fundamental indexes are used to characterize the complexity of each architecture:

- Order: number of elementary traction systems connected to achieve the hybrid configuration
- Index: number of links between the elementary traction systems
- Energy route: number of available energy pathways equal to the square of the order number

Another "hybridisation ratio" can be evaluated starting from the previous two:

$$R_{ch} = (\sum R_{h \text{ paral.}}) \cdot (\sum R_{h \text{ serie}})$$

This classification it's useful because starting from this ratio there are several considerations that can be obtained; for example, two complex hybrids with the same order and index can have the same flexibility if uses the same type of components but to completely identify the potentiality of a system it's necessary to consider the product among all the efficiencies of each component (at least the mean value). Then through these indexes it's possible to identify the first information for sizing of storage sources and powertrain components. To conclude this brief review, it's necessary to highlight that V2G services could be suitable especially for hybrid and electric vehicles with medium/high capacity on-board battery packs, then with hybridisation ratios near to zero and, moreover, with the possibility to be recharged directly from the grid (plug-in vehicles) but not all the hybrid vehicles on the market have this opportunity.

2.2.2) Market analysis

The Electric and Plug-in Hybrid Vehicles Roadmap presented a detailed scenario for the evolution of the electrification process in the automotive field.

This roadmap covered the two main types of electrification for light-duty vehicles: pure battery electric vehicles (EVs) and plug-in hybrid electric vehicles (PHEVs); it's of high interest analyze the differences between these two "philosophies" because directly affect auxiliary infrastructures, driver behavior and technological development.

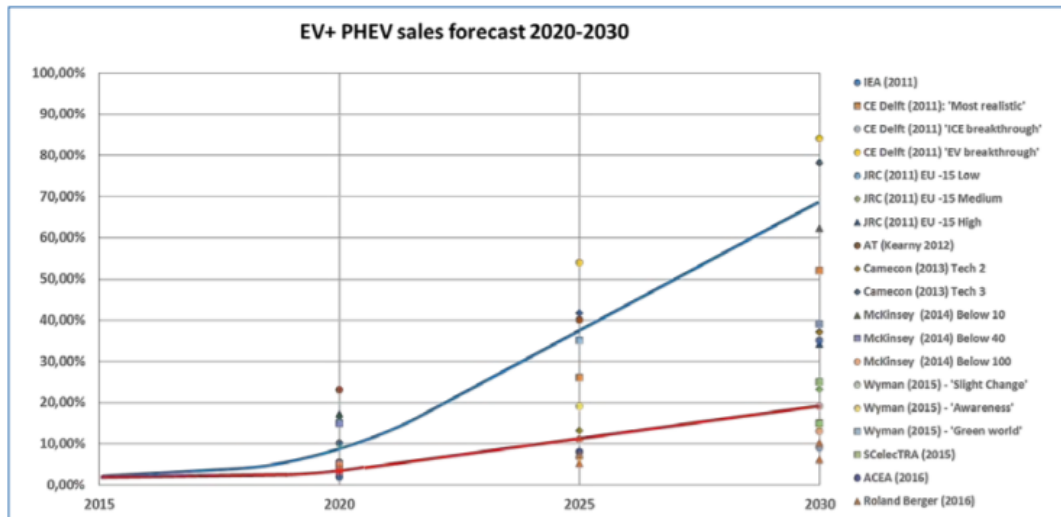


Figure 2.12: European market forecast from literature

In figure 2.12 and 2.13 there are two major trends that will probably describe the sales evolution of BEVs/PHEVs in the European market:

- LOW SCENARIO: the electrification it's boosted by the new CO2 targets but the main electrification source is the hybridisation of ICE-based vehicles.
- HIGH SCENARIO: achievable with several breakthrough developments in the EVs technology (battery price, lifespan...)

Being probable a rapid increase of the electrification degree in the next years, such trends must be studied and decision must follow the best trade-off between the expectations and the technological feasibility.

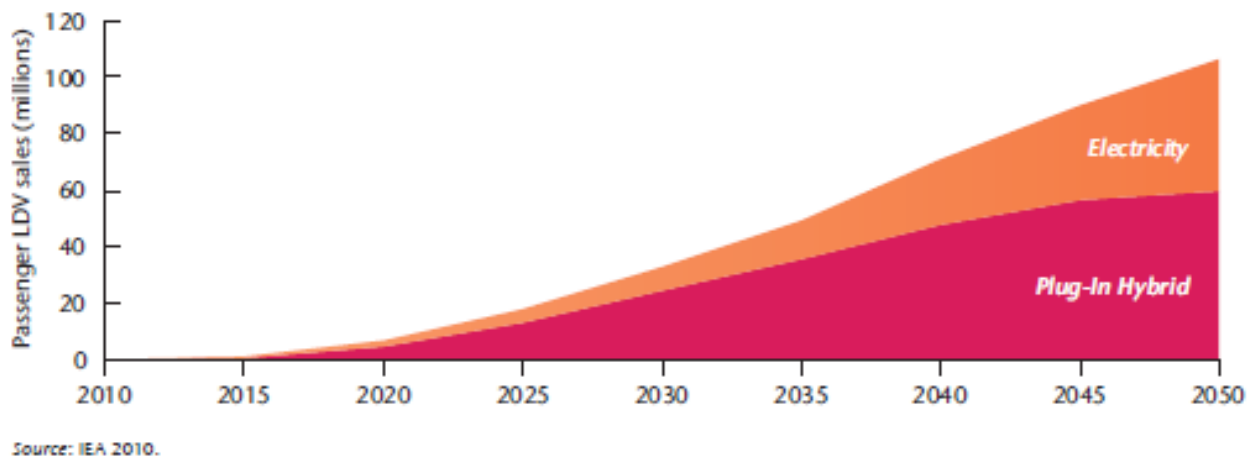


Figure 2.13: Expected market share between BEVs/PHEVs from "BLUE MAP SCENARIO" [11]

From [11] it's possible to identify the most important differences between requirements, targets and constraints derived from the adoption and deep diffusion of BEVs and PHEV while a complete comparison between the two different paradigms is reported in the next rows.

PHEVs		EVs
Consumer adoption:		Consumer adoption:
<ul style="list-style-type: none"> Many consumers may be willing to pay some level of price premium because it is a dual-fuel vehicle. People interested in PHEVs may focus more on the liquid fuel efficiency (MPG) benefits rather than the overall (liquid fuel plus electricity) energy efficiency. Metrics should encourage looking at both. Electric range should be set to allow best price that matches the daily travel of an individual or allow individuals to set their own range (e.g., providing variable battery capacity as a purchase option). 		<ul style="list-style-type: none"> Early adopters may be those with specific needs, such as primarily urban driving, or having more than one car, allowing the EV to serve for specific (shorter) trips. More research is needed to better understand driving behaviour and likely EV purchase and use patterns. With involvement from battery manufacturers and utilities, consumers may have a wider range of financing options for EVs than they have for conventional vehicles. EVs will perform differently in different situations and locations; therefore utility, and operating costs may vary significantly.
Fuel standards:		Fuel standards:
<ul style="list-style-type: none"> SAE J1711 (Recommended Practice for Measuring Fuel Economy and Emissions of Hybrid-Electric and Conventional Heavy-Duty Vehicles) and UN-ECE R101 (Emissions of carbon dioxide and fuel consumption) are possible candidates for the standard for measuring PHEV fuel economy. 		<ul style="list-style-type: none"> SAE J1634 (Electric Vehicle Energy Consumption and Range Test Procedure) is currently undergoing review, and UN-ECE R101 (Emissions of carbon dioxide and fuel consumption) is a possible candidate for a testing procedure for EVs.
PHEVs		EVs
Infrastructure:		Infrastructure:
<ul style="list-style-type: none"> Home recharging will be a prerequisite for most consumers; public recharge infrastructure may be relatively unimportant. 		<ul style="list-style-type: none"> Greater need for public infrastructure to increase daily driving range; quick recharge for longer trips and short stops; such infrastructure is likely to be sparse in early years and will need to be carefully coordinated.
Economies of scale:		Economies of scale
<ul style="list-style-type: none"> Mass production levels needed to achieve economies of scale may be lower than those needed for EVs, for example if the same model is already mass-marketed as a non-PHEV hybrid; 		<ul style="list-style-type: none"> Mass production level of 50 000 to 100 000 vehicles per year, per model will be needed to achieve reasonable scale economies; possibly
Vehicle range:		Vehicle range:
<ul style="list-style-type: none"> PHEV optimal battery capacity (and range on grid-derived electricity) may vary by market and consumer group. Willingness to pay for additional batteries (and additional range) will be a key determinant. 		<ul style="list-style-type: none"> Minimum necessary range may vary by region: possibly significantly lower in Europe and Japan than in North America, given lower average daily driving levels.

Starting from these considerations and looking at foresights trying to understand the potential diffusion till 2050, it's necessary to highlight that at least for HEVs the path seems to be quite established: due to more stringent CO2 requirements cars manufacturers will surely adopt such a solution and HEVs, in different configurations, will lead over EVs for many years [12].

Drawbacks like the limited specific energy of the battery, the lack in infrastructures and the necessity of deep analysis of well-to-wheel efficiency could be an obstacle to the rise of the full electric mobility.

These problems could be faced passing from the current storage system, based as said on electrochemical batteries, to breakthrough alternative storage methods but nowadays there are not enough mature technologies that could be applied in mass production vehicles.

2.2.3) Trends and technological evolution

In a short prospective there are not technological developments that could lead to an immediate passage from hybrid vehicles to pure electric vehicles, at least in large-scale markets, then it's necessary a review of the available solutions, of the evolving regulations and of the possible future alternatives.

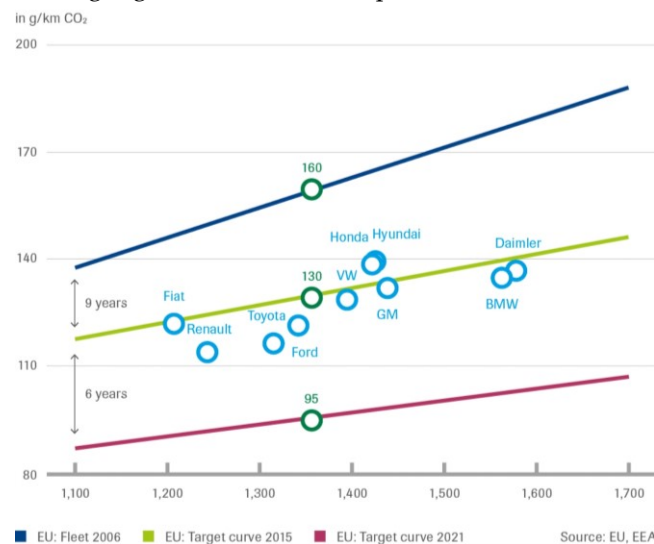


Figure 2.14: CO₂ target values for the automotive industry and fleet values from different manufacturers

One of the crucial reasons to point the attention on the hybridisation of the ICE-based vehicles is the increasing penalties for each gram of carbon dioxide that overtakes the target set for the whole fleet of a car manufacturer (excess emission premiums).

MAKE	AV. CO ₂ 2016 (g/km)	AV. CO ₂ 2015 (g/km)	VAR. (g/km)	POSITION 2015	Car	Engine/Powertrain	CO ₂ g/km
1 PEUGEOT	101.9	103.5	-1.7	1	GM Volt	Series Hybrid or Range	27
2 CITROEN	103.3	105.6	-2.3	2	Vauxhall Ampere	Extended Electric	
3 TOYOTA	104.0	107.6	-3.6	4	Chevrolet Volt		
4 RENAULT	105.6	105.9	-0.3	3	Volvo V60	Diesel PHEV	
5 SKODA	111.8	115.4	-3.7	6	Toyota Prius	SI PHEV	49
6 NISSAN	115.0	114.1	+0.8	5	Toyota Yaris	SI Hybrid	79
7 SEAT	115.8	116.7	-0.9	7	VW	Natural Gas SI Engine	79
8 FIAT	116.0	117.6	-1.6	9	Renault Clio	1.5L diesel	83
9 MINI	116.4	117.0	-0.6	8	Hyundai i20	1.1L CRDi Blue	84
10 DACIA	117.6	121.9	-4.3	12	VW Golf	Bluemotion 1.6 L diesel	85
11 VOLKSWAGEN	117.7	117.8	-0.1	10	KIA Rio	1.1L CRDi Eco85	85
12 FORD	120.1	118.0	+2.1	11	Ford Fiesta Titanium ECONetic	Diesel 1.6L Duratorq TDCi with stop/start	87
13 VOLVO	122.0	122.8	-0.8	13	Citroen C3	e-HDi 70 Airdream EGS SI Hybrid	87
14 OPEL/VAUXHALL	122.4	126.3	-3.9	14	Peugeot 3008	Diesel Hybrid 4	88
15 BMW	123.2	128.0	-4.8	19	Fiat 500	SI Petrol	89
16 KIA	124.5	127.7	-3.1	18	Lexus CT200h Luxury car	Petrol Hybrid	94
17 AUDI	124.7	127.3	-2.6	15	Honda Civic	1.6L-DTECI	94
18 HYUNDAI	124.8	127.4	-2.5	16	Fiat Panda Twin Air	Diesel	95
19 MERCEDES	127.5	128.1	-0.6	20			
20 MAZDA	127.7	127.5	+0.2	17			

Figure 2.15: Different powertrains and manufacturers with the relative CO₂ emissions

As introduced before and as evident in figure 2.15, the HEVs can respect the constraints in terms of CO₂ emissions with higher efficiency with respect to other powertrain technologies.

In the next rows are reported the principal (past and future) steps that determine the limits that must be respected:

- 2015: definition of a threshold at 130 g/km.
- 2017: from the New European Driving Cycle (NEDC) to the Worldwide harmonized Light vehicles Test Procedure (WLTP), a more severe procedure will lead to higher fuel consumption.
- 2019: the fine will be of 120 euro for each g/km over the limit.
- 2020: fleet-average CO₂ emission target of 95 g/km must be met by 95% of each manufacturers' new passenger cars registered in 2020, and by 100% of cars from 2021.

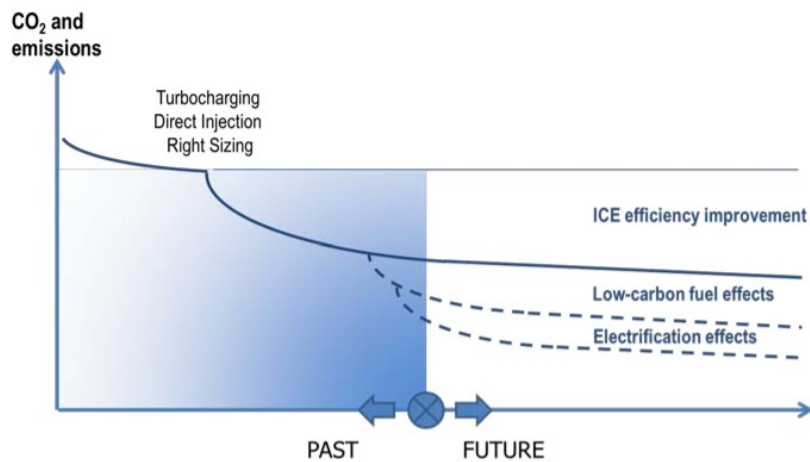


Figure 2.16: CO₂ emissions reduction strategies between past and future

In figure 2.16 and 2.17 it's possible to understand how the improvements in the fuel conversion efficiency (then the reduction in CO₂ emissions in g/km) will lead to a deeper and deeper electrification: there are no other alternatives that allow to respect the future limits and, moreover, this will require an increase in powertrains complexity and costs.

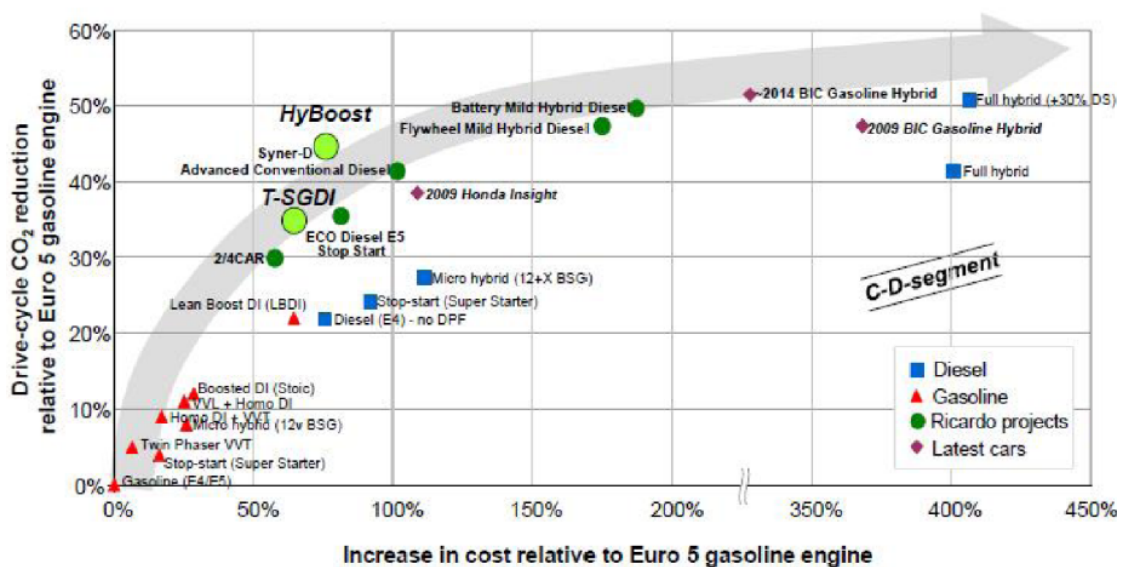


Figure 2.17: Automotive technologies: CO₂ emissions reduction vs increase in cost

Furthermore, in last years, the focus is passing from the emissions measured with the test cycles toward the value measured in real driving conditions: in figure 2.18 it's possible to see how the reduction in NOx limits from 2000 to 2014 (reduction about 80%) was not mirroring the real driving emissions that were reduced about 40%.

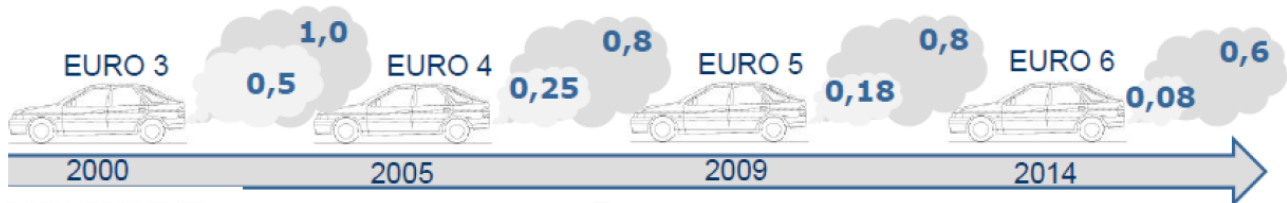


Figure 2.18: Real NOx emissions (dark grey) versus European NOx emissions limits (light grey)

This lack of correlation can be explained due to:

- Insufficient reproducibility of the dynamic operating conditions of a ICE during real driving operations (the emissions limits considered the NEDC as reference cycle)
- Real vehicle specifications different from those considered during type approval and more auxiliary devices affecting the ICE performance
- Variable environmental conditions and road structures

For this reasons WLTP (figure 2.19) will substitute the actual cycle and , moreover, real-driving emissions tests (RDE), using portable emissions measurement systems (PEMs), will be inyntroduced in two steps to determine and measure real values:

- From September 2017 for new models and from September 2019 for new vehicles the “conformity factor” (ratio between the measured emissions and the standard limit) will be equal to 2.1 (will be tollerated emissions twice the limit).
- From January 2020 for new models and from January 2021 for new vehicles the CF will be equal to 1 plus the error margin set to 0.5.

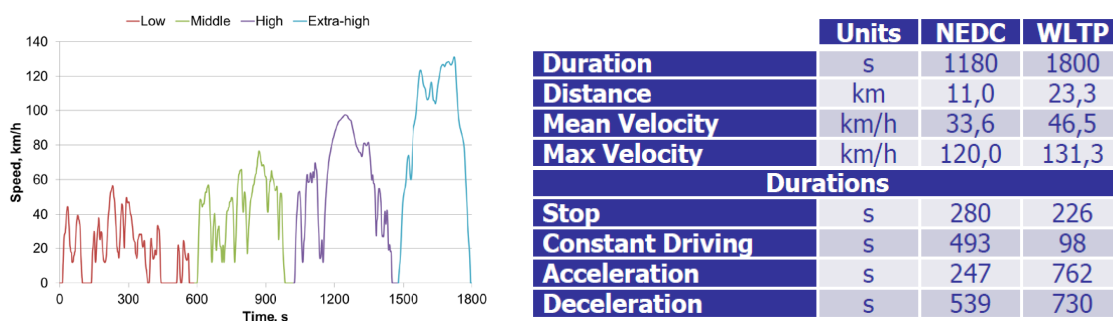


Figure 2.19: WLTP cycle (on the left) and the technical comparison with NEDC (on the right)

After all these considerations it's useful to look at the forecasted emissions limits (at least in terms of CO2) and the relationship with the introduction of the described variations; in figure 2.20 there are the past present and future evolutions of the CO2 fleet limits and of the measurement procedures.

Can be seen that after 2021 the limits will be influenced by the measured emissions after the adoption of WLTP while till the 2020 both the cycles will be utilized; as far as RDE and low temperature test (for CI engines) are concerned there is an introduction phase to evaluate the impact on the measured emissions and to set adequate limits without to compromise the automotive market.

Emission Limits	Euro 5b			Euro 6b			Euro 6c				Euro 6d			
	2012	2013	2014	2015	2016	2017	2018	2019	2020	2021	2022	2023	2024	
CO ₂ Fleet	130 g/km					95 g/km - NEDC Based Target				To be Defined on WLTP test results				
Driving Cycle	NEDC Testing Only					Double testing NEDC/WLTP				WLTP Testing Only				
Low Temperature Test (-7°C) for CI Vehicles						Introduction				New Limits				
Real Driving Emissions						Phase-In				New Limits				

Figure 2.20: EU – LD Emissions Testing Roadmap from FEV, ICCT and Delphi

Also if, as introduced before, it's really improbable to see a fast passage from ICE based vehicles (considering also hybrid electric vehicles) in the next years, it's necessary to review the possibility, as far as the On-Board energy storage system are concerned, to understand the alternatives that are being studied and developed.

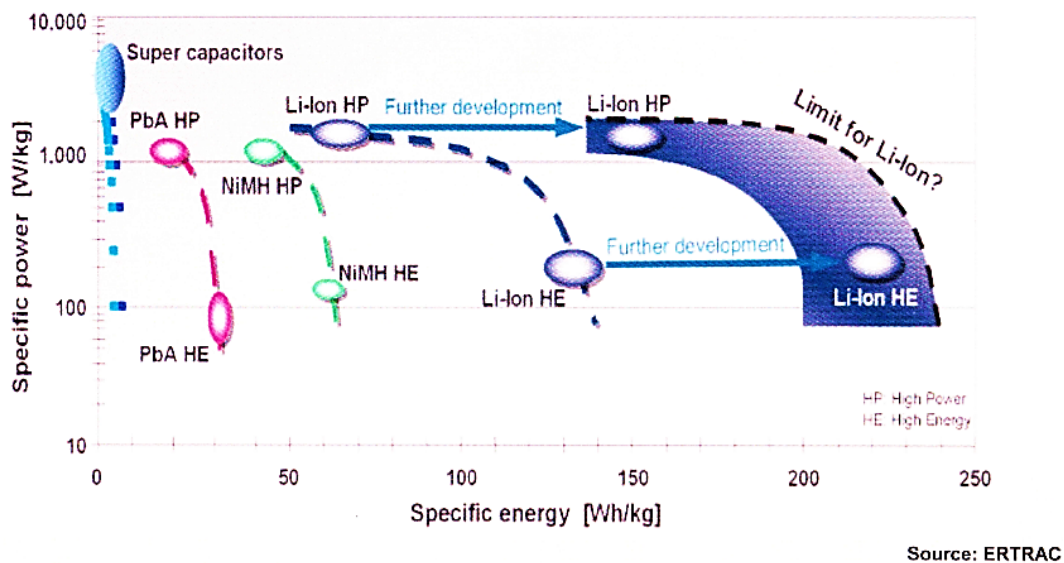


Figure 2.21: Pareto plot describing the trade-off between high-power/energy designs for different storage systems

Nowadays Li-Ion batteries are the first choice in the automotive field also considering the high cost: this because the high specific power and high specific energy potential (figure 2.21). Specific energy is still improvable but being far away from the hydrocarbons capabilities. Other important features promoting the rapid diffusion of EVs could be:

- Recharge time (till 5 minutes for 80% of the battery capacity)
- Lifetime (should be close to the vehicle's calendar life, thus 10 years/200.000 km)
- Battery pack cost (Should be lower than 150 euro/kWh)

Then electric vehicles commonly store the energy in electro-chemical form (with specific energy between 30 to 180 Wh/Kg) while ICE based vehicles can use gaseous (stored at hundreds of bars) and/or liquid fuels (around 10 kWh/Kg).

Other possible storage systems could exploit very different energy forms for example:

- Elastic energy (with specific energy from 2 to 10 Wh/Kg)
- Kinetic energy (with specific energy from 6 to 20 Wh/Kg)

The advantages of liquid fuels start from the higher specific energy, the maturity of the technology till to the highly extended refuelling infrastructure; on the other side elastic, kinetic and electrochemical energy sources have the possibility to recover the kinetic energy during braking phase and to remove the pollutant emissions (NO_x, HC, PM) from the utilization sites.

Nevertheless, the R&D process of the alternative energy sources does not seem to achieve sufficient improvements and without new breakthrough technologies there are few possibilities to easily and rapidly replace the ICE based fleets.

2.3) Toward V2G: scale effect and deployment issues

Depending on the widespread of V2G infrastructures, the economic costs and the impact on the power grid during charge/discharge would change drastically.

Smart control, through an aggregator, it's the first step to mitigate the most important drawbacks:

- Increased peaks load
- Stress on the grid and its components
- Power losses and reduced electric distribution quality
- Increased battery degradation

Numerous simulations have been conducted in different geographic locations and then in different grid configurations [18]-[26]:

<i>"Dumb charge"</i>			
<i>Location</i>	<i>Reference</i>	<i>Penetration level [%]</i>	<i>Peak load increase [%]</i>
<i>Los Angeles</i>	<i>[18]</i>	5	3,03
	-	20	12,47
<i>California</i>	<i>[19]</i>	10	17
	-	20	43
<i>Portugal</i>	<i>[20]</i>	11	14
<i>New York</i>	<i>[21]</i>	50	10
<i>Western Australia</i>	<i>[22]</i>	17	37
	-	31	74
<i>Belgium</i>	<i>[23]</i>	30	56
<i>U.K.</i>	<i>[24]</i>	10	17,9
	-	20	35,8
<i>Netherlands</i>	<i>[25]</i>	30	7
<i>Belgium</i>	<i>[26]</i>	10	22
	-	30	64

Figure 2.22: Effect of uncoordinated charging at different geographic locations [6]

In [13] uncontrolled and smart charging strategies are compared: it's evident the negative effects on the daily power peaks, in case of "dumb" (uncontrolled) charge, and on current and voltage fluctuations.

The simulation takes into account different levels of penetration in different geographic locations; worsening of the operating conditions are unavoidable but, with a "smart" charging strategy, it's possible to mitigate these effects decreasing also the deviations in current and voltage (figure 2.23).

	Without EVs load	Un-coordinated charging	Coordinated charging
Line current (A)	105	163	112
Node voltage (V)	220	217	220
Peak load (KVA)	23	36	25
Power losses (%)	1.4	2.4	2.1

Figure 2.23: Power quality degradation in case of un-coordinated and coordinated charging [13]

Considering different levels of BEVs diffusion, in [14][15] the effect on Power Systems are simulated in different nations (Germany, UK, Portugal, Spain, Greece) and with different charging strategies (Dumb charge, Multi-tariff charge, Smart charge) identifying the additional energy requirements.

If it's evident that a larger adoption means higher load levels and higher possibility to obtain a congested grid, many BEVs connected during the parking time (most of the time a vehicle is parked at work or at home) could damp these positive and negative peaks reducing the detrimental effect on whole the energy system. The impact of large-scale deployment of PEVs on the California grid is summarized in [16]: as penetration increases, so does the total annual electrical energy demand and the total peak requirements (figure 2.24 and 2.25). Thus, a high level of PEV penetration could disrupt distribution systems, depending on the charging power and schedule.

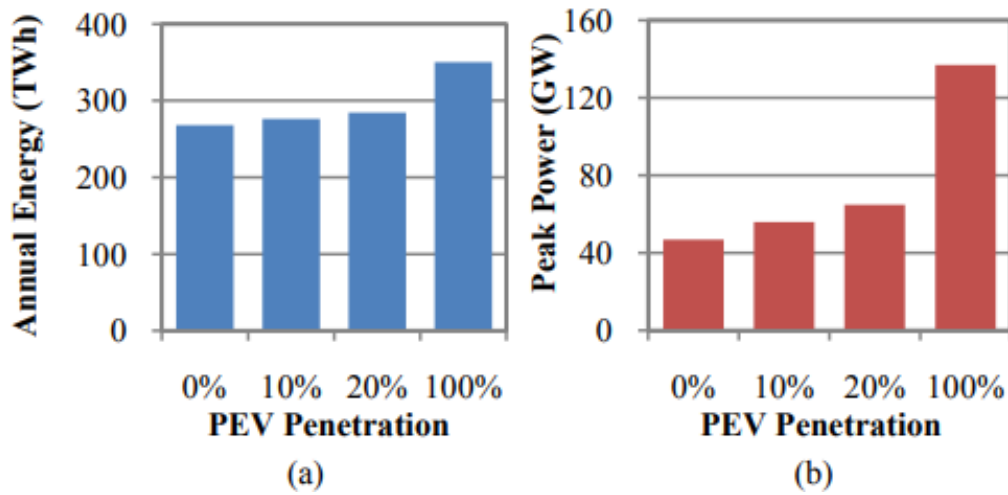


Figure 2.24: Impact of BEVs on California's annual electrical energy (a) and peak power (b) demands [16]

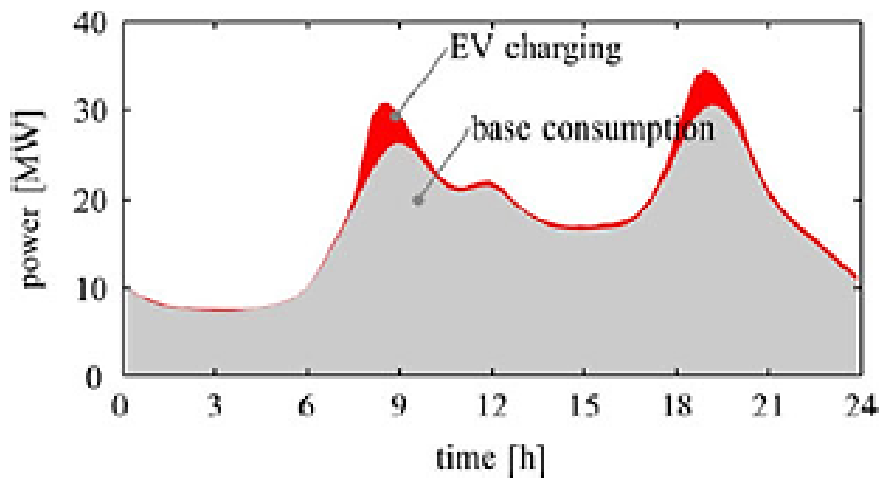


Figure 2.25: Resulting peak power from the un-coordinated charging of 2200 BEVs [6]

From this study the maximum allowable EVs integration percentages in the MV grid were 17 % with the dumb charging, 20 % with the multiple tariff, and 63 % with the smart charging approach.

Economic costs, emissions reductions benefits, and distribution system impacts of PEVs depend on vehicle and battery characteristics as well as on charging frequency and strategies.

When no smart charging schemes or embedded controller are available, vehicles are charged like any other load. Coordinated smart charging and discharging procedures to optimize time and power demand appears to be the most beneficial and efficient strategies for both grid operator and PEV owners.

In [17] and [6] the potential high penetration of EVs and PHEVs it's seen as a problem by the grid-side prospective: EVs, during charging operations, represent a burden on the distribution grid (increasing peaks and oscillations of the absorbed power); without a coordinated charging strategy, and considering nowadays architectures, there is the risk to overload the grid causing aging and malfunctions of many devices (transformers, relays...).

Again, this scenario will surely result from the so-called "dumb charge", in which there are not high-level controls to achieve an optimization of the energy distribution.

Instead with "smart charge" control it's possible to minimize the line's losses postponing the energy delivery, and then the charge, at the nodes farer from the slack bus, in periods with a low demand. This second strategy does not require an excessive upgrade of the actual infrastructures but just requires an advanced Energy Management System (EMS) with "smart-meters" that can send/receive load data analysing the state of the grid.

These are clear signals to the necessity of a new design of the power grid architecture: this is particularly true considering the e-mobility targets that could be achieved in the next decades.

3. V2G potentialities, hardware and architectures

3.1) V2G applications

In the next chapters, all the services that can be supplied to the grid from a sufficient number of vehicles connected, through a bidirectional charger, to the grid, will be presented: as introduced before an “Aggregator” allows to consider the total capacity available like in a unique Electric Energy Storage (EES).

Will be described also the potential benefits that a BEV owner could gain from the most promising applications, furthermore after a first introduction, the description will sub-divide the possibilities in “services that affect the battery SoC and then life time”, such those that imply an exchange of active power, and “services that does not involve battery degradation”. EES can supply the following services [1]:

- Bulk-energy services:
 - Energy time-shifting
 - Electric capacity

- Ancillary services:
 - Regulation
 - Spinning reserves
 - Voltage support
 - Black start

- Distribution infrastructure services:
 - Distribution-upgrade
 - Congestion relief
 - Voltage support

- Customer energy management services:
 - Power quality
 - Power reliability
 - Retail energy time-shift
 - Demand-charge management

In figure 3.1 it's suggested another classification subdividing the different available V2G applications for factors like storage period, available power, AC voltage...

Application	Storage (in min)	Power	AC voltage in kV	Duty cycle requirements	Floor space (importance)	Portability (importance)
Spinning reserve	10^1 – 10^2	10^1 – 10^2 MW, LC	10^1 – 10^2	10^1 /year, random, discharge only	Medium	Low
Area control & Frequency responsive reserve	Charge/discharge Cycles of $<10^1$	10^1 – 10^2 MW, LC	10^1 – 10^2	Random, continuous charge/discharge cycle clustered in 2-h blocks daily	Low	Low
Load levelling	10^2 – 0.5×10^3	10^0 – 10^2 MW, LC	10^1 – 0.5×10^3	10^2 /year, regular, periodic, weekday block discharge, increased use in shoulder months	Medium	Negligible
Transmission system stability	10^{-3} – 10^{-1}	10^1 – 10^2 MVA, SC	10^1 – 0.5×10^3	10^3 /year, random, charge & discharge cycles	Medium	Low
Transmission voltage regulation	10^1 – 10^2	10^0 – 10^1 MVAR, SC	10^1 – 10^2	10^2 /year, random charge & discharge cycles typically weekdays, seasonal by region—at least 6–7 months	Medium	High
Transmission facility deferral	10^2	10^{-1} – 10^1 MVA, LC	10^0 – 10^1	10^2 /year, most likely during weekday peak, charge & discharge	Medium	Medium
Distribution facility deferral	10^2	10^{-1} – 10^0 MW, LC	10^0 – 10^1	10^2 /year, most likely during weekday peak, charge & discharge	Medium	Medium
Customer energy management	10^1 – 10^2	10^{-2} – 10^1 MVA, LC	10^{-1} – 10^1	10^2 – 10^3 /year, regular periods	High	Varies
Power quality & Reliability	10^{-3} – 10^0	10^{-2} – 10^1 MVA, SC	10^{-1} – 10^1	10^2 – 10^3 /year, irregular periods, charge & discharge	High	Varies
Renewable energy management	10^0 – 10^3	10^{-2} – 10^2 MVA, LC	10^{-1} – 10^1	10^2 – 10^3 /year, regular periods, discharge only, unpredictable source	Varies	Varies

Figure 3.1: Summary of different grid services and their technical requirements [1]

In [27] a simulation on 533 homes, with an equivalent number of EVs connected to the grid, was designed to study the simultaneous connection of a high number of vehicles, simulating a high EV load penetrance in an already unbalanced local power network; then the focus is shifted from the LV bus to the MV bus analysing the capability of Level III inverters to face this new scenario (a suitable layout is schematized in figure 3.2). It resulted in two main conclusions:

- 1) Mass adoption of BEVs is a necessary step to obtain benefits from V2G ancillary services
- 2) Further improvements of the inverter technology must be achieved

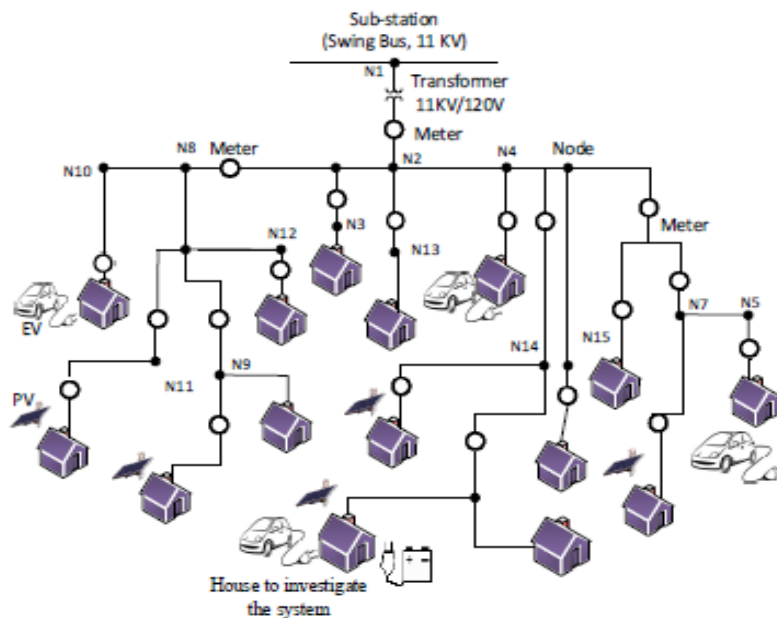


Figure 3.2: MV to LV scheme representing the local power network with V2G applications [32]

In [28] a clear list of technical obstacles that must be overtaken:

- Energy Management System (EMS) must be able to manage in real time the balance between generation and load then acting on sources that behave like both sources/loads.
- Small capacity in early stages would be far from matching the capacity of the actual powerplants and the early adopters should be sponsored, by the operators, in order accelerate the process of adoption and testing.
- The SoC, when the owner needs his vehicle, cannot be affected by all these services; this means that vehicles can be bypassed and a lost in regulation capacity must be managed.
- Standards in the interconnection between car and grid should be able to overcome the problems relative to many different configurations of batteries, chargers and inverters.
- The grid topology must be optimized to control the new bidirectional flows and complex strategies.

3.1.1) Peak shaving and Load levelling

These two are similar services, because both store energy during low demand phase and supply energy into the grid during a high demand phase, nevertheless with different targets:

- In “peak shaving” the main target is to act smoothing the peaks whenever they start
- In “load levelling” the whole trend is considered and the target is to reach a nearly constant load curve (reducing the effect of high/low peaks)

Peaking power plants operate only during times of peak demand, caused by diffused and intensive air conditioning, cyclic demand peaks in different hours of the day... Typical peaking power plant should start up a few hours before the foreseen peak (scheduling and dispatch) and shut off a few hours later (their activity it's well represented in figure 3.3).

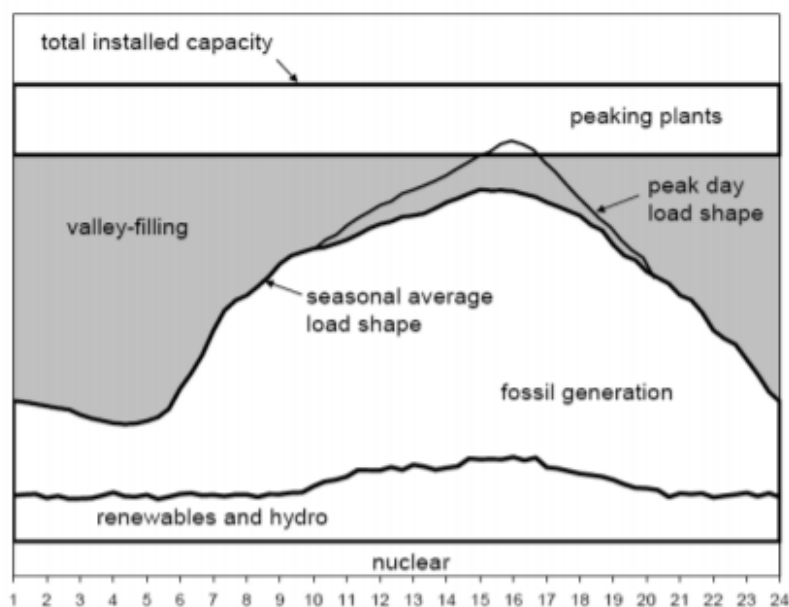


Figure 3.3: Peak shaving and valley filling between system capacity and system load

The classical architecture of these plants includes hydroelectric and gas turbine power plants.

Instead, load following power plants run during the day and early evening curtailing output power during the night and early morning, when the demand for electricity is the lowest.

Time of operation depends on numerous factors:

- Efficiency converting fuel into electricity (The most efficient plants are activated first)
- Status of the electrical grid in that region and base load generating capacity
- Variation in demand
- Variations in the periods of the year and in days of the week

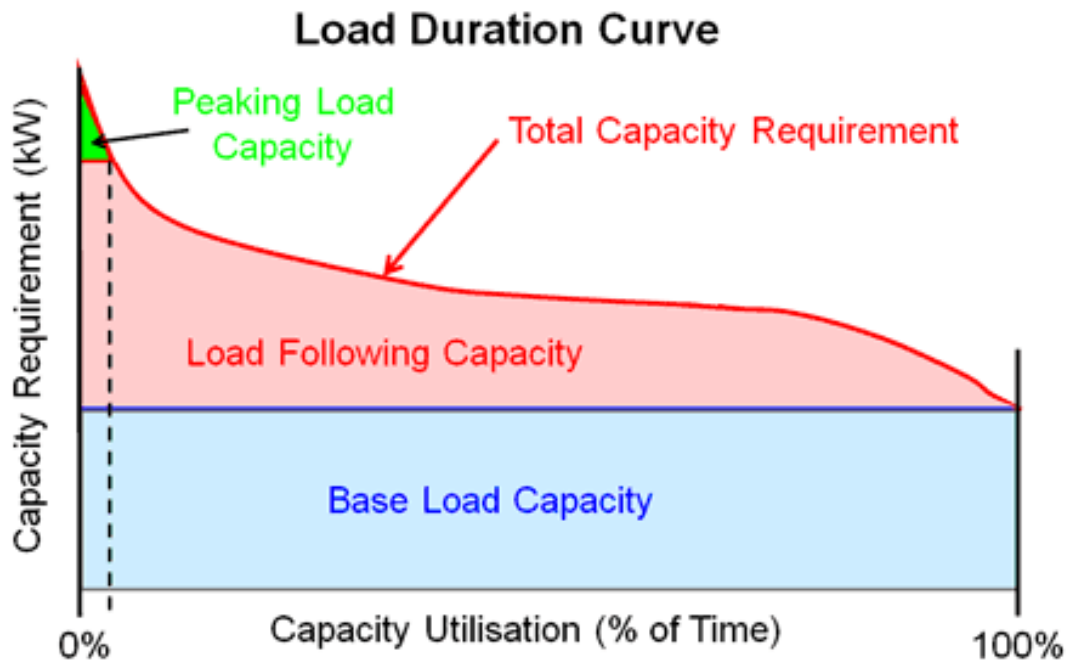


Figure 3.4: Load following capacity [33]

In figure 3.4 it's possible to see the deep differences between peaking capacity and load following capacity: these two services differ in the amount of energy and power deployed but moreover in the utilization period. Compared with other peak-shaving and valley-filling methods, V2G can be a more economical and effective solution, with the added advantage of rapid response to the grid-demand variations [29][32][5].

In highly industrialized realities the peak demand can assume values as high as 50% of the average demand, with V2G technology it's possible to reduce the cost of such services taking advantage by the intrinsic fast-response of the grid connected EVs with a more efficient control based on the grid-demand variation.

The price for kilowatt-hour in different periods of the day and for charge or discharge, can be an available index to control peak shaving or valley filling (figure 3.5).

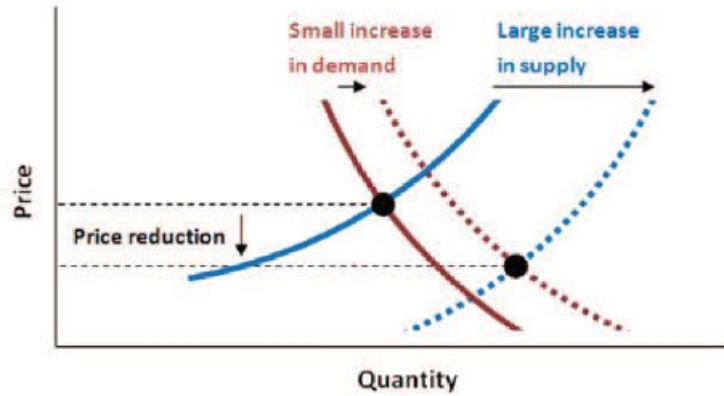


Figure 3.5: Relationship between price and energy supply [39]

This implies also costs and a complex layout of the “smart chargers” that must be able to connect bi-directionally the EVs but also have to control a flow of data in order to coordinate the vehicles and the grid status, all considering a set of constraints related to the battery architecture and characteristics and, moreover, requirements of the EVs owners that should not be worried about the performance variations (in terms of range and readiness) of their cars.

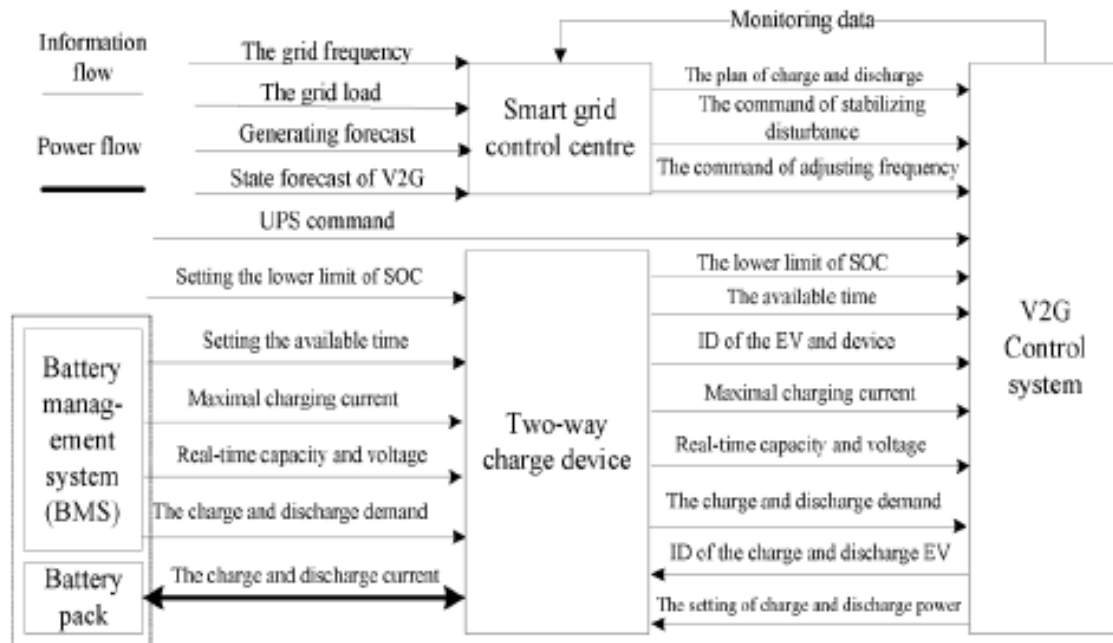


Figure 3.6: ICT systems in V2G applications [29]

A control centre or an aggregator should exploit these communication channels, and the relative information flow, to optimize the energy distribution acting on each single EVs connected but, of course, considering also the vehicle status, then “speaking” with the Battery Management System installed on the vehicle: for this purpose, a complex scheme of communication channels and control devices are necessary (figure 3.6).

Through statistical data, extrapolation and predictive models, it’s possible to get load curves in order to forecast the demand and to pre-set a control strategy, taking into account the randomness of the EVs connected: for this reason, a redundancy in the number of active vehicles connected to the grid is necessary and should guarantee a reliable service (high penetration level of BEVs/HEVs is mandatory).

3.1.2) Frequency regulation

Frequency control, often called “regulation”, it’s compose by several different, but cooperating, methods to achieve a nearly constant and ideal grid frequency value; among these methods there are so-called ancillary services, provided by users to the network. The scope of the regulation is to maintain grid frequency within a specific range and deviations are mainly caused by the mismatch between electric generation and load demand.

Regulating reserves of active power are automatically supplied whenever the grid is affected by a deviation in frequency and also regulation down must be feasible.

Three levels of controls are used to maintain the balance between load and generation [34][39]:

- Primary frequency control: local automatic control (frequency-responsive) that modifies the generation and the consumption (controllable loads) counteracting frequency deviations (limits and stops frequency excursions) i.e. in case of generators outages.
- Secondary frequency control: centralized automatic control that regulates the active power production of the generating units (in coordination) bringing back the frequency, already deviated, to the nominal value.
- Tertiary frequency control: generators are manually regulated to restore the primary and secondary frequency control reserves and to manage congestions in the transmission network.

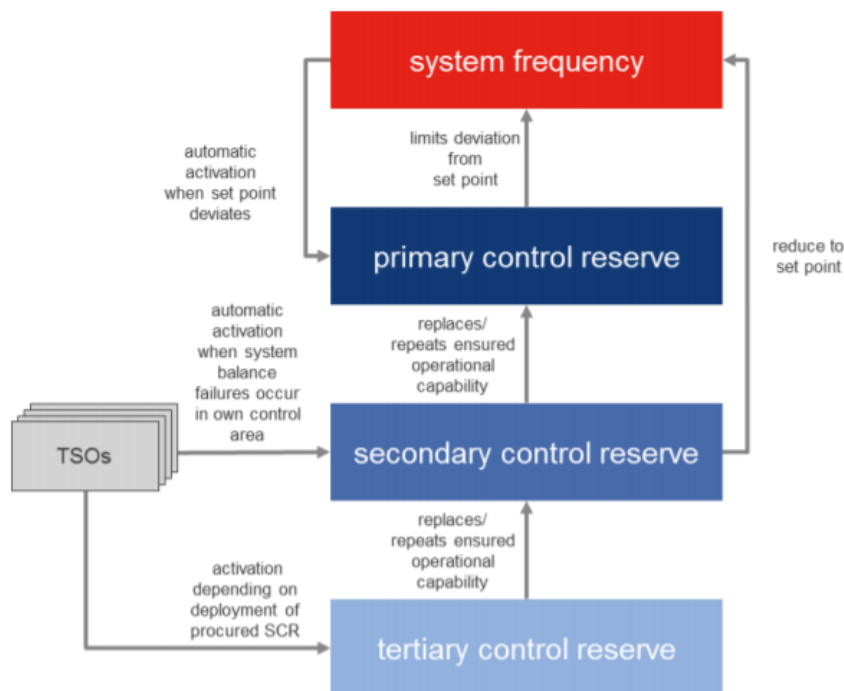


Figure 3.7: Representation of the different levels of frequency regulation [30]

The main factors characterizing different types of regulation are “deployment start” that describes the maximum delay between the TSO request and the beginning of the frequency control service, the “full availability” that instead describes the time necessary to pass from zero to full delivery and finally the “deployment end” describing the maximum time that a service can be continuously provided. These three main characteristics and their declination in the different regulation levels are represented in figure 3.8 with the response of the grid frequency.

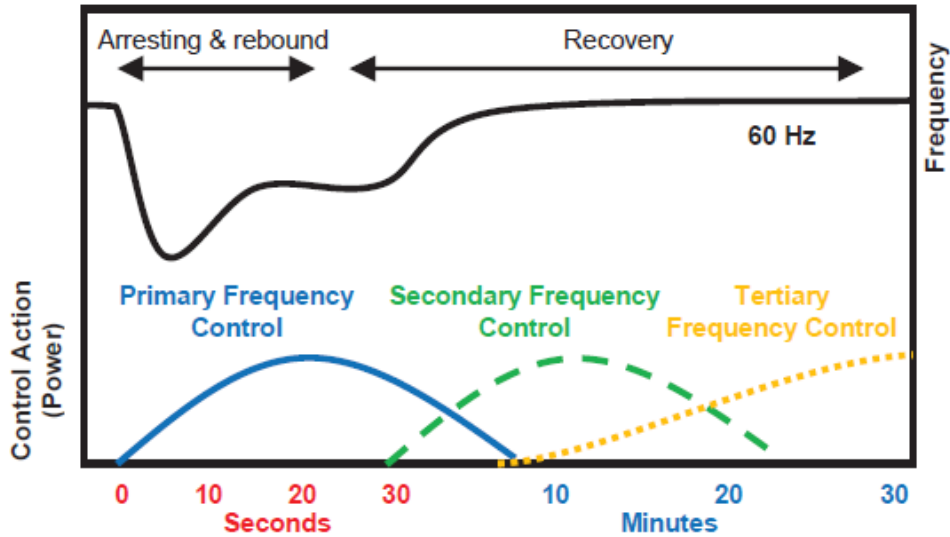


Figure 3.8: Primary, Secondary and Tertiary frequency control with respect to the activation time [39]

At this point it's necessary to establish a clear definition of the so-called spinning reserves [35]:

“the spinning reserve is the unused capacity which can be activated on decision of the system operator and which is provided by devices which are synchronized to the network and able to affect the active power”

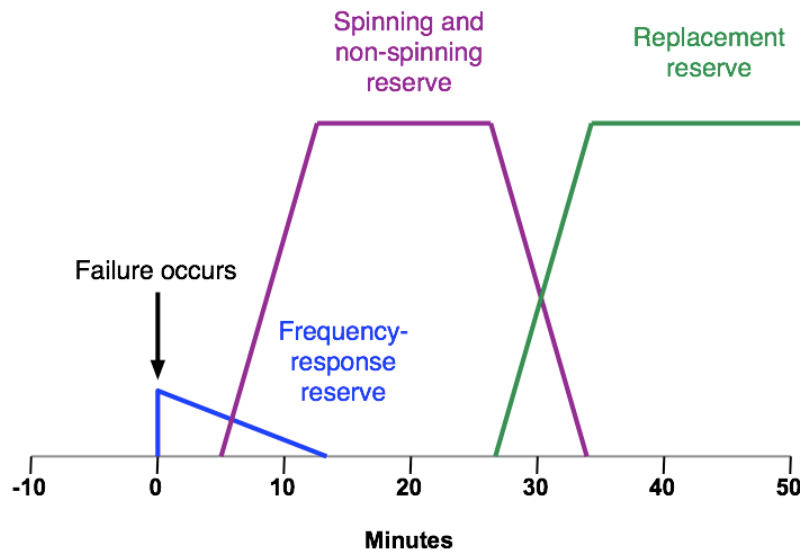


Figure 3.9: Spinning and non-Spinning reserves and their temporal activation [40]

In figure 3.9 there is another classification to identify the on-line capacity, more than the load demand, sufficient to cover the loss of the largest generating unit plus a safety margin; to ensure the right level of safety margin it's necessary to consider several major aspects:

- The variability of new renewable sources requires a higher safety margin.
- Spinning reserves should be distributed over numerous generators.
- Generators have limits on the rate at which they can increase output

Growing diffusion of renewable sources (PV, WT...) with highly intermittent generation, cause of unbalancing transient and oscillations in the available power.

In [36] and [37] has been proposed a distributed control strategy based on DC-link voltage sensing for small installations: the variation of the DC voltage is considered in order to choose the operating mode; this simple control allows the best utilization of DERs for charging PHEVs and EVs reducing the intrinsic intermittent behaviour and optimizing the energy flows management.

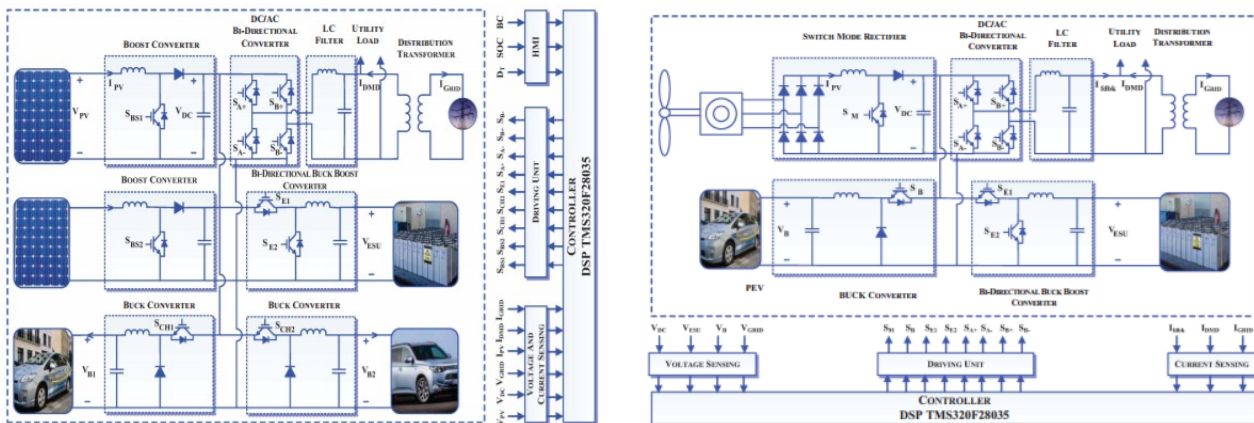


Figure 3.10: Layouts to promote the integration of photovoltaic/wind turbines with BEVs [36][37]

These reserves must be “frequency-responsive”, then effective with full capacity in few seconds/minutes and synchronized to the grid to maintaining the system frequency as close as possible to the nominal value: this is feasible exploiting the EVs batteries achieving very good performances.

Furthermore, the owner could be paid for the whole time the vehicle remains connected, to reward its reserve potential in case of generator failures (availability).

Again, the challenge is to assure the adequate redundancy, facing random connections and disconnections over many points of the grid: this could lead to an insufficient capacity in case of necessity.

These factors are subjected to many variations considering different geographic locations and their directives. It's then finally important to highlight the difference among the approaches of different states and the different standards with different procedures and terminology [34], should be necessary to take into account these characteristics during the design process of new technologies.

	Primary frequency control reserves	Secondary frequency control reserves	Tertiary frequency control reserves			
PJM [33]	Frequency response	Operating reserve				Reserve beyond 30 min
		Regulation	Primary reserve		Secondary reserve	
			Spinning reserve	Quick start reserve		
CAL [16]	(no name)	Operating reserve			Replacement reserve and supplemental energy	
		Regulating reserve	Contingency reserve			
		Spinning reserve		Non-Spinning reserve		
DE [20]	Primärregelreserve	Sekundärregelreserve	Minutenreserve		Stundenreserve and Notreserve	
FR [19]	Réserve primaire	Réserve secondaire	Réserve tertiaire			
			Réserve tertiaire rapide 15 minutes		Réserve tertiaire complémentaire 30 minutes	Réserve à échéance ou différée
ES [34],[35]	Reserva primaria	Reserva secundaria	Reserva terciara			
NL [28]	Primaire reserve	Secundaire reserve	Tertiaire reserve			
BE [17]	Réserve de puissance pour réglage primaire	Réserve de puissance pour réglage secondaire	Réserve de puissance pour réglage tertiaire			
GB [22]	Operating reserve	(does not exist)	Operating reserve		Contingency reserve	
	Response		Regulating reserve	Standing reserve	Fast start	Warming and hot standby
	Primary Secondary High frequency					
SE [36]	Frekvensstyd Normaldriftsreserv and Störningsreserv	(does not exist)	Seven different types of reserves			
AU [13],[14],[15]	Contingency services	Regulating services and network loading control	Short-term capacity reserve			
	Fast Slow Delayed					
NZ [30]	Instantaneous Reserves	Frequency regulating reserve	(no name)			
	Fast Sustained Over frequency					

Figure 3.11: Comparison of the different terminology of different regulation levels in different countries [34]

Looking at figure 3.11 it's possible to highlight that the same regulation roles are sometimes called with different names passing from a national power system to the others. There are also differences in the number and in the typologies of the services (i.e. secondary frequency control reserves do not exist in the GB power system).

In figures 3.12 and 3.13 there is a technical comparison among primary and secondary frequency control services in different countries; tertiary control is not included being out of the possibilities of V2G applications.

Technical Comparison of Primary Frequency Control Parameters in Various Systems								
	NERC	UCTE	DE	FR	ES	NL	BE	GB
Full availability	No rec.	<30s	<30s	<30s	<30s	<30s	<30s	<30s
Deployment end	No rec.	> 15 min	>15 min	> 15 min	> 15 min	> 15 min	> 15 min	> 30 min
Frequency characteristic requirement	10 % estimated yearly peak	20,570 MW/Hz	~4,200 MW/Hz	~ 4,200 MW/Hz	~ 1,800 MW/Hz	-740 MW/Hz	-600 MW/Hz	~ 2,000 MW/Hz
Droop of generators	5 % in 2004; no rec. anymore	No rec.	No rec.	3-6%	< 7.5 %	5-60 MW: 10 % >60 MW: 4-20%	No rec.	3-5%
Is an adjustable droop compulsory?	No rec.	No rec.	Yes	Yes	No rec.	>60 MW: Yes	No	Yes
Full deployment for or before a deviation of:	No rec.	± 200 mHz	± 200 mHz	± 200 mHz	± 200 mHz	70% for ±50-100 mHz	± 200 mHz	+/- 500 mHz

Figure 3.12: Technical comparison of Primary Frequency control parameters in different systems [34] [35]

Technical Comparison of Secondary Frequency Control Parameters in Various Systems							
	NERC	UCTE	DE	FR	ES	NL	BE
Deployment start	No rec.	<30s	Immediate or <5 min	<30s	No rec.	30 s-1 min	<10s
Full availability	No rec.	< 15 min	<5 min	<430 s or <97 s	<300-500 s	< 15 min	< 10 min
Deployment end	No rec.	As long as required	As long as required	As long as required	> 15 min	> 15 min and as agreed	As long as required
Control organisation	No rec.	No rec.	Pluralistic	Centralised	Hierarchical	Pluralistic	Centralised
Measurement Frequency	T<6s	T: No rec.	T = 1s	T=1s	T = 2s	T = 4s	T: Variable
Exchanges	T<6s	T<5s	T=1 s	T=10s	T = 4s	T = 4s	T: Variable
Controller cycle time	<6s	1-5 s	1-2 s	5 s	4 s	4 s	5 s
Controller type	No rec.	I or PI	PI	I	P or PI	PI	PI
Proportional term	No rec.	0-0.5	Unknown	0	Unknown	0.5	0-0.5
Integral term	No rec.	50-200 s	Unknown	115-180s	100 s	100-160s	50-200 s
K-factor (ACE)	The frequency characteristic	110% of the frequency characteristic	Unknown	Unknown	Unknown	900 MW/Hz	-660 MW/Hz

Figure 3.13: Technical comparison of Secondary Frequency control parameters in different systems [34] [35]

Multiple levels of frequency control.

Trying to minimize the detrimental effect on the battery, due to additional charge and discharge cycles, first frequency regulation will be studied and results of different simulation in V2G will be presented.

Powerplants base the power generation on locally-sensed grid frequency and usually have slow transient during output power variation reducing the efficiency of the regulation [38].

Optimal regulation implies fast-response variation of the generated power above and below a baseline value: looking at figure 3.14 these fluctuations have approximately zero net energy variation over the whole operation time (no battery discharge), for this reason V2G applications seem to be well suited if implemented with a bi-directional charger (there is not an effect on the available range and very low energy is exchanged).

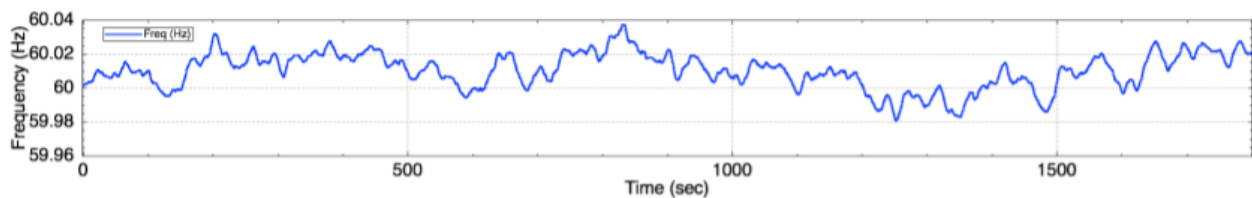


Figure 3.14: Frequency oscillations around the nominal value (60 Hz) [38]

To optimize the operations and to obtain an adequate power capacity, an aggregator should be created and directly controlled by the grid operator as depicted in figure 3.15.

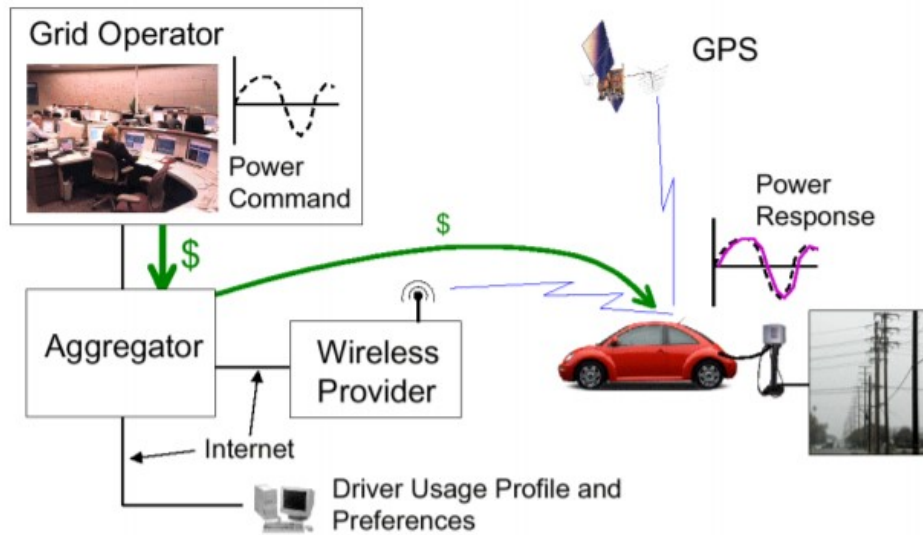


Figure 3.15: communication layout between grid operator, aggregator and BEVs [28]

In order to avoid deep discharge, regulation must not be extended for long periods thus specific strategies must be applied: this scenario is not common in first frequency control, usually lasts for second or few minutes, while in secondary frequency control could be necessary a longer activity and then specific limits. In the next pictures (figures 3.16 and 3.17) there are two examples of regulation, one with a classic hydro power plant and the second with V2G approach:

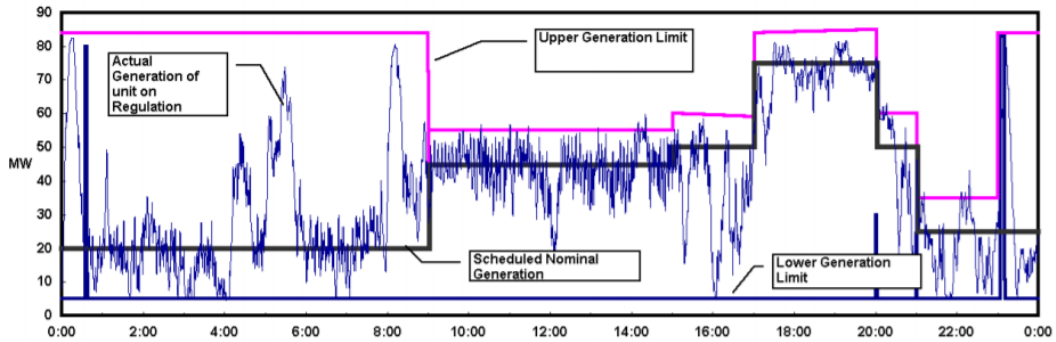


Figure 3.16: Frequency regulations UP and DOWN [28]

EVs performing frequency regulation should have null net energy exchange close to zero due to symmetric limits both up (battery discharging) and down (battery charging).

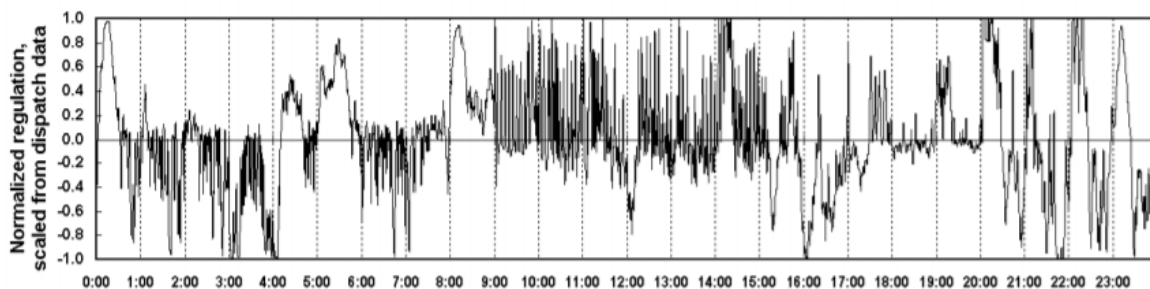


Figure 3.17: Frequency regulation performed using V2G [28]

There are several clear deployment issues [28]:

- Aggregator receives grid status information by the EMS (high amount of data exchanged due to very short update intervals) and detailed EVs status to select the available vehicles respecting several constraints; for this reason, an upgrade of the communication system it's required.
- The required power capacity (comparable to that of the traditional power plants) it's much more than the achievable power, furthermore in the early stages of deployment, this is an obstacle to the integration of first vehicles participating to the regulation (figure 3.18).

Power Generation Type (Assumes 33% Peaker Dispatch)	Generation Capacity (MW)		
	WECC	SMUD	$C_f, Total$ F.R.
Steam – Coal & Other	43,150	N/A	432
Hydropower	61,277	688	29,686
Combined Cycle Gas Turbine	41,489	837	415
Steam – Nuclear	9,463	N/A	95
Steam – Gas	19,496	N/A	195
Simple Cycle Gas Turbine	17,746	158	5,856
Wind	7,434	102	N/A
Internal Combustion Engine	1,172	6	12
Solar	526	155	N/A

Figure 3.18: Frequency responsive capacity subdivided among different sources in WECC and SMUD markets [39]

- EVs connected to the smart grid, should not be part of the regulation service in case this would lead to a problem for the owner: under a limit SoC value, depending by many factors, the vehicle should be considered offline by the aggregator.
- Robust and widespread standards should assure the correct coordination of many different vehicles and their equipment.

Finally, in [38] a frequency responsive EVSE is proposed to perform primary regulation, this device measures the local grid frequency with a resolution of 10 μ Hz and an update interval of 1 second adjusting the charging rate on the basis of the deviation from the target value of 60 Hz.

This configuration has several advantages:

- Eliminate need for communication
- Fastest reaction
- Low cost modification to EVSE

The simulation results showed that such a regulation can provide characteristics similar to the conventional solutions but with higher efficiency and faster response and then it's particularly appealing for V2G applications. Secondary frequency control deserves to be further studied: current market prices are similar but the market demand is expected to grow.

In secondary frequency control, labelled as Automatic Generation control (AGC) in [39], independent grid operators (ISO) manage different control areas tuning continuously the balance between power generation and consumption.

These operators must be synchronized with on-line generators and, analysing a signal called Area Control Error (ACE), regulate the power capacity (ramp up and down) to assure the frequency target under real time control as reported in figure 3.19.

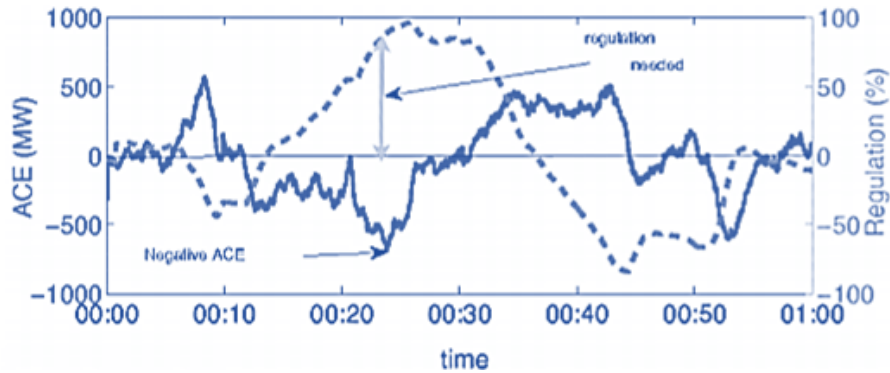


Figure 3.19: Secondary Frequency control through the analysis of ACE signal

To conclude both primary and secondary regulation can be improved through the implementation of a wide and extended network of V2G-enabled vehicles and chargers: this configuration could be particularly convenient in primary frequency control because the performance of a BEV, in terms of time to respond and time to reach the full availability of the service, are much higher than those of the actual regulation methods. Nevertheless, it's necessary to consider the complex communication system necessary to activate and coordinate each vehicle.

In secondary frequency control the structure would be centralized and less complex but, the larger regulating periods in which the vehicle is supplying the service to the grid, would lead to higher periods in which the vehicle should be connected to the grid without being used by the owner, higher energy exchange and then higher battery degradation and finally higher minimum bid amount to activate the service (figure 3.20).

	PCR	SCR	TCR
tender period	weekly	weekly	daily
tender time	as a rule on Tuesdays (W-1)	as a rule on Wednesdays (W-1)	as a rule Mo-Fri, 10 a.m.
product time-slice	none (total week)	peak: Mo-Fri, 8 a.m. to 8 p.m., without public holiday off-peak: residual period	6 x 4 blocks of hour
product differentiation	none (symmetric product)	positive / negative SCRL	positive / negative TCR
minimum bid amount	1 MW	5 MW	5 MW (submission of bid for a block of max. 25 MW possible)
increment of bid	1 MW	1 MW	1 MW
call for tender	capacity price merit-order	energy price merit-order	energy price merit-order
remuneration	pay-as-bid (capacity price)	pay-as-bid (capacity price and energy price)	pay-as-bid (capacity price and energy price)

Figure 3.20: Detailed description of the characteristics of regulation reserves in Germany [30]

3.1.3) Reactive power compensation and Voltage control

Reactive power transmitted into the grid it's a consequence of AC systems and the passive components inside the network: this power is exploited to build up magnetic fields (capacitors) and electric fields (inductors); this fraction of the transmitted power cannot be exploited by the users but is paid to the distributor.

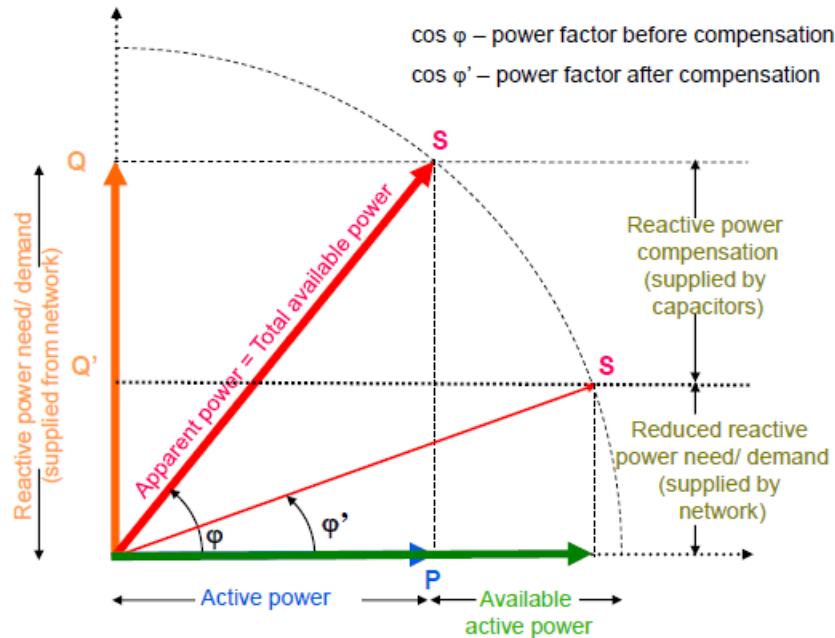


Figure 3.21: Reactive power compensation concept [31]

Correcting the power factor (ideally should be equal to 1), as can be seen in figure 3.21, could directly affect the cost of the electric power for factories, buildings, local networks...

Through the capacity of BEVs and the bidirectional power converters inside the chargers would be possible to reduce the phase gap between current and voltage of the grid.

Among the benefits in power compensation:

- Reduced network losses
- Avoided penalties for excessive consumption of reactive power
- Reduced necessity in equipment development/upgrade/expansion
- Improved voltage regulation capability and power availability

Reactive power injection can be used to compensate voltage drops, this compensation must be provided close to the loads and it's suitable to distributed energy sources like in case of BEVs connected to the grid.

Shunt compensation of reactive power can be employed either at load level, substation level or at transmission level (figure 3.22).

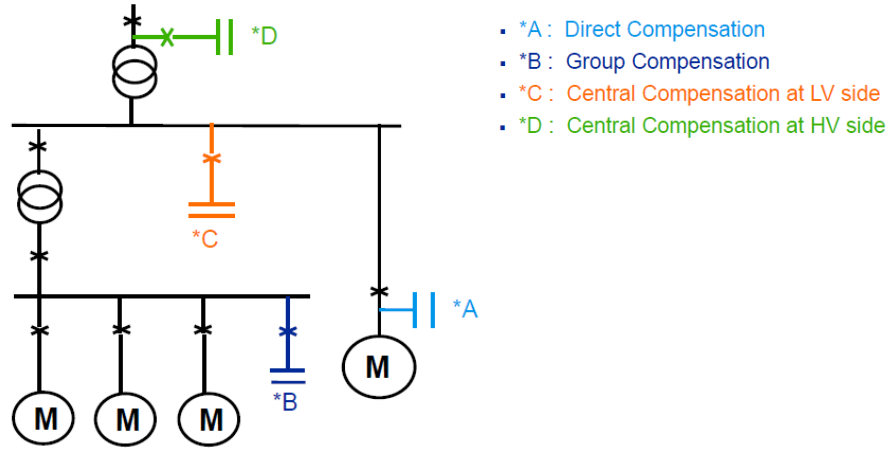


Figure 3.22: Different levels of reactive power compensation [31]

Also this time it's possible to subdivide three different levels of the service:

- Primary voltage control, that is local automatic control maintaining tuned the voltage sensing a determined bus (traditional solutions are Automatic Voltage Regulators and STATCOMs).
- Secondary voltage control, is a centralised automatic control coordinating many local regulators in order to inject reactive power in regional voltage zones.
- Tertiary voltage control, refers to manual optimization and regulation of the injected power in the whole power system.

A comparison among different applications should be done considering the configuration of the surrounding network, for this reason it's better to compare the requirements in terms of available reactive power to control the voltage.

POD is the point of delivery, considered as the point of the compensation provider nearest to the transmission network and can be used to compare the different requirements at the terminals.

Reactive power absorbed by auxiliaries, step-up transformer, and transmission line until the POD is usually around 15% of the nominal apparent power, then the power from the generator is estimated as:

$$Q_{\text{POD}} \approx Q_{\text{Stator}} - 0.15 \times S_n$$

Reactive power requirements are evaluated from the dimensioning voltage (U_{dim}), that is the actual average voltage at which the generating unit is connected, or for the nominal voltage of the network (U_n).

In the considered survey, the two voltage values are considered equal while the possible reactive power/voltage pairs are given by the U/Q diagram of the unit, case by case.

In primary voltage control, the deployment time should be equal to zero and the service should operate continuously keeping the voltage as near as possible to the nominal value and improving the stability of the system (together with the voltage controller parameters).

In figure 3.23, being impossible to compare P/Q diagrams, are reported maximum power requirements for the nominal active power delivered.

Reactive power connecting conditions, reported in the analysis, do not mean that one system uses more or less reactive power than another, TSOs can contract for additional reactive capabilities or use some of their own reactive power sources.

Technical Comparison of Voltage Control Parameters in Various Systems						
	DE	FR	ES	NL	BE	GB
Absorption capability requirement (lagging)	pf=0.95 or 0.975 at the POD for Pn and Un	-0.35*Pn at the POD for Pn and Udim	pf = 0.989 at the POD for Pn and Un	pf = 0.8 at the POD for Pn and Un	-0.10*Pn at the POD for Pn and Un	pf = 0.85 at the terminals for Pn
Production capability requirement (leading)	pf = 0.925 or 0.9 at the POD for Pn and Un	0.32*Pn at the POD for Pn and Udim	pf = 0.989 at the POD for Pn and Un	pf = 0.8 at the POD for Pn and Un	0.45*Pn at the POD for Pn and Un	pf = 0.95 at the terminals for Pn
Estimated absorption requirement at the POD for Pn and Un	-0.33*Pn or -0.23*Pn	-0.35*Pn	-0.15*Pn	-0.75*Pn	-0.10*Pn	-0.80*Pn
Estimated production requirement at the POD for Pn and Un	0.41*Pn or 0.48*Pn	0.32*Pn	0.15*Pn	0.75*Pn	0.45*Pn	0.17*Pn

Figure 3.23: Technical comparison of voltage control parameters in different systems [34]

The basic or mandatory reactive energy service (described in figure 3.24) includes the requirements that the production units must meet to be connected to the network. Enhanced Reactive Power Service is a non-mandatory service that is provided based on basic requirements. The terminology of voltage control is much more uniform than frequency control and it is not necessary to discuss it further.

Characteristics of the Markets for Basic Voltage Control Ancillary Service				
	France	Great Britain	New Zealand	PJM
Type of market	Compulsory and bilateral contracts	Compulsory and tendering process	Compulsory and bilateral contracts	Compulsory
Frequency of the market clearing	Every two or three years	Every six months	No recommendation	Every year
Structure of remuneration	Fixed (€/month) + Availability (€/Mvar/h)	For each capability slice: Fixed (£/Mvar/h) + Availability (£/Mvar/h) + Utilization (£/Mvarh)	Fixed (\$/Mvar) + Availability (\$/Mvar/h) + Utilization (\$/Mvarh)	Fixed (\$/month) + Opportunity cost
Type of price	PBP	PBP or RP	PBP	RP
Price cap	None	Fixed: offer cap at 999.999 £/Mvar/h Availability: offer cap at 999.999 £/Mvar/h Utilization: offer cap at 999.999 £/Mvarh	None	None
Revision of the asked volume	As soon as the generating unit is connected	Every 6 months	Every half-hour	Unknown
Market creation	2000	April 1998	September 2004	September 1999

Figure 3.24: Market characteristics for basic voltage control ancillary service [34]

V2G could be particularly suitable to offer voltage regulation to the grid for several characteristics related to the technology already used with EVs and to further development:

- EVs are most of the time connected to the grid, also with full SoC, the availability it's a main feature that can be exploited, and then paid, by the grid operators.
- The battery is not affected by the exchange (absorption and supply) of reactive power with the grid.
- Chargers need passive components (capacitors and inductors) to filter the oscillations and distortions caused by AC/DC and DC/DC conversions, then converters and passive components can be exploited in the voltage control.

Of course, there are many developments that must be accomplished to enhance this service opportunity: the most important and studied is the adoption of bidirectional chargers in order to control four power quadrants in output.

Charger type	Active power operation	Reactive power operation
PFC unidirectional	Grid-to-vehicle charging	Limited ^a
Four-quadrant bidirectional	Grid-to-vehicle charging or Vehicle-to-grid discharging	Inductive or capacitive

Figure 3.25: Reactive power services deliverable with different chargers [41]

Then different levels of voltage regulation can be achieved with different charger's typologies (figure 3.25): from [41] resulted that also unidirectional chargers could deliver a certain amount of reactive power but with very low performance and introducing low-frequency current harmonics.

Looking at the picture 3.26 it's possible to see how an electric vehicle could be placed between the voltage conversion and the loads of the local network.

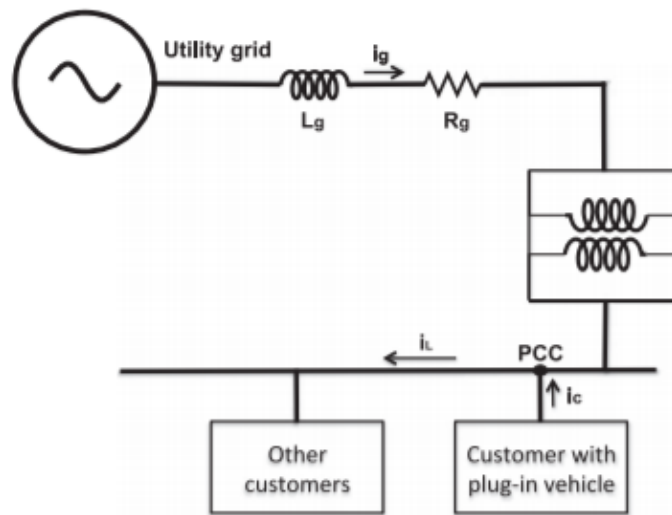
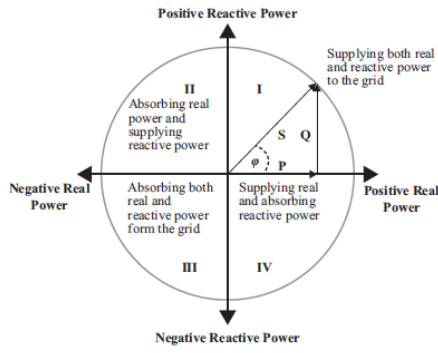


Figure 3.26: Possible configuration of power grid support using a BEV [41]

In figure 3.27 all the operation modes obtained in [41] with the adoption of a bi-directional charger are reported and can be seen how the voltage regulation can be achieved with both inductive or capacitive operations exploiting the high flexibility of the converter.

Studying the effects on grid side and on battery side [41], in different operation modes and using a common bidirectional charger, there are not evident drawbacks and additional losses are not significant.



#	P_s	Q_s	Operation Mode of the Charger
1	Zero	Positive	Inductive
2	Zero	Negative	Capacitive
3	Positive	Zero	Charging
4	Negative	Zero	Discharging
5	Positive	Positive	Charging and inductive
6	Positive	Negative	Charging and capacitive
7	Negative	Positive	Discharging and inductive
8	Negative	Negative	Discharging and capacitive

Figure 3.27: Operating region in the P-Q plane and available mode for a bidirectional charger [42]

The possibility to exploit all the four quadrants at the same power levels leads to the necessity to increase the size of passive components (especially the capacitors) and consequently the weight and cost of these devices: this significant result is obtained in [41] and an idea about the value of this over-sizing can be seen in figure 3.28.

Converter type	DC-link ripple current (120 Hz) and capacitance increase (for $L_c = 1.0 - 2.0$ mH)	
	3.3 kVA	6.6 kVA
Dual-buck	4.2% – 8.6% (total)	8.6% – 15.2% (total)
Half-bridge	4.2% – 8.6% (total)	8.6% – 15.2% (total)
Full-bridge	2.1% – 4.3%	4.3% – 7.6%

Figure 3.28: Capacitor increase for 100% reactive power compensation [41]

In [43] different setpoints, with different amount of active and reactive power supplied, are studied to get the best efficiency, performance and to set limits using two common bidirectional charger topologies (single and dual stage) considering three main operational scenarios:

- 1) Minimum Voltage Solicitations to minimize the voltage solicitations across AR and BDDC by setting Vdc at Vdc,m.
- 2) AR Current Rating Exploitation to fully exploit the AR current rating by setting Vdc at 3.55 Vg (This feature is attained at the expenses of voltage solicitations across AR and BDDC that are 1.3 times higher than with the first hypothesis).
- 3) Mixed Solution to make AR functioning at rated current during the CC stage of the battery charging, and under input voltage limitation during the CV stage (appears a good compromise between reactive power compensation and voltage solicitations across AR and BDDC).

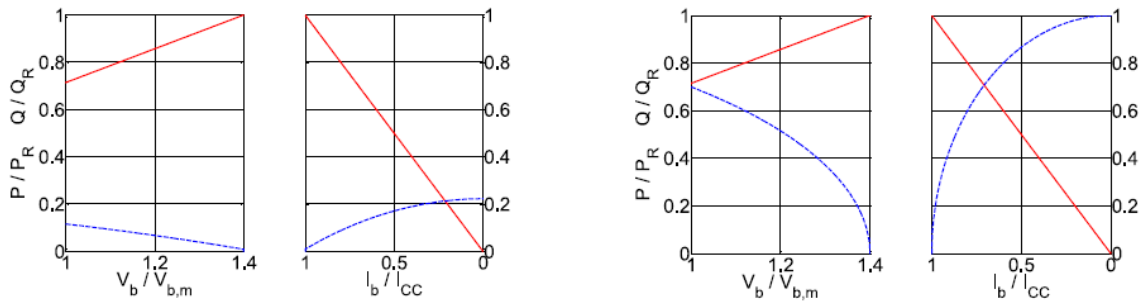


Figure 3.29: Active (RED) and Reactive (BLUE) power with Vdc=2.7Vg (left) and Vdc=3.55Vg (right) [43]

The maximum amount of reactive power that BBC is able to manage as a function of the state of charge of the battery has been calculated with the help of the phasor diagrams. Key operating points of BBC have been identified in the phasor plane in correspondence of the transition of the operation of AR embedded in BBC from rated current to input voltage limitation and vice versa.

Finally, it's important to recap the main assumptions and the derived results: adoption of bi-directional chargers seems to bring flexibility and potentiality to V2G applications; this technological choice would not affect the efficiency of the chargers but would affect price and complexity of these devices.

Nowadays the whole scenario is characterized by just unidirectional chargers and, before to start the technological upgrade, it's necessary to focus the attention on the economic feasibility considering both the higher initial investment and the value of voltage regulation services.

3.1.4) THD control

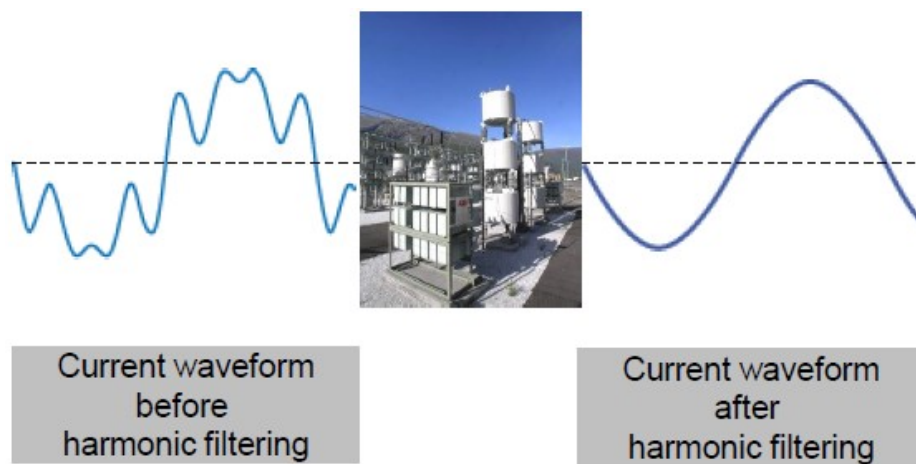


Figure 3.30: Schematization of the harmonic filtering process [31]

Harmonic currents are generated by the non-linear loads, like rectifiers, drives, converters; there are many advantages in filtering current signals mitigating this phenomenon:

- Improvements in control system, metering system and network protection reliability.
- Reduced grid losses, equipment overloads and stress.
- Reduced cost and outages with higher power availability.

Total Harmonic Distortion is the ratio of the energy in the output signal that is not related to the input sine tone and it's usually measured over a range of frequencies determining a value at each frequency of interest (calculating the RMS value over a frequency range or around the main harmonic).

$$\text{THD} = \frac{\text{Energy unrelated to Input}}{\text{Total Energy}}$$

The procedure to evaluate the THD index consists in putting a single frequency into a system, and measuring the output.

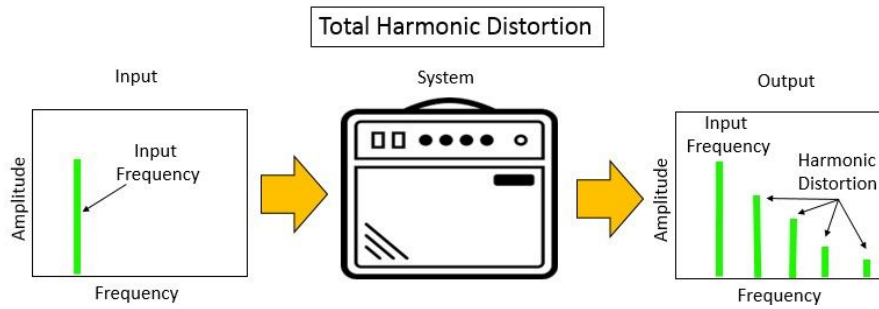


Figure 3.31: Difference between input and output signals

THD index can assume values between zero and one for each frequency tested:

- Values close to zero means that the output has low harmonic distortion (sine wave of the output has similar frequency content as the input).
- Values close to one means that there is a lot of harmonic distortion present in the signal (almost all the frequency content in the signal is not at the same frequency as the input signal).

In practice, there are differences in how THD may be calculated for a given spectrum. For some methods, only the energy at harmonics are considered. Sometimes the calculation is limited to first five or ten harmonics of the output signal. Other methods consider the total RMS of the output signal. These methods are sometimes designated as THD+N, because the noise between harmonics is included in the calculation. The N is short for noise.

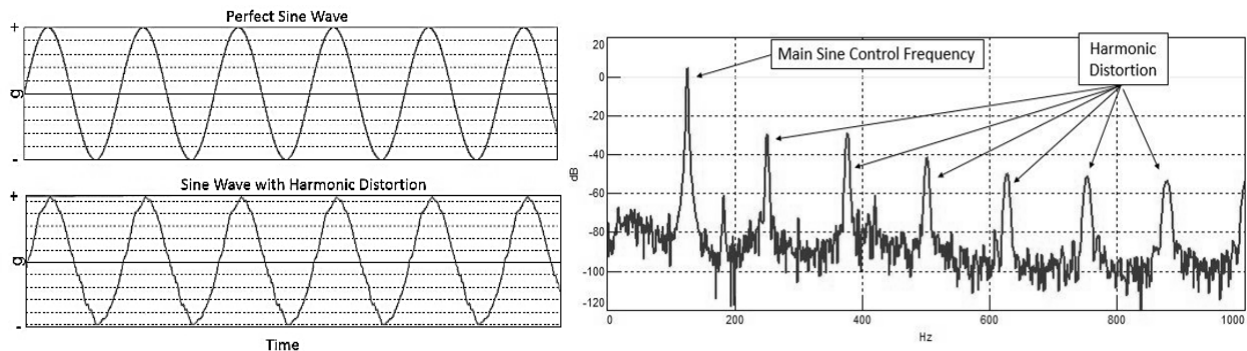


Figure 3.32: Deviation from the sine wave due to harmonic distortion and evidence in the spectrum analysis

An ideal sine wave has a single frequency in its spectrum, without harmonics. Harmonics are present when the sinusoidal vibration of the output does not replicate the pure sine wave of the input. Trying to control a system with a high THD can be difficult: typically, a single frequency is the input into the system with a controlled amplitude. High amounts of harmonic distortion create vibration at other frequencies, which are not controlled. This increases the vibration amplitude levels on the test object in an uncontrolled, and therefore, unpredictable manner. Low THD for unity power factor converters is achieved mainly through choosing an appropriate converter topology and precisely controlling the switches. There are three main methods to decrease THD if too high:

- Multi-level inverters, more than two voltage levels exist in the converter.
- Larger inductor, or additional filter elements, to decrease current ripple.
- Increase switching frequency, which is a trade-off between additional switching loss and THD.

The twelve pulses converter of HVDC network (figure 3.33) is a great source of harmonics in power systems [44]: to reduce the harmonics current PHEV park is connected at the converter terminal of HVDC as a virtual shunt active filter reducing harmonics from source to converter, where the harmonics current in source is higher than the load due to the use of virtual active filter.

Figure 3.33: grid active filtering through the connection of BEVs with bi-directional converters [44]

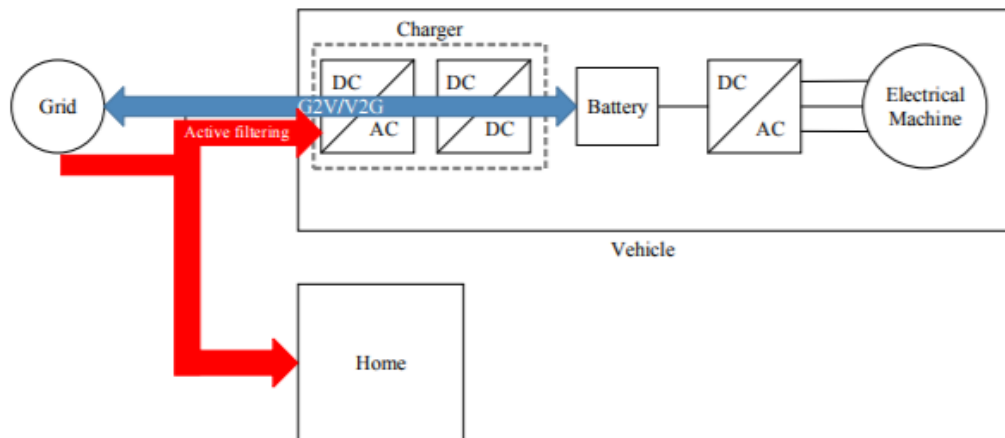


Figure 3.34: power flow between grid, vehicle and home [45]

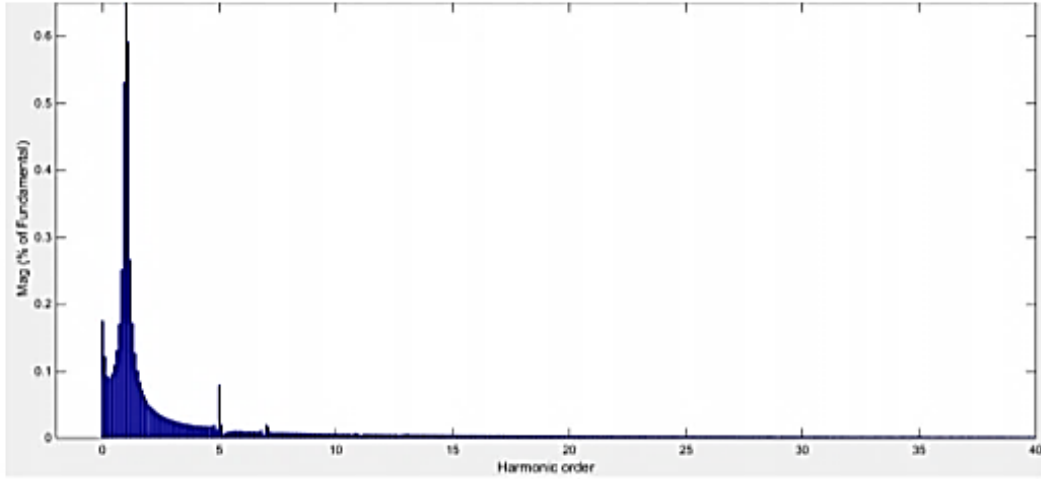


Figure 3.35: Current harmonic spectrum after the filtering process [45]

The charger ensures that the grid current is as much sinusoidal as possible and in accordance with IEEE 519 limits, which specifies the maximum permissible percentage of every current harmonic, this is clearly shown by the source current harmonic spectrum in Figure 3.35.

When the charger is operating as a shunt active power filter for the load, the grid current is in phase with the voltage demonstrating that the DC/AC converter acts as an active filter providing a unity power factor in addition to being able to regulate the DC link voltage to 700V (figure 3.36).

The shunt active filter is therefore able to eliminate a big part of the current harmonics and reduce the THD index so that it complies with the IEEE standards (the charger topology and control work well enough in: G2V, V2G and active filtering modes).

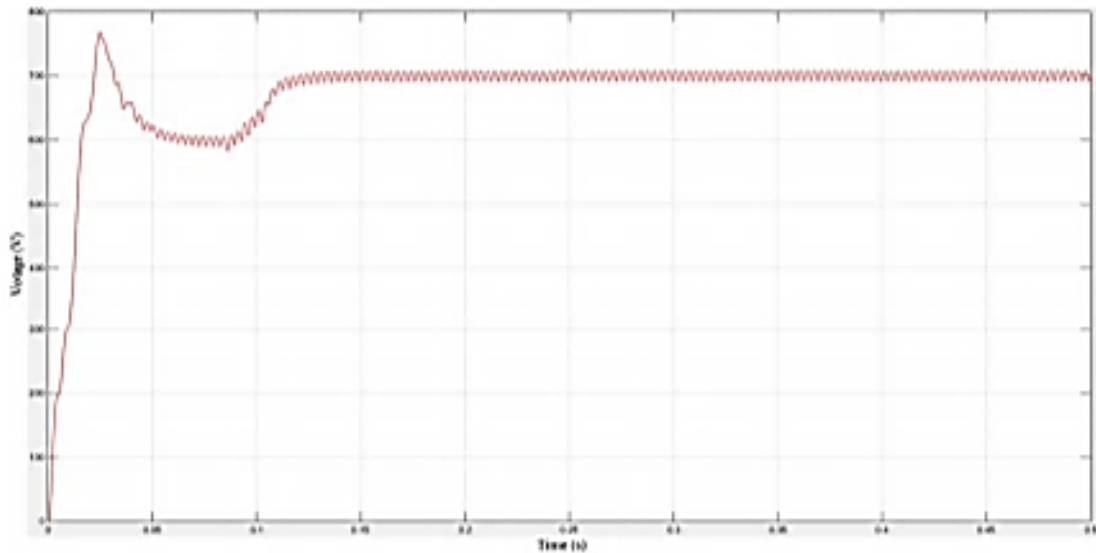


Figure 3.36: DC link voltage during active filtering [45]

3.1.5) Conclusion

System services	Base load	Peak shaving	First Frequency control	Second Frequency control
Description	Constant part of power demand	Fluctuating part of power demand	Quick power in case of outages	Power for frequency stabilization
Utilization time	24h/day	2-3h/day	Short	Very short
Utilization frequency	-	Daily	Low	High
Cost	Low	Moderate	High	High
General feasibility	Bulk power plant	Gas turbine	Quick power generators	Batteries
Feasibility of V2G	n/c	Higher battery degradation	Very good	Good

Figure 3.37: List of the most significant grid support services and their suitability with V2G [46]

V2G shows a lot of possibilities and alternatives to supply services to the grid; the possibility to inject active and reactive power into the grid, exploiting the On-Board capacity, could represent a key feature in the large scale adoption and diffusion of BEVs.

There are some major issues and requirements that will determine the success of this technology or will stop the development of this concept:

- 1) It's mandatory an evolution of the chargers that should be bidirectional in order to obtain the maximum degree of flexibility.
- 2) It's necessary to assure the minimum amount of stress on the battery during V2G services, this to avoid negative effects on the lifespan of the device and to allow the maximum economic benefit for the user.
- 3) It's necessary to establish a regulatory scenario that allows to promote such services: facilitating the new users to enter in the market and optimizing the management and communication systems.

As reported in figure 3.37 primary and secondary regulation methods should be furtherly investigated and also the characteristics of these two different markets will lead to the choice of a solution instead of the other.

Other services constitute a promising alternative: i.e. the compensation of reactive power would minimize the detrimental effect on the batteries but, as described before, could determine an increase in complexity and cost of the chargers and their control strategies.

3.2) EVs/PHEVs chargers: common topologies and standards

This chapter will describe the most diffused topologies, in the market and in technical publications, explaining the reasons under some choices and showing the possible developments.

The unidirectional chargers, today the most diffused technological solution, have several important advantages with respect to the bi-directional ones [47]:

- 1) Low complexity and costs (typically a diode bridge, a filter and a DC-DC converter in dual stage applications)
- 2) Easy control strategies
- 3) Reduced weight and volumes (particularly important in On-Board devices)

Such important aspects could represent an obstacle to the implementation of more sophisticated bidirectional systems.

Older studies [47] showed that it's physically possible to inject an amount of reactive power into the grid with the traditional unidirectional solutions: this is achieved by commutating the current flowing through the diodes. Nevertheless, the limited amount of phase difference introduced it's dependent on the configuration of the boost inductor and the performance cannot be easily improved.

There are also many other disadvantages that lead to research new technologies:

- 1) Low current harmonics introduction
- 2) Low power factor
- 3) High passive components oversizing
- 4) Compensation can be done just while charging (if SoC=100% it's not possible to compensate reactive power)

Furthermore, the possibility to get bi-directional power flows open the doors to many other ancillary services, for example the frequency regulation; in the next chapters will be described the most common solutions adopted today and the viable alternatives for the future, with a focus on the differences among them.

3.2.1) AC/DC and DC/DC converters

AC/DC converters:

These converters are the fundamental components that allow an interface between the grid and the battery: unidirectional single stage chargers are based on this type of converters.

In numerous studies [47][48][49][50][51] three common AC/DC topologies have been highlighted:

- Half -Bridge layout
- Full-Bridge layout
- Bridge-Less layout

Each configuration can be selected according some characterizing parameters: number of switches, stress on switches (voltage and current), passive components size (capacitors and inductors), low harmonic contents and highest power reachable.

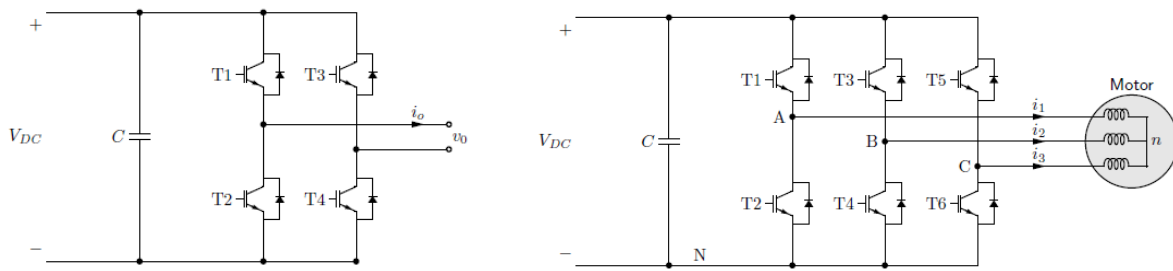


Figure 3.38: Four-quadrant Full-Bridge single/three-phase converters

Half bridge layouts are the simplest, the switches are directly facing the battery voltage (V_{dc}) and require two bulky and expensive capacitors also affecting the life expectancy.

Full-bridge single/three-phase converters (shown in figure 3.38) seem to be the most convenient layouts, the first for low output power (till 1.9 kW) and the second for higher power levels.

Among the advantages of these configurations:

- Lower current per switch (considering the same power each switch operates at half the current of the previous case) leading to lower switching losses with respect to the half bridge
- Higher efficiency for higher output power
- DC output voltage with a lower harmonic content (notch filter is still necessary)
- Simplest control and lower number of components with respect to other configurations

Among the drawbacks of these devices there is a larger number of switches and a low frequency harmonic content in the voltage leading to quality problems for the battery.

Increasing the power size of the charger, more complex and expensive solutions must be adopted: the stress on the switches must be reduced because is a limiting factor.

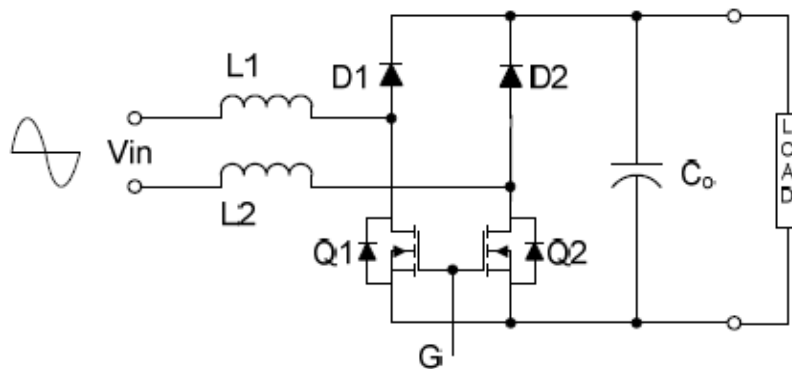


Figure 3.39: Bridgeless PFC boost converter [48][49][50]

To reach higher energy density and a high efficiency at the same time, the bridge it's a limit due to heat management difficulties [52]; bridgeless layouts offer the advantage to remove such critical component, in order to get higher charging power but with a negative effect in EMI and a complex circuitry.

The solution proposed in [52] it's called Bridgeless Interleaved boost converter (BLIL) and it's designed to achieve power levels above 3 kW with low EMI thanks to the interleaved topology: two MOSFETs and two fast diodes are necessary and then the cost increases (figure 3.39).

For level 2 charge in European and American automotive fields, two layouts are identified to supply power up to 8 kVA: BLIL (figure 3.40) and Bridgeless Interleaved Resonant PFC boost converter [51].

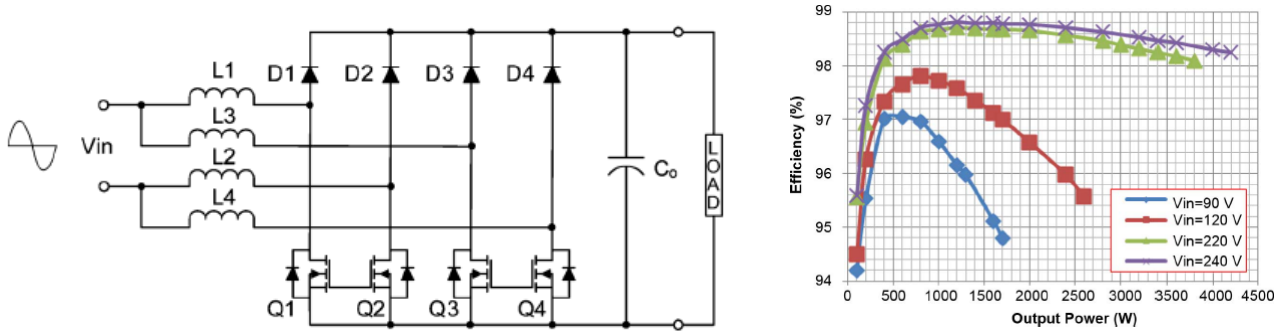


Figure 3.40: Bridge-less interleaved PFC boost converter and its efficiency with different input voltages [48] [49] [50]

In [51] further configurations are listed and their differences in terms of cost, complexity and performance are described:

- Multilevel PWM AC-DC converter
- Diode clamped converter
- Switched clamped converter
- Capacitor clamped converter

A single-stage charger it's an architecture in which there is just a single AC/DC converter (one of the previous mentioned topologies) directly interfacing grid and battery leading to different advantages:

- Simplest structures
- Lowest component count
- Reduced switching losses

Single stage topologies are mainly used for Level 1 charge, this can be a constraint in high power applications and in EVs, where the battery capacity increases drastically, the time required to reach 100% SoC could be inaccessible.

In dual-stage topologies a second device is interposed between grid and the vehicle to obtain a power factor correction and moreover to regulate the output dc voltage exploiting the possibility to recharge the battery at different charging levels.

Recapping the AC/DC stage controls the input currents (in case of three-phase grid) and the DC output voltage while DC/DC stage controls the current charging the battery. Almost whole the topologies presented in [53] are dual-stage, to supply the required output power necessary for automotive and V2G applications.

A fundamental limit that leads to the passage from single-stage to dual-stage architectures is explained in [43]: the choice depends on the minimum level of the battery voltage; the AC/DC output is connected, through a LC filter, to the battery:

$$V_u = \frac{V_{dc}}{\sqrt{2}\sqrt{3}} = \frac{V_{dc}}{\sqrt{6}}$$

Where V_u is the upper limit of the V_{rms} from the single-stage rectifier and must not be lower than V_{grid} then the minimum allowable value of V_{dc} is: ($k \geq 1$)

$$V_{dc,m} = k\sqrt{6} V_g$$

In most cases this condition is not satisfied and a second stage supplies to the inconvenience. Just to conclude it's possible to include the proposed solutions and the relative characteristics in the table of figure 3.41:

Topology	Conventional PFC boost converter	Phase shifted semi-bridgeless PFC boost	Interleaved PFC boost converter	Bridgeless interleaved PFC boost converter	Bridgeless interleaved resonant PFC converter
Power Rating	< 1 kW	< 3.5 kW	< 3.5 kW	> 5 kW	> 5 kW
EMI / Noise	Poor	Fair	Fair	Best	Best
Capacitor Ripple	High	Medium	Low	Low	Low
Input Ripple	High	Medium	Low	Low	Low
Magnetic Size	Large	Medium	Small	Small	Small
Driver	2 LS	2 LS	2 LS	2 LS	2LS+2HS
Efficiency	Poor	Best	Fair	Best	Fair
Cost	Low	Medium	Medium	High	Highest

Figure 3.41: Topologies comparison [48]

DC/DC converter

Looking at the second stage of a dual stage charger [6], classic dc/dc converters such as buck, boost and buck/boost topologies are commonly adopted.

- BUCK: when the required output voltage is lower than the input voltage, small number of components and low losses.
- BOOST: Increased number of switches and passive components' size; output voltage can be higher or lower than the input one.
- BUCK-BOOST: Negative polarity output achievable, small number of components but higher stress levels (high voltage ripples).

The more frequent solution, at least in unidirectional chargers, is the second one (figure 3.42):

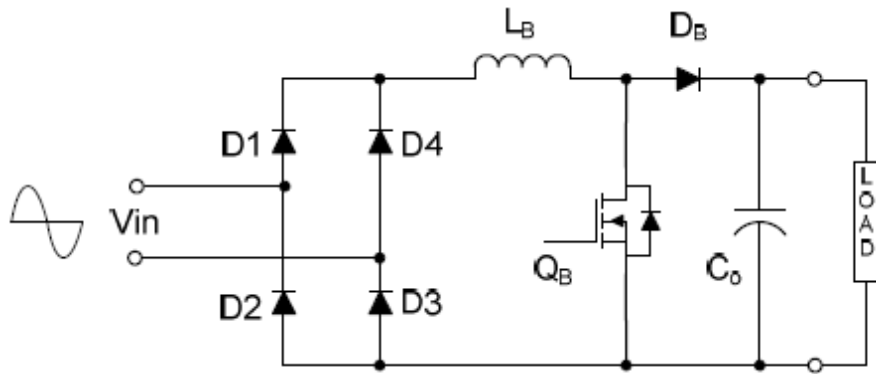


Figure 3.42: conventional Power Factor Correction boost converter [48]

But many other layouts offer different advantages:

- Interleaved solution (figure 3.43): Reduces the battery charging current, reduces inductors' size and the stress on the capacitors.

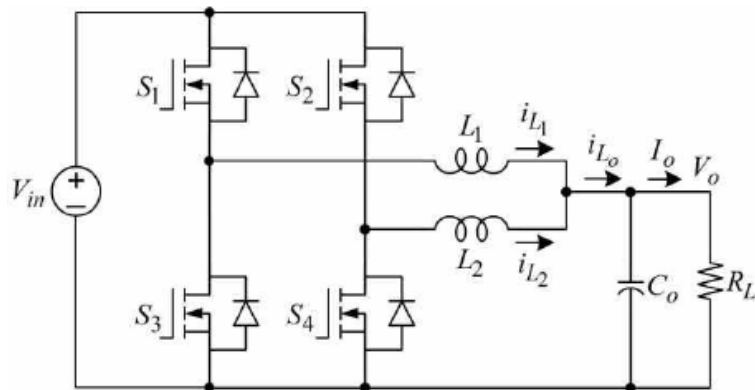


Figure 3.43: Interleaved layout

- Resonant solution (figure 3.44): Achieve a higher efficiency reducing switching stress and losses.

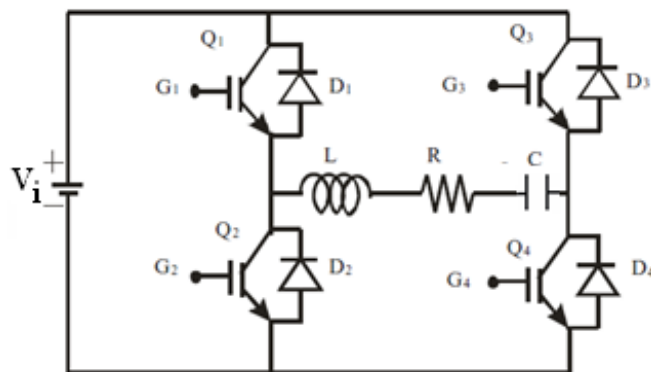


Figure 3.44: Resonant layout

- Zero Current Switching (ZCS represented in figure 3.45): Reduces size and weight (fundamental characteristics for On-Board device).

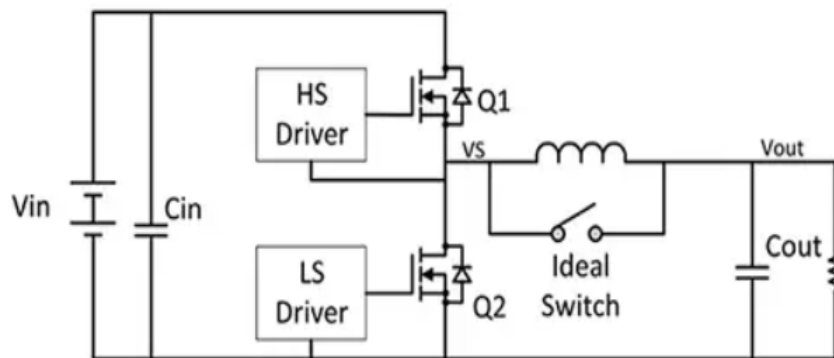


Figure 3.45: ZCS layout

- Zero Voltage Switching (ZVS represented in figure 3.46): Excellent efficiency vs power density trade-off.

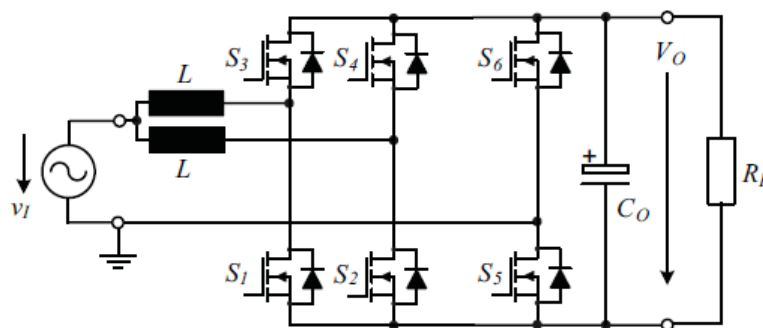


Figure 3.46: ZVS layout [54]

There are also less common topologies, sometimes including isolation characteristics, with a more complex circuitry and larger passive components:

- Fly-back converter (isolated)
- Push-Pull converter (isolated)
- CUK, SEPIC, LUO converters (not isolated)

Finally, some diffused dual-stage topologies for bidirectional converters from automotive chargers applications are reported from [51]:

- Full-bridge AC/DC + Two-Quadrant Buck-Boost
 - Popular on bi-directional On-Board chargers
 - AC/DC converter regulates the DC link voltage
 - DC/DC controls charging/discharging current
 - High DC link voltage ripple at twice grid frequency

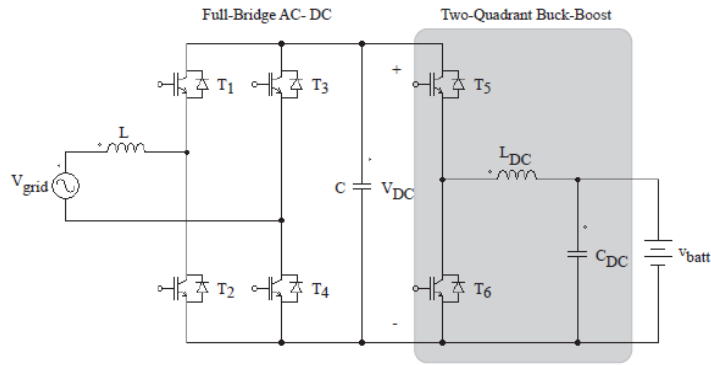


Figure 3.47: Bidirectional Full-bridge + Buck-Boost converter [51]

- Full-bridge AC/DC + Dual-Active Bridge DC/DC:
 - Allows to reduce the DC link capacitor
 - DAB for galvanic isolation (high power applications)
 - DAB controls DC link voltage
 - Full-bridge AC/DC regulates the current
 - Added cost for DAB but reduced cost of capacitor

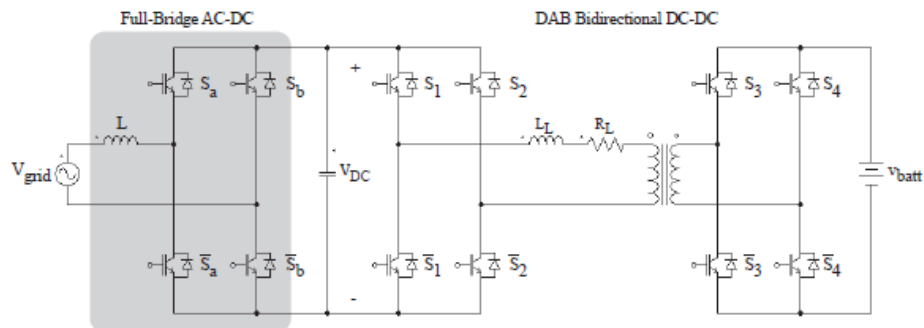


Figure 3.48: Bidirectional Full-bridge + DAB converter [51]

- Direct/Indirect Matrix converter (figure 3.49):

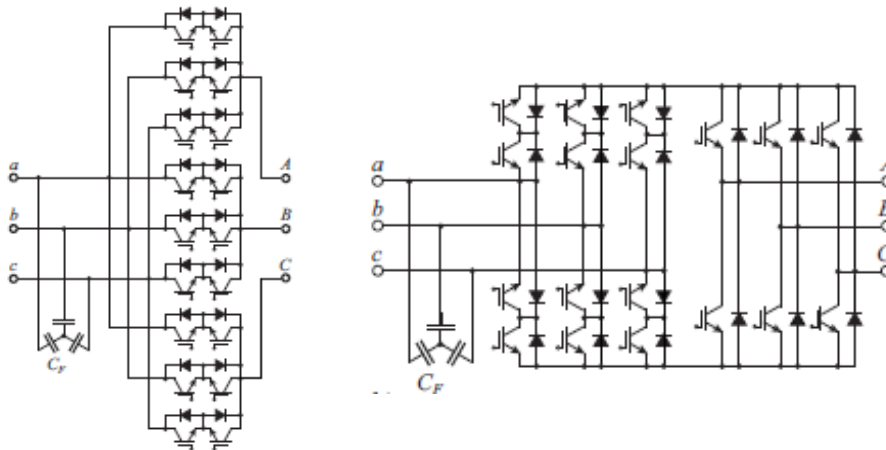


Figure 3.49: Bidirectional Direct/Indirect matrix converters [54]

3.2.2) On-Board vs Off-Board solutions

This further classification focuses the attention on the point in which the input power (AC single-three phase) from the grid is converted in a DC power suitable to charge the battery.

On-Board chargers face directly the voltage of the grid and manages the conversions (AC/DC and DC/DC), with embedded devices sized for the charging level defined by the manufacturer.

Off-Board charge bypasses on-board devices, the conversion is made in the charging station and just the DC power feeds the battery.

These are two completely different philosophies, with many pros and cons on each side and the concepts can be understood looking at the figure 3.50.

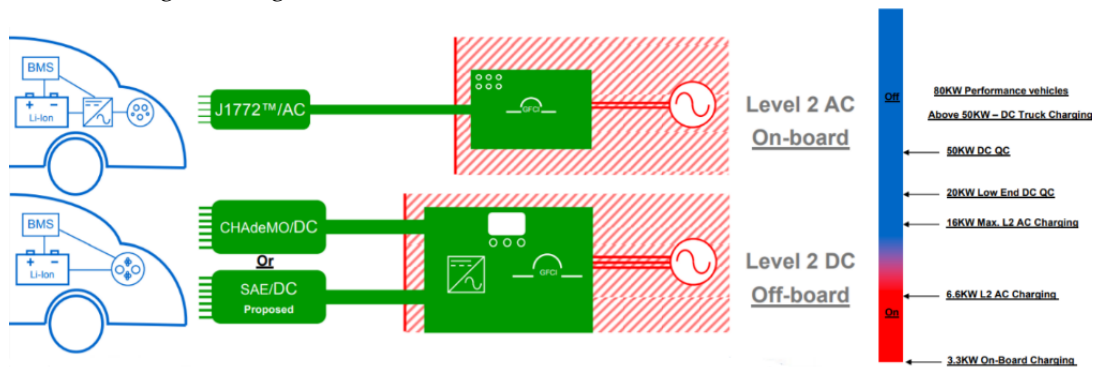


Figure 3.50: On-Board vs Off-Board layouts [55]

The differences between these two opposite configurations concern mainly weight, volume and price: the first two factors directly affect the vehicle performance if the converter is installed On-Board.

Price is a fundamental argument for both On/Off-Board solutions: DC off-board chargers are typically 10-40 times more expensive than the equivalent AC solution: this considering the same output power delivered to the battery.

The same considerations hold as far as the weight is concerned: the off-board solutions have weights ten times larger than the on-board ones but allow to reach very high charging power and do not have a direct detrimental effect on the vehicle performance.

ON-BOARD

Today all electrified vehicles (PHEVs and BEVs) have an On-Board charger, these are redundant devices because are parallel to the converters used in the electric drive: it's naturally to wonder if could be possible to eliminate this extra weight and cost.

On the other side, On-Board chargers are suitable to be used in Level 2 charge (this through EVSE that manages correctly the connection to the grid) and are designed and sized to get maximum efficiency at these power levels while the drive converters are oversized for charging operations.

Recapping main characteristics of such configuration:

- Sized for low/medium power conversion
- Better management of battery heating through embedded thermal management systems
- Operated by pilot signal j1772
- BMS manages directly the on-board rectifier
- Constraints in volume and weight

Considering the constraints in weight and size of such On-Board components, it's interesting to notice that just two vehicles, on thirteen analysed, have overtaken an output power of 8 Kw.

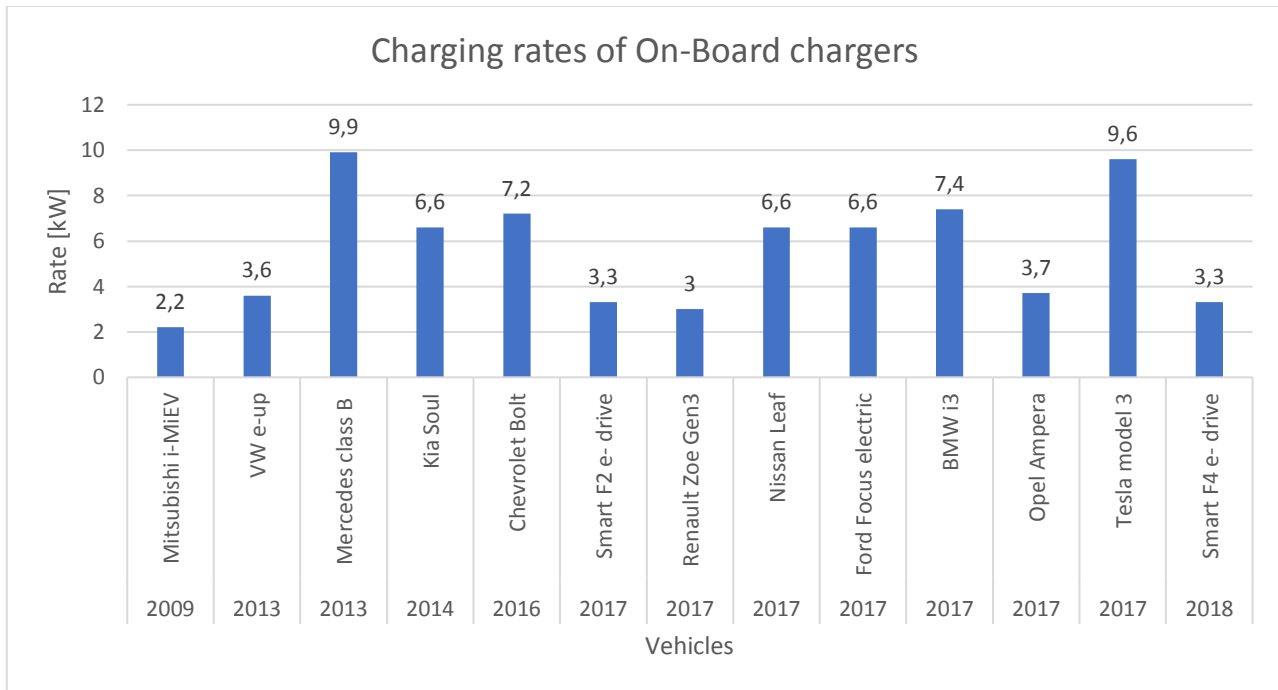


Figure 3.51: Power size of On-Board charger mounted in different BEVs

This is probably a trade-off result: larger chargers would negatively affect the car weight, layout and cost; this is especially true in large scale vehicle productions.

In [54] has been demonstrated how the developments in power electronics have reached a limit as far as the compromise among performance, complexity and costs is concerned.

Through a multi-objective optimization, a roadmap has been created: first considering the maximum performance achievable with the current technology (topologies, modulation techniques and control strategies), then the effect on performance of future developments from base technology has been forecasted.

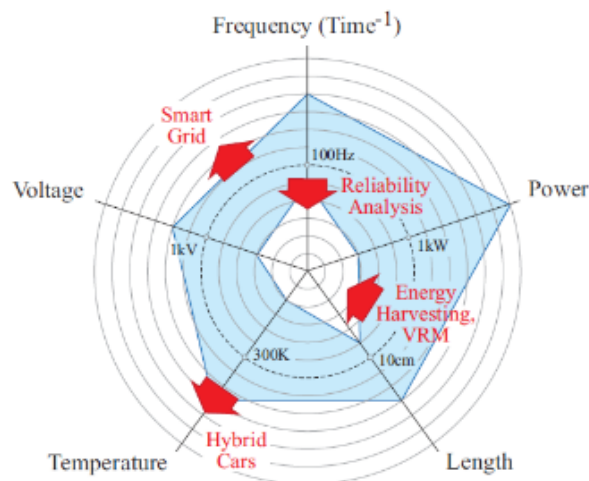


Figure 3.52: Performance evolution trends for different power converter applications [54]

From figure 3.52 it's possible to note how different power converters are necessary for different applications: this will lead to specific performance evolutions for each specific field (i.e. for hybrid cars the requirements will lead to the development of devices working at higher operating temperatures).

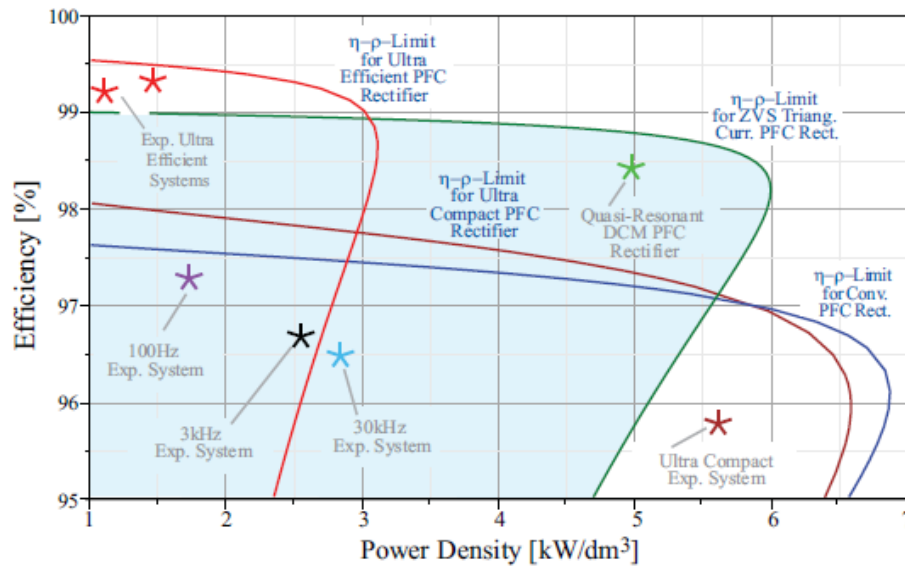


Figure 3.53: Pareto plots for different converter topologies [54]

In figure 3.53 the plots describe the trade-off between efficiency and power density for different converter topologies and forecasted limits: this is extremely useful to select the converter suitable to reach targets and requirements of each application with a focus on the possibility in the future developments and improvements.

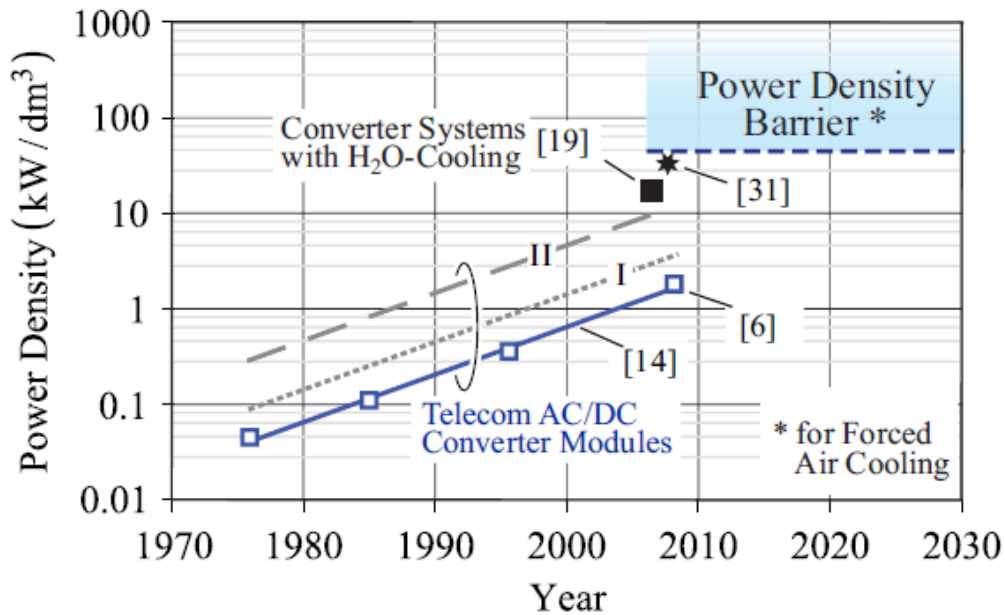


Figure 3.54: Evolution of the power density in the next years [54]

Nevertheless, in figure 3.54 the results of the analysis [54] determines that probably, also with advanced thermal management systems, the power density barrier of 90-100 kW/dm³ will not be easily overtaken.

To solve these problems, a promising studied solution is to use the electric drive power electronics also for charging purposes; this will require high research and development, a brief review of the most promising alternatives will be discussed in next chapters.

OFF-BOARD

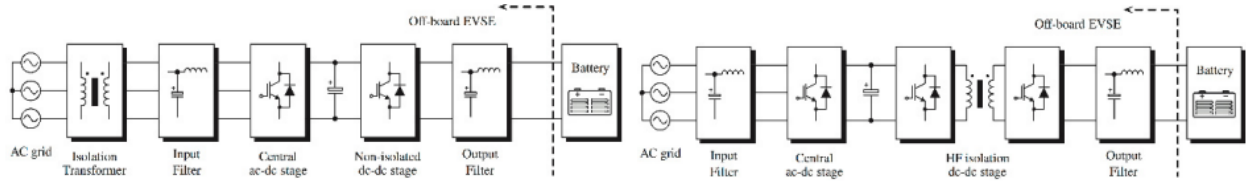


Figure 3.55: Generic structure of an off-board charger (LF isolation on the left and HF isolation on the right [56])

Among the reported vehicles, just two are not configured to support a Level 3 charge (thus supporting the use of an Off-Board charger), the tendency is clear, a fast charge opportunity is mandatory to boost the EV diffusion and to overcome the obstacle of the “Range anxiety” that limits the potential customers. The picture above shows the main components of an off-board charger for level 3 and the main steps of the conversion from the grid to the battery:

- 1) Three-phase AC input is managed by a PFC circuit.
- 2) AC input is rectified by the active rectifier into a high-voltage DC of about 400 V.
- 3) This voltage passes to a DC/DC converter generating the correct DC level to charge the battery.
- 4) One or more MCUs monitor and control AC/DC and DC/DC power-conversion operations.

All EVSE stations use high level communications to support the charging process (figure 3.56): the power line communication (PLC), with its CAN interfaces, allows the EVSE to communicate with a high-speed communication link to the vehicle.

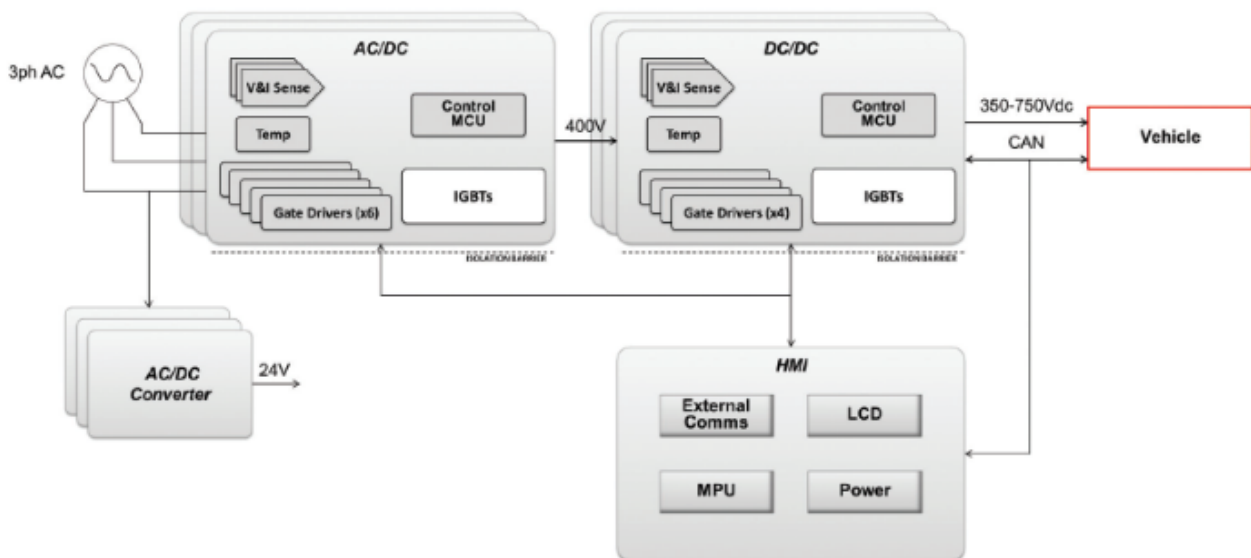


Figure 3.56: EVSE system block diagram

Off-Board chargers have advantages and drawbacks with respect to the On-Board ones:

- Higher power transfer
- More complex BMS, based on strict standards, must take into account the large number of battery chemistry.
- Advanced communication with buildings/homes/grid.
- Less constrained as far as weight and volume are concerned

Looking at some charging station on the market, reported in figure 3.57, it's possible to characterize their performance in terms of output power and charging currents.

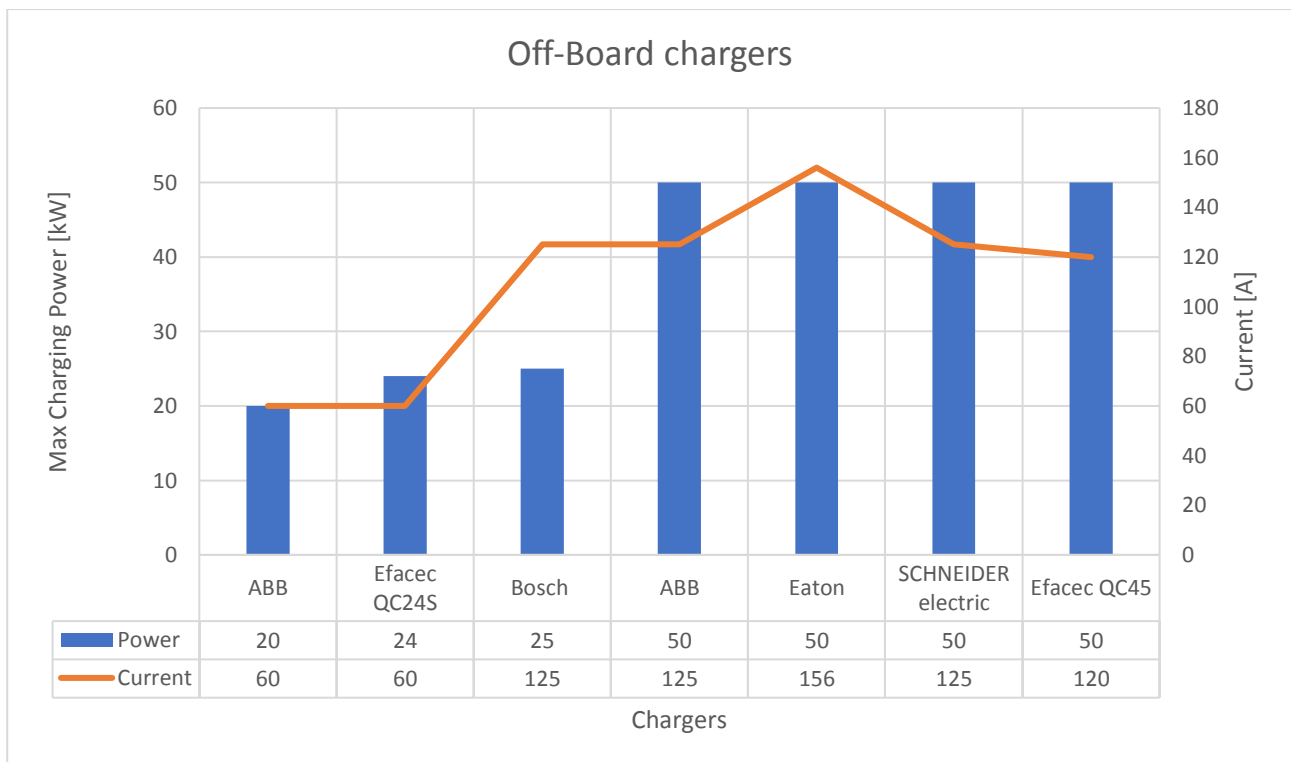


Figure 3.57: Output power and operating current of several Off-Board chargers available in the market

Analysing again the possible application of these chargers, it's interesting to highlight the limitations of Level 3 charging stations:

- 1) Households, without upgrade in the electric system, may only support 16 A then would be necessary to de-rate the charging level inhibiting most of the advantages of such type of chargers.
- 2) PHEVs, with the limited capacity of their batteries, would not use Level 3 fast charge that could be unsupported and, in any case, senseless.
- 3) Most DC charging stations stop the charge operation at 80% SoC because, at this point, the power must be reduced entering in the constant voltage region (power reduced through the decreasing current).

Nevertheless, many studies highlighted the necessity to have Level 3 Fast charger diffused in strategic points in order to reduce, as much as possible, the "range anxiety" that seems to be the most relevant obstacle between potential customers and electric vehicles [57].

3.2.3) AC vs DC charge procedures





SAE charging configurations			
	AC LEVEL 1 (SAE J1772) (OnBoard charger) 1,9 kW at 120 Vac and 16 A		DC LEVEL 1* (OffBoard charger) 36 kW at 450 Vdc and 80 A
	AC LEVEL 2 (SAE J1772) (OnBoard charger) 19,2 kW at 240 Vac and 80 A		DC LEVEL 2* (OffBoard charger) 90 kW at 450 Vdc and 200 A
	AC LEVEL 3* (OffBoard charger) > 20 kW Single/Three-phase		DC LEVEL 3* (OffBoard charger) 240 kW at 600 Vdc and 400 A
NOTE: In this table are reported value related to the maximum output power			
*To be definitely defined			

Figure 3.58: AC/DC levels and suitable charging connectors

There are studies identifying AC level 2 operations as the only profitable solution for V2G services [6] and there are several aspects that can appear as weaknesses of DC fast charge with respect to the AC:

- Higher installation and hardware cost due to higher volumes and weights
- Lower time in which the vehicle is connected to the grid resulting in less time for V2G services
- Lower flexibility and lower scalability
- Usually are devices oversized for PHEVs (≥ 20 Kw)
- Higher control complexity facing many different battery systems (strict standards are required to avoid incompatibilities or damages)
-

Nevertheless, there are other factors pushing the market toward the DC fast charge adoption:

- Limit in volume, weight and cost of On-Board chargers (today with a max power around 10 kW)
- Increasing battery system capacity resulting in longer charge time
- Mitigation of "Range anxiety"

Connectors and Standards

A huge barrier to the diffusion of EVs is surely the lack in strong and robust standards shared among different OEMs and different states/continents.

During the years many attempts have been made but there are several different architectures that can be equivalently utilized and, many times, chargers' manufacturers must offer different configurations of the same product in order to be sure to satisfy each requirement (figure 3.57).

Briefly the main adopted solutions for Vehicle Conductive Charge Coupler will be introduced and described.

SAE J1772 (IEC Type 1)

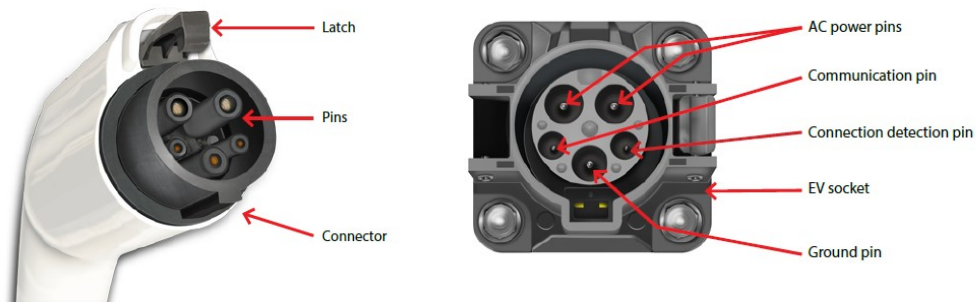


Figure 3.59: SAE J1772 connector

This connector is often used for AC Level 1 and AC Level 2 charge (up to 19.2 kW) controlled by the EVSE. SAE requirements define the configuration, the communication protocol and the safety standards (NEC 625, UL 2231 and L 2594): when the connector is attached to the EV the charging station detects the connection and communicates the maximum allowable current to the vehicle; at this point the BMS of the vehicle sends back a response signal (Pilot signal) enabling the charge (charging operations are managed by the On-Board charger).

With this configuration and its standards, would be possible to support DC Level 1 and DC Level 2 charge but, being not actually used, will not be discussed.

IEC 62196 Type 2 connector (Mennekes)

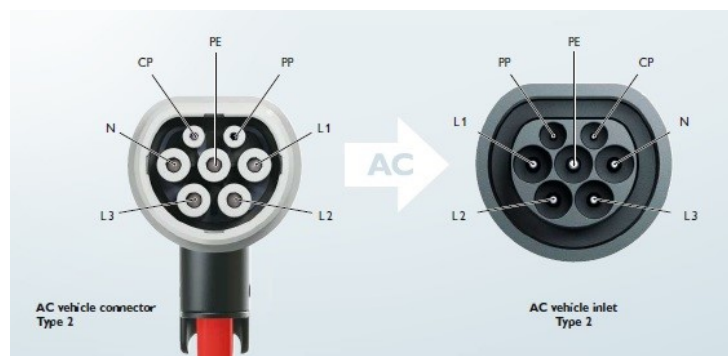


Figure 3.60: IEC 62196 connector

It's the main European standard, this because in January 2013 the IEC 62196 Type 2 connector was selected by the European Commission as official charging plug within the E.U.

The connectors contain seven contacts: two small contacts for signalling (CP and PP), the centre pin for the Earth connection (PE), two pins on the bottom row are always for power supply (L2 and L3) and the other two pins in the centre row are dedicated to a further power line and the neutral (N and L1).

Recapping there are pins always used for the same functions:

- Proximity pilot (PP) for pre-insertion signalling.
- Control pilot (CP) for post-insertion signalling.
- Protective earth (PE) for full-current protection.
- The allocation of the four power supply pins varies:
- Neutral (N) and line (L1) for single-phase AC power supply.
- Neutral (N) and line phases (L1, L2, and L3) for three-phase AC power supply.
- Neutral (N) and line (L1); negative (-), and positive (+) for combined single-phase AC and low-current DC power supply.
- Negative (-) and positive (+) for low-current DC power supply.
- Negative (-, -) and positive (+, +) for mid-current DC power supply.

The Type 1 and Type 2 connectors have been used as base technology to develop a third connector suitable for DC Level 3 fast charge, this topology will be described in next pages.

Combined Charging System (SAE J1772 Combo standard)

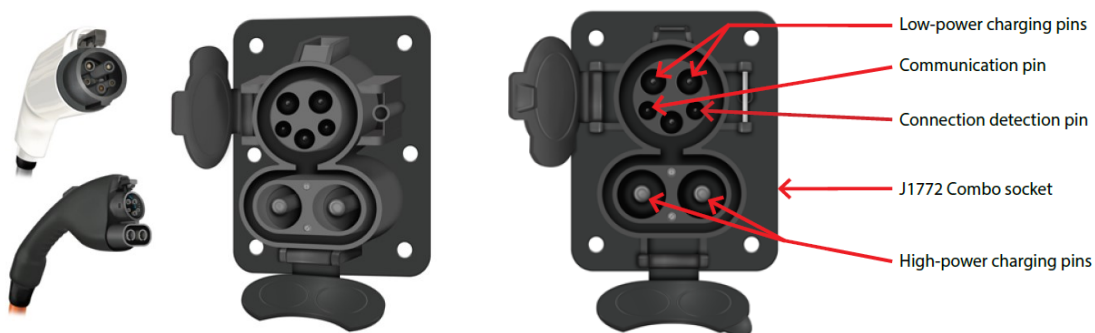


Figure 3.61: SAE J1772 combo connector

It's a more complex solution that, supplying high DC power, must have higher insulation capabilities (at least 1.12 MΩ isolation from the chassis) and other phenomena like short-circuits and electrostatic discharges must be avoided.

The architecture it's enabled for DC Level 2 fast charge, built with the combination of the standard j1772 Type 1 connector or the type 2 connector plus two additional high-power pins supporting up to 200 A. The connection protocol is very similar to the previous ones: the connection starts just with a pilot signal from the vehicle to the charging station after an exchange of information to determine the charging rate suitable for both EV and charger.

CHAdeMO standard

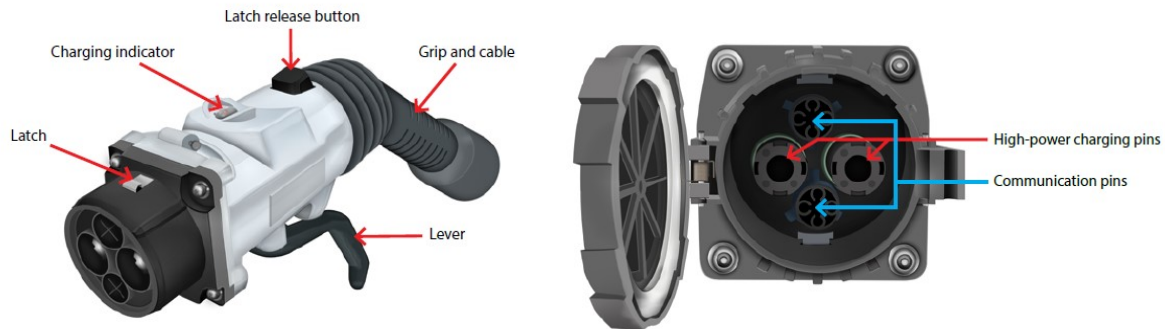


Figure 3.62: CHAdeMO connector

This is a Japanese standard appositely designed (hardware and protocols) for DC fast charge stations; In the same way of the SAE J1772 Combo standard, robust safety requirements have been implemented:

- Redundant communication signals (Analog + CANbus)
- Latch mechanism to avoid disconnections during the charging process (the connector need to be de-energized before the disconnection)

Communication protocols are designed to transmit battery status (SoC, SoH...) to the station, including when to stop fast charging (usually 80% of the SoC), target voltage, and battery capacity allowing the charger to set the adequate output current.

Pros and cons of each solution

Standard SAE J1772 defines six charging levels: this classification is evolving and not all the classified levels are currently in use; the development of a charging mode with respect to the other will depend by many factors, starting from the evolution of PHEVs and EVs vehicles and the development of batteries' capacity, OEMs choices and customers' behaviour.

The high grade of discontinuities among different geographic locations and different applied standards will slow the EVs market and focused initiatives should share a common target encouraging the potential customer to buy an electric vehicle.

AC Level 1

Nowadays all EVs are equipped with On-Board Level 1 chargers that can be plugged into an ordinary power outlet: this is a way to increase the flexibility of such vehicles compensating the lack in infrastructures and at the same time, minimizing the stations installation costs.

Power consumption and then distance travelled per kWh, vary according to vehicle, road conditions, driver behaviour and number of On-Board devices used.

Charging time is also a function of the energy consumed by the vehicle since the last full charge.

Different analyses have been conducted taking into consideration the average behaviour of EVs owners: this charge mode seems to be insufficient for both the normal driving conditions and as far as V2G task is concerned.

AC Level 2

Level 2 charging stations can limit the time required for a full charge but must be considered the typology of the on-board charger, by the state of the battery, and the grid architecture (household applications).

This charging mode is the most promising, among the AC chargers, and is currently achievable by the larger number of On-Board converters; furthermore, it's a good trade-off between charging time and level of stress applied during the charging process to the battery and to the grid.

DC fast charge

All carmakers, with fast-charge enabled vehicles, adopt one of the two described standards (except Tesla): the configuration of the charging plug and the EV socket and the communication protocols between the charging station and the EV have light differences but the basic principles are the same.

Since an external device manages the charging current, it needs to take into account several fundamental parameters: i.e. the communication protocol handles the sharing of data about the battery's voltage ranges and ampacity, which allows the charging station to supply the correct charging voltage and current level to the EV battery.

Considering DC Level 2 charge, the maximum charging power specified by the CHAdeMO standard is 62 kW (125 A at 500 Vdc), while the J 1772 Combo standard sets the maximum power at 100 kW (200 A at 500 Vdc).

In practice, very few batteries support 500 V, and charging stations are commonly equipped with both standard connectors limiting the rated power to 50 kW

In contrast, Tesla Supercharger stations are rated 120 kW and the major automakers have announced higher output levels in the near future passing to DC Level 3 charge.

Since most EV batteries have a rated voltage of around 350 V, they cannot take full advantage of fast-charge stations. Consequently, for comparison it is useful to establish charging times using a feasible output of about 40 kW [57].

3.2.4) New scenarios: Integrated and Wireless chargers

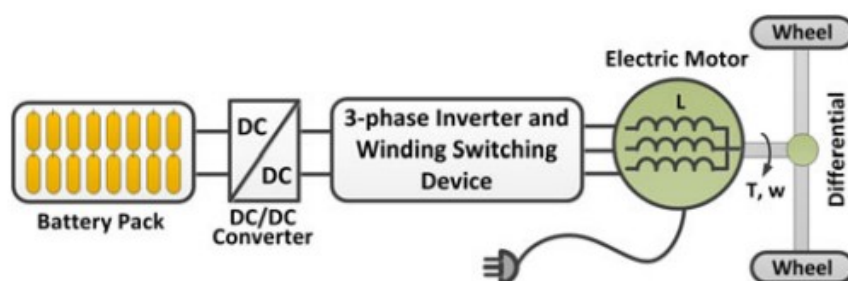


Figure 3.63: Base layout of an integrated charger [47]

There are several key technologies that can be a target to enhance the EVs diffusion and adoption:

- High performance moto-generators with wide speed range and field-weakening control.
- Equipment to provide optimal DC-link voltage regulation for the motor drive
- Battery charger with high efficiency, power quality and advanced control strategies;
- Integration of the electric drive power electronic and charger equipment.

Integrated chargers are a way to save weight, volume and cost exploiting the electric drive system for the charging operations: it's then possible to avoid redundant devices such as the onboard chargers, when the electric drive is not used for traction, the idea is to access the motor centre tap to use its structure as a coupling inductor.

Fully integrated chargers use windings of the motor as a part of the charging circuit together with the traction inverter and in figure 3.63 there are the schematic representation used to describe stator and rotor windings. Being designed for high power levels (related to the traction operation) these architectures could lose efficiency if used at lower charging power [58].

A complete review of the possible architectures is presented in [59], in which both isolated and not isolated topologies are considered (isolated when just three motor terminals are accessible), in this chapter just the most promising solutions are described, with a particular interest in solutions suitable for V2G applications.

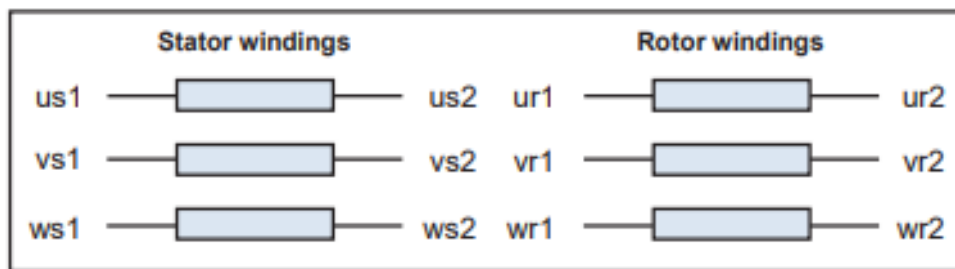


Figure 3.64: Representation of stator/rotor windings from [59]

Wound Rotors Asynchronous Motors (WRAM)

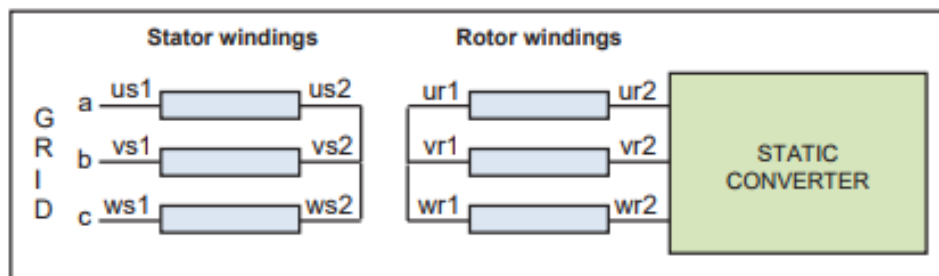


Figure 3.65: WRAM layout [59]

This solution behaves as a transformer (stator as primary and rotor as secondary) and there are different pros and cons.

Advantages

- Galvanic isolation between battery and grid
- V2G ready
- Low THD
- Power Factor Correction capabilities

Disadvantages

- Necessity to have power contactors
- Motor windings work at a different voltage than that of design
- Need of mechanical locking of the rotor

Permanent Magnet Synchronous Motors (PMSM)

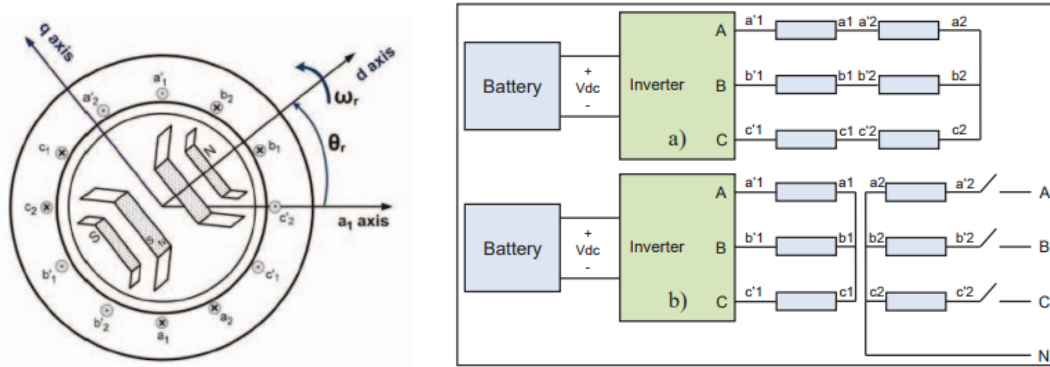


Figure 3.66: PMSM layout [59]

Six windings are evenly distributed around the stator with a lag equal to 30° and two operating modes are showed in the scheme above:

- 1) Traction mode: a classic series connection is performed
- 2) Charging mode: windings are dissociated and then a three-phase transformer behaviour is achieved to charge the battery pack (the stator would rotate if not locked)

In addition to the classical configuration it's necessary to add a rectifier filter for THD.

There are many patents, starting from 1990s until today, in [47] and [51] a detailed list of the most promising architectures is presented:

- Non-isolated/Isolated Cases for Induction Motors

-

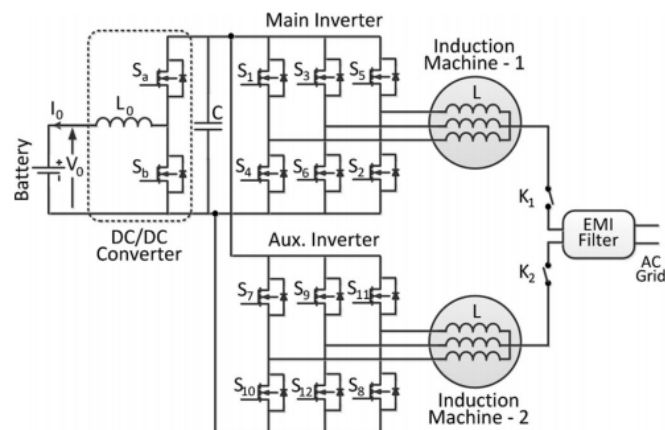


Figure 3.67: Integrated charger with two inverters and two motors [47]

This configuration, studied for plug-in hybrid vehicles, tends to minimize size and weight, simplifying the control strategies and does not require extra hardware except a transfer switch.

Charging system composed by two motors, in combination with interleaved layouts, has the benefit to get low input current ripple: interleaved control can be employed when the motor inductors are too small [60].

Disadvantages include high magnetization currents and the extra costs of the wound rotor and contactors.

- *Non-isolated/Isolated Cases for Permanent Magnet Motors*

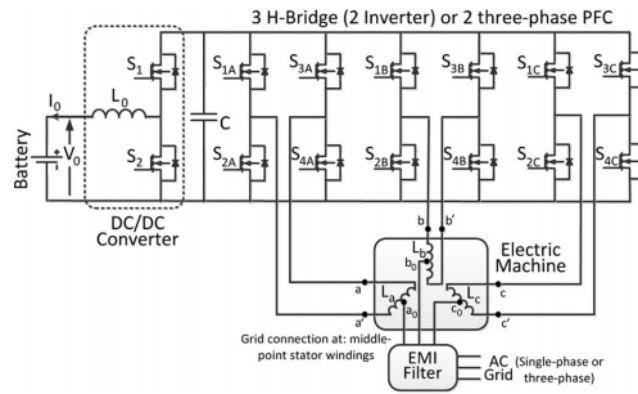


Figure 3.68: PM non-isolated integrated charger with connection through multiple points [47]

Permanent-magnets synchronous motors are well suited for traction purposes and widespread in EVs thanks to the high efficiency.

Controlling PFC converters, it's possible to set the DC link voltage, at a constant value, while the buck-boost chopper regulates the battery charging current at the desired rate.

Each AC phase is connected to two parallel boost converters through the midpoint of each winding of the moto-generator. Winding inductances, used as a filter, require a different control with respect to a classic boost converter in PFC mode [61].

There are three full bridge PWM converters to manage grid connection and traction while a two-quadrant buck-boost chopper controls DC side. The grid is connected to centre taps in each phase, splitting the currents into equal and opposite portions, this topology is complex as it must control three independent currents: a magnetic coupling exists between the six inductances; controlling the current in one of the winding could have effects on the other currents resulting in a more complicated current control. No additional filtering is needed since the PWM ripple is minimized by means of phase interleaving operation and uses inductances in the motor windings for filtering purposes.

Disadvantages include extra hardware, higher number of switches, a single-phase rectifier bridge with a mechanical switch to access the centre tap of the motor, a capacitor... To overcome isolation safety problems, various possibilities have been investigated i.e. an electric machine configuration with an extra set of windings.

- *Non-isolated/Isolated Cases for Switched Reluctance Motors (SRM)*

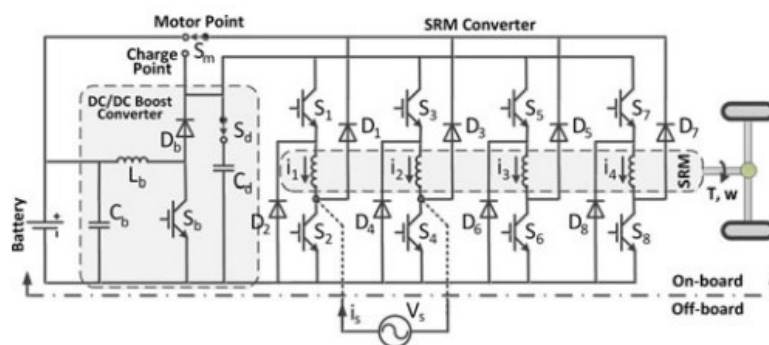


Figure 3.69: SMR integrated charger layout [47]

On-board charger is formed by the embedded components of SRM windings and the traction converter: in driving mode, the DC/DC boost converter is controlled to assure well-regulated DC-link voltage for the SRM drive from the battery.

For a BEV, a suitable DC/DC front-end converter to regulate the battery voltage has several advantages:

- 1) reduction of battery voltage variation on the motor converter and reduction in DC-link capacitor ratings;
- 2) smoother developed torque and improved performance;
- 3) reduction of the back-EMF effect to enhance the performance at high speeds;
- 4) increase in the motor output power, without increasing the sizes of motor and battery pack;

In charging mode, power devices embedded in the traction converter and the three motor-phase windings are used to form a buck-boost rectifier to charge the battery from the grid with good power factor [62].

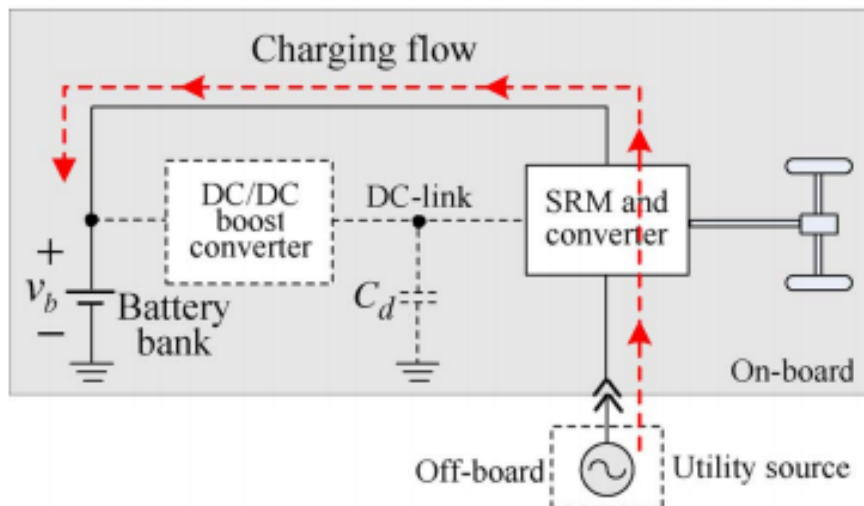


Figure 3.70: Charging flow in a vehicle equipped with integrated SRM charger

When the EV is in idle status, the onboard charger circuit is formed using the motor windings and converter embedded power devices, then only the insertion of power cords is needed. In the proposed SRM converter, the winding stored energy can directly be sent back to the battery during each demagnetization stroke and during braking, the SRM is arranged in the generator mode to let the mechanical stored momentum energy to be recovered back to the battery pack during deceleration.

Concluding this rapid overview on the integrated topologies, it's necessary to highlight the most important characteristics that could lead to the choice of a configuration instead of another one [58]:

- Necessity of bulky add-on components introduces increased complexity and reduces cost saving
- Access to inaccessible points of the machine winding (neutral and mid-point) requires inconvenient hardware rearrangements
- Requirements in terms of insulation can lead to different layouts
- Interactions between rotor and stator magnetic fields during the charging process could lead to dangerous rotation of the electric machine and an opportune locking system must be designed

Wireless technologies

Increasing interest in wireless charging solutions is explained by the enormous advantages that, with a development in the technology and satisfying a series of requirements, would deeply modify the e-mobility paradigm:

- Avoided battery deep-cycling, through frequent charging sessions, increasing the life cycle.
- Decreased capacity of on-board batteries with savings in weight and costs.
- Removed cables and cords with a better galvanic isolation.
- Reduced necessity of fast-charging infrastructures.

Nevertheless, this is an evolving technology not yet suitable to diffused implementations:

- Low efficiency.
- Low power density.
- High manufacturing complexity, and costs.
- Poor magnetic coupling and high leakages flux.

Inductive charging it's based on the magnetically transmission of the power; there are several methodologies [47] [63], three will be reported in this chapter:

- 1) **Stationary inductive charging:** the working principle is similar to the transformers concept where the primary transducer is a paddle and the second is the vehicle charge port; when these components are coupled is built a magnetic circuit and power can be transferred through an high frequency converter (0.5-50 kW with air gaps of 1-150 mm).

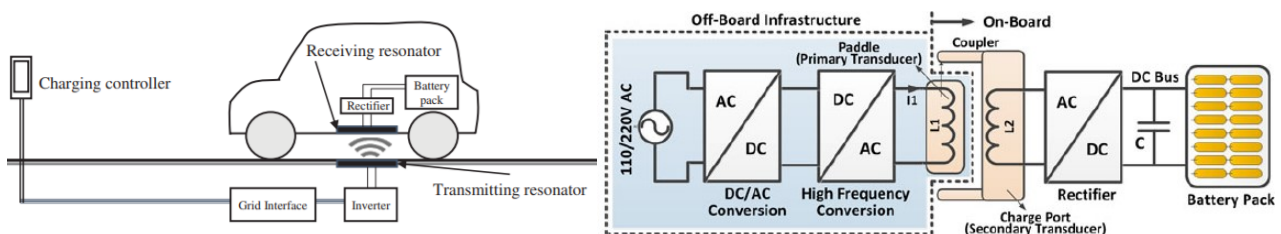


Figure 3.71: Stationary WTP (external view on the left and hardware layout on the right [47])

These solutions offer the best performance in terms of coupling, tuning, lateral alignment, and efficiency but to meet THD standards an active front-end is necessary.

- 2) **Contactless Roadbed EV charging:** focusing on the contact-less moving-roadbed, the main benefit is the potential reduction of battery weight and size. Transfer power occurs between a stationary primary source, below the pavement, and one or more secondary loops installed in the vehicle.

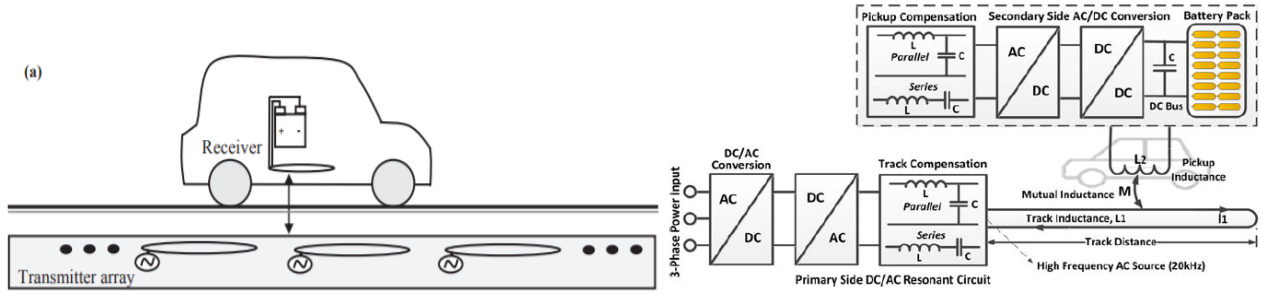


Figure 3.72: Inductive coupling roadbed (external view on the left and hardware layout on the right [47])

There are challenges that must be faced before a widespread adoption: high power ratings requirement, poor coupling characteristics, high supply voltage, loop losses, high magnetization currents and high lateral misalignment.

- 3) **Resonant and compensation circuit topologies:** the target is to maximize the power transfer minimizing supply voltage and current rating. In order to deliver high power with small devices it's necessary to work at high frequencies but reactive power compensation is required for both the sides (primary and secondary) of the inductive charger.

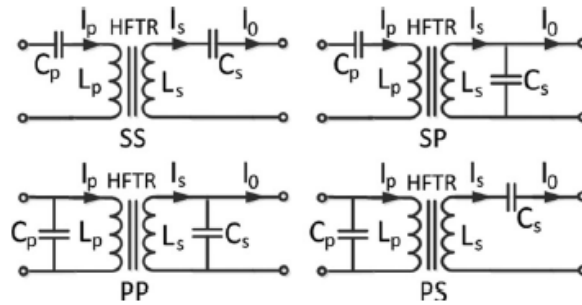


Figure 3.73: Main compensation topologies [47]

For these topologies the critical parameters are the frequency range, low magnetizing inductance, the high leakage inductance and the capacitance needed to set up resonance and for the reactive power compensation. High-frequency source can be an inverter or combination of a power amplifier and a signal generator. In EV charging applications battery is connected through a rectifier and regulator circuit while load impedance consists of the impedance of the charging circuit.

In conclusion a recap of the most interesting solutions and their main characteristics is reported in figure 3.74:

Technology	Performance			Cost	Size / Volume	Complexity of System	Suggested Power Level
	Efficiency	EMI	frequency				
Inductive Power Transfer (IPT)	medium	medium	10 - 50 kHz	medium	medium	medium	medium/high
Capacitive Power Transfer (CPT)	low	medium	100 - 500 kHz	low	low	medium	low
Permanent Magnet Coupling Power Transfer (PMPT)	low	high	100 - 500 Hz	high	high	high	medium/low
Resonant Inductive Power Transfer (RIPT)	medium	low	1 - 20 MHz	medium	medium	medium	medium/low
On-Line Inductive Power Transfer (OLPT)	medium	medium	10 - 50 kHz	high	high	medium	high
Resonant Antennae Power Transfer (RAPT)	medium	medium	100 - 500 kHz	medium	medium	medium	medium/low

Figure 3.74: technical comparison of the most promising wireless charging architectures [64]

3.2.5) Conclusion

Speaking about V2G applications, in particular about active power exchange between vehicle and grid, can be reasonable to exclude AC Level 1, AC Level 3, DC Level 2 and 3 chargers because:

- For AC Level 1 chargers (up to 1.92 kW) the low power exchangeable would be a limit to the amount of Active and Reactive power that could be supplied to the grid.
- For AC Level 3 chargers (above 19.2 kW) the time in which the vehicle is connected to the grid is drastically reduced (tens of minutes).
- For DC Levels 2 and 3 the output power overtakes 36 kW and holds the same argument of AC level 3 chargers

This type of services has been studied and tested many times in these years, the situation and the choice of a charging architecture with respect to the other could be different speaking about ancillary services. Speaking about grid regulation services, i.e. in which the exchanged power is delivered almost instantaneously but for very short period when requested (UP and DOWN regulation), the previously described review could be modified.

Net revenues are originated considering payments for the available capacity offered by connected EVs plus the payment of the active power effectively supplied into the grid and minus the costs to provide the service [65].

$$\text{Revenue_in_a_month} = P_{\text{charger}} * \text{Tariff} * \text{TIME_connection}$$

This type of service could be profitable for owners of Level 3 chargers but a detailed analysis must consider the high initial investment, the realistic net revenues in the reference national grid and the negative effect on the battery lifespan.

There would be some constraints requiring a certain amount of available power in order to start the service (minimum number of EVs connected at the same time) this will lead to the definition of aggregators that will manage many vehicles in many different locations in order to satisfy the entering rules.

In any case will be necessary to have a household electrical system able to support upper charging currents, then with adequate fuses and protection systems: for domestic applications, nowadays, just a maximum current of 16 Amps could be theoretically feasible and this is a limiting factor also in AC level 2 chargers.

An upgrade in the electric system for domestic applications is a must looking at smart-grid concepts.

Finally, a further advantage in off-board chargers is the possibility to use the passive components, always connected to the grid, compensating reactive power also without a connected vehicle [66]: The proposed architecture is composed of two stages sharing the same dc-link, one to interface the power grid and the other to interface the batteries. This novel architecture was experimentally verified where the results obtained validate the proposed charger-to-grid (C2G) operation mode, in which the ac-dc converter of the battery charger is also used to produce capacitive or inductive reactive power without using energy from the batteries. In the next studies will be important to understand if level 1 bi-directional off-board chargers (10-15 kVA) could be used to effectively mitigate quality problems in the installation location.

4. Batteries: evolution in the automotive scenario

A battery is a device that converts chemical energy into electrical energy and vice versa; this section starts with a comparison among the available energy storage alternatives and with a summary introducing the terminology used to describe and classify different technologies, characterizing the different operating conditions and specifying the manufacturer recommendations.

4.1) Characterization and classification

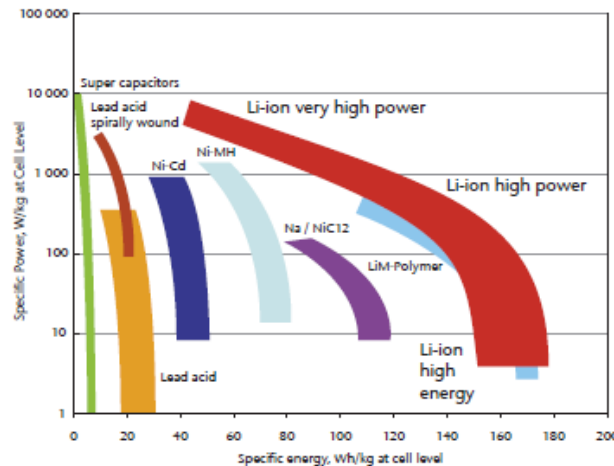


Figure 4.1: Specific energy vs specific power of different battery typologies (Johnson control -SAFT 2005/2007)

As previously described, batteries are the crucial components determining the performance and then the electrification degree of HEVs and moreover of EVs: thus, it's necessary to explain main features and factors that allow to understand the possibilities of different types of batteries, highlighting potential, advantages and disadvantages. Batteries for hybrid plug-in and electric vehicles are all secondary batteries (are rechargeable). This component constitutes the limiting factor for the large-scale adoption of electric vehicles not connected continuously to the grid: one of the biggest problem is the compromise between specific energy and specific power shown in the Ragone plot.

Liquid fuels show a much higher specific energy and have several other advantages.

Liquid fuel characteristics:

- Simple and fast refuelling procedures
- High specific energy (11.8 kWh/kg for gasoline and 13.7 kWh/kg for diesel)
- High energy density
- Widespread infrastructures

In automotive, battery modules are obtained connecting, in series or in parallel, different battery cells that are composed by four main components as illustrated in figure 4.2:

- Anode electrode (positive pole with coated catalyser substrates)
- Cathode electrode (negative pole with coated catalyser substrates)
- Separator material between anode and cathode
- Electrolyte carrier for ions flow (lithium-ion cells) or active participant in the electrochemical reaction (lead-acid cells) in liquid, gel or solid form.

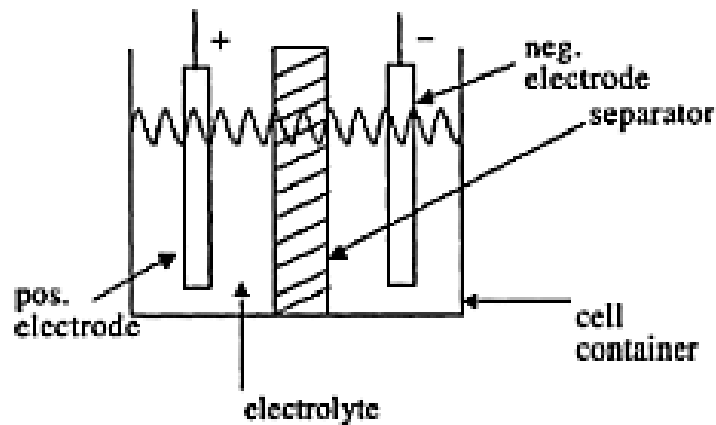


Figure 4.2: Basic scheme and components of a conventional battery cell [69]

Batteries with the same chemistry are not always equal: it's necessary to design the battery pack with specific targets in terms of energy and power; a trade-off between these two characteristics must always be found (it's not possible to have both at high levels) for this reason batteries for different applications are often categorised as high-power or high-energy batteries.

Cells and modules must be properly assembled to get the required high voltage necessary in automotive applications: the cell is the smallest unit while the battery pack is built assembling cells in module and then modules together.

4.1.1) Figures of merit

Battery Basic Terminology

Terminology used to describe battery cells, modules, and packs characteristics and parameters are briefly introduced [68]:

- Terminal Voltage (V): Voltage between the battery terminals with a load applied; varies with State of Charge and discharge/charge currents.
- Open-circuit voltage (OCV): Voltage between the terminals without a load.
- Internal Resistance (Ohm): Generally different for charging and discharging phases; as internal resistance increases, the efficiency decreases with thermal stability and more energy is dissipated into heat.
- Nominal Voltage (V): Reference voltage of the battery.
- Cut-off Voltage (V): Minimum allowable voltage that generally defines the “empty” state of a cell.
- Nominal Energy (Wh for a specific C-rate): Energy capacity available when the battery is discharged at a certain discharge current from 100% SoC to the cut-off voltage, calculated multiplying the discharge power (Watt) by the discharge time (hours). Energy decreases with increasing C-rate.
- Cycle Life (for a specific Depth of Discharge): Cycles that the battery can experience before it fails to meet performance requirements for specific charge and discharge conditions. The actual operating life

of the battery is affected by the rate and depth of cycles and by other conditions such as temperature and humidity.

- Specific Energy (Wh/kg): Nominal battery energy per unit mass (also called gravimetric energy density), is a characteristic of the battery chemistry and packaging.
- Specific Power (W/kg): Maximum available power per unit mass, is a characteristic of the battery chemistry and packaging.
- Energy Density (Wh/L): Nominal battery energy per unit volume (also called volumetric energy density), is a characteristic of the battery chemistry and packaging.
- Power Density (W/L): Maximum available power per unit volume, is a characteristic of the battery chemistry and packaging.
- Maximum Continuous Discharge Current (A): Maximum current that can be continuously sustained during discharge; limit usually defined by the manufacturer to prevent excessive discharge rates that would damage the battery or reduce its capacity.
- Charge Voltage (V): Voltage that the battery reaches when fully charged. Charging schemes generally consist of a constant current charging (CC) until the battery voltage reaches the charge voltage, then constant voltage charging (CV) to complete the process.
- Float Voltage (V): Voltage at which the battery is maintained after being charged to 100% SoC to conserve that capacity compensating self-discharge rates of the battery.
- C- rate: Index used to describe the discharge current in order to normalize against battery capacity, which is often very different between batteries; C-rate is a measure of the rate at which a battery is discharged relative to its maximum capacity (i.e. 1C means that the discharge current will fully discharge the battery in 1 hour).

This section describes some of the functions used to describe the actual condition of a battery:

Capacity

The amount of free charge generated by the active material at the negative electrode and consumed by the positive electrode, when it is fully charged before reaching a fully discharged condition, is called battery capacity.

$$Q_{\max} = \int_{t_{\text{charged}}}^{t_{\text{discharged}}} i(t) dt$$

The capacity is measured in Ah (1 Ah=3600 Coulomb, where 1 Coulomb is the charge transferred in 1 second by 1 Ampere current in the MKS unit of charge).

It is worth to note that the standard discharge conditions (i.e. constant current, 20 hours discharge at 27 °C) need to be specified in the definition of the capacity, since the maximum charge that can be delivered is significantly affected by the discharge current and by temperature.

In particular, it depends on the discharge current according to Peukert's law:

$$Q_{\max} = Q_{\max,0} \left(\frac{I}{I_{20}} \right)^{\alpha}$$

Then coulometric capacity, (Ah available when the battery is discharged at a certain discharge current) from 100% State-of-Charge to the cut-off voltage, decreases with increasing C-rates and can be calculated multiplying the discharge current (Amps) by the discharge time (Hours).

The cells in a battery are typically connected in series, and the capacity of the battery is dictated by the smallest cell capacity.

State of Charge (SoC)

$$\text{SoC} = \frac{Q}{Q_{\max,0}}$$

The capacity of a battery is not constant but varies with operating conditions (can be clearly seen the dependence with temperature in figure 4.3): the state of charge (SoC) of an accumulator is the ratio between the electric charge Q that can be delivered by that accumulator under standard slow discharge conditions and its nominal capacity.

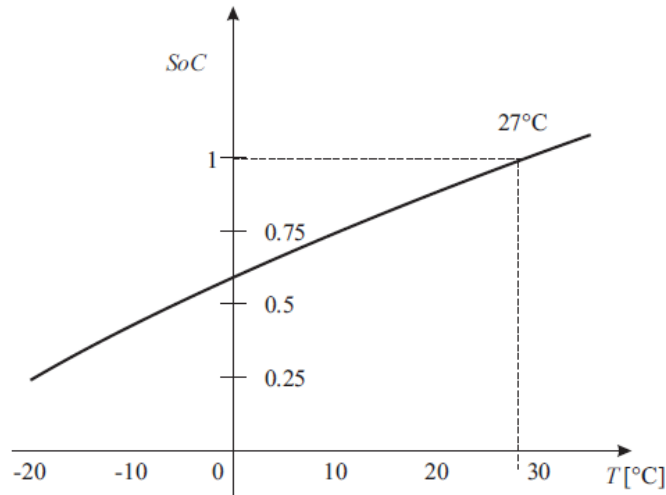


Figure 4.3: SoC variation due to different temperature conditions

SoC is generally calculated using current integration to determine the change in battery capacity over time.

State of Health (SoH) and State of Life (SoL)

SoH takes into account the progressive reduction of the capacity and the possibly increase of the internal resistance due to reversible phenomena while SoL considers irreversible phenomena such as corrosion, wear... These are ratios between the capacity of the brand-new battery and then actual residual capacity of the battery, both measured in standard slow discharge conditions.

Degradation mechanisms make a battery soon or later unsuitable thus, trying to address this issue, vehicles are equipped with Battery Management Systems which monitor the battery (terminal voltage, terminal current, temperature...) in real time and estimate these indexes during everyday utilization.

$$\text{SoH} = \frac{Q_{\max,0}}{Q_{\max,0,\text{new}}}$$

Depth of Discharge (DoD)

The depth of discharge is the percentage of battery capacity (rated capacity) to which a battery is discharged expressed as a percentage of the maximum capacity.

The depth of discharge can be expressed as:

$$DoD(t) = \frac{Q_T - SoC_T(t)}{Q_T} \times 100\%$$

$$= \frac{\int_0^t i(\tau) d\tau}{Q_T} \times 100\%$$

Where Q_t is the deliverable capacity that depends on the allowable energy at the actual temperature and power level; it's important to note that this index is strictly related to the State of charge being: $DoD = 1 - SoC$.

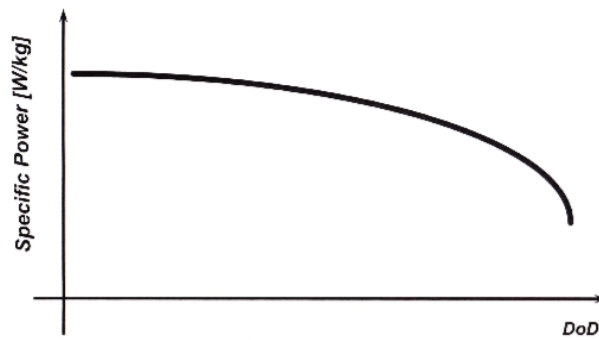


Figure 4.4: influence between Specific power and DoD

The withdrawal of at least 80% of battery (rated) capacity is referred to as deep discharge.

The available power tends to decrease with lower and lower temperatures and with higher DoD values (figure 4.4); these values fall dramatically close to 0°C then no recharging current is possible in this condition.

4.1.2) Batteries in the automotive market and future developments

Battery Type	Specific Energy, Wh/kg	Specific Power, W/kg	Energy Efficiency, %	Cycle Life	Estimated Cost, US\$/KWh
Lead-acid	35–50	150–400	80	500–1000	100–150
Nickel-cadmium	30–50	100–150	75	1000–2000	250–350
Nickel-metal-hydride	60–80	200–300	70	1000–2000	200–350
Aluminum-air	200–300	100	<50	Not available	Not available
Zinc-air	100–220	30–80	60	500	90–120
Sodium-sulfur	150–240	230	85	1000	200–350
Sodium-nickel-chloride	90–120	130–160	80	1000	250–350
Lithium-polymer	150–200	350	Not available	1000	150
Lithium-ion	80–130	200–300	>95	1000	200

Figure 4.5: List of available battery technologies and their technical specifications [69]

There are many alternatives that have been considered for automotive applications and many other will be studied in the next years; in figure 4.5 a group of different battery typologies are compared and it's possible to see how large are the ranges of specific energy, specific power, efficiency...

Nevertheless, the experience allowed in first approximation to establish, considering the performance targets and the requirements attributable to an On-Board energy storage in automotive applications, which technologies are possible candidates for future researches.

A way to identify the most promising technologies for future applications is to rely on the "experts' judgement". In [70] 15 experts (list in figure 4.6) of batteries, with various backgrounds and from several EU geographic locations, have been interrogated on the evolution of cost, performance of different solutions and, moreover, on the impact that different scheduling of the RD&D programs could have on the technical development of these storage devices in the next years. Such a method is useful in case in which there are not historic data available to make probabilistic decisions for the future strategies, through many alternatives. The selection process consisted in the identification of a first group of experts (core group) then these first participants were asked to find other relevant figures in the so-called "snowball sampling technique". This balanced pool it's composed by exponents of the institutions and private sectors and are engineers, policy makers, economists etc. being representative of the active players in the sector.

Name and surname	Affiliation	Country	Expertise
Michel Armand	Université de la Picardie	France	Battery technology
Pierpaolo Cazzola	International Energy Agency	Italy	Policy
Damien Crespel	Société Véhicules Electrique	France	Vehicle tecnology
Claudio Fonsati	Micro-Vett	Italy	Vehicle tecnology
Sergio Leonti; Vittorio Ravello	FIAT	Italy	Vehicle tecnology
Giuseppe Lodi	FIAMM	Italy	Battery technology
Adolfo Perujo y Mateos del Parque	Joint Research Centre	EU	Policy
John L. Petersen	Fefer Petersen & Cie	Switzerland	Policy
Bruno Scrosati	Università degli Studi di Roma "La Sapienza"	Italy	Battery technology
Patrice Simon	Université Paul Sabatier	France	Battery technology
Jean Marie Tarascon	Université de la Picardie	France	Battery technology
Christian Thiel	Joint Research Centre	EU	Policy
Margaret Wohlgahr-Mehrens	ZSW ULM	Germany	Battery technology
Karim Zaghib	Ireq	Canada	Battery technology

Figure 4.6: List of experts participating in [70]

Results, obtained from such type of questionnaire, can be exploited to establish significative policy recommendations, RD&D choices and targets.

The focus on these activities should be divided between the private and public investment accelerating the technological maturity of the production process. In 2008 almost all the funds (94%) came from private investments, and a stronger national activity would lead to significative steps forward in the cost reduction. Of course, cost estimates in the literature change basing the evaluation on different initial assumptions and the market for light duty vehicles is now a niche and few data are available.

In applications for PHEVs and EVs different chemistries and layouts to maximize respectively the specific power and the specific energy of the battery pack lead to different costs: considering the price for the unit of energy stored (i.e. euro/kWh) it's possible to see that PHEVs' batteries are 1.3/1.5 times more expensive than the equivalent battery pack for EVs (of course it's necessary to consider the different total capacity required between the two powertrains).

Finally, they were asked to highlight several potential prototype technologies (some of those are represented in figure 4.7) that could reach a superior performance level and could substitute the actually adopted battery chemistries (this just after years of research and development).

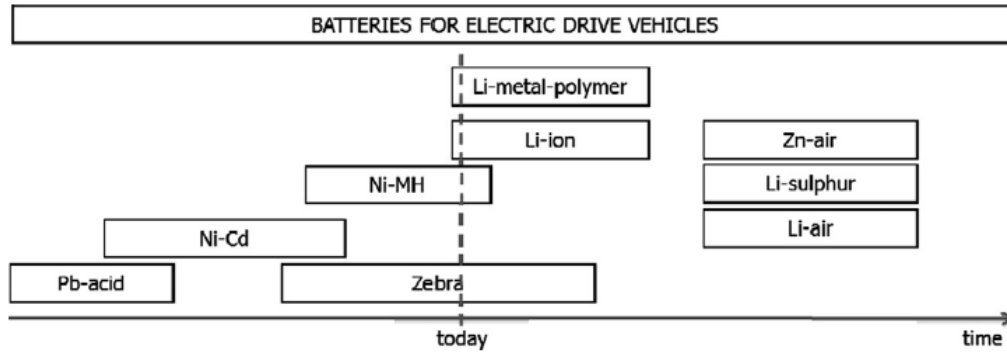


Figure 4.7: Technology path and state of development of some alternatives from [70]

Briefly describing the procedure utilized to get data and furthermore to assess the importance of the results, a first step was to define the preparation of each expert, asking them to declare their level of knowledge of each battery typology.

In this way it was possible to assure a homogeneity in the outcomes, avoiding lack of knowledge on certain battery technologies and topics; this was done with a self-evaluation on the degree of preparation attributing a level from 1 to 5 for each type under consideration (figure 4.8).

- All the technological alternatives are covered by at least one figure with a high level of expertise
- All the experts declared a wide knowledge of Li-Ion batteries
- Two third of the participants declared a good knowledge of the Ni-MH batteries (Nickel Metal Hydride)
- Half the experts reported a good expertise on LMP batteries (Lithium Metal Polymer)
- All the other proposed alternatives are less studied, maybe due to the high immaturity of the technologies

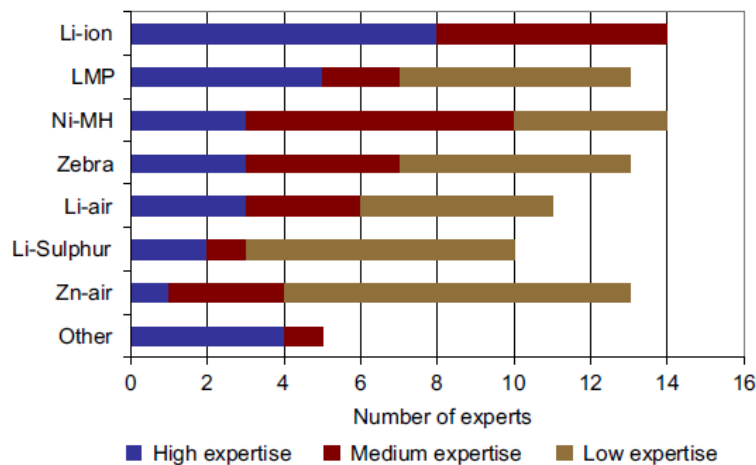


Figure 4.8: Classification of the experts following their level of expertise for each technological alternative [70]

A second target consisted in the establishment of the optimal allocation for the public investments, that could boost in a near future the RD&D process, in order to identify the technologies that most probably could satisfy the technical and economic targets, for the diffusion in the automotive field, by 2030: for this task a budget of 100 chips has been assigned and then a distribution among the possibilities identified the confidence of each participant on each battery technology (results in figure 4.9).

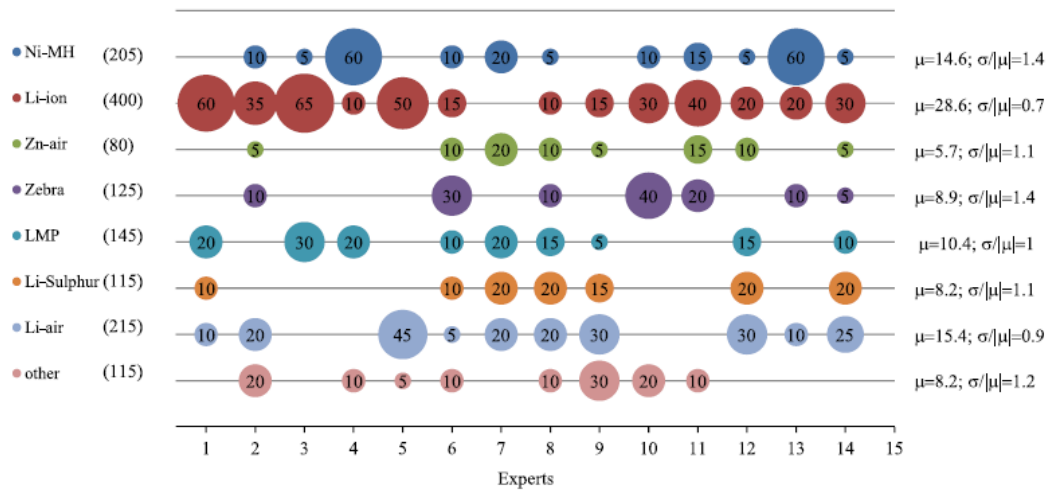


Figure 4.9: Suggested allocation of the RD&D budget for the period 2020-2030 [70]

As described before, this second step allows to determine the likelihood of achieve cost-competitiveness ranking the different scenarios; a further important line-guide it's the subdivision of the budget in different RD&D levels:

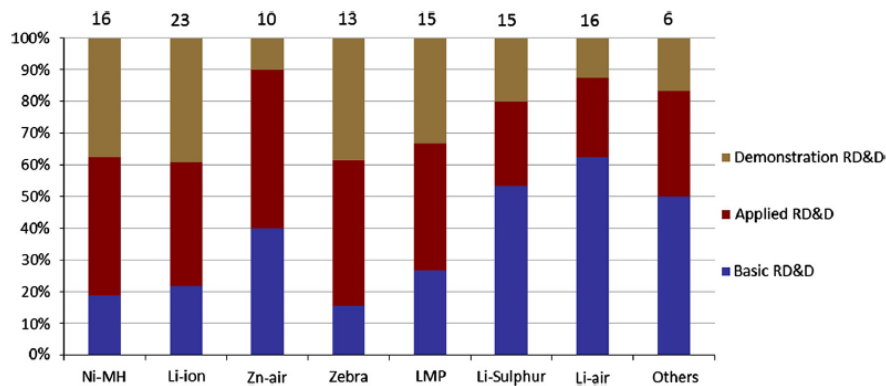


Figure 4.10: Suggested subdivision of the available RD&D budget among different development phases [70]

Without to enter in the details, a very significant result, that can be easily derived from a rapid analysis of the distribution of the opinions, is the uncertainty that covers all the candidates: on average each expert chose to “spend” their chips on 5 different technologies, this is a clear sign of the necessity to explore parallel ways at the same time, supporting a diversified portfolio not being able to identify a clear technological supremacy of one or two possibilities.

The dispersion in the estimates can be attributable to different expectations in the evolution of factors like:

- Base material availability
- Improvements in the specific energy and power
- Production volumes
- Safety issues
- Price and cycle/calendar life

Finally, from figure 4.10 can be understood that the subdivision of the available funds should be for roughly: 60% directed on the actually marketed products (such as Li-Ion and Ni-MH batteries) while the rest 40% should be devoted for immature solutions than need most of the investments in basic RD&D (such as Li-Air, Zn-Air and Li-Sulphur).

The focus of the chapter will be on the three candidates with an introduction on the characteristics and the possibilities of such immature battery typologies with a further contribution from [71]:

- Li-Air
- Li-Sulphur
- Zn-Air

A first aspect that can be noticed, relevant in the evaluation of the materials necessary for each cell, is the substitution of the graphite anode, the most adopted in current battery's cells, with a metallic Li anode to get higher energy density.

On the opposite the cycle life could be affected negatively due to the high reactivity of such a metal, especially as far as the non-linear degradation behaviour is concerned, with the unpredictable formation of dendritic elements that should be avoided with stronger safety strategies [71].

Li-Air

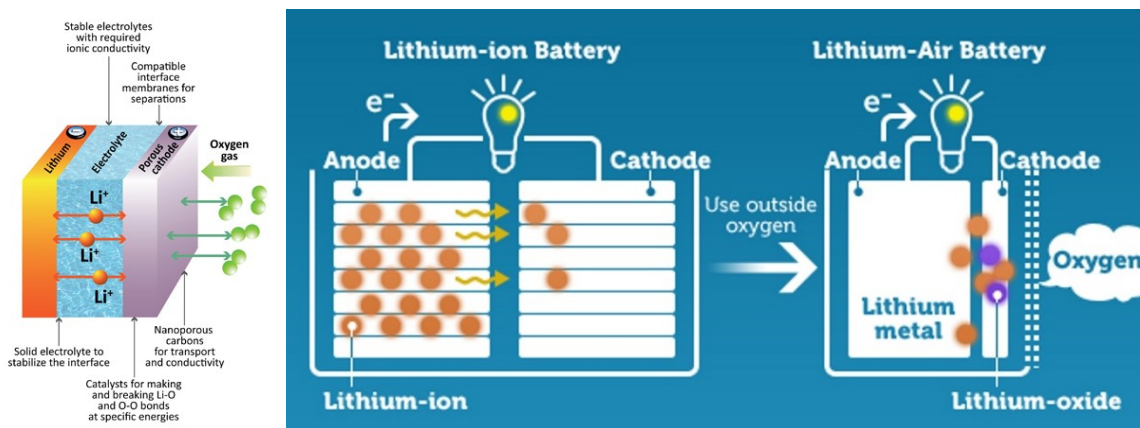


Figure 4.11: Scheme of a Li-Air battery and comparison of the working principle with the Li-Ion technology

Lithium-air battery is an electrochemical cell, in the early stage of development, that involves oxidation of Lithium at the anode and reduction of Oxygen at the porous carbon cathode (in which the oxygen is trapped).

The working conditions don't require molecular oxygen stored in the battery, this is an "open system" near to the fuel cell operating mechanism (figure 4.11), then the energy must be evaluated considering the growing mass at the cathode during the discharge phase.

The Li-Air cell has the highest theoretical energy with a cell voltage of 2.9 V and a specific energy of 5.200 Wh/Kg (near those of fossil fuels) but the real value droops dramatically due to several major drawbacks [71]:

- The real gas participating in the reaction could not be generic air but instead it's necessary to use Oxygen without a contamination of moisture, humidity or dust otherwise extremely fast degradation phenomena occur leading to a cycle life under 300/500 cycles.
- There are strong phenomena of passivation of the cathode due to the solid discharge products leading to high hysteresis and low efficiency.
- The high reactivity of the Lithium anode results in highly non-linear degradation and severe safety issues (as seen before).

Values of specific energy above the one reported, can be found in literature, this because several studies consider just the Lithium mass and not the mass of the Oxygen flow. Other correction can take in consideration the fact that Li₂O₂ product is formed at higher rates than Li₂O during the reaction, then the theoretical specific energy falls at about 3500 Wh/Kg but the experiments reported in lead to a more realistic value of 500 Wh/Kg. Oxygen is easily accessible in the atmosphere (dioxygen consists in 20.8% of its volume) and comes from a sustainable cycle, exploiting the photosynthesis process.

There are several connection points between Li-S and Li-O₂ batteries: both use a Lithium metal anode and pure chalcogens as main cathode material; despite these similitudes, there are different problems to be faced for a commercialization stage.

The first huge difference is the physical state of dioxygen, that is in gaseous state, and Sulphur, that is in solid state at standard conditions: the basic idea under this “ultrahigh-energy density electrochemical cell” is to couple the most electropositive metal lithium anode with the most electronegative one, considering also the elements with lowest equivalent weight (S, O, Cl and F).

Despite F and Cl could reach the best performance, the high toxicity of such gases represents an insuperable barrier to whatever alternative application.

Lithium-dioxygen batteries have been categorized depending on the electrolyte adopted:

- 1) non-aqueous electrolyte
- 2) aqueous electrolyte
- 3) hybrid electrolyte
- 4) all-solid-state electrolyte

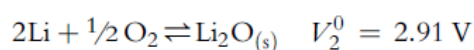
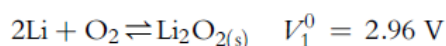
In this work will be introduced the two first types using carriers called “protic” (or aqueous) and “aprotic” (non-aqueous) electrolytes.

Non-aqueous Lithium/Oxygen Batteries

The main components can be rapidly listed:

- Anode: made of metallic Lithium.
- Electrolyte: organic or ionic liquid solution with dissolved Lithium salt.
- Separator: made of glass fibre or Celgard.
- Cathode: porous O₂-breathing component composed of black carbon particles often blended with catalyst particles, both connected to a metallic current collector thanks to a binder.

Starting from the fundamental cell reactions:



During the discharge phase, the gas (dioxygen or air) passes through the porous cathode and it's reduced in Lithium oxides that, being insoluble species, will cover the porosity.

The positive electrode determines the amount of Oxygen that can participate to the reaction: this value depends on the available surface area, on the pore structure and on the number of sites (diffusion is enhanced as the porosity increases, resulting in improved kinetics of the reduction reactions).

Two suitable alternatives to express the capacity consist in the expression in mAh/g, considering all the active player in the battery operation (carbon material, binder, catalyst...), and a further possibility, useful to compare the potentialities with other types of batteries, is to include the capacity expressed in mAh/cm².

In the figure 4.12, a typical discharge and charge profile it's reported: the discharge phase has a slightly decreasing trend, around 2.6 V, till the ohmic drop due to the formation of Li₂O₂ products.

The observed capacity ranges from 600 to a few thousands of mAh/g (grams of cathode) depending on the electrolyte, carbon, binder, applied current, and oxygen partial pressure.

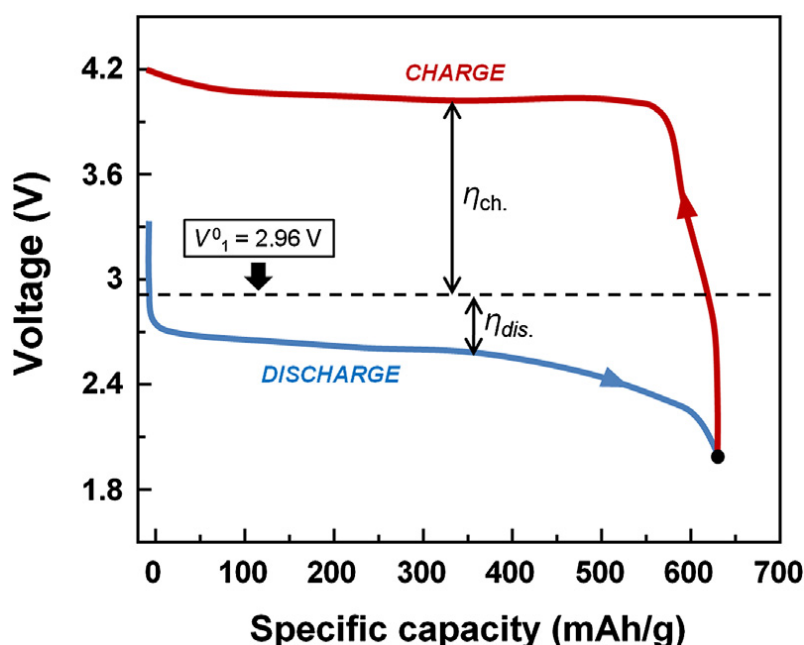


Figure 4.12: potential vs capacity curve (1st cycle) for a non-aqueous Li-O₂ battery [75]

Each oxygen reduction reaction (ORR) and oxygen evolution reaction (OER) exhibits different catalytic reaction mechanisms, thus a bifunctional catalyst is favourable to decrease the resistances of both reactions.

The limited cycle life (hundreds of cycles against thousands of cycles for the Li-Ion batteries) is the most challenging and critical aspect together with the low current density (increasing the discharging current leads to a decrease in the cell capacity).

The efforts are concentrated to find a suitable chemically stable electrolyte: ionic liquids despite the relatively high stability (i.e. hydrophobic ionic liquids are not mixable in water) cannot be considered as an optimal solution due to the lower electrochemical performance.

Pore clogging it's another relevant issue that must be faced designing new cathode structures reduce phenomena like the deposits formation and the volume variation during operations.

A possible future development to overcome the described problems, is the adoption of solid-state Li-O₂ cells, in order to solve the liquid electrolyte weaknesses thanks to a protective and highly conductive membrane that isolates the Lithium anode.

Such a configuration would allow to exploit directly the ambient air avoiding parasitic reactions due to the high reactivity of Lithium with water, carbon dioxide...

Aqueous Lithium/Oxygen in Batteries

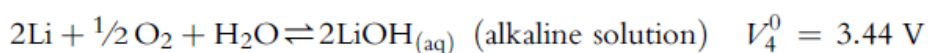
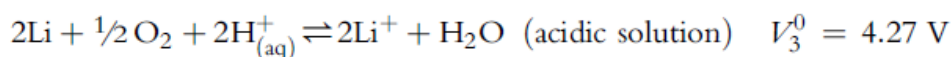
In this configuration the electrolyte is composed by an aqueous solution with dissolved Lithium salts; the reactions occurring in the process are furtherly complicated by other inorganic anions and precipitation reactions.

The advantage is that the atmosphere within the air-breathing cathode is not, anymore, an issue.

As described before the contact between Lithium and water must be avoided because would lead to dangerous dihydrogen gas production by corrosion reaction: to avoid this violent corrosion the structure requires an intermediate layer to prevent any direct contact.

A proposed solution, that effectively improved the performance and the reliability of the system, is represented by the implementation of an ion-conducting glass ceramic but other limitations persist, just like the precipitation of Lithium Hydroxide: saturation is theoretically reached at 5.25 M, but water is consumed during the discharge process and the saturation is anticipated (reaching 170 mAh/g), thus enhancing the precipitation of LiOH to allow the delivery of high energy and power but with consequences such as the covering of the protecting ion-conducting glass ceramic and the clogging of the porous cathode.

This implies an impedance increase and different solutions are being investigated: the larger part of the efforts are in the direction of the integration of a discharge product reservoir, detached from the cathode, allowing the electrolyte circulation.



Another of the problems affecting the commercial use of this technology is the occurrence of side reactions, for example when the carbon dioxide in the air, using alkaline electrolytes, produces insoluble Li_2CO_3 .

Despite the lower performance, in terms of capacity and specific energy, with respect to the aprotic version, this different typology could allow more flexibility in case, some of the most relevant issues will be solved. Nevertheless, the requirements concerning coulombic/energy efficiencies, rate capability and cyclability are far from being achieved in few decades.

To conclude it's necessary to point out that most of the reported experimental data were obtained under specific operating conditions: under pure Oxygen or artificially mixed O_2/N_2 then far from real usage conditions concerning much more complex reactions and mechanisms.

Li-Sulphur

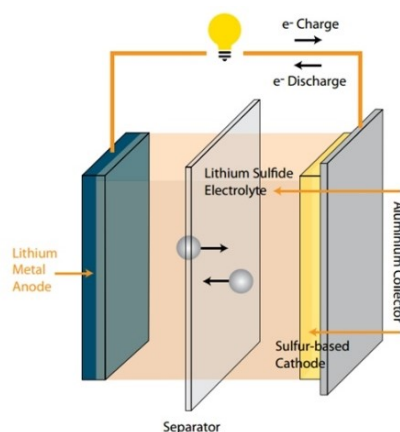
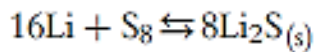


Figure 4.13: Scheme of a Li-S cell

In figure 4.13 there is an illustration of the basic structure of a LI-S cell and, also this time, the negative electrode is made of lithium metal while the positive electrode is made by a mix of additives and Sulphur to replace the gaseous oxygen of the Li-Air batteries and then producing Li₂S instead of Li₂O₂ (solid state products). The electrochemical reaction can be written as follow:



The real mechanisms are much more complex and the occurrence of many intermediate species and radicals makes difficult to establish a clear and solid description [71].

The high theoretical specific energy (2.500 Wh/Kg) and the cell voltage (about 2 V) make this solution an interesting candidate for automotive applications, but with the same concerns about the Lithium anode and its drawbacks.

The measured specific energy can be estimated as 5 times the value of the Li-Ion batteries, between 400/600 Wh/Kg, at the battery pack level [72][73][74][75].

The main phenomena affecting the performance of such a technology and then its practical use are [71][72][73][74][75]:

- polysulfides, formed during discharge, tend to be dissolved in the electrolyte (organic electrolytes such as glyme but also electrolyte of the Lithium Metal Polymer (LMP)) attacking the Lithium anode, lowering the capacity during cycling operations (polysulfide shuttle mechanism) and potentially reducing the maximum SoC reachable during the charge phase.
- the insulating capability of Sulphur (electron conductivity in the range of $5 \cdot 10^{-30}$ S/cm) leads to the adoption of a large amount of conducting additives reducing the specific energy.
- high volume variation of the cathode (about 22% volume expansion during the first discharge and 11% during the second ones).
- other aspects like poor coulombic efficiency, self-discharge (more than 0.8% per months) and safety issues.

In order to improve the performance enhancing aspects like the specific energy, the cycle life and the safety characteristics, it's necessary to improve all the main components of the cell (Lithium Anode, Sulphur cathode and electrolyte).

The aim of the research is to study new designs of the cathode in terms of additives, thickness and porosity (Oxygen diffusion is facilitated as the porosity increases, resulting in an improvement of the kinetics of the reduction reaction), to develop other electrolytes less affected by the polysulfide shuttle mechanism and, of course, to solve the problems related to the adoption of the Lithium anode that, once more, constitutes the crucial issue to ensure the commercialization of Li-S batteries [72][73][74][75].

Capacity and cyclability performance were improved by enlarging the contact surface between Sulphur, the additives and the electrolyte.

These are mandatory requirements to reach an adequate level of marketability: the literature shows a high degree of uncertainty in the results, with large fluctuations among the reports, then much more time and energies must be dedicated to basic RD&D phase.

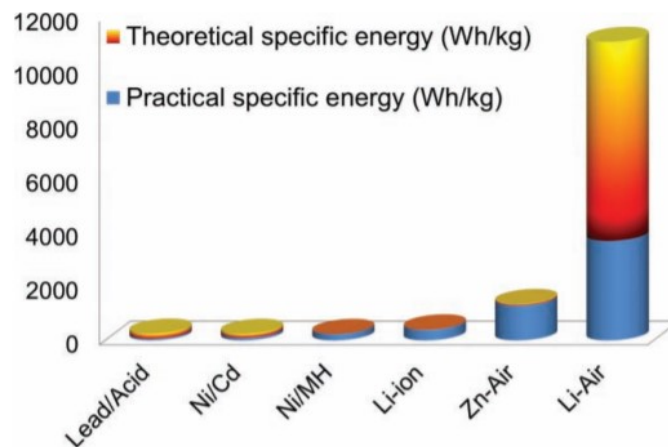


Figure 4.14: Theoretical/Practical specific energy of many battery technologies [76]

Comparing Li-Air and Zn-Air batteries [76] it's possible to highlight the higher stability that the Zinc-based solution can achieve: the components are stable also in presence of humidity therefore is easier to manufacture and utilize these batteries, also under ambient conditions. In figure 4.14 it's possible to see the theoretical and practical specific energy (Wh/Kg) among the possible alternatives for the automotive field.

This characteristic, whit the price competitiveness due to the lower cost of Zinc and of the electrolyte, represent the strong points that could make preferable the adoption of this solution, accepting a loss in the energy density, with respect to the Li-Air technology. For these reasons the maturity of such a typology seems to be nearer to the commercialization step.

On the other side, the reversibility and the operating potential of the Lithium based batteries are larger resulting, as said before, in higher energy density.

Nevertheless, there are many mechanisms not completely understood requiring additional studies in order to get the required reliability for the automotive sector.

Zinc morphologies involving particles with high surface areas, can affect the electrochemical behaviour of the system and the efficient reaction with the electrolyte.

The most severe issue in Zn-Air batteries it's represented by the slow reaction of Oxygen that originates high overpotentials for both ORR/OER and affects the cathode performance: catalysts such as perovskite and pyrochlore together with the electrode structure have an important role in the reduction of this phenomenon. Finally, the pore size of the separator must be optimized to maximize the electrochemical performance and reducing at the same time the migration of Zinc ions from the anode to the cathode (causing a loss in capacity).

4.1.3) Conclusion

The target of this short preview was to highlight the high hype behind some new technologies that for different reasons are very attractive for the future of the electric mobility.

Each of the proposed alternatives would represent a tough competitor with respect to the LIB batteries (if the judgement is about the potential specific energy), in fact all the described solutions show a theoretical and experimental energy density of several degrees of magnitude above the current batteries in the automotive.

Besides these considerations, the early stage of development does not allow to identify these technologies (or at least one of them) as a clear breakthrough solution for On-Board energy storage systems and then in the e-mobility scenario.

In fact, the most important and challenging obstacle is the determination of a stable and efficient electrolyte, allowing reversible cycling (this can be seen from the detailed analysis of both ORR/OER reactions) then lengthening the cycle life.

In the aqueous version some of the issues are reduced, but further improvements in terms of safety, reliability and cost reduction must be promoted in the next decades.

Not all the opinions, among the researchers, are optimistic on the feasibility of future developments of Li-Air batteries: this is clear also in the interview reported at the beginning of the chapter.

Also Li-S batteries have already surpassed the typical energy density of LIBs (about 180 Wh/Kg at cell level), but this performance is measured just for few hundreds of cycles.

Sulphur is an interesting candidate as active material for the positive electrode being abundant in nature and relatively cheap; a main drawback is the necessity of a large amount of high conductive additives reducing the specific energy together with the high reactivity of the Lithium anode with the dissolved species and the electrolyte.

Further developments will have as target to better understand the polysulfide shuttle mechanism (due to the Sulphur species dissolution) and of the anode/electrolyte interface behaviour in order to achieve higher safety levels, lower self-discharge rates and higher rate capabilities.

4.2) Li-Ion batteries: present and future

4.2.1) Classification

A first wide classification considers the anode material as a first parameter and the electrolyte structure as a further distinctive factor (figure 4.15).

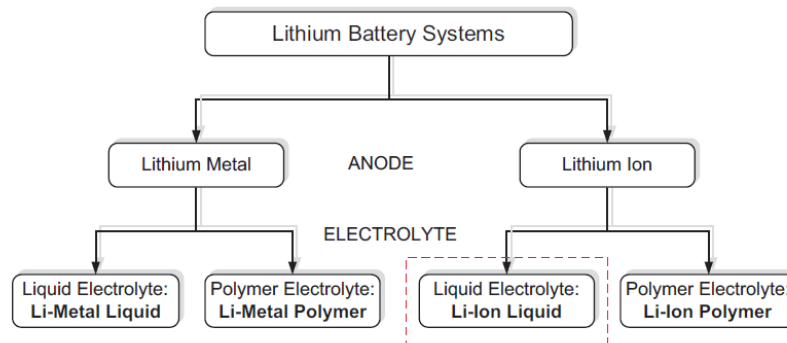


Figure 4.15: Lithium battery systems classified considering anode and electrolyte characteristics [77]

From Lithium Metal to Lithium-Ions [77]

Alkali metals, in particular Lithium, are optimal candidates as Anode:

- High cell voltage (up to 4V) that allows to reduce the cell's number in a module
- High specific energy (beyond 200 Wh/Kg)
- Wide range of operating temperatures
- High power density
- Flat discharge profiles
- Longer shelf life

But many issue are related to such a type of anode:

- High reactivity with water
- Not uniform plating during the charge
- Risk of dendritic short-circuit
- Overheating

For these reasons, nowadays almost all BEVs are based on the Lithium-Ions batteries, with different chemistry, structures and manufacturing processes for Anode and Cathode: these characteristics allow to optimize the battery cell performance to satisfy a set of features of interest (FOI) in the best way.

LIBs with liquid electrolyte

Looking at the most diffused solutions in the current scenario, the Anode is made by a graphitic carbon with a layering structure, the Cathode is made by a Lithium metal oxide and finally the electrolyte is a solution of lithium salt in a mixed organic solvent (this element works as a carrier for ion flow between the electrodes).

It's out of the objective of this work to enter in the details but just a recap of the functioning mechanism of the most important examples on the market will be done.

The base mechanism of the Li-Ion batteries is the intercalation and de-intercalation of the positive Lithium ions inside the electrodes materials matrixes, possibly in a reversible way and without excessive deformation and stresses (figure 4.16).

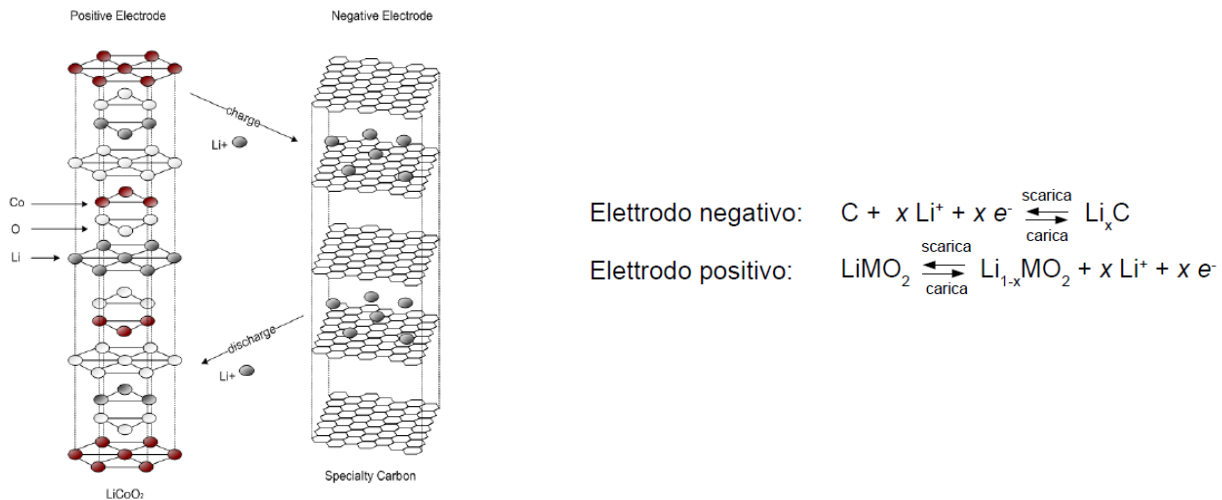


Figure 4.16: Intercalation and de-intercalation mechanisms

In discharge mode the current moves out from the positive pole of the battery, through the external circuit, and free ions travel into the electrolyte between the electrodes; the reverse process occurs during the charge mode, as clearly depicted in figure 4.17.

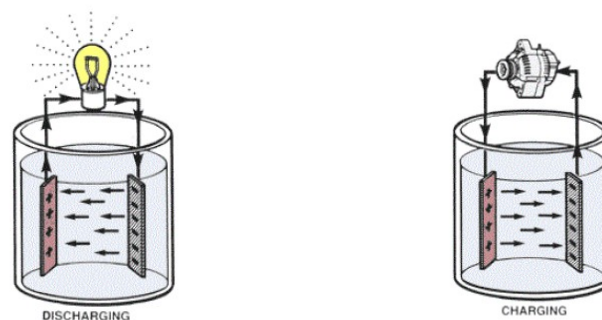


Figure 4.17: Charge and discharge phases

Elementary electrochemical cells are then connected in series or in parallel in order to achieve the desired power/energy: generally speaking the cells must be connected in series till the necessary operating voltage is obtained then it's necessary to connect several series in parallel to reach the target capacity.

This type of batteries has several fundamental advantages that explain the success in a wide range of fields, such as the automotive and the Hi-tech industries:

- High specific energy and density
- Cell voltage between 205 and 4.2 V
- Wide range of operating temperatures
- High rate capability (up to 5C)
- Long cycle life (beyond 1000 cycles)

In automotive applications there are several important characteristics that must be carefully studied and improved:

- **Abuse tolerance:** for example, overcharging and over-discharging conditions
- **Cycle and calendar life:** due to the high costs, a battery must guarantee the required performance for at least 10 Years/150.000 Km with low degradation
- **Wide temperature range:** the operating temperatures must be considered between -30/+60 °C and an adequate heat management system must provide safety and optimal conditions
- **Environmental impact, reliability and price:** Battery reuse and material recycling plans have a fundamental role in the BEVs diffusion and sustainability

Solid-state Lithium batteries

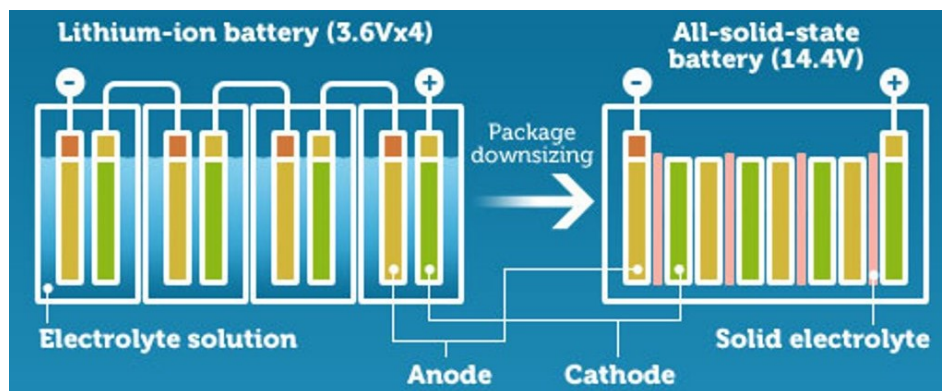


Figure 4.18: Lithium-ion battery vs Solid-state Lithium battery layouts

Solid polymer electrolytes can be classified in:

- a) Dry solid polymer electrolytes
- b) Polymer gels
- c) Polymer composites

LIBs with polymer electrolyte differ from the conventional solutions because they have conducting membranes playing the role of electrolyte (figure 4.18) offering many advantages [72][73][74][75]:

- Higher energy density
- Avoid excessive dendritic growth and then short-circuits
- Limit the electrodes volume variation
- Reduce the electrolyte reactivity
- Improve safety and abuse tolerance

There are also several drawbacks: the most important is the lower ionic conductivity of solid-electrolytes: this is particularly critical at low temperatures limiting the available specific power.

For these reasons the research is focused on the development of solid electrolytes with high ionic conductivity (should be at least between 1-10 mS/cm) in the temperature range required in the electric vehicles [71].

To obtain target requirements there are several operating conditions that must be respected: the electrolyte layers and the electrodes must be kept in strong contact, through high mounting pressures, resulting in higher manufacturing complexity and costs. Moreover, ion transporting along the polymer chains requires energy

for forming and breaking chemical bonds during the solvation of Li-ions and energy to transport the ions from one coordination site to the others.

Finally, exploiting the layer structure, of some of these electrolytes, is possible to simplify the recycle process (reducing costs). In fact, one of the most challenging and expensive process is the extraction of Lithium, from the liquid electrolytes, due to complex solutions of many compounds and solvents.

This last characteristic could be a key factor in the creation of profitable processes to recover Lithium (nowadays there is no interest in lithium recovery but, in the future, could be a necessary operation to avoid Lithium shortage).

Anode and Cathode materials

A brief description of the different chemistries will be reported and a final comparison will allow to understand strong and weak points of each solution [77] [78].

ANODE

Lithium metal anodes, despite the higher achievable performance, are affected by several serious drawbacks (high reactivity, run-away reactions, poor cycle-life...) that lead to the research of other materials suitable to build the negative electrode.

Nowadays carbon anodes are the largely diffused in the market due to their poor cost, the material availability, the high conductivity and the relative low volume change; it's a mature technology that enhanced the evolution and diffusion of Li-Ion batteries in many fields; the intercalation process exploits the graphene planes that show a good electrical conductivity and mechanical stability during the Li transport (the whole process is depicted in figure 4.19).

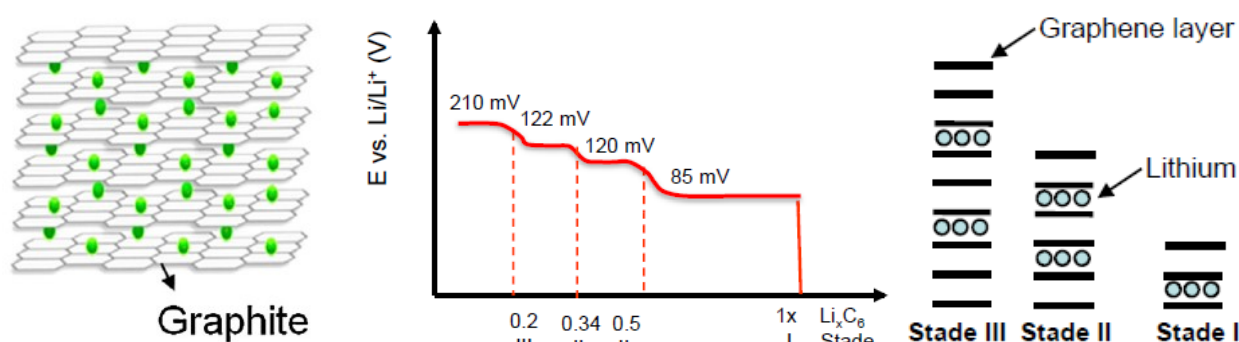


Figure 4.19: Intercalation in the graphitic anode layers with voltage evaluation in different stages [72][73]

It's possible to subdivide the carbon anodes in two categories:

- Graphitic (soft) carbons: with large grains able to achieve a capacity very close to the theoretical one but with poor compatibility with propylene carbonate electrolytes because this element intercalates in the planes causing exfoliation and strains in the anode. In the last applications, the soft carbon material is coated with a layer of amorphous carbon to protect the graphene planes.
- Hard carbons: with smaller grains and disordered orientation, are less exposed to exfoliation; very small void spaces, between the grains, allow to reduce the volume variation and to reach capacity values above the theoretical one.

Hard carbon anodes could seem as the most convenient solution due to higher performance in terms of high capacity and cycle life but, large voltage hysteresis, high irreversible losses and lower volumetric capacity leads to the scarce diffusion in the market with almost no applications.

Lithium titanium oxide

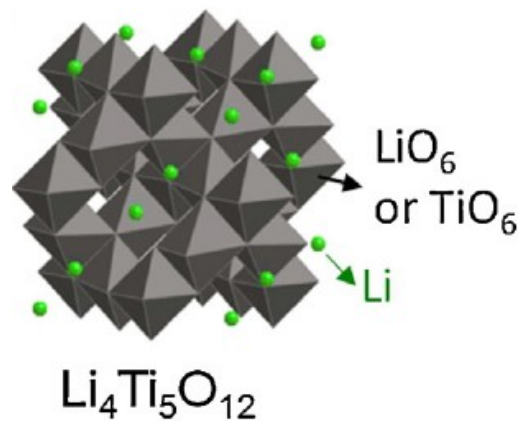


Figure 4.20: Lithium Titanate Oxide crystalline structure [78]

The lithium titanate oxide negative electrode uses a lithium titanate nanocrystals (figure 4.20) on the anode surface instead of carbon.

LTO anode have been largely commercialized achieving higher thermal stability, volumetric capacity and cycle life also if is more expensive than the carbon anode, due to the high cost of Titanium, but have lower voltage (however, this lower operating voltage brings advantages in terms of safety) and capacity.

It operates with a “zero-strain” mechanism because the intercalation and de-intercalation processes occur with just 0.2% variation in the volume.

This configuration has several other advantages:

- Small voltage hysteresis
- Low SEI growth
- Higher rate performance
- High potential prevents dendrite formation

LTO anode shows weak Lithium diffusivity and electric conductivity and side reactions take place between the electrode and the electrolyte: this last issue is often faced with a carbon coating that, especially at high temperatures, catalyse the formation of SEI.

CATHODE [77]

Intercalation cathode materials constitute a solid host for the traveling ions that are inserted, stored and removed during charge and discharge phases. The main material categories that can be evaluated as alternatives for the positive electrode are metal chalcogenides, transition metal oxides, polyanion materials. Further classifications can consider the crystalline structure of these materials: layered, olivine, spinel and tavorite (all represented in figure 4.21).

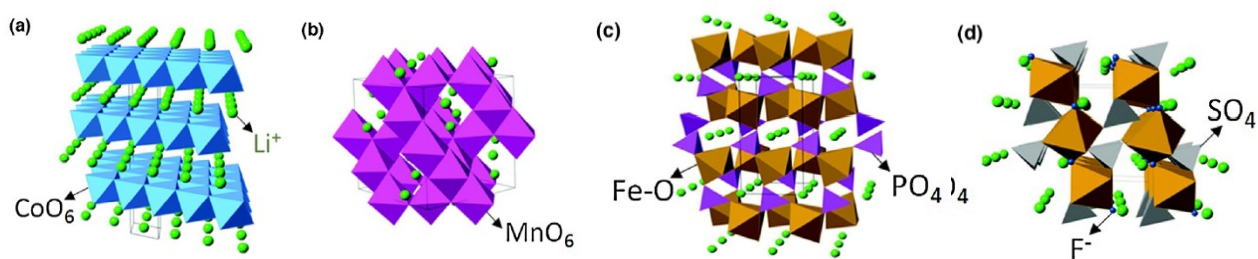


Figure 4.21: (a) layered, (b) spinel, (c) olivine, and (d) tavorite [78]

In this section will be briefly described just the most important alternatives among the transition metal oxides because they show, higher operating voltage and higher specific energy.

Lithium cobalt oxide-based batteries (LCO)

The lithium cobalt oxide (LiCoO_2) based battery is a mature battery technology characterized by long cycle life time and high energy density.

LCO consists of a cobalt oxide positive electrode, as cathode, and a graphite carbon negative electrode as anode (LCO cell is rated at 3.7 V).

Cobalt and Lithium are located in the octahedral sites occupying alternating layers; the high specific capacity (theoretically around 274 mAh/g) and high volumetric capacity (theoretically around 1363 mAh/cm³) together with low self-discharge properties are among the best characteristics of this solution.

High cost, low thermal stability and safety issues are fundamental weaknesses: above a certain temperature the exothermic release of oxygen leads to an irreversible run-away process.

This dangerous behaviour is common for all the transition metal oxide cathodes but, LCO chemistry is one of the most affected due to the very low thermal stability: this phenomenon is highly influenced also by cell design choices and manufacturing process.

Deep cycling, very common condition in BEVs, induces distortion of the octahedral structure reducing significantly the cycle life.

Then due to concerns with safety and reliability and high price of Cobalt, LCO batteries are not an ideal solution for automotive applications (at least for large-scale production volumes).

Many other elements were studied to substitute the Cobalt as dopant but all with poor performance results.

Lithium manganese oxide-based batteries (LMO)

The lithium manganese oxide (LiMn_2O_4) based battery, have a higher nominal voltage rated between 3.8 and 4 V but with a lower energy density (approximately 20% less) than the previous solution.

Manganese is much cheaper than the other cathode materials and it's also less toxic compared to Nickel and Cobalt. Other important attributes of LMO battery cells are high thermal stability and improved safety.

There are many drawbacks that lead to difficulties in the adoption of such a chemistry for the automotive field: the most relevant are the short cycle life, due to change in the crystalline structure from layered to spinel layouts during operation, high capacity losses and low specific power.

In all the cathodes containing fraction of Manganese, dissolution in electrolyte has been observed with destabilizing effects on the carbon anode chemical equilibrium (not in LTO anodes): this phenomenon increases with ageing and leads to an acceleration of the SEI growth with increase in the anode impedance

Lithium nickel oxide-based batteries (LNO)

The lithium nickel oxide (LiNiO_2) based battery has the same crystal structure of the LCO type and a similar specific capacity (275 mAh/g) but with a lower cost: for this reason, it's particularly interesting and there are many research activities.

Also in this case the high energy density is accompanied with a very low thermal stability (Ni^{3+} ions are more readily reduced than Co^{3+}) and a cell voltage below 3.6 V.

However, pure LNO cathodes are not common because Ni^{2+} ions substitute the Li^{+} ions in the intercalation sites during cycling, blocking the Lithium diffusion.

To solve the most significative issues, an effective way was to substitute a fraction of Nickel with Cobalt, reducing the cationic disorder, to dope the electrode with Magnesium increasing the thermal stability at high SoC and to include a small fraction of Aluminium improving both thermal stability and electrochemical performance.

Lithium nickel cobalt aluminium oxide-based batteries (NCA)

The lithium nickel cobalt aluminium oxide (LiNiCoAlO_2) based battery, has a lower voltage and a better safety characteristic, compared with LCO; it's widely adopted in automotive industry, i.e. in Tesla vehicles due to good characteristics in terms of power density, energy density and lifespan.

Thermal management is crucial since this cathode typology suffers of high capacity fade at high temperatures (more than 40-50°C) due to high SEI growth rates.

Lithium nickel manganese oxide-based batteries (NMO)

It's an interesting solution thanks to the high energy density (near to that of LCO) but with a reduced cost due to lower Cobalt content. Nickel allows to enhance the Lithium extraction capacity but may result in cation disorder and then low Li-Ions diffusivity and low C-rates capability.

In the last models synthetized through ion exchange method, has been achieved a good specific capacity (around 180 mAh/g) and good response at high C-rates.

Lithium nickel manganese cobalt oxide-based batteries (NMC)

The cathode of lithium nickel manganese cobalt oxide, LiNiMnCoO_2 (NMC) is composed by Cobalt, Nickel and Manganese (most commonly used NMC composition contains equal amount of all three transition metals) reaching very good results in terms of high capacity, rate capability and high voltages.

NMC cathode materials for LIBs have been attractive in recent years because of their higher capacity and lower cost compared with commercial LCO ones. [79]

One of the critical issue is the continuous voltage fade during cycling with decrease in energy density, limiting the useful life in automotive applications where long-term performance must be achieved, to overcome this problem have been considered variations in the crystalline structure (passing from layered to spinel structures), doping and coatings.

Lithium iron phosphate-based batteries (LFP)

Lithium iron phosphate (LiFePO_4) based battery represents an extremely attractive battery chemistry, due to characteristics such as high capacity, low cost, flat voltage profile, low environmental impact and high safety degree. Moreover, LFP batteries are considered suitable for being used in stationary, automotive and back-up power applications. This chemistry has lower specific energy with respect to LCO, higher safety levels (highest among the alternatives), low cost due to the absence of Cobalt and low environmental impact making this typology one of the most promising player in the EV diffusion challenge.

To conclude, the described chemistries can be summarised in a table with the theoretical performance achieved, highlighting the intrinsic characteristics of each solution in order to select the most convenient alternative for different missions.

Material	Specific capacity [mAh/g]	Nom. voltage [V]	Energy density [Wh/kg]	Cycle life [cycles]	Properties
LCO	140	3.7	110 - 190	500 - 1000	High safety risk, good lifetime
LMO	146	3.8	100 - 120	1000	Cheaper, safer than LiCoO_2 and LiNiO_2
NCA	180	3.6	100 - 150	2000 - 3000	High energy, high density, expensive
NMC	145	3.6	100 - 170	2000 - 3000	High voltage, good specific capacity, high safety risk, good lifetime
LFP	170	3.3	90 - 115	> 3000	Long lifetime, high stability, basic low cost
LTO	170	2.2	60 - 75	> 5000	Negligible volume expansion, basic low cost, stable electrochemical operation, high thermal stability

Figure 4.22: Technical comparison among many electrodes' chemistries

Comparison of Li-ion battery chemistries

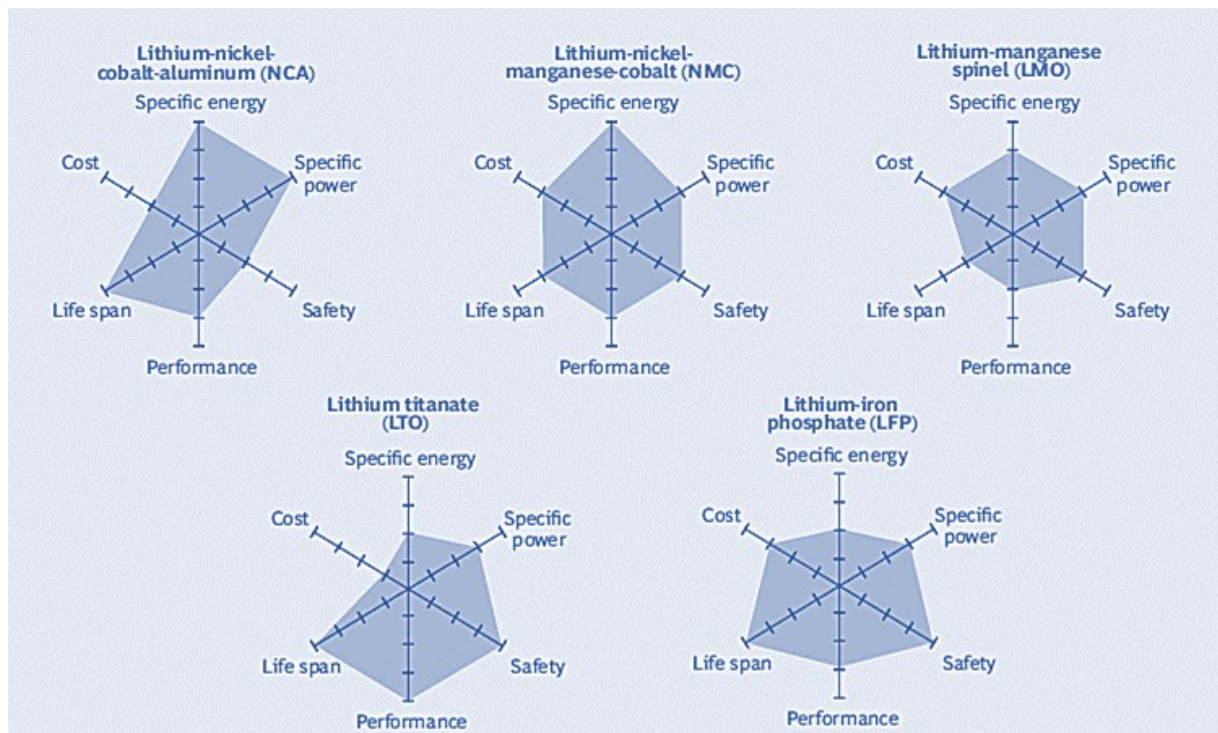


Figure 4.23: Graphical characterization of the features of interest among different Li-Ion chemistries [80]

Li-ion battery chemistries can be compared considering six main features of interest [80]:

- Specific energy [Wh/kg]
- Specific power [W/kg]
- Safety
- Performance
- Life span
- Cost

It's evident how the selection of the chemistry must be a function of the performance target that must be achieved and then of the working conditions.

Li-ion batteries: stationary vs automotive applications

As said before, the chemistry, the manufacturing process and the layout of a battery pack can lead to different performance, then the target that must be achieved influences the choice of the typology.

A further classification can then be made as a function of the purpose and the services that the battery system must accomplish. The classification based on the application becomes less relevant speaking about the V2G services, in which these two categories are coexistent; a trade-off between the automotive requirements and the services performance must be obtained (the vehicle requirements in terms of range, power and durability must have the priority to not affect the user experience).

Automotive applications

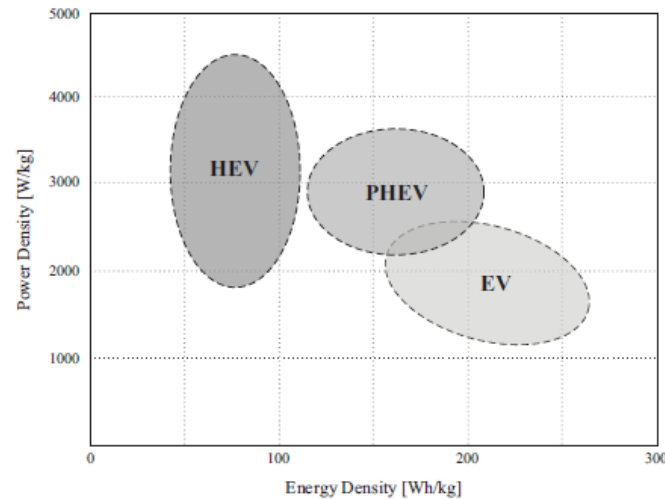


Figure 4.24: Requirements of the battery pack for different electrification levels [77]

In the automotive field, different behaviours are requested to the battery system of different vehicles, then considering three main electrification levels (figure 4.24):

EVs) This kind of vehicles need the largest energy amount in order to ensure the longer driving ranges; at the same time there is a necessity of high output power to ensure the driving performance.

Other important factors are the requirement of a long life-time and the necessity to support high charging power to reduce the charge time, indeed these vehicles have a larger capacity with respect to the other ones.

The necessity to reach the longest possible driving range leads to high Depth of Discharge (DoD) and, due to the consequent higher stress working in these operating conditions, abuse tolerance must be improved.

Nevertheless, requirements in terms of lifespan must respect the automotive standards (10 years/100.000 Km) making challenging to obtain a battery pack with sufficient performance.

HEVs) There is an integration of a traditional powertrain with one or more moto-generators and a battery pack, but of course the main energy source is the fuel tank that feeds the internal combustion engine; the electric traction system helps the vehicle during accelerations and to recover the energy during braking.

Electric energy stored in the battery pack comes totally from the fuel burnt in the ICE and from the recovered kinetic energy (there is not the possibility to connect the battery pack to the grid for charging operations).

For this reason, there are low energy requirements (On-Board storage system shows a low capacity) but high-power requirements (in terms of power density).

PHEVs) It's an intermediate solution, this time the vehicle can be purely electric (at high SoC) for short/medium ranges, actuated with both electrical and ICE powertrains or driven just by the ICE.

This kind of vehicle shows the maximum flexibility and, as said before, have characteristics between the other two architectures as can be seen from pictures 4.24 and 4.25.

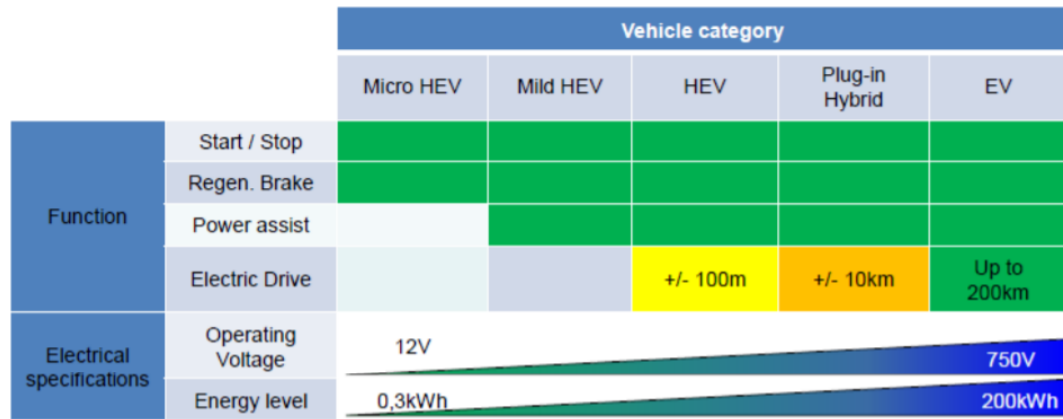


Figure 4.25: Distribution of the main electrical specifications among different electrification levels

As said, different layouts lead to different usage profiles:

- Charge Depletion mode: The battery is fully charged through an external source and progressively depleted during the driving; then the battery is sized to get the maximum specific energy (BEVs)
- Charge Sustaining mode: The battery is continuously charged and discharged around a target SoC and the design tries to maximize the specific power (HEVs and FCHEVs)
- Dual mode: at the beginning (max SoC) the vehicle is in CD mode but can be switched to CS; the priority is the power but enough energy must be able to assure a pure electric range (PHEVs).

Stationary applications

Among the possible features of storage systems for stationary applications, frequency regulation (upward and downward) is the most interesting: it's a method to improve and accelerate the penetration of RES reducing the effort from the centralized system and improving power quality and reliability.

The key parameter, in order to get the minimum cost from the battery degradation, is the lifetime of the ESS: in first approximations and considering Li-ion batteries, the services implying small oscillation in the state of charge seem to be the less impacting on the battery life.

The evolution of this work has the scope to identify V2G operating conditions, during the ancillary service supply, that minimize the degradation of the battery pack, then affecting in the best possible way, the durability of the ESS.

After these conditions will be identified, the study will allow to understand which V2G applications can be suitable to respect these requirements describing the potentiality and the effect of such a utilization.

Service	Energy storage requirement							Applications	Li-ion battery chemistries						
	High power	High energy	Long cycle life at partial cycle	Long cycle life at full cycle	Low cost/cycle	Fast response	Low self-discharge		LCO	LMO	LNO	NCA	NMC	LFP	LTO
Grid frequency regulation	✓		✓	✓	✓	✓		Stationary	Grid frequency regulation			✓		✓	✓
Forecast accuracy improvement	✓	✓	✓		✓				Forecast accuracy improvement			✓	✓	✓	
Power gradient reduction	✓		✓		✓	✓			Power gradient reduction	✓	✓	✓	✓	✓	✓
Peak shaving		✓													
Black start		✓		✓			✓	Automotive	EV	✓	✓		✓	✓	
Energy arbitrage		✓		✓			✓		HEV	✓	✓		✓	✓	✓
									PHEV		✓		✓	✓	✓
								Back-up	UPS			✓	✓	✓	

Figure 4.26: Energy storage requirements to supply different grid-support services (on the left) and feasibility analysis of different Li-ion chemistries to satisfy stationary/automotive targets (on the right) from [77]

In [77] a first analysis compared different Li-Ion chemistries with respect to the feasibility in supplying both stationary and automotive services also highlighting the required features: it's possible to see in figure 4.26 that NMC and LFP chemistries show the highest flexibility and could be candidates in V2G applications.

4.2.2) Main degradation mechanisms

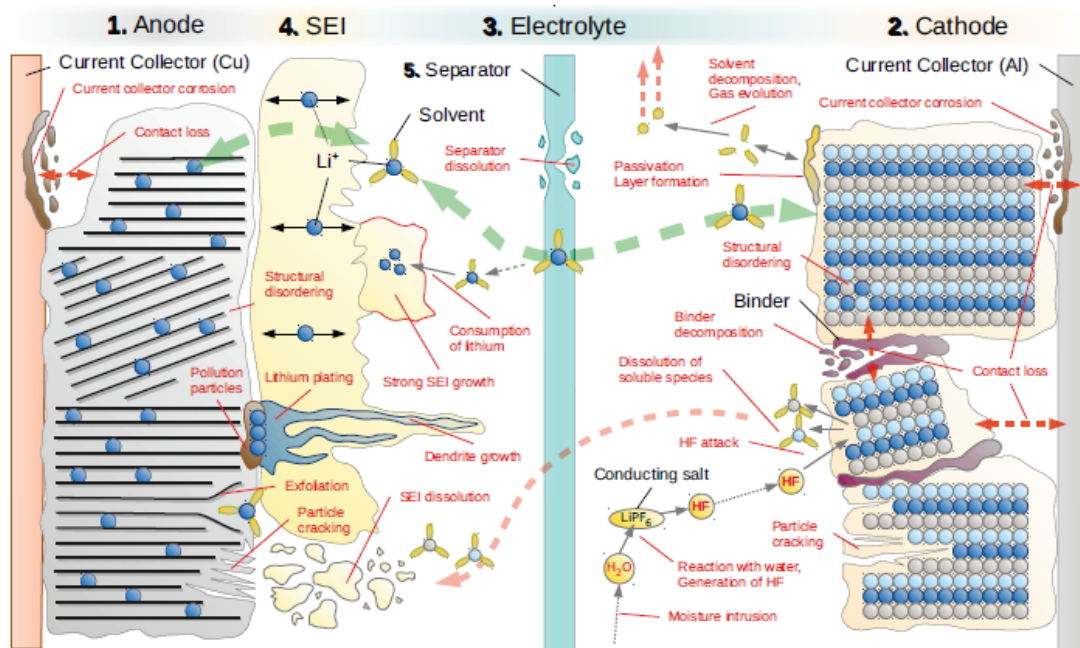


Figure 4.27: Review on the aging mechanisms in Li-ion batteries for electric vehicles based on the FMEA method [81]

The degradation of Lithium-ion batteries is a complex process and is characterized by different intrinsic and extrinsic factors. [72][73][74][81]

Intrinsic factors: manufacturing processes, types of materials used, quality controls and battery design.

Extrinsic factors: Operating conditions, current and temperature distributions and unbalance in the battery pack.

In the next pages will be presented the mechanisms (illustrated in detail in figure 4.27) participating to the ageing of the Li-ion batteries' components.

Anode)

Speaking about carbon anode (the most diffused in the market) there are several major phenomena affecting the performance of the system:

- **Current collector corrosion:** the corrosion can lead to the contact loss and then to an increased internal resistance (particularly serious with copper collectors). Collector corrosion is promoted by potential values close or above than its electrochemical stability window that is dependent on the material and on the cell design.

- **Change in anode structure:** effect deriving from a structural disordering of the inner particles of the electrode due to mechanical stresses, vibrations and/or temperature variations. Another phenomenon is the change in the morphological structure at the electrode surface mainly due to solvent intercalation in the graphitic material.
- **Lithium plating:** catalysed by high charging currents and low temperatures, positive Li-ions intercalation does not occur enough fast and then metallic Li it's deposited on the anode surface.

A further development of the process leads to the growth of these deposits (dendrites) and the risk of damaging of the separator causing dangerous short-circuits.

Intercalation and de-intercalation in the negative electrode (at potentials close to that of Li/Li^+) constitutes one of the biggest advantages in the use of carbon anodes: on the contrary at very low potentials Li^+ ions can be deposited in metallic form on the surface creating obstacles to the intercalation phase. The process is not completely reversible since Lithium, also if dissolved again, may form other compounds.

- **SEI layer:** The electrode surface state is one of the most important aspects influencing the battery performance [81]; one of the fundamental mechanisms is the formation of an irreversible passive layer on the Anode. Being the result of the decomposition of the electrolyte, this layer is called SEI (Solid Electrolyte Interphase); can work as a protection layer that avoid further decomposition in the liquid carrier, protecting the graphite anode from exfoliation or, if excessively thick, can bring to a severe capacity loss (figure 4.28).

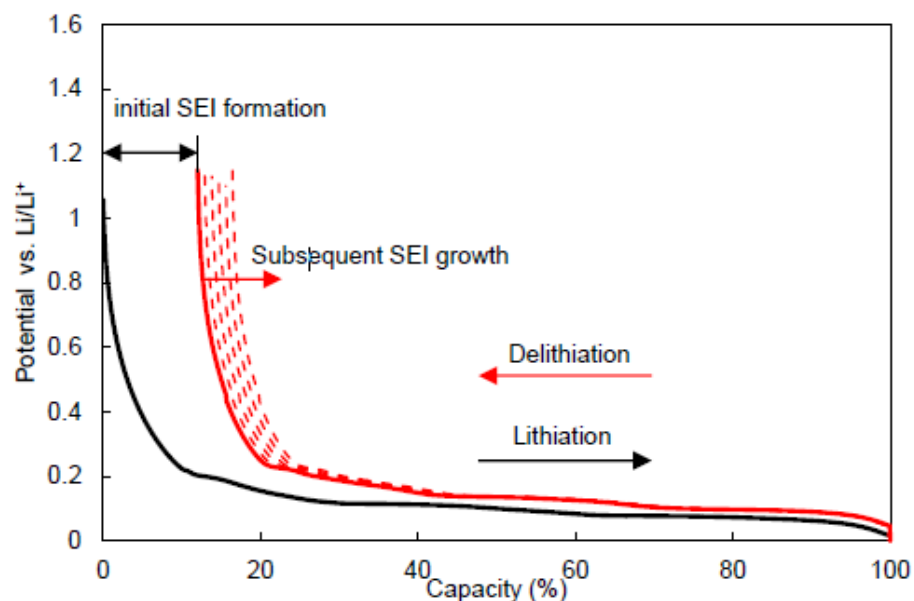


Figure 4.28: SEI layer growth and corresponding evolution in potential vs capacity plot [90]

Solid Electrolyte Interphase formation occurs due to the electrochemical instability of graphite when is in contact with the most common liquid electrolytes.

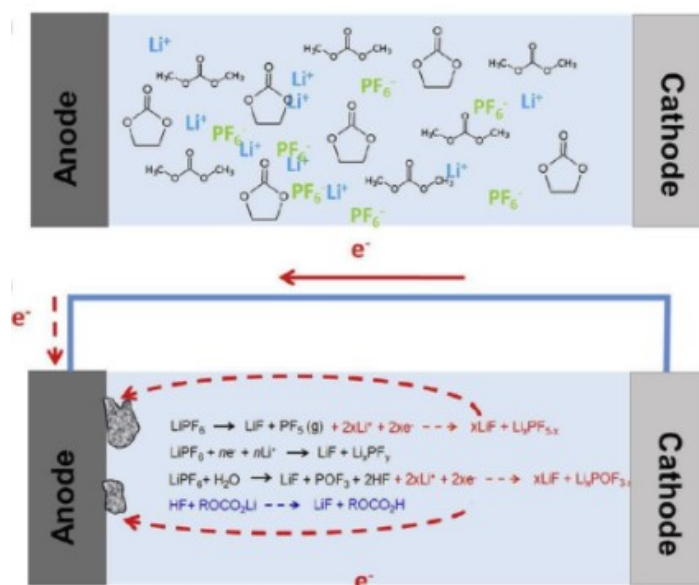


Figure 4.29: representation of the SEI formation in early steps [73]

During the first cycles Lithium reacts with the anode surface creating a thin SEI layer. If the thickness does not grow too much (and then there is not a high lithium consumption) the ion conductivity of the electrode is not deeply affected and a stable condition can be reached but if the process continues further formation of SEI would have a significant effect on the cell's impedance. Then a certain limit must not be overtaken but, at the same time, without SEI the anode would be subjected to continuous side reactions resulting in very poor lifespan.

High temperatures and volume variation during deep cycling (intercalation and de-intercalation in the host matrix) can induce respectively to dissociation and cracks in the surface film, then to Lithium inventory losses.



Figure 4.30: representation of the SEI formation in final steps [73]

Then the SEI layer should be stable along different cycles, along a wide range of temperatures and without excessive water content, but moreover should be homogeneous avoiding unbalances on the electrode surface. The generic schematization of the process and the structure of the SEI layer are summarized in figures 4.29 and 4.30; obviously the composition can vary as a function of the solvent type, concentration and contaminants.

Cathode)

The most significant mechanisms are:

- **Current collector corrosion:** due to the vulnerability of the Aluminium there are reactions with the electrolyte especially working at low SoC where the anode potential becomes to positive versus Li/Li⁺. This could lead to loss in contact between the current collector and the cathode material and also to products with poor electronic conductivity causing overpotentials, current unbalances and Lithium plating.
- **Change in the cathode morphology:** variation in the available surface with respect to the initial conditions it's caused by volume expansion and contraction inducing stress in the host matrix and then crystalline disorder and cracks on the surface.
- **Decomposition of the binder:** again, it's a phenomenon similar to the one described for the anode and is accelerated during operations at low SoC.
- **Contamination and dissolution of the soluble species:** performance decreases due to the presence of air and vapour in the cell; other contaminations derive from manufacturing processes and from electrodes active materials dissolution and SEI dissolution (it's a critical issue in LMO cathodes).

The classification reported in figure 4.31 helps to correlate original causes with the main degradation mechanisms that are finally classified in three main degradation modes.

Moreover, this useful representation, highlights the links of each stress factor with the successive ageing mechanisms/ modes till the final effects on the battery performance: power and capacity fade phenomena.

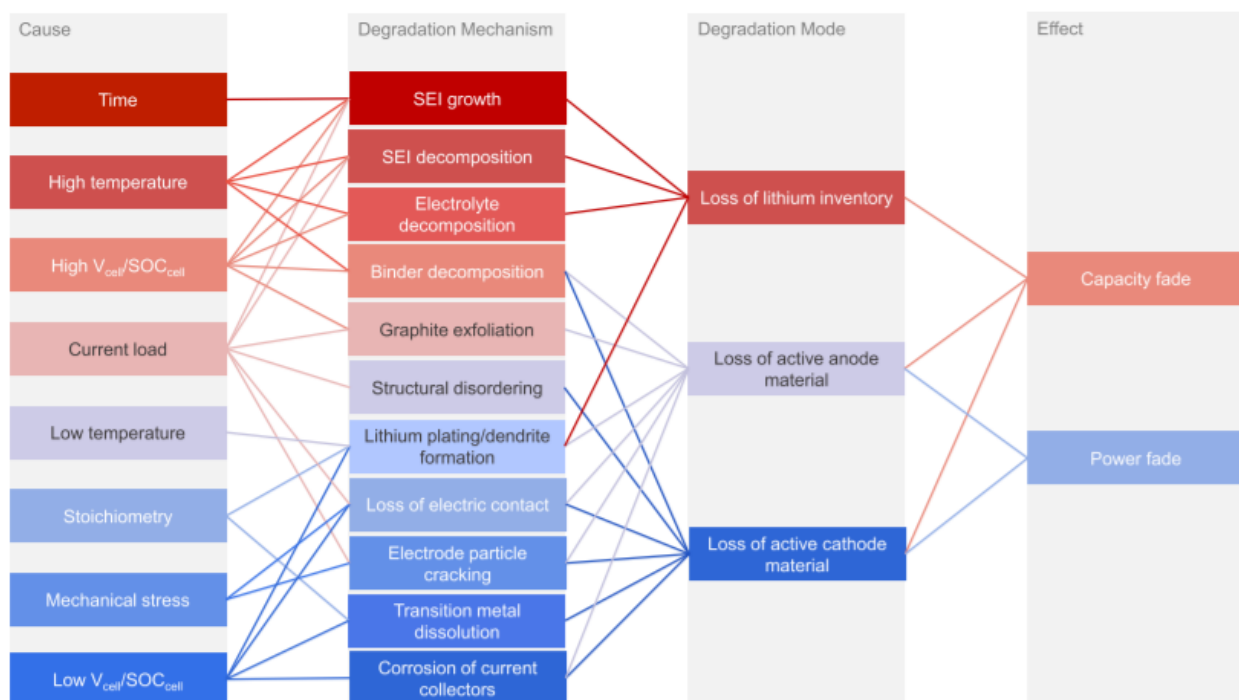


Figure 4.31: Interconnections between stress factors, degradation mechanisms, degradation modes and effects

4.2.3) BMS and On-Board control strategies

High level communication between the vehicle and the Electric Vehicle Service Equipment (EVSE) is fundamental to manage smartly the charging operation and this become even more important in V2G application where complex strategies are implemented. The communication protocol (IEC 61851-1) enables the high-level communication through the pilot wire in the charging cable (in each the levels as represented in figure 4.32).

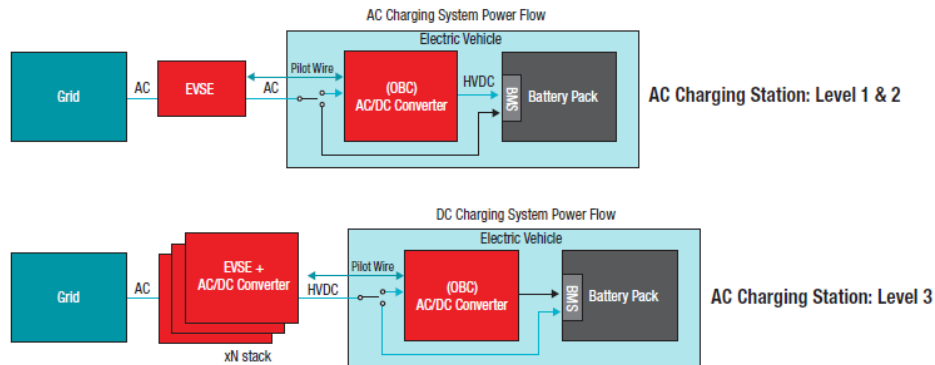


Figure 4.32: AC and DC charging systems power flows

A microcontroller (MCU) manages the monitoring, control and communications circuits [82], while one or more communications ports complete the EVSE.

In EVSE the pilot port lets the AC source to “talk” with the vehicle (On-Board charger and its battery system). The “pilot” wire allows data communication between the vehicle and the charging station: the charge starts just if the following information are verified:

- Vehicle connection
- Vehicle earthing
- Indication of the maximum power allowed by the charger

As far as the voltage is concerned: for single-phase solutions, the voltage is between 208-240 Vac while for the three-phase ones it’s between 360-440 Vac.

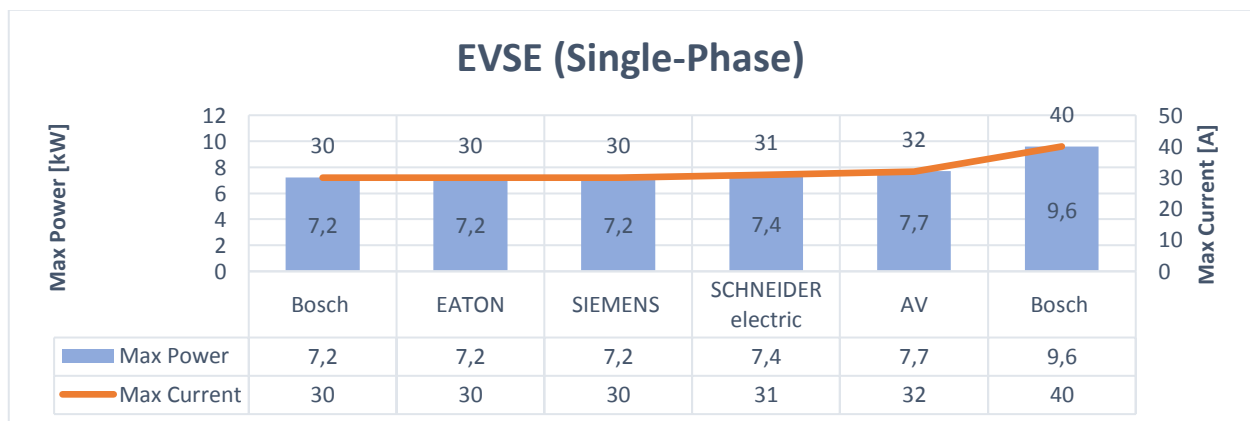


Figure 4.33: List of some EVSE on the market and relative values of output power and current

Thanks to the EVSE it's possible to control the charging rate acting on the charging current; in some cases, the limit of the household fuses constrains the operation and the EVSE de-rates the charge to avoid damages.

In figure 4.33 several EVSE on the market are classified considering maximum output power and current (these devices can manage the charging process inside these limits): the connection of BEVs through an EVSE can be suitable for level 1 and level 2 charging operations. In many nations this kind of systems are mandatory to assure the required safety standards, especially in case of domestic charge.

Battery Management Systems (BMSs)

HEVs and BEVs are equipped with battery management systems (BMS), which monitor the battery (terminal voltage, terminal current, temperature) in real time and estimate the SoH during everyday use by rather complex algorithms, to early detect the onset of critical failure conditions for timely battery replacement. This On-Board technology is still in early stage of development: differs from the equivalent systems in portable devices because in these applications there are hundreds of batteries connected to reach targets in terms of high power, high energy then high voltage and current.

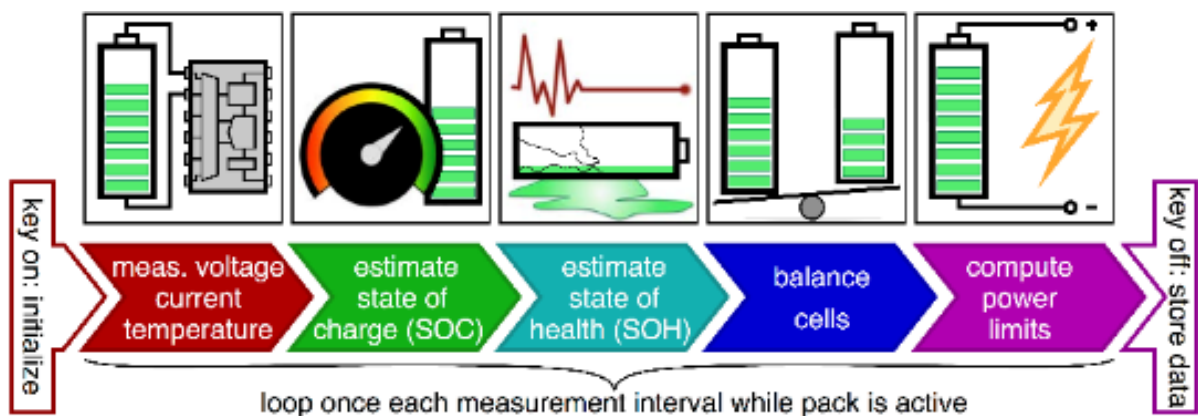


Figure 4.34: features and processes running inside a BMS

Manufacturing differences among the modules are the reasons of degenerative behaviours (due to cell-to-cell variations) causing:

- Performance reduction
- Irreversible damages

Thus, it's a control system of the battery pack with diagnosis and safety functions managing high voltage devices and coordinating cells-balancing and the thermal balance (figure 4.34).

Another task is to minimize the performance reduction, then to improve the lifetime, with the actuation of the thermal management system (active or passive) keeping the modules in a temperature and voltage window (figure 4.35).

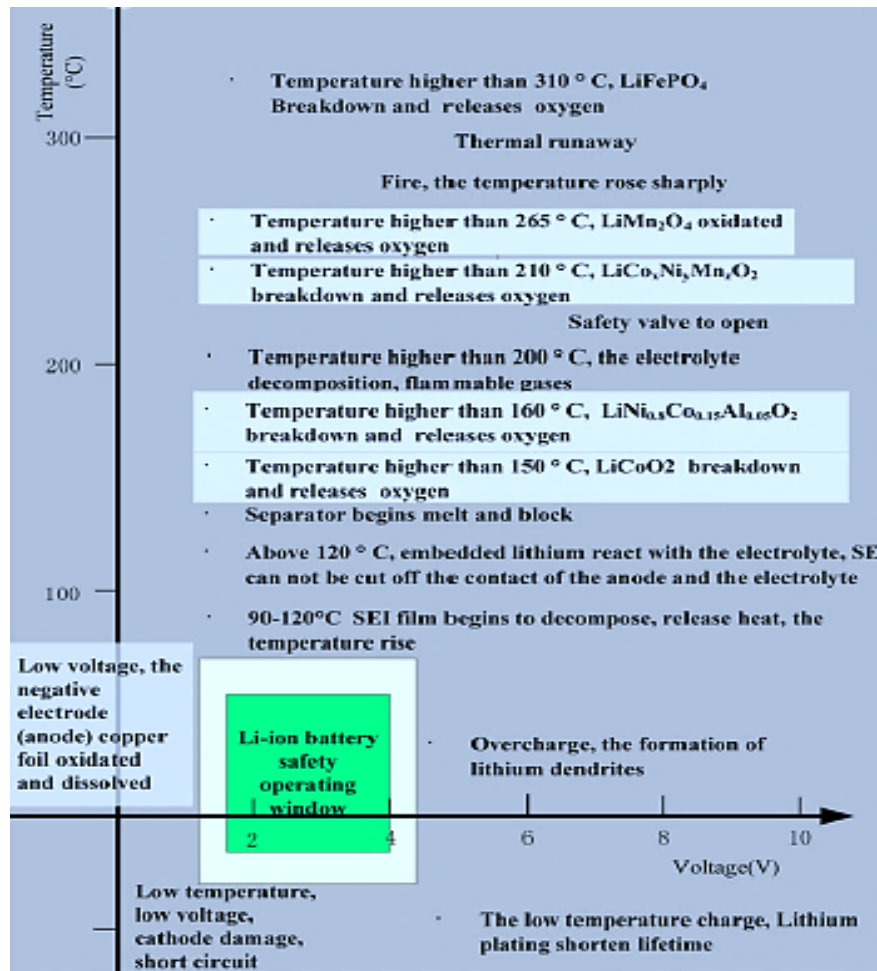


Figure 4.35: Safety operating window for Li-Ion batteries [84]

BMSs can be designed using a variety of functional blocks and design techniques: battery requirements and targets will guide in the choice of architecture, functional blocks and related ICs to create layout and strategies to optimize battery lifespan.

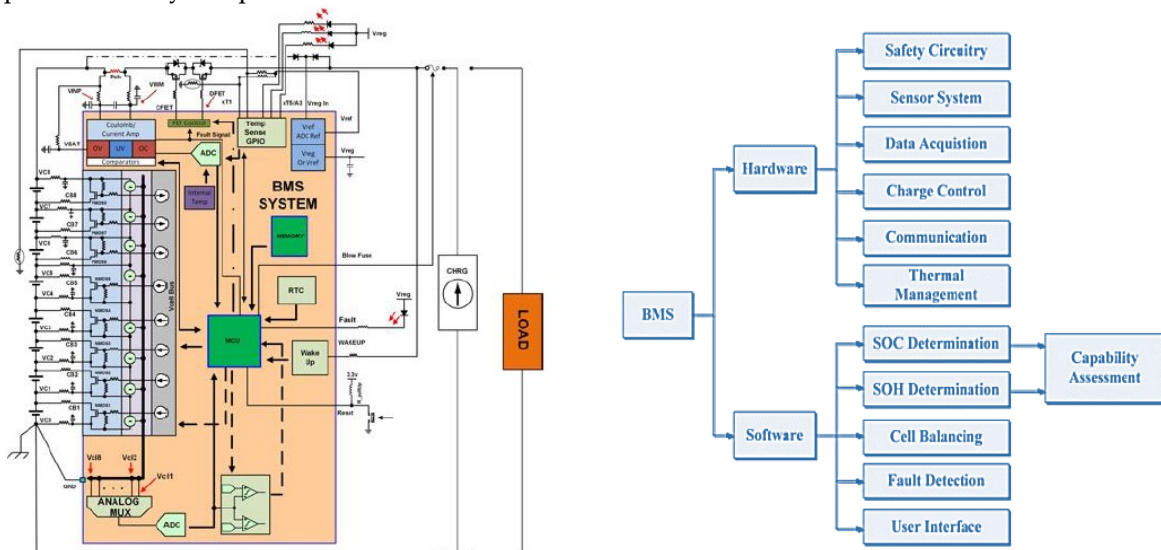


Figure 4.36: Building blocks of a BMS (on the left [83]) and list of the main hardware/software sub-systems [86]

Hardware

A short and concise description of the main building blocks in the structure of a BMS will be reported [83]: among the many functional blocks it's worthwhile to list cut-off FETs (field-effect transistors) and FET driver, fuel gauge, cell voltage and temperatures monitors, cell voltage balance, real time clock and a state machine (operable to receive outputs from the comparators and generate a digital output).

The schemes of the functional blocks vary with the complexity of the BMS that could be a simple analogic front-end or a standalone integrated device.

FET driver it's the block that has the role to isolate the battery from the load and the charger and it's driven by data coming from other blocks: battery cell voltages, currents and real-time detection circuitry status.

This component must be designed to be connected at the high or low side of the battery pack: in the first case the system requires a charge pump to activate FETs but obtaining a solid ground reference for the rest phase, while in the second case it's possible to reduce the costs, not requiring high voltage devices, but could be affected by noise in the measures with impact on the performance.

Fuel gauge tracks the charge entering and exiting (product between current and time), and can be designed to measure the current at high or low resolution.

In the generic layout there are a current amplifier and a MCU (micro-controller unit) with a low/high resolution ADC (analogic-digital converter) but in the low-resolution layout just poor dynamic performance can be achieved.

On the contrary, high resolution ADC guarantees rapid response in case of erratic connections, avoiding the formation of high frequency spikes delivered to the load.

Erratic behaving loads require fast scan times to monitor a cell's out of bounds condition: SAR ADCs are often used to achieve fast measurements in short periods but consume more power and have less resolution.

Most of the blocks that are used to obtain measures are connected to analogic comparators and with the FET driver to monitor short-circuit or over-currents events minimizing the response latency.

Cell voltage monitoring and balance

The equilibrium among the cells must be guaranteed as much as possible (during cycling the cells are subjected to different operating conditions and then unbalances), in terms of voltage, SoC and temperatures; this is one of the critical issues that must be faced to prolong the battery lifetime.

All the cells must operate inside a determined voltage window (dependent on the electrodes chemistry) and during charging and discharging some limits must not be overtaken otherwise the battery life can be seriously affected.

The task to keep an adequate level of homogeneity among the cell's voltage isn't easy: cells are connected in series to build modules (to increase the overall voltage) that, one more time, are connected in parallel to get the final layout of the battery pack. This complex structure, composed by many cells, must be controlled because assuming great unbalance, the first cell to reach the upper voltage limit during the charge phase, would stop the recharge also of the cells at lower SoC limiting the total capacity of the battery pack. In the same way during discharge, the first cell to reach the lower admissible voltage level, would cause a range limitation also if other cells have residual charge.

For these reasons, the BMS must assure an optimized charge scheme to assure the higher possible balance and uniformity among cells, this operation will affect directly the cycle number and the battery life.

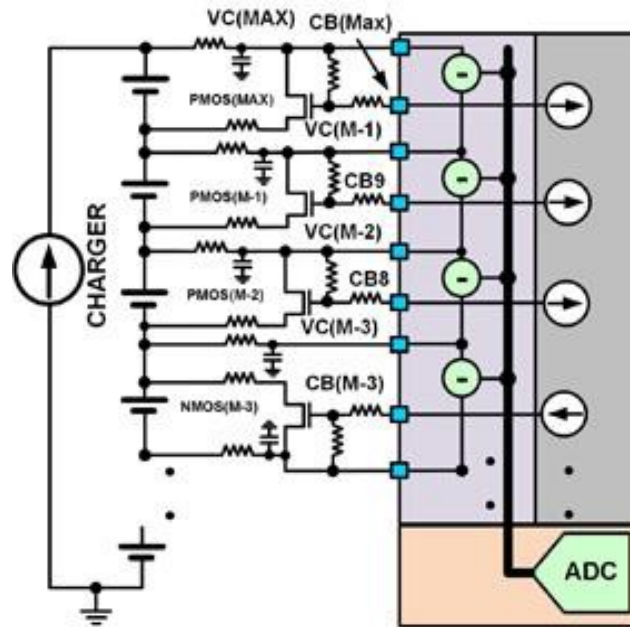


Figure 4.37: Bypass Cell Balancing FETs Used to Slow the Charge Rate of a Cell During the Charging [83]

There are two main architecture and charging/discharging strategies that allow to minimize cell-to-cell differences: with the layout represented in the figure 4.37, it's possible to slow down the charge of the strongest cell (alpha cell) to allow the weakest cells to complete the charging procedure. Results are obtained through a by-pass FET that connects the cells to a resistor limiting the charging current in order to allow the other units to reach the same maximum voltage level then maximising the capacity of the battery pack.

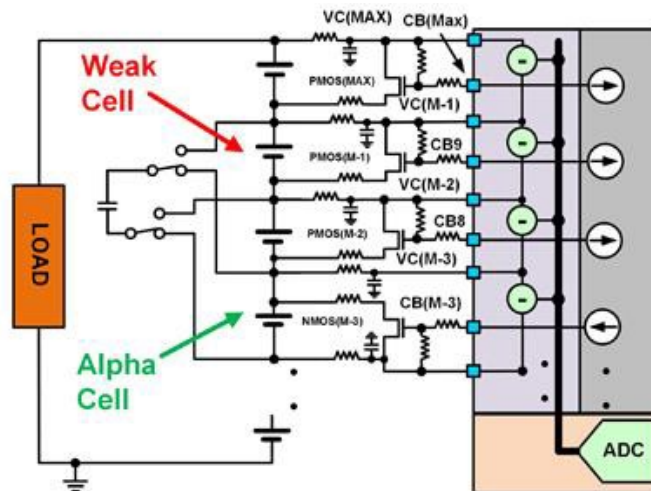


Figure 4.38: Active Balancing During the Discharge Cycle [83]

In this second scheme (figure 4.38) the so-called active balancing is implemented during discharge procedures and is achieved by taking charge via inductive coupling or capacitive storage from the strongest cell (alpha) and injecting the stored charge into the weakest cells.

It's interesting to note that more parallel connections lead to easier support to the weak cell (the charge transfer is shared by more cells in parallel) but at the same time it's tough to identify the weak cells in the battery pack. To conclude it's important to highlight that components like diodes, resistors and capacitors are widely adopted to damp the transients.

Temperature monitoring

Particular attention is required to the temperature monitoring and appropriated thermal management strategies must be adopted to assure the temperature balance among the cells in order to achieve the maximum performance and the necessary safety conditions: high unbalances could lead to uncontrollable run-away phenomena and the consequent battery auto-combustion.

Temperature sensors and thermistors are used to monitor each cell and circuit: this is done using an internal reference voltage to avoid errors due to change in the ambient conditions.

Other building blocks

Among the remaining building blocks, it's necessary to list some fundamentals components:

- Battery authentication: prevents the BMS electronics from being connected to a third-party battery pack.
- Real time clock and Memory: used for black box applications where the RTC is used for a time stamp and memory is used for storing data, allowing to know the battery pack's behaviour before a trigger event.
- Voltage reference and regulator: to power peripheral circuitry around the BMS system
- Daisy chain circuitry: used to simplify the connection between devices and replaces the need of shifting circuitry.
- The daisy chain block replaces the need for optical couplers or other level shifting circuitry.

Software [84] [85] [86]

It's the operative core of the system controlling the hardware and the signals from the sensors to estimate the best strategies to manage cell balancing, switch control and safety circuits.

The software also performs online data analysis to determine and update many key parameters (single cell voltage, overall battery voltage, total current, impedance, temperature and smoke detection) fundamental in the fault identification and state estimation.

Battery state estimation is a complex and challenging task since it's focused on the determination of SoC (estimated using voltage, current and temperature) and SoH (related to capacity fade and power fade) indexes: these values can be evaluated starting from many different working conditions and models/algorithms.

In the table below (figures 4.39) there is a list of different methods to obtain the required SoC estimation and the main advantages and disadvantages related to each solution:

Method	Advantage	Disadvantage	Input
Discharge test method	Accurate, easy	Long time needed, offline, energy loss.	Remaining charge, capacity.
Ampere-hour integral method	Easy to implement, accurate if the initial SOC value, the current measurement and the efficiency is precise.	Depends on the initial SOC value. Needs accurate value of the self-discharge rate and the coulomb efficiency. Needs high accurate measurement of the current. Not suitable for batteries under very dynamic conditions.	Current, capacity, coulomb efficiency, self-discharge rate, initial SOC value.
Open circuit voltage method	Easy to implement. Accurate.	Needs some rest time. For some kinds of battery like LFP, it is only suitable when the SOC is very high or very low.	Rest time, voltage.
Battery model-based SOC estimation method	Needs no rest time. Insensitive of the initial SOC value.	For some kinds of battery like LFP, it is only suitable when the SOC is very high or very low. Sensitive to the measure noise.	Current, voltage, Battery model.
Neural network model	Suitable for all kinds of batteries.	Needs large amount of training data.	Current, voltage, cumulative charge, initial SOC, etc.
Fuzzy logic	Fuzzy thinking of human beings.	Not accurate.	Current, voltage, etc.
Resistance based methods		AC impedance: hard and cost. DC resistance: not so accurate.	Resistance.
Weighted fusion algorithm	Consider both the Ampere-Hour integral method and the battery model-based SOC estimation method.	Lot computation. Instability if the weight factor is not suitable.	Current, voltage, capacity, coulomb efficiency, self-discharge rate, initial SOC value, Battery model.
Kalman Filter	Accurate, dynamic. Insensitive of the noise and the initial SOC value error.	Lot of computation. Complicated. Instability if the gain is undesirable.	Current, voltage, capacity, coulomb efficiency, self-discharge rate, initial SOC value, Battery model.
Sliding mode observer	Accurate, robustness, dynamic. Insensitive of the noise, model error and the initial SOC value error.	Nonlinear. Not easy to implement.	Current, voltage, capacity, coulomb efficiency, self-discharge rate, initial SOC value, Battery model.

Figure 4.39: Comparison among different SoC methods from literature [84]

Cell balancing tries to reduce the gap among SoC of the cells, this helps to reduce the risk of abnormalities and can be improved with an intelligent data control system recording historical data: all these actions are required to protect the battery from damaging and to communicate to the driver the state of the storage system.

Thermal management strategies in the BMS

The last important factor affecting the performance and lifespan of the battery pack is the architecture of the thermal management system and its strategies.

The objectives are to maintain the maximum temperature of the pack within an ideal temperature range, to ensure small local temperature differences between cells but there are also two main problems encountered at low temperatures: the drop of the available capacity and, moreover when charging at cold temperatures, the plating of metallic lithium onto the anode and the growth of SEI layer which accelerates ageing phenomena. To optimize the lifespan of the battery it's necessary to design specific warming phases, using an efficient active heating strategy and to cool-down the battery with different intensity based on the output power (there are different optimal temperature windows for different C-rates as depicted in figure 4.40).

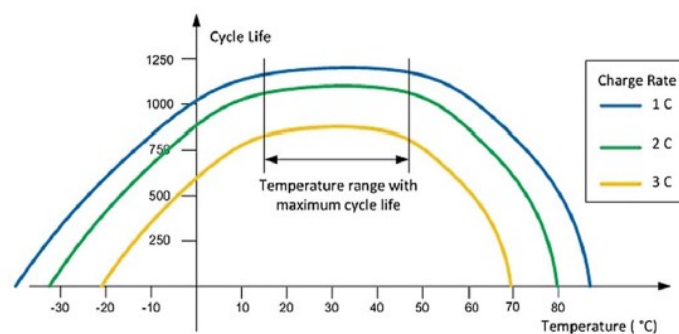


Figure 4.40: Relationship between cycle life and operating temperature for different C-rates [85]

These devices can be “active” (with external or internal heating/cooling sources) or “passive” (cooling exploiting the external air) and can also be characterized into system based on air, liquid and Phase Changing Materials (PCM). [87]

Air management

As described before, the battery pack is a complex structure of cells connected in parallel and series to build modules and the whole system; passive air cooling systems are common due to the simplicity, their low cost and the low occupied volume. Series and parallel cooling case could be considered to design the thermal balancing system but, the second one, seems to achieve better results considering the temperature distribution.

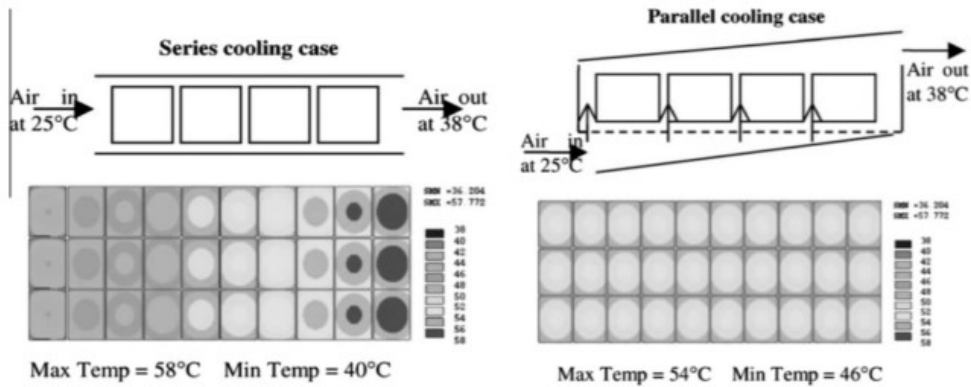


Figure 4.41: Serial and parallel cooling system layouts [87]

Active air cooling, placing fans to force the air flow in different locations of the battery pack, allows to achieve more degrees of freedom in the control strategy: one of the most efficient layouts (cooling action and cost) is the cubic arrangement with the same number of cells along the length and the width of the pack and with the fan on the top.

As anticipated, heating strategies, in cold weather, for cold start-up optimization has the target to pre-heat the battery pack, thanks to an internal or external source, allowing the battery to retain greater capacity warming the area surrounding the battery pack before to start the vehicle.

External convective heating systems, using fan and heater, require the shorter warming time but with an increase in complexity and cost.

Liquid management

Above certain temperatures ($>60^{\circ}\text{C}$) the low conductivity of air is not suitable to achieve efficient cooling operations, then at high charge/discharge rates a liquid cooling system (water, oil, acetone, glycol, or refrigerant) is more appropriate.

There are three main approaches:

- Modules surrounded by a jacket or a plate containing heating/cooling liquid
- Modules directly immersed in the heating/cooling liquid
- Heat pipes (sealed container filled with a working fluid) instead of circulating liquid

In the last architecture the working fluid is a saturated liquid that vaporizes and travels to the condenser, where it is cooled and turned back into a saturated liquid.

The condensed liquid is returned to the evaporator via the capillary process acting on the liquid phase.

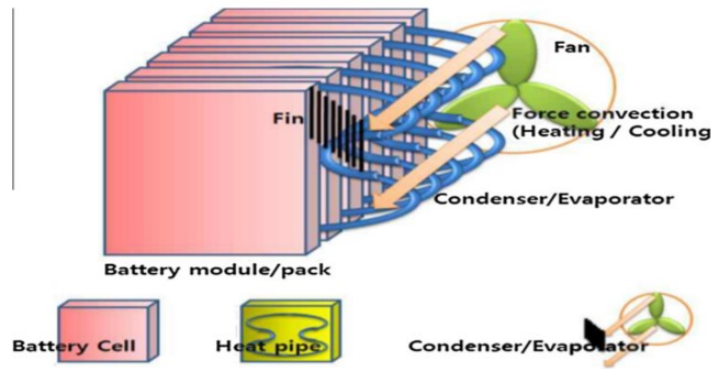


Figure 4.42: Heat-pipe battery cooling system [87]

Liquid cooling systems are often large, convoluted, and costly in terms of air vents, fans, pipes, pumps, etc.

Phase-change materials

A Phase-Change material is a substance capable of storing and releasing large amounts of heat at a given temperature as a result of its melting and solidification processes.

Heat is released or absorbed whenever the substance changes from solid to liquid and vice versa.

PCMs actually performed better results than “traditional” thermal management systems, but their development is still in the experimental phase.

PCMs can achieve higher temperature uniformity in a module regardless of whether it is under normal or stressed conditions.

For low-temperature operations, PCMs can also be used as heating materials; if the battery temperature drops below the melting point of the PCM, the heat stored by the PCM is released to the battery pack.

Development in the control strategies

SoH estimation is a crucial point in the management of the battery system and its performance; this index describes the ability of a battery to store or deliver energy and power and its evaluation is necessary to assure efficient, reliable and safe operations.

This is a challenging task because the degradation evolution is dependent on many operating conditions then the cells degrade differently depending on how are utilized.

From this necessity, several adaptive models have been developed: they are quite accurate methods but requires high computation power that could not be available in the On-Board BMSs: for this reason, advanced operando methods must be able to identify the main degradation modes and, at the same time, to maintain low computational complexity. [88]

The proposed method rely on the measurement of the voltage thus could be enough light to be suitable in BEVs/PHEVs applications.

Two promising techniques to estimate the evolution of the described ageing mechanism are reported in [89]:

- 1) Electrochemical Impedance Spectroscopy (EIS)
- 2) Incremental Capacity-Differential Voltage (IC-DV)

As already said, the target is not uniquely to estimate the entity of the degradation modes but also to use these analysis inside the control strategies of the Battery Management Systems: for this reason, the study is centred on IN-SITU methods that are suitable for real-time applications.

The configuration of the battery pack in the automotive field, with cells connected in series and parallel to obtain modules, causes uneven current distribution and then unbalances; there are also variations in the

properties due to manufacturing tolerances and operating conditions that contribute to diversify the working conditions of the cells.

Cell-to-cell SoH difference makes un-reliable evaluations of the battery aging uniquely based on the currently used indexes; improved lifetime strategies in the BMS could be achieved just with other techniques relating the DMs in a mechanistic way.

The purpose is then to substitute the SoH index (based on Capacity and Power Fade, related to the driving range and power) with indicators of the physical state of the battery, in order to forecast in a better way, the development of non-linear and/or hidden degradation mechanisms/modes.

A simple classification in [89] identifies three main degradation modes:

- Conductivity Loss (CL): affects the electronic parts of the battery and results in current collector corrosion and/or binder decomposition
- Loss of Active Material (LAM): implies structural transformation in the active material and in the electrolyte
- Loss of Lithium Inventory (LLI): variation in the number of ions available for the intercalation and the de-intercalation

The proposed step-by-step methodology has been illustrated and verified in [89] to highlight the possibility to implement on the vehicle this new diagnostic method (using NCA modules with initial unbalance between the SoH of the cells).

It's important to highlight that different electrode materials might not react in the same way to the same operating conditions: it's then necessary a large testing procedure combining as many combinations as possible (experiments in laboratory) before the implementation in the vehicle [88].

Thus, the implementation must be preceded by the compilation of multidimensional lookup tables (as shown in figure 4.43), containing experimental values describing the variation of the most important FOIs (features of interest) upon different degradation paths and operating conditions; in this way only a lookup table is embedded to the system and the SoH is estimated comparing the measured FOI values with the one recorded in the tables.

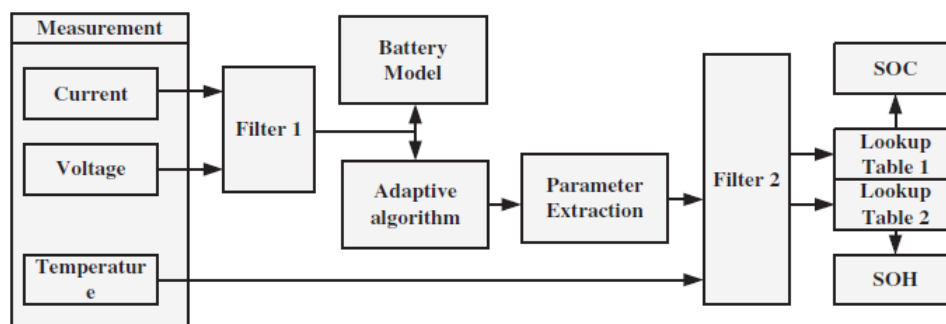


Figure 4.43: Adaptive control strategies

Drawbacks related to the difficulty in the achievement of a good Signal to Noise ratio in the EIS methodology, leads to prefer, as far as the On-Board application is concerned, the IC-DV method. Moreover, the characteristics of the actual battery management systems are not adequate, in terms of available frequencies, for the EIS spectra that covers a range between 2 mHz and 100 kHz.

Then less computational demand is a further advantage of the selected method (also filtering and differentiation steps in IC-DV procedure are less demanding than the fitting procedure used correlating EIS spectra to a representative ECM), anyway the decision to implement in the BMS a technique or another depends on many factors and pros/cons are reported in figure 4.44.

Technique	Advantages	Disadvantages
EIS	(a) Quick test duration (25 min/cell). (b) Possible for on-board implementation subject to SNR and time invariance. (c) Enable measurements at particular frequencies and SoC.	(a) Accuracy dependent on different sources: measurements and model. (b) Complex computation (requires fitting a model). (c) Not universal (model dependent).
IC-DV	(a) Accuracy dependent mostly on the measurement (C-rate used). (b) Possible for on-board implementation subject to charge/discharge C-rate. (c) Simple calculation. (d) Universal (model independent).	(a) Long test duration (10 h/cell). (b) Do not enable measurements at particular frequencies and SoC. (c) The effect of some DMs can be neglected (e.g. CL).

Figure 4.44: Advantages and disadvantages comparison between EIS and IC-DV techniques [89]

Incremental Capacity-Differential Voltage (IC-DV)

This non-invasive in-situ methodology allows to track the most important degradation modes starting from Incremental Capacity (IC) and the Differential Voltage (DV) curves. SoH estimation in the BMS must be as efficient as possible to reduce the computational resources required: in this prospective a subset of parameters involved in the analysis must be identified [88].

These “features of interest” (FOI) and their evolution can be observed in the voltage curves (and the relative IC-DV curves) and, thanks to the utilization of look-up tables describing the investigated phenomena, can be exploited to track the development of the chosen degradation mechanisms.

The process is applicable to many different cells chemistries based on the intercalation mechanism but, as described before, a deep knowledge of the ageing phenomena, for each different battery typology, must be acquired (specific multidimensional look-up tables must be embedded) in order to compare the obtained results with the historical ones.

Before to enter in the details of the procedure, it’s relevant to list some of the most important FOIs that could be considered, and for this reason it’s convenient to divide the features in four main categories (figure 4.45):

- Voltage based: peak position, front and back tail voltage, peak half width, voltage variation, resistance increase...
- Intensity based: peak intensity, intensity at front/back tails, intensity variation.
- Capacitive based: area under IC-DV curves.
- Derivative based: peak slope.

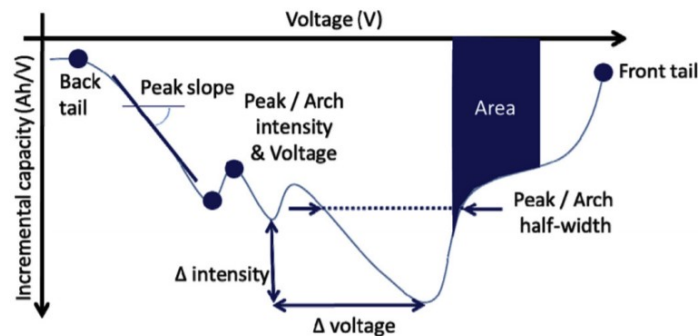


Figure 4.45: Features of interest individuated on the IC curve [88]

This selection assumes a fundamental role in the applicability to On-Board systems because, individuating a small set of essential FOIs, it's possible to reduce the database volume, required to describe the degradation modes for a determined battery chemistry, from Gigabytes to Megabytes, reducing the requirements on the BMS.

The procedure to identify the evolution of the main degradation modes can be subdivided in two main steps: [89][90][91]

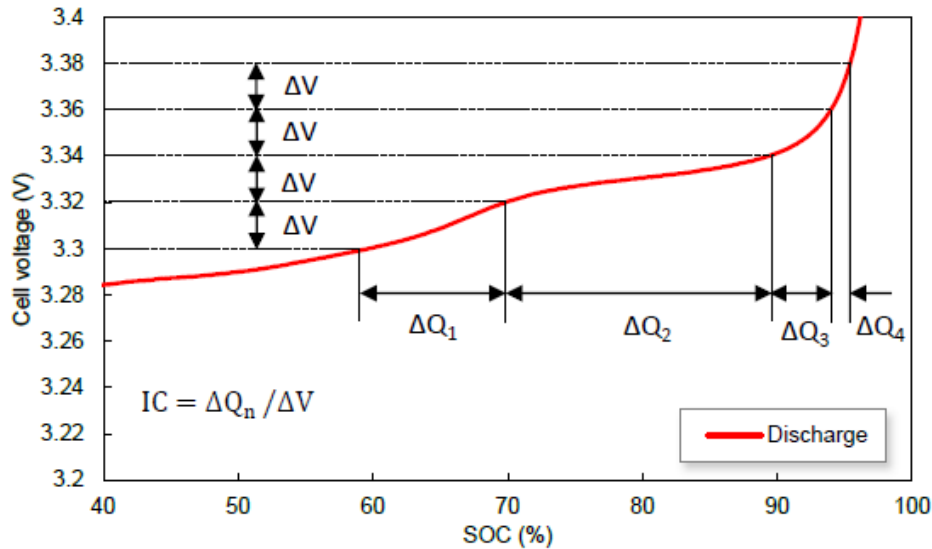


Figure 4.46: IC-DV, calculation of the incremental capacity curve for equally spaced capacity intervals [90]

The first step (figure 4.46) starts considering fixed voltage windows and the consequent increment in capacity: the procedure implies a constant current charge or discharge; just very low C-rates can be adopted because the process should be executed in thermodynamic equilibrium: this means to operate at rates around C/25 but in automotive applications, due to the time constraints, a full charge at C/10 could be employed.

Such operation can be repeated once a year, with a 10 hours test that can be easily scheduled during the night without effects on the owner routine: this because slow evolution of the ageing processes in LIBs, allows to perform the test one-two times in a year (DMs do not require to be analysed regularly [89]).

Important indications in [90] allow to setup an adequate measurement procedure, this because the IC curves are highly dependent on the accuracy and the precision of the measures of voltage and capacity: the fixed voltage steps should be at least about 5 mV and better accuracy could be achieved reducing the sampling rate.

The filtering procedure proposed in [89], necessary to achieve a good Signal to Noise ratio, consists in:

- 1) Averaging the pOVC values related to any repeated measurement.
- 2) Linear interpolation using the remaining points to obtain values of pOVC equally spaced.
- 3) Comparison of the filtered data with the original ones to assure a correspondence: the median of the absolute deviations of the recorded data about the filtered line must be below 2%.

Both IC and DV plots offer two different points of view on the development of different degradation phenomena: mathematically speaking IC curves can be obtained differentiating the measured Q vs pOVC curves while the inverse of IC yields the DV curve [89].

IC CURVE: gradient of Q with respect to pOVC:

$$\frac{dQ}{d(pOCV)} \approx \frac{\Delta Q}{\Delta(pOCV)}$$

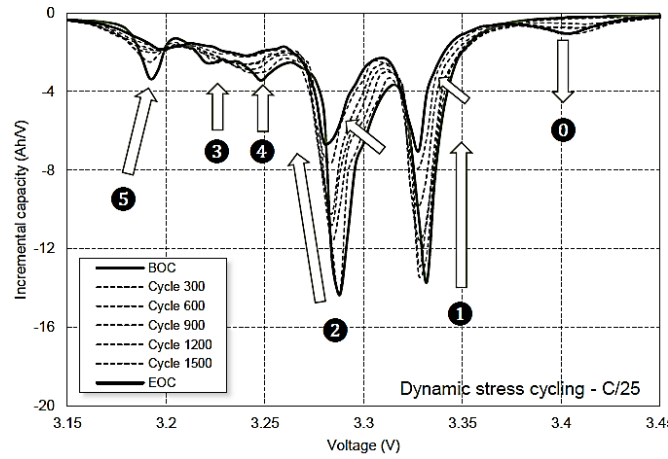


Figure 4.47: IC curve [89]

DV CURVE: inverse of the IC curve:

$$\frac{d(pOCV)}{dQ} \approx \frac{\Delta(pOCV)}{\Delta Q}$$

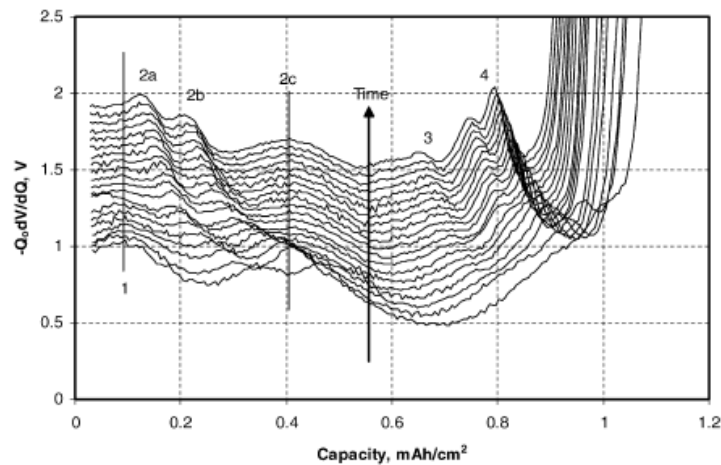


Figure 4.48: DV curve [89]

Phenomenologically speaking IC plot (dQ/dV) describes equilibrium phase, where two or more phases with different Lithium concentrations have the same Lithium chemical potential vice versa DV plot describes phase transitions. Must be clear that measured data, and corresponding peaks, contain both the electrodes contribution if not obtained from half-cell data (figure 4.49):

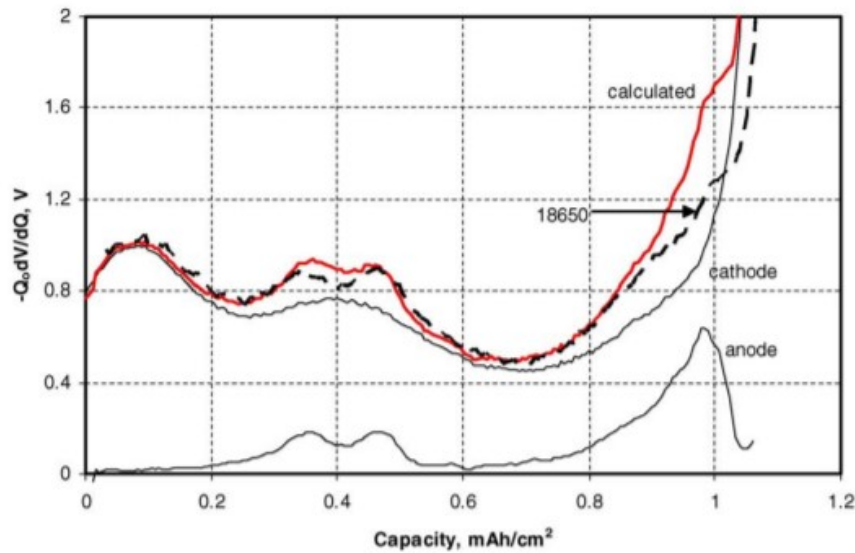


Figure 4.49: cathode and anode contributions [92]

Between voltage plateaus/ramps and the cell's electrochemical reactions there is a strict correlation then, through the analysis of these behaviours, it's possible to establish the evolution of the different electrochemical mechanisms occurring inside the cell: i.e. voltage plateaus are linked to high capacity increase and in the IC curve will appear as peaks [90].

IC peaks (i.e. those in the right plot of figure 4.50) are the electrochemical signature of both positive and negative electrodes and correspond to different ageing phenomena at a certain stage for the specific cell considered (each different chemistry exhibit different signatures).

Through the interpretation of these peaks, in terms of position, shape and intensity, it's possible to track the ageing phenomena upon cycling extracting fundamental qualitative information.

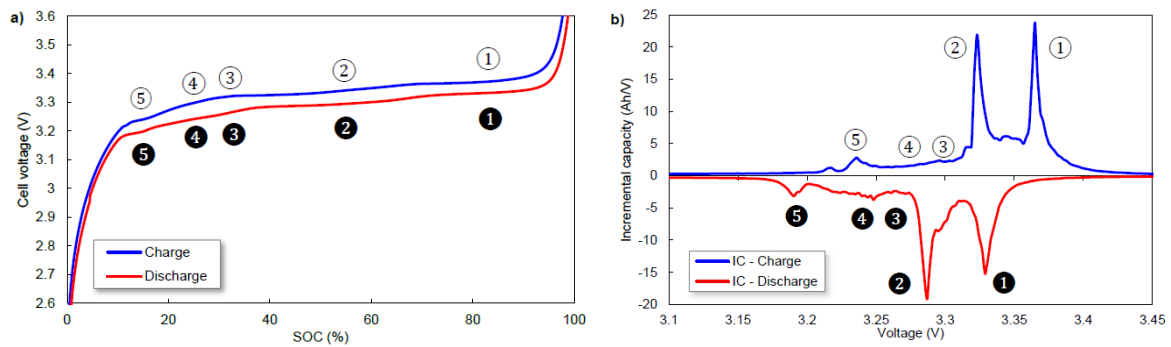


Figure 4.50: Charge/discharge curves (on the left) and relative IC curve (on the right) [90]

It's in this step that the thermodynamic equilibrium is essential: the IC curves and the related peaks are sensible to the current rate and for conditions far from the equilibrium the peaks are not distinguishable.

Identification of degradation modes using IC-DV

Variations in IC-DV plots during calendar and cycle ageing can highlight the evolution of the investigated degradation modes: also if there are differences between many chemistries in the market, it's possible to list the main relationships between these variations and several of the main modes [88][89].

Change in IC curve	Unit	Change in DV curve	Unit	Most pertinent DM	Potential ageing mechanisms	Most pertinent observed effects
Shifting toward lower voltages.	[V]	Lack of change.	[Ah]	CL	Current collector corrosion. Binder decomposition.	PF CF
Decrease of the height of the peaks and shift toward lower or higher voltages.	[Ah V ⁻¹] and [V]	Shifting toward lower capacities.	[Ah]	LLI	Electrolyte decomposition. Oxidation of electrolyte Lithium plating. Formation of Li grains. Solvent co-intercalation.	CF & PF PF CF & PF CF & PF CF & PF
Decrease of the height of the peaks at approximately constant voltage.	[Ah V ⁻¹]	Decrease of the depth of valleys at approximately constant capacity.	[V Ah ⁻¹]	LAM	Electrode decomposition. Oxidation of the electrolyte. Intercalation gradient strains in the active particles. Formation of Li grains. Crystal structure disordering. Transition metal dissolution. Solvent co-intercalation.	CF & PF CF & PF CF & PF CF CF & PF PF CF & PF

Figure 4.51: Relationship between IC-DV curves and the main degradation modes [89]

Shift to lower voltages (IC curves) and capacities (DV curves) are related to current collector corrosion and then to Conductivity Loss (CL). Decreasing trend of the peak's height, variations in the voltages (IC curves) and shifts to lower capacities (DV curves) are linked to decomposition and oxidation of the liquid electrolyte, Lithium plating and grains formation, thus to Loss of Lithium Inventory (LLI).

Finally, decreasing peak's heights at approximately constant voltage and reduction of the valleys' depth at approximately constant capacity are related to electrodes decomposition, oxidation of the liquid electrolyte, strains in the active particles with structure disordering and transition metal thus to Loss of Active Material. The listed ageing mechanisms are usually followed by Power and Capacity fade effects and through a simple model of the battery (model based on the Ohm's law), the previous effects can be explained:

$$V_{poc} = V_{oc} - V_{ohm} = V_{oc} - I \cdot R_{ohm}$$

A reduction in the intercalation and de-intercalation processes will lead to a decrease in V_{pocv} (pseudo open circuit voltage) and in capacity loss; these effects are mainly related to LLI phenomena and can be seen in the plots as a reduction in the height of the peaks (considering IC) and a shift toward lower capacity (higher evidence in DV curves). At an approximately constant pOVC, the effect of LAM with, number of cycles, can be seen as the reduction of the peaks in IC curves (most relevant and evident effect).

Thus, these two tools can be used in cooperation due to differences in the evidence of each phenomenon with respect to the other.

Finally, CL mode are negligible using IC-DV technique due to the lack of information derived from the curves, this is not seen as a major issue being these effects less relevant with respect to the other two degradation modes.

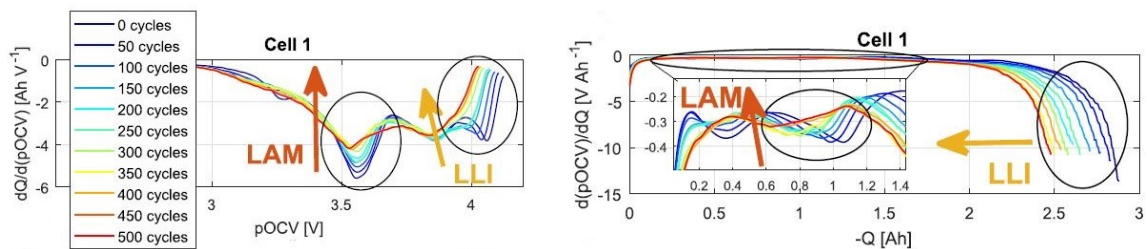


Figure 4.52: Graphical representation of the evolution of the main degradation modes in IC and DV curves [89]

In the figure 4.52 the above described DMs and the results achievable from IC-DV plots are synthesized. Recapping, the purpose of this technique is to obtain a deeper and reliable description of the ageing mechanism to avoid hidden phenomena (not detectable using SoH) that could shorten the cycle life of the battery pack. Identification and quantification of different degradation modes in real conditions can be also useful tools to improve the control strategies of the batteries mitigating extrinsic factors and limiting the effects of non-linear and/or hidden degradation mechanisms.

Procedures and concepts described are suitable to other cell chemistries and technologies that must be explored, furthermore there is the necessity to investigate more boundary conditions (storage applications, dynamic cycling, C-rates, different initial SoC...). For example, it's been advised a variation in the development of the DMs with different SoC levels: this can be verified through the measurement of ionic conductivity and diffusion in the electrodes.

The implementation of advanced control strategies under real driving conditions, would enhance the process of optimization of materials, manufacturing alternatives and battery design preventing accelerated and unexpected accelerated ageing phenomena thus extending the battery useful life.

4.2.1) Economic and Geo-politic considerations

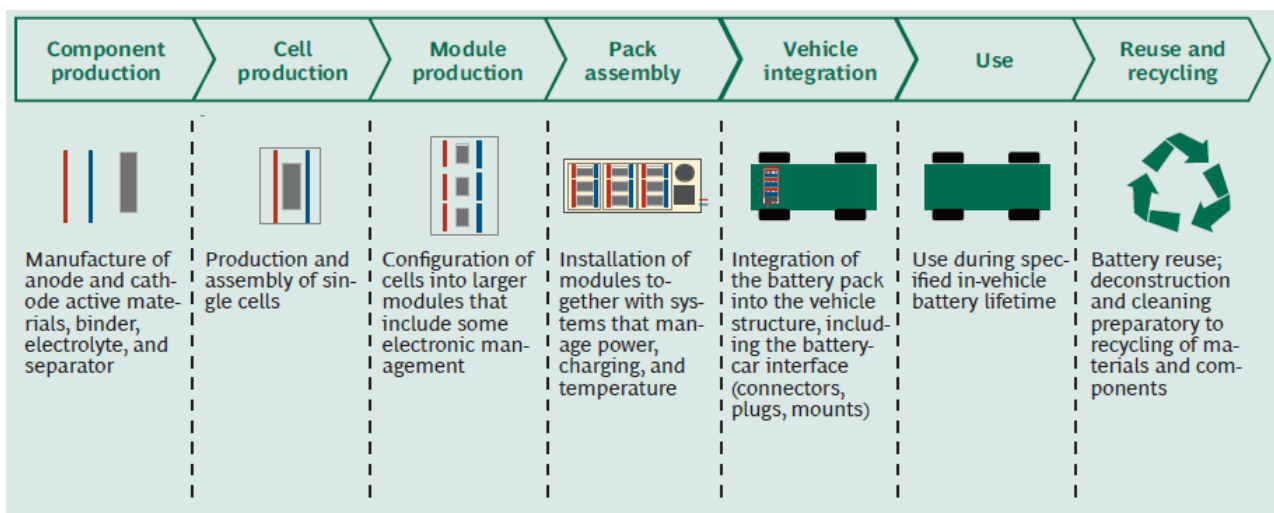


Figure 4.53: Value-chain of a battery pack for EVs/PHEVs [80]

In the value chain proposed in figure 4.1 from [80], there are the major steps from the evaluation of the raw material, necessary in the manufacturing process, to the recycling procedures, then there is the description of the whole life of the battery.

Studying economic and technological constraints, along the different phases of the value-chain, it's possible to understand which are the obstacles that do not allow to decrease the final price of the battery pack (in terms of euro/kWh) and, moreover, the possibilities to improve the entire structure.

Finally, the sustainability of the whole process will be studied with the opportunities to reuse and/or recycling of the exhausted batteries.

Two questions can fix the attention on several strategic targets that could determine the success of the Li-Ion batteries for automotive applications (especially in case of deep penetration of EVs):

- 1) What are the challenges to satisfy the market criteria?
- 2) What will be the price range of the Li-ion batteries?

As already described, the features of interest for an on-board energy storage system can be synthesized in 6 main points:

- 1) **Safety:** it's a particularly severe argument in the automotive applications due to the large number of cells and modules in the battery pack, subjected to risky unbalances, and due to the challenging environmental conditions (temperature, vibrations, incidents...); for these reasons each pack must be tested to assure an adequate abuse tolerance [93]. Safety/Abuse tolerance testing, such as the procedures described in the SAE Abuse Test Manual J2464, consider critical conditions (Mechanical, Electrical, Thermal) through a series of high stressing tests:

- 1 & 10 mohm short circuit
- 1C & 32A Overcharge/Overdischarge
- Thermal Ramp @ 100% SOC & 90%SOC
- Mechanical crush on both the positive and negative sides @ 100% SOC
- Nail penetration @ 100% SOC

The main dangerous phenomenon that must be avoided is the so-called “thermal runaway”: secondary chemical reactions lead to heat generation and can start a reaction with the electrolyte resulting in fire as can be seen from the abuse test in figure 4.54.



Figure 4.54: Run-away process resulting in flames

This failure can be triggered by misuses like overcharging, too high discharge rates, too high temperatures, unbalances among the cells and short circuits. OEMs, during the selection of the electrodes' chemistries, have to face a compromise between high performance cells (i.e. NCA) and higher safety cells (i.e. LFP), and there are not alternatives to maximize both these aspects. Nevertheless, efforts to assure the highest possible safety level, through the development of robust cell chemistries, of new battery pack designs and new thermal/electric control strategies, allow to manage these risks in the right way.

- 2) **Life Span:** cycle stability and battery age are two possible points of view that can be used to define the lifespan of a battery. Speaking about the cycling stability, referred to the case of BEVs, the definition can be described as the number of charge/discharge cycles before the reduction of the available capacity falls under 80% of the initial one. A common way to “dope” this characteristic, usually

adopted by EV manufacturers, is to oversize the battery pack in order to assure the performance along the expected electric vehicle life (around 200.000 km/10 years), this does not seem an efficient method because the high price and weight of the battery pack negatively affect the vehicle's performance. Another way could be to simply consider the years of activity experienced by the battery pack, forecasting a certain reduction in the performance in correspondence to a certain period.

- 3) **Performance:** a wide range of ambient conditions and driving profiles must be considered to assure the right performance level in each case. Also this time, the manufacturers are in front of a trade-off because configurations equally satisfying the opposite conditions (hot and cold climates, high and low SoC...) cannot be found. One possible approach could be to specifically design the battery system for a precise climate and so optimizing the vehicle characteristics looking at the place where the vehicle will be driven. This of course would require efforts to tune each different configuration reducing the flexibility of each product.

<i>Vehicle</i>	<i>Consumption (kWh/100km)</i>	<i>(km/kWh)</i>	<i>Available capacity (kWh)</i>	<i>Measured range (km)</i>	<i>Test Units</i>	<i>NEDC range (km)</i>
Hyundai Ioniq elettrica	12,21	8,19	28	229	16	250
Volkswagen e-Up!	13,04	7,67	18,7	143	10	160
CitrJen C-Zero	14,09	7,1	14,5	103	13	150
Peugeot ion	14,2	7,04	14,5	102	18	150
BMW i3 60 Ah	14,83	6,74	21,6	146	18	190
Mitsubishi i-Miev	15,38	6,5	16	104	14	160
Volkswagen e-Golf 24 kWh	15,69	6,37	24,2	154	26	180
Renault Zoe R90 22 kWh	15,77	6,34	22	140	78	240
Kia Soul EV	15,91	6,29	27	170	11	212
Renault Zoe Q90	16,19	6,18	23,3	144	13	370
Nissan Leaf 24 kWh	16,34	6,12	21,3	130	41	199
BMW i3 94 Ah	16,53	6,05	33,2	201	6	312
Renault Zoe R90	16,9	5,92	41	243	5	403
Tesla Model S 60	19,4	5,15	60	309	6	400
Tesla Model S 85	21,27	4,7	85	400	36	500
Mercedes Classe B	23,54	4,25	28	119	6	200

Figure 4.55: EVs on the market ordered for decreasing efficiency (from the top to the bottom)

In [95] several EVs have been tested (real driving data) to obtain significative information in terms of consumption, range, efficiency and the results are reported in figure 4.3 to highlight the most efficient vehicles.

For each model under investigation at least 5 test units/measures are available and the median, instead of the mean, has been considered to obtain an index not affected by anomalous values.

In the table the vehicles are ordered with decreasing efficiency, this can be easily verified looking at the consumption expressed in km/kWh.

A second interesting result comes from the comparison of the values obtained in the real driving conditions against the values obtained through the New European Driving Cycle (figure 4.4):

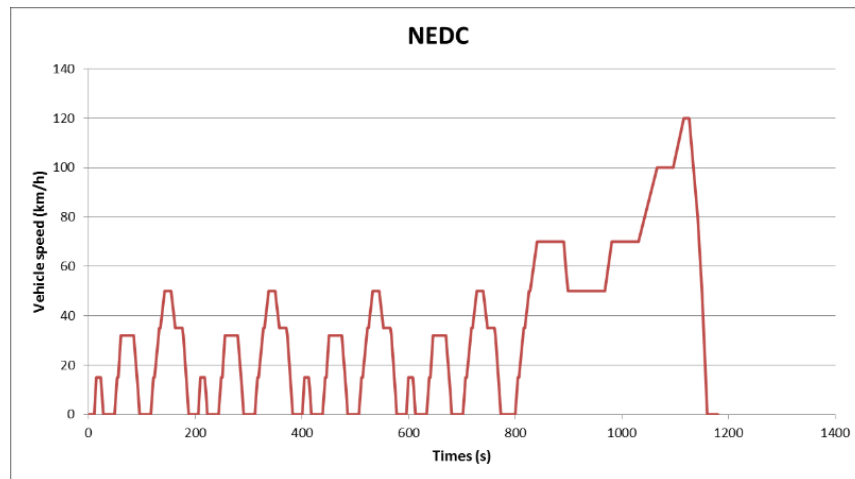


Figure 4.56: NEDC

This homologation regime is far from simulate real driving conditions and gives total overestimated between 8-40% as clearly reported in figure 4.5:

Vehicle	Difference between measured data and NEDC [%]
Hyundai Ioniq elettrica	-8
Volkswagen e-Up!	-11
Volkswagen e-Golf 24 kWh	-14
Kia Soul EV	-20
Tesla Model S 85	-20
Tesla Model S 60	-23
BMW i3 60 Ah	-23
CitrJen C-Zero	-31
Peugeot ion	-32
Nissan Leaf 24 kWh	-35
Mitsubishi i-Miev	-35
BMW i3 94 Ah	-36
Renault Zoe R90	-40
Mercedes Classe B	-41
Renault Zoe R90 22 kWh	-42

Figure 4.57: Difference between data from real driving conditions and data from NEDC

The range reduction resulting from the passage between this cycle and the real values it's dependent on many aspects of the vehicle: weight, rolling resistance of the wheels, aerodynamic efficiency and so on...

However, the data from NEDC are suitable to investigate the efficiency of the power electronic of the vehicle being measured at wheels level.

Moreover, NEDC is going to be substituted by the World-wide harmonized Light-duty Test Procedure (WLTP) that would surely represent a more significative regime but to reach higher levels of fidelity, with real driving emissions and consumptions, further steps forward are necessary.

- 4) **Specific power/Energy:** while the specific power is not a critical issue, it's currently addressed, the specific energy is the real key parameter that limits the driving range of BEVs.

With values, at battery pack level, within 120/180 Wh/Kg (against 12/13 kWh/kg of liquid fuels) the allowable range is limited to values under 300 km (obviously the dependence of these values from the driving profiles, the operating conditions and the battery pack SoH is fundamental).

There are viable solutions, that are investigated, to increase the specific energy [71]:

- Acting on the cathode is possible to increase the content of Nickel in the layered compound, reaching capacities higher than 200 mAh/g but reducing the thermal stability; otherwise it's possible to use Cobalt in order to increase both the specific energy and specific power, but affecting negatively the price due to the high cost of such an element.
- An alternative is the improvement of the battery voltage limits but with drawbacks in terms of durability and safety.
- There are several possible developments considering the anode material: graphite, with its layered crystalline structure (figure 4.6), is the most common choice in actual BEVs; a substitute could be a Silicon based anodes (Si has a specific capacity of 4.200 mAh/g) but 300% change in volume during charge/discharge leads to very poor cycle life.

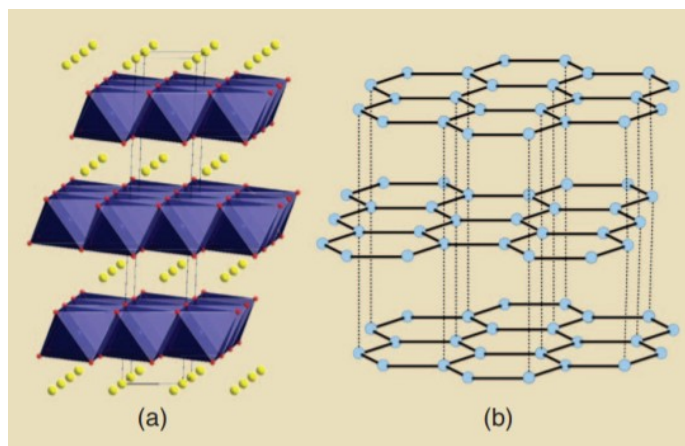


Figure 4.58: Layered cathode (a) and graphite anode (b) structures from [71]

- 5) **Charging time:** another technological and commercial barrier is represented by the customers' requirements in terms of fast and ultra-fast charge procedures (level 2 and level 3 charge methodologies) that would allow to reduce the recharge time from hours to minutes but, from both vehicle side and grid side, there are unsolved problems that would result in:

- Accelerated battery degradation due to the high charging rates
- Overloads in the grid in case of a large-scale adoption of PHEVs and EVs

- 6) **Cost:** Price of batteries will play one of the most important role in the diffusion of BEVs being a large fraction of the electric vehicle cost (till 75% in small vehicles); the drop in the price under 150 \$/kWh

would enlarge the possibility of a deep penetration of the electric vehicles nullifying the price difference with respect to the conventional ICE based vehicles (as depicted in figure 4.7).

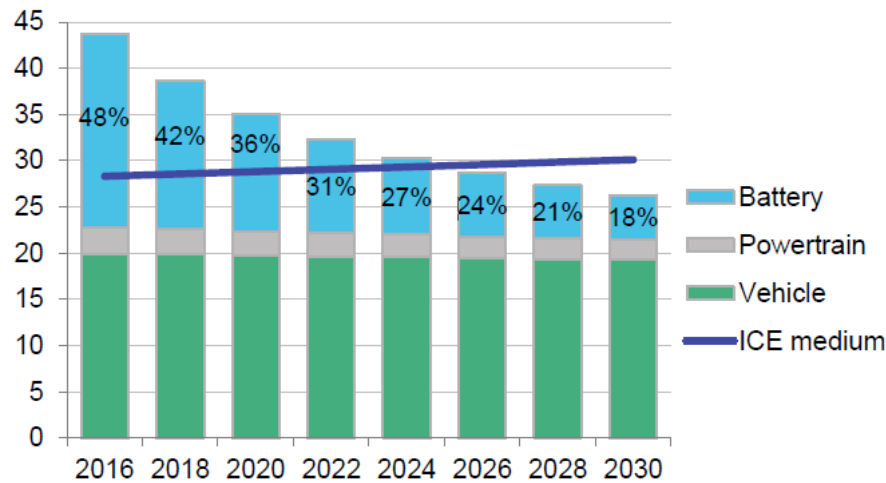


Figure 4.59: BEV and ICE prices (pre-taxes) in U.S.A. in thousands of \$ (source: Bloomberg New Energy Finance)

In [96] a comparison between the studies in the literature highlights that the oldest predictions, relative to the price forecast in 2020, are the ones with the highest battery cost while, earlier studies, continuously corrected the estimation reducing the forecasted values, this is a sign of an optimistic trend that is supported by the real data: it's interesting to see, in figure 4.8, how the cost reduction resulted in a drop around 50% of the starting specific cost, at both cell and pack levels, from 2013 to 2016.



Figure 4.60: historical data of the evolution of battery specific cost between 2013 and 2016

In 2016 an average price, at battery pack level, of 273 \$/kWh has been registered, moreover, a reduction in the battery price of the 35% and 22%, relatively to the periods 2014/2015 and 2015/2016, makes plausible a further drop under 250 \$/kWh, maybe near the soil of 200 \$/kWh, in the next years. Two types of battery (battery I and II described in figure 4.9) have been studied in [96] and respectively represents an example of a battery already present in the market (I) and a possible solution with a different anode chemistry that could be developed in the future (II).

	Battery I	Battery II
Positive electrode	NMC (6:2:2)	NMC (6:2:2)
Negative electrode	Graphite	Silicon Alloy [50]
Pack energy density	155 Wh/kg	205 Wh/kg

Figure 4.61: battery typologies studied in [96]

The same case study has been used to estimate the values, of production and recycle/reuse steps and will be considered in the evaluation of the End of Life value of the Li-Ion batteries.

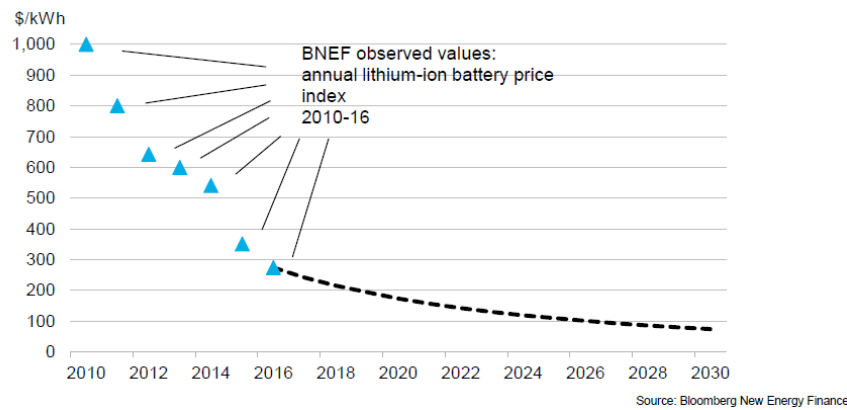


Figure 4.62: prediction of the battery cost, in the next decade, starting from the record from 2010 [97]

The drop in the price of the battery packs leads to very optimistic considerations for the future in [97] forecasting a value of 73 \$/kWh in 2030 (figure 4.62), motivating the result with several reasons:

- Hard competition among manufacturers leading to strong improvements in the production efficiency and in production volumes (in [80] 70% of the components in a battery pack are considered volume-dependent).
- Development of new chemistries (R&D) with higher performance and/or lower costs

Process-based cost modelling

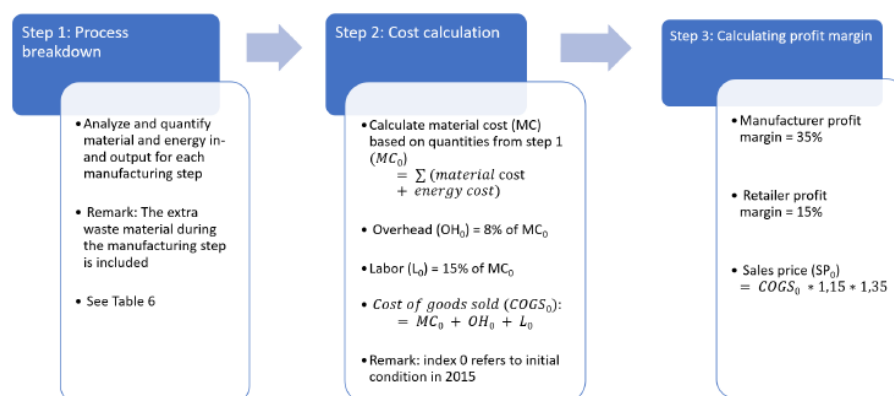


Figure 4.63: Process-based cost modelling from [96]

As illustrated in figure 4.63, the proposed cost modelling procedure can be represented by three main blocks, respectively:

- Process breakdown
- Cost calculation
- Profit margin calculation

The procedure starts from the analysis of energy/material input and output flows; after the evaluation of these quantities it's necessary to calculate, with a first approximation, the cost of each "player" in the process: considering the product between the amount in weight of each single raw material and its specific cost (\$/Kg) it's possible to identify the most relevant elements in the process (in terms of cost). In the second step it's possible to integrate learning and/or dynamic curves in order to forecast the evolution of these costs due to the optimization in the production plants and the variation of the labour cost. In the last step it's necessary to include several aspects like manufacturer margin and retailer profit to finally get the sales price.

It's then fundamental to describe in detail the manufacturing and assembling phases and this can be done in 7 main steps, but it's also reported in figure 4.12:

Step 1) The first phase is the electrodes manufacturing, the active material, the conductive agents, solvent and binder are mixed together and the current collector is coated with this compound (positive collector is made of Aluminium while the negative one is made of Copper).

Step 2) The cells are dried and the solvent is vaporized; to assure a good conductivity between the compound and the current collector, the assembly is calendared through high pressure between the components.

Step 3) The electrodes manufacturing process ends with a correct size cut.

Step 4) Cells are assembled or it's created a multilayer structure composed by alternating levels of positive electrodes, separators and negative electrodes.

Step 5) Cells are packaged and temporary sealed for a further drying procedure: in order to assure the absence of solvent.

Then the cells are filled with the liquid electrolyte and are permanently sealed.

Step 6) To ensure thermal and electrical stability, some "formation cycles" are necessary stabilizing the chemical structure.

Step 7) The final step consists in a quality test measuring the electric performance.

Manufacturing Process		Material
Electrode Manufacturing	Slurry Mixing	+ Active Material + Conductive agent + Solvents + Binder
	Coating	+ Al/Cu foil
	Drying	– Solvents
	Calendaring	
	Cutting	+ Remaining al/Cu foil
Cell Assembly	Stacking/Winding	+ Separator + Adhesive Tape + Al/Cu tabs
	Packaging (Pouch/Case)	+ Pouch Foil/casing
	Temporary sealing	+ Solvents
	Drying	
	Filling	– Remaining al/Cu foil
	Permanent Seal	
Formation	Formation	
	Cell Testing	

Figure 4.64: Cell manufacturing process including input/output material flows [96]

To proceed with the price evaluation, it's necessary to know the exact composition of the selected battery and then, for new chemistries, a careful knowledge of patents and publications must be studied. In the proposed case study, the calculation steps allow to estimate the cost of the different chemistries: in this case battery I (NMC(6:2:2) + Graphite) and battery II (NMC(6:2:2) + silicon alloy).

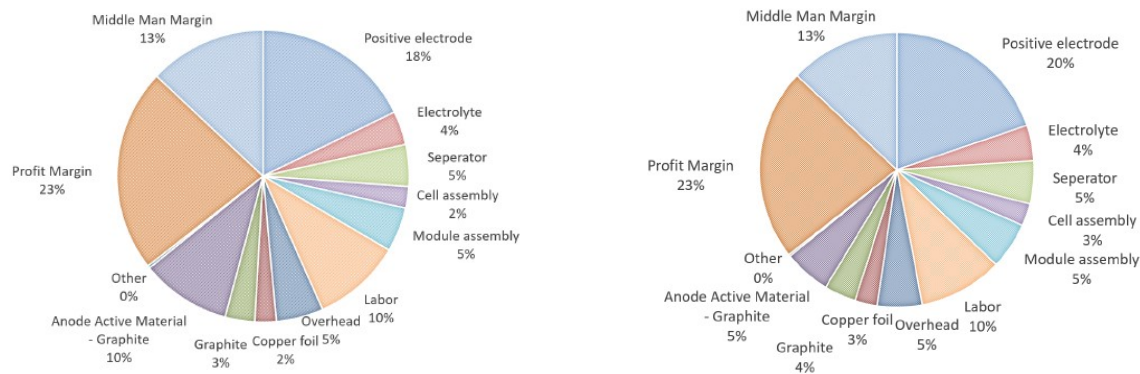


Figure 4.65: Sales price of battery I (on the left) and battery II (on the right) [96]

The result highlights that almost 50% of the price derived from the material and almost 20% from the production for both the batteries: this fact allows to reasonably think that upscaling the number of production plants and volumes will lead to a significative reduction in the final price.

Materials

As far as the fraction of price dependent on the materials is concerned, it's useful to look at the review [78] that covers and compare many families of the materials suitable to be used in the electrodes; in particular in figure 4.14 there is a periodic table with the availability of each element (expressed as a fraction of the Earth's Crust) and the corresponding forecasted price range:

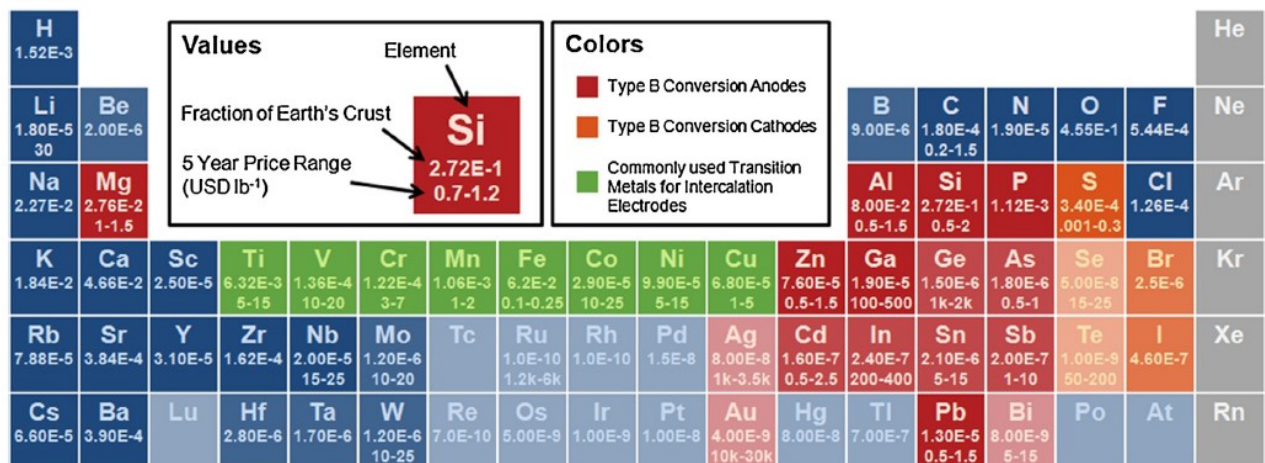
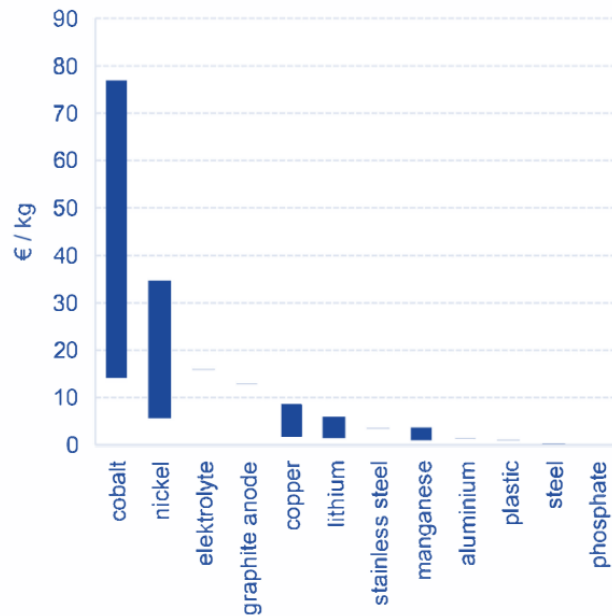


Figure 4.66: Periodic table with identification of the main elements for anodes and cathodes in Li-Ion batteries [78]

Considering the historical trend of the cost of the main raw materials present in the Li-Ion batteries, it's evident how much the oscillations of these values can have an impact on the value-chain determining the feasibility in large-scale production targets [98].

Figure 4.67: Price ranges of the main raw materials utilized in Li-Ion batteries [98]



These large uncertainties in the raw material cost and the different chemistries adopted by manufacturers make difficult to set up an economic relation with the suppliers predicting an effect on the final product.

Lithium availability

To simplify such a complex study, seems reasonable to focus the attention on the base element common to all the chemistries of the Li-ion battery technology.

In literature numerous authors analysed the relationship that occurs between the Lithium availability and the growth of BEVs/PHEVs/HEVs fleets [100].

Discontinuous and sometimes opposite point of view are difficultly to be integrated because rely on very diversified base assumptions: pessimistic studies highlight that the Lithium could result in a bottleneck for the increasing production rate of battery based vehicles, others estimate that the amount of Lithium on the Earth crust is sufficient to cover the necessity for a future world fleet, nevertheless it's important to establish that the rate of extraction of such an important metal could be a main obstacle.

Among the boundary conditions, to define a specific scenario for the analysis, there are:

- Time horizon considered and the rate of production of electric vehicles (BEVs/PHEVs/HEVs).
- Share, in the EV market, of vehicle based on Li-Ion batteries.
- Size of the battery for different electrification levels and the quantity of lithium per unit of capacity.

While, the main variables affecting the estimation of future supply, required to satisfy the demand without obstruction in the production of Li-Ion batteries, are:

- Estimates of Lithium reserves.
- Future production rate.
- Future recycling rate.

Lithium content per unit of energy (BEVs and PHEVs)

Particularly interesting is the investigation on the amount of Lithium necessary to get a unit of energy in the battery pack [100].

Ideally would be required the knowledge of a set of characteristics to determine such value:

- Deliverable voltage during the operation
- Specific capacity
- Chemical composition of the active materials

To solve the lack of information (these data are available only for the manufacturers) in [100] four different methods are introduced:

Method A) The easier way would be to quote industry data from the past experiences, obviously when are accessible.

Method B) Starting from the measure of voltage and specific capacity, the procedure continues with disassembling the battery and analysing the composition of the components in a laboratory; this can be labelled as “reverse engineering” and present different drawbacks because it’s a very expensive method leading to very specific results not transferrable to other chemistries.

Method C) This third method can be applied using the published data relative to battery voltage and specific capacity then through assumptions and comparisons an estimated composition can be obtained with an acceptable degree of uncertainty.

Method D) The last possibility is to evaluate the amount of Lithium starting from the theoretical value required under ideal conditions (underestimation) and then referring the value to the operating conditions through a correction. This latter method is the one used in [100] to minimize the effort necessary to get a first indicative result, nevertheless it represents an oversimplification that cannot be reliable for whatever application.

A brief description of the theoretical assessment of Lithium inventory seems to be useful to address a first attempt in the evaluation of Lithium content per unit of energy.

Such approximation should take into account several key factors that could vary and then could affect the result:

- Lithium inventory varies with different chemistries.
- During the operation, the battery delivers just a fraction of the chemical energy stored while the rest is dissipated as heat due to the internal resistance.
- Actual capacity of a Li-Ion battery is usually much higher than the rated capacity in order to increase the durability.

Variation in lithium intensity among different chemistries and energy losses

Calculating the amount of Lithium per unit of energy (g(Li)/kWh) in the ideal conditions will lead to the evaluation of a minimum and not the real quantity in a battery.

This value is anyway useful to highlight the intrinsic differences among the chemistries as a result of each different electrochemical process.

However, the real value of the amount of Lithium per unit of energy must account for two main phenomena:

- Energy losses
- Lower voltage (V) with respect to the electromotive force (E_0) due to the internal resistance (R_i)

Briefly, the difference between V and E_0 , called overpotential, it's affected by the discharging rate and the operating temperature but also depends on the chemical composition and the structure of the electrodes. The "Lithium Intensity" in g/kWh it's calculated as:

$$I = \frac{m \times 10^3}{E_0 a c}$$

Where:

- "I" is the Lithium intensity in g/kWh
- "m" is the molar mass of Lithium in g/mol
- "E0" is the electromotive force in Volts
- "a" is the available fraction of Lithium
- "c" is the charge of 1 mol of Lithium ions in Ah/mol

Being V smaller than E_0 , the substitution of the real voltage value leads to a higher required Lithium intensity. To conclude, the voltage difference must be measured experimentally for any battery chemistry because derives from complex phenomena and cannot be generalised for each case.

Over-specification on lithium intensity

A common strategy to compensate the capacity fade of the Li-Ion battery pack (to improve the rated useful life) is to "over-specify" the battery, therefore using higher quantities of Lithium: the main priority currently pursued by EV manufactures is increasing vehicle range rather than decreasing material intensity. This method becomes an obstacle in the direct evaluation of the Lithium intensities, leading to prefer estimations based on the literature (figure 4.16).

Source	Vehicle application	Material intensity (kg Li/ kWh)	Methodology ^a
Chemetall GmbH [28]	BEV (25 kW h)	0.165	A
	PHEV (16 kW h)	0.176	
	HEV (1 kW h)	0.375	
Meridian International Research [7]		0.300	A
Meridian International Research [20]		0.563	D
Kushnir and Sanden [18]	Average for four chemistries	0.160	D
Rade and Andersson [19]	Li-ion (Mn)	0.140	D
	Li-ion (Ni)		
	Li-ion (Co)		
Argonne National Laboratory [26]	HEV4 (1.2 kW h)	0.308	C
	PHEV20 (6 kW h)	0.244	
	PHEV40 (12 kW h)	0.246	
	EV100 (30 kW h)	0.246	
Gruber et al. [17]	Li-ion (Co, Mn, Ni)	0.114	D
Evans [29]		0.113	A
Evans cited by Reuters [30]	Chevrolet Volt (16 kW h)	0.158	A
Engel [25]		0.050	A
Fraunhofer ISI [12]	LiCoO ₂	0.180	D
	LiFePO ₄	0.120	
Dundee Capital Markets [11]		0.080	A
National Renewable Energy Laboratory [27]	HEV (1.7 kW h)	0.100	Internal modelling study (C or D)
	PHEV12 (5.6 kW h)	0.108	
	PHEV35 (17.5 kW h)	0.110	
	BEV75 (29.5 kW h)	0.112	
	BEV150 (67 kW h)	0.112	

Figure 4.68: Estimations of Lithium carbonate usage per kWh found in literature [100]

From the table in figure 4.16 it's evident that, looking at the uncertainty in the studied methods, the most reliable solution should be (A) but not all the reported values derive from industry data; due to these

difficulties could be acceptable to rely on the other procedures, accepting a significative risk of inaccuracy. [101]

Reference	EV (kg)	PHEV (kg)
Falås and Troeng [101]	2.7–4.3	1.2–2.0
Gruber et al. [16]	5.1–7.7	1.5–2.3
JOGMEC [102]	2.8–5.7	1.4–3.1
Kushnir and Sandén [18]	5.8	1.4
Mean value	4.9	1.9

Figure 4.69: Estimations of the Lithium amount for different vehicles batteries from the literature [101]

In 2015 worldwide, 88.6 million of units were produced, but the forecast for 2020 is the achievement of 100 million: also if just a fraction would be electric vehicles it would requires hundreds of kilotons of Lithium (in part could be from recycle process).

Many scenarios have been drawn to predict the sales of the new generations of electrified vehicles: in figure 4.18 have been reported the results of two of the most important ones; obviously the identification of a realistic case it's fundamental to evaluate the Lithium demand in the next years and further data will correct these estimations leading to a clearer result.

	HEV	PHEV	BEV	FCV
Blue map	14	62	47	34
Blue EV shifts	6	20	104	0

Figure 4.70: Vehicle sales, in millions of units, for 2050 [100]

Balance between future lithium supply and demand

Applying the last method (C) and historical production data (showing an approximately geometric growth in supply), it's possible to get the plot in figure 4.19 where there are two limits scenarios ('low' and 'high' material intensity cases) representing the evolution in the demand of Lithium for BEVs and PHEVs in different years till 2050.

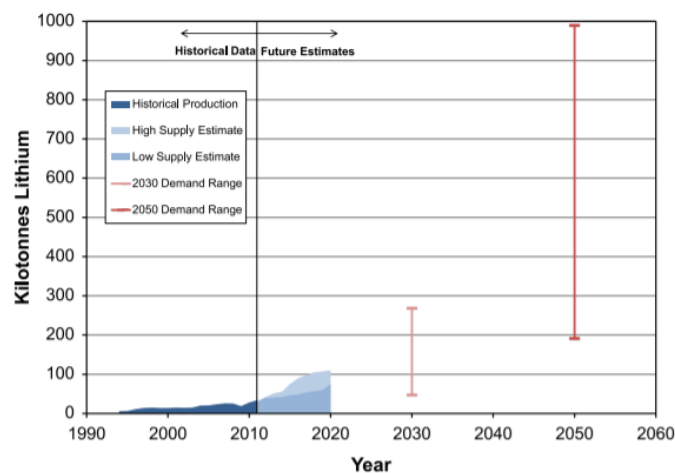


Figure 4.71: Lithium production scenarios and uncertainties from historical data to 2050 [100]

In the “low material intensity” scenario has been considered an average battery pack of 4.3kWh and 16kWh, respectively for PHEVs and BEVs, obtained from the most conservative values found in literature (probably underestimating the real On-Board capacity of these vehicles).

The “high material intensity” scenario it’s based on the highest capacity values of the batteries mounted on today’s electric vehicles, thus neglecting the fraction represented by PHEVs and HEVs. With this second prospective, the highest possible demand is estimated in one million tonnes of Lithium necessary annually to cover just the demand of the automotive sector.

Geological overview [100] [101]

The review shifts from the demand side to the supply side, starting from a geological and geographic identification of the most significative reserves and resources till the possible production rates to satisfy the future requirements without bottlenecks.

Lithium, represented by the symbol Li and with the atomic number 3, belongs to the first group (alkali elements); in its pure form, is a soft, silver-coloured metal that rapidly oxidizes when in contact with air or water, for this reason, it’s never in pure form in nature and only appears in compounds, usually ionic compounds.

Under standard conditions, Lithium is the least dense solid element and, as all alkali elements, is highly reactive and flammable.

Can be found in four main deposit types: ores, brines, sedimentary rocks and seawater (ores and brines are the largest world’s source of Lithium today) as illustrated in figure 4.20.

Lithium carbonate (Li_2CO_3), from brine, constitutes the main form used to manufacture Li-Ion batteries while other sources like Lithium in sedimentary rocks and Lithium from seawater are not exploited today due to high uncertainties in the economic viability and sustainability of such processes.

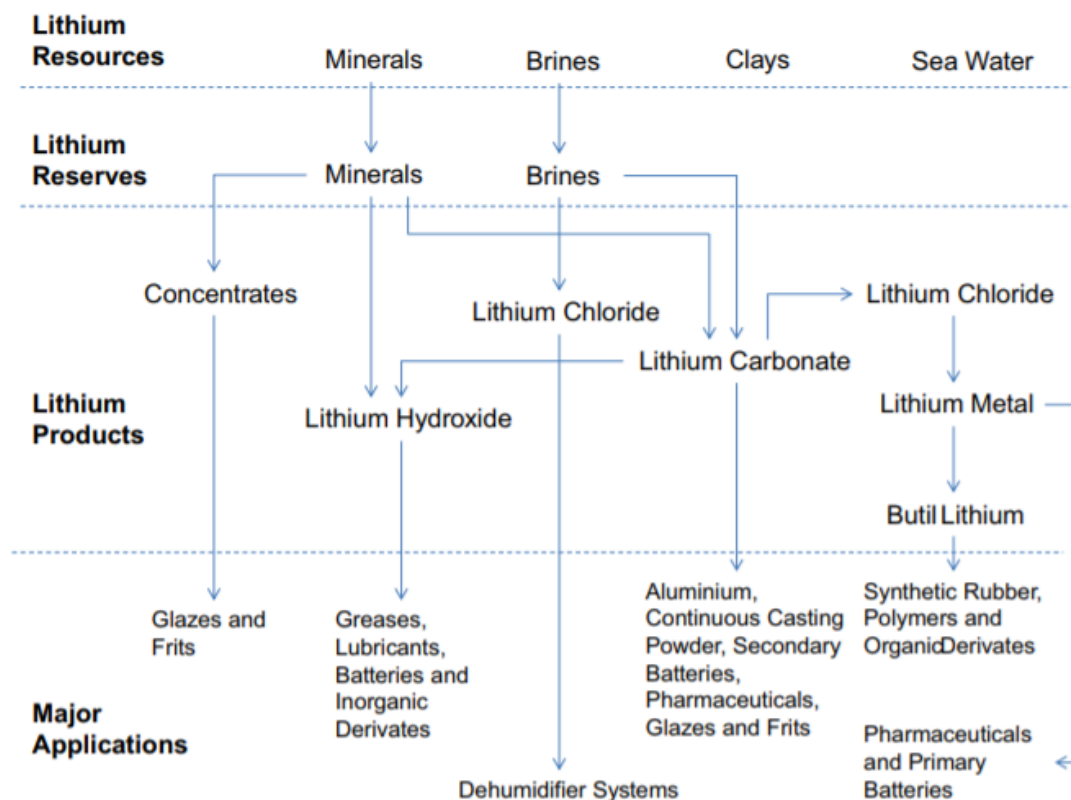


Figure 4.72: Sources of Lithium in nature and main applications [100]

Geographic overview [100] [101]

As anticipated, brine deposits are, nowadays, the cheapest and most economically sustainable sources of Lithium: these sites are highly concentrated in dry lakes, such as the Salar de Atacama in Chile, geothermal deposits and saline aquifers [100].

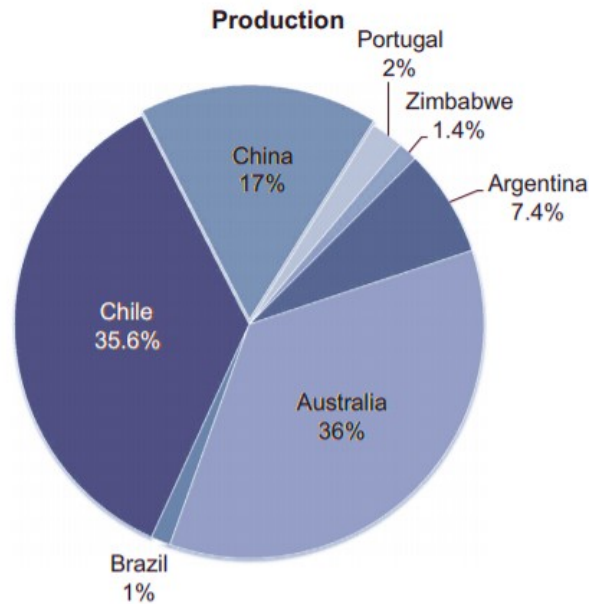


Figure 4.73: Distribution of Lithium reserves in 2011 [100]

Almost 95% of the production and revenues in 2011 are subdivided in four states as reported in the chart of figure 4.21:

- Australia (Lithium in minerals recovered from spodumene deposits)
- Chile (Lithium carbonate from brine)
- China (35% from minerals and 65% from brines)
- Argentina (Lithium carbonate from brine)

Despite the amount of Lithium in the Earth crust would cover the entire future demand (also supposing to substitute the whole the vehicles fleets in the world) it's mandatory to precise that just a small fraction of the existent material can be exploited by the society: the small fraction that can be extracted at a certain rate in order to supply the manufacturers.

The distribution of Lithium reserves is less critical with respect of other materials (i.e. rare earth metals) and then should be less constrained by geopolitical questions.

Resources and reserves

Assumes an absolute importance, the clarification of the terminology adopted in order to describe and discuss Lithium availability: this is due to wrong and/or diversified definitions and classifications utilized in many works as synonymous, contributing to complicate the aggregation of the data.

Two basic definitions can be assumed to distinguish "resources" and "reserves" [101]:

- Resources: defined as the "geologically existent quantity of an element that is available for exploitation"

- Reserves: defined as the “quantity of an element that is exploitable with current technical and socioeconomic conditions”

Results clear that the reserves are those that are significative in order to evaluate the cumulative amount of material that can be exploited in the industry and then represent the supply potentialities.

Actual reserves are not stationary, there are variations in the amount of raw material that is considered accessible and exploitable in different periods due to:

- Available technology
- Demand and price magnitudes
- Political conditions in the reserves location
- Material concentration in the extraction sites
- Legal issues or environmental policies

Resources, on the other side, must be converted, if possible through changes in the technology or thanks to different political/economics conditions, in reserves before to enter in the supply-chain.

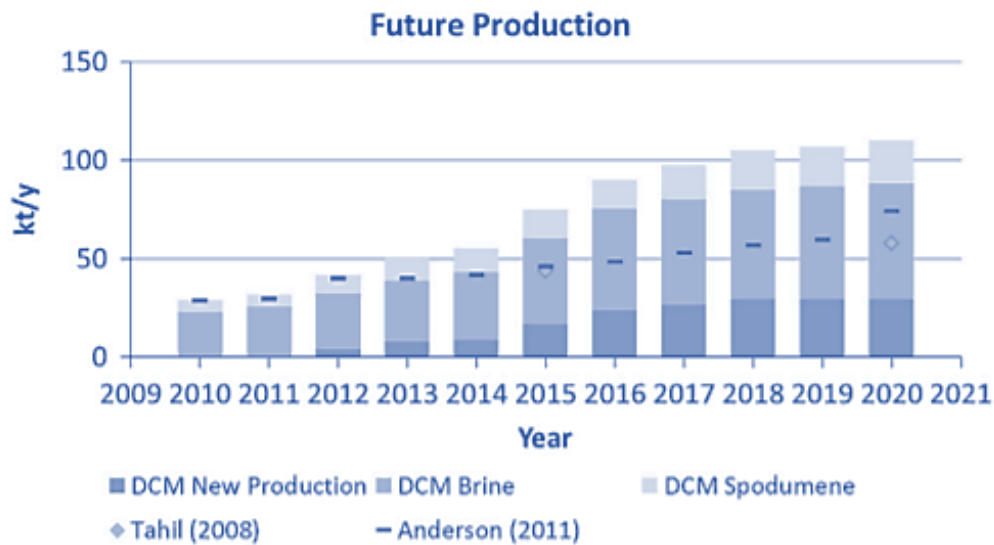


Figure 4.74: Lithium production prediction, subdivided among brine, spodumene and new reserves [100]

Increasing production will be probably accompanied by increasing reserves because the immaturity in the exploration, together with the increasing demand, will push many states to invest funds to discover new resources sites (as described in figure 4.22).

Nevertheless, nowadays brine represents the first Lithium source (and the largest) but several critical drawbacks must be faced: for example, the very large water consumption (65% of the fresh water in the Salar de Atacama region [Tahil]) and the varying concentration could modify the economic sustainability of these sites.

Production model results [101]

There are many works trying to evaluate, through models and historical data, the peak year and maximum production for the future (figure 4.23).

	Base case			High case		
	Logistic	Gompertz	Richards	Logistic	Gompertz	Richards
Peak year	2074	2098	2078	2088	2129	2095
Maximum production	208	81	165	403	134	305

Figure 4.75: Maximum production in kilo-tonnes predicted through different models [101]

These results are obtained fitting the models to historical production data through numerical methods and least squares minimization; also recoverable resources and the previously extracted volumes of Lithium (0.5 Mt using USGS gross product data considering Lithium content of 6%) are included in the procedure. All the models show a significant future potential for the development of higher production rates. In particular in figure 23 there is a prediction concerning the global production of Lithium (till 2100) starting from historical data (since 1900) and representing the results of different studies from the existent literature.

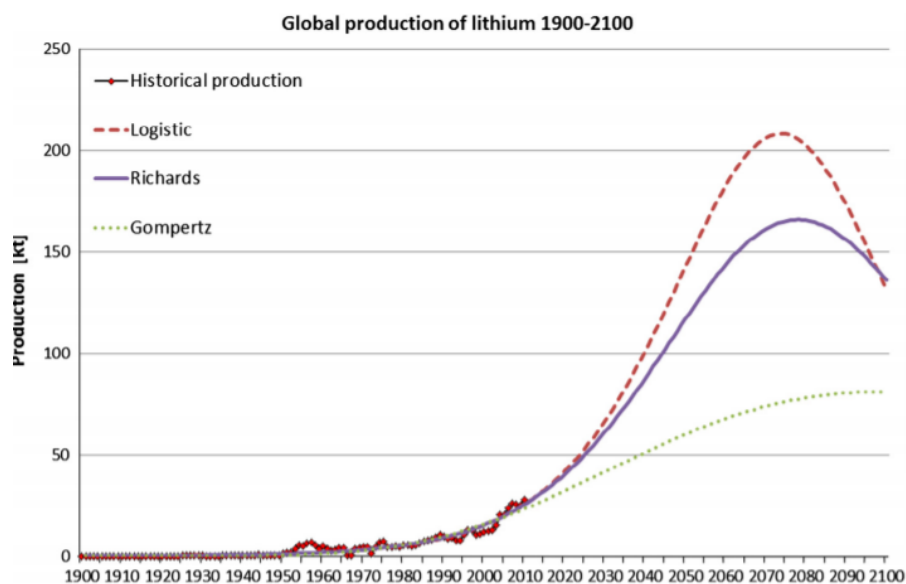


Figure 4.76: Medium-Long term projected future Lithium production [101]

Many other studies faced the possibility to match e-mobility targets established to design a roadmap; medium-long scenarios seem to be covered by the projected production rates, anyway, the boundary conditions strongly affect the result and each variation should be accurately studied:

- Target performance of PHEVs and EVs
- g(Li)/kWh
- Number BEVs/PHEVs produced

Author	Forecast lithium supply constraint on EV manufacture	EV manufactured (millions per year)	By year	Lithium intensity per vehicle (kg)
Evans [10] Evans [11]	No	5 EV	2015	HEV: 0.23 PHEV: 1.35 BEV: 2.81
Gaines and Nelson [12]	No	~35 BEV & ~65 PHEV	2050	HEV: 0.17-0.64 PHEV: 0.93-5.07 BEV: 3.38-12.68
Gruber et al. [13]	No	> 600 EV	2100	HEV: 0.05 PHEV: 1.14 BEV: 3.85
Kushnir and Sandén [14]	No	4500 EV (cumulative)	2100	PHEV: 1.44 BEV: 5.76
Neubauer [15]	No	47 BEV and 60 PHEV	2050	PHEV: 0.6-1.9 BEV: 3.3-7.5
Tahil [7] Tahil [8]	Yes	4-8 PHEV	2015-2020	PHEV: 1.5
Yaksic and Tilton [9]	No	~	2100	EV: 1.27

Figure 4.77: Comparison of the most important studies in literature about the possible Lithium constraints [100]

In [102] the production capacity of lithium from the rock, clay, and brine resources is considered as a bottleneck to meet the growing lithium demand: future supply crisis could be prevented through LIBs recycling with minimum high degree lithium recovery. Progressive lithium demand for LIB and the controlled thermonuclear fusion reactor may exceed the current availability of the mineral and brine reserves in the next few decades.

Recycle/Reuse

To establish an “End of Life market” for the Li-Ion batteries not anymore suitable for the automotive sector, it is necessary to define the monetary residual value of their components [98].

Three main possible alternatives, for the last step in the value-chain, can be identified:

- Recycling the raw materials
- Remanufacturing of specific components/systems of the battery pack
- Second-life in application with lower performance requirements (stationary energy storage)

At the actual premature state of these processes, it's difficult to address the future potentialities selecting the most economically convenient, was also because there is a strong dependence on factors like the evolution of the Li-Ion battery price and of the alternative services (i.e. V2G applications).

There are several exogenous parameters affecting the choice among the possibilities and the feasibility related to the costs and the revenues:

- Percentage of discarded batteries
- Variation in the Li-Ion cells price
- Variation in the raw materials price

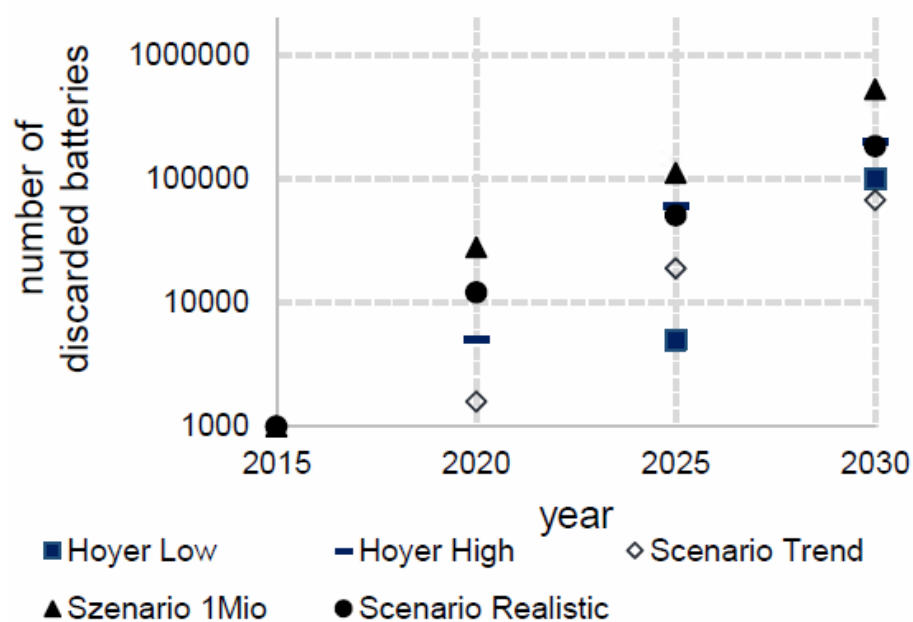


Figure 4.78: Estimated number of discarded batteries from BEVs [98]

While the other parameters have been treated in previous sections, the percentage of discarded batteries can be estimated from the data of the past 5 years production and, through an interpolation, it's extrapolated a trend for the future (represented in figure 4.26).

In the next chapter just the recycle scenario will be described: it's a new and highly premature sector (just about 3% of exhausted LIBs are currently treated) with many different obstacles against a fast development and most of the projections seem to overestimate the real possibilities at least in the short-medium period.

Extraction of lithium and other metals is beneficial to:

- keep all the hazardous metals in one place
- reuse metals reclaimed
- save cost of landfilling the batteries
- achieve good environmental policy (such as waste electrical and electronic equipment WEEE directive)
- save natural resources

There are many different procedures, with many different target materials, that can be found in literature and in recycle plants around the world; in figure 4.27 is represented a flowchart describing a possible procedure starting from the pre-treatment, on the discharged and dismantled components of the battery, till the recovery and the thermal management of some precious materials.

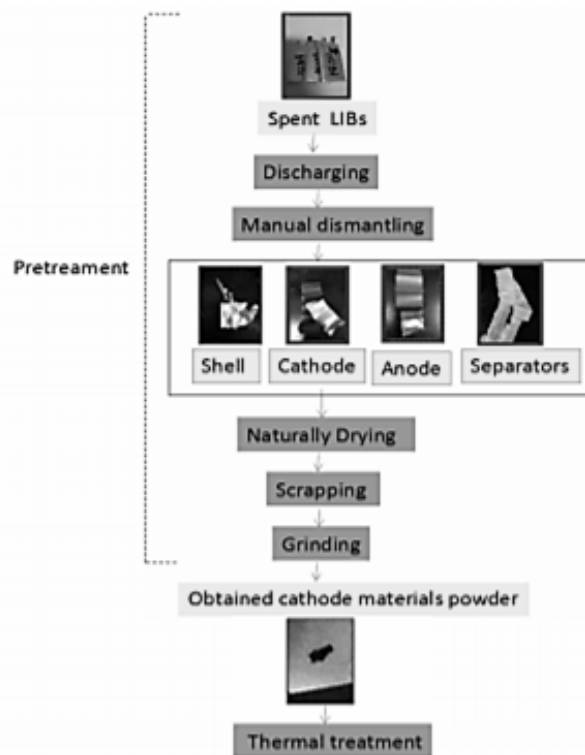


Figure 4.27: Flowchart of one among the available processes to recover raw materials from the spent LIBs [78]

In [98][78] disassembly has been investigated looking at the recoverable materials of three different chemistries and at the time necessary to conclude each operation in the reuse process: from these results is possible to see (figures 4.28 and 4.29) weight percentages of each material that could be recovered and the hours required to conclude each step before to reuse the components in another battery pack (cleaning and testing the electric parts and remanufacturing the battery).

	NMC	NCA	LFP
Alu cathode	3.9	4	3.4
Aluminium	0	0.25	0
Cobalt	3.9	1.6	0
Copper anode	6.6	7	6
Elektrolyte	11.4	10.1	8.5
Grafite anode	14	13.1	11.1
Lithium	1.4	1.3	0.76
Manganese	3.6	0	0
Nickel	3.9	8.6	0
Phosphate	0	0	3.4
Separator	5.4	5	4.3
Iron	0	0	6.1
Alu cell housing	2.1	2	1.7

Figure 4.80: Materials weight percentages for three cell's chemistries [98]

Process step	Time [h]
Disassembly Pack	0,7
Inspection pack	0,5
Testing time pack (equipment)	4,8
Testing time (employee)	2,0
Testing electronics like BMS	1,0
Remanufacturing Frame/Housing	2,5
Cleaning components	1,0

Figure 4.81: Time in hours required to conclude each of the operations involved in the reuse process [98]

Several risks come from the utilization of recovered materials inside new LIBs: both performance and lifetime could be affected by this manufacturing choice; non-linear variations in capacity fade, cell-to-cell inhomogeneity have been verified in the literature and represent the major risk of such a policy.

Increasing price of Lithium (due to higher demand) could boost the interest in the recycling that today is almost inexistent (less than 1% of the total amount of Lithium in LIBs is recovered), this because the recycle process is not focused on Lithium but tries to recover more precious metals like Cobalt and Nickel.

Many issues seem to make difficult a growing interest in Lithium recovery plants:

- LIBs are still evolving and it's difficult to establish efficient recycle processes
- The economic feasibility is highly dependent on the Lithium price and availability
- The process to extract Lithium from the batteries are complex and expensive

These barriers make difficult to imagine fast development in this field, at least in short-medium terms: It is also important to separate the recycling rates from the recycled content in new products.

Even if the recycle rate would become sustainable and effective, concerns on the suitability of these recovered materials, to be used in new automotive On-Board storage systems, should be further analysed and probably the best solution, to avoid drop in reliability and performance, will be to use such materials in other applications (i.e. static storage systems).

Large part of the literature includes recycling as a major player of future lithium production, this assumption can have very large implications on the results and conclusions drawn (figure 4.30).

Publication	Time-scale	Recycle Rate (%)	Effects on production
Kushnir, Sandén	Medium time	80%	Significant
Gruber et al.	2010–2100	90–100%.	35/50% of the demand
Wanger	Short time	40% or 100%	10/25% of the demand
Mohr et al.	Medium-Long time	limit of 80%	Significant
IEA	2020-2030	100%	Very Significant
Gaines, Nelson	2050	100%	over 40,000 t

Figure 4.82: Predicted recycle rates in different studies and different time-scales

A fundamental factor in the evolution of this sector will be the national regimentation and a specific incentive policy on the wasted batteries [100]. Some initial steps have already been initialised: in Europe, from 2012, member states must collect at least 25% of EoL batteries and, from 2016, the percentage increased to 45%; must be clear that this does not mean that the same percentage of Lithium is recovered, as said other materials have the priority due to their higher costs, but with further variations would be possible to accelerate the process. In order to effectively be able to recycle LIBs it's necessary to know exactly the different chemistries and develop specific processes for each cathode/anode combination; this implies to have automatic sorting procedures (using magnetic, electrodynamic, photographic and x-ray sensors) to adequately separate the different typologies [100]. Proposed processes basically are Pyro-metallurgy, Hydrometallurgy, Bio-Hydrometallurgy and Hybrid processes.

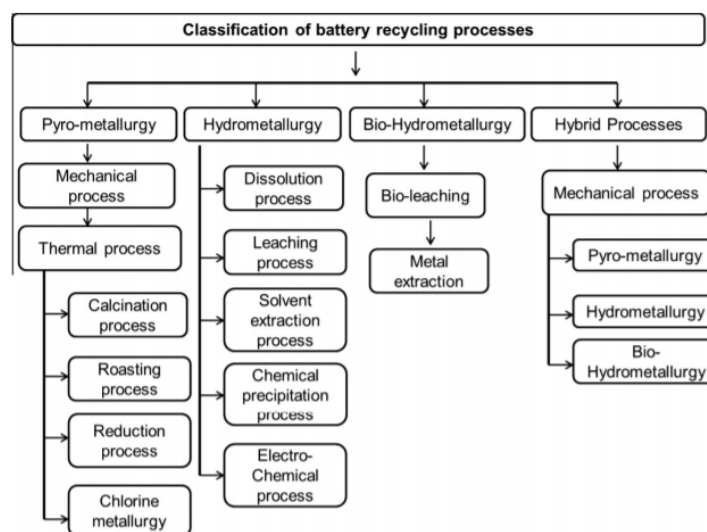


Figure 4.83: Alternative recycling processes [102]

Considering technological advantages of hydrometallurgy such as, smaller scale, minimal energy investment and minimal CO₂ emission, lithium recovery by hydrometallurgy processes seem to be the most promising alternative for the near future.

5. Minimization of V2G impact on the storage system

The last part of this work aims to identify the behaviour of the On-Board Energy Storage System (ESS) evaluating the performance degradation, during drive cycles, V2G services and storage periods. Starting from a synthetization of the experiments found in literature involving the analysis of the most important stress factors acting in the capacity and power fade phenomena, will be extrapolated a base set of conditions to build different strategies in different applications (minimizing the negative effect on the battery pack). In the first step, the most important and significative test procedures, fundamental to get valuable data from the experiments, will be described. Almost all the reported tests derive from the USABC test manual, reference document to analyse performance and behaviour of the batteries in the EVs (for HEVs other procedures are described by both USABC and PNVG associations).

5.1) Test procedures from USABC manual

5.1.1) Introduction

U.S. Advanced Battery Consortium (USABC), formed in January 1991, it's a branch of the U.S. Council for Automotive Research (USCAR), born from the cooperation of FCA, Ford and GM; the mission of this team is to develop ESS technologies to promote the commercialization of new types of power-trains and vehicles (fuel cells, hybrid and electric vehicles). [103]

To support the electric mobility and to achieve the performance targets, the main strategy was to start long-term R&D programs involving cooperation with industries, automotive manufacturers, laboratories and universities. One of the most important activities that have been addressed was the publication of technical goals, to allow benchmarking of the available technologies and to develop the required test procedures. Then, the “electric vehicle battery test procedures manual” helps to obtain comparable results and to identify the right tests for different applications providing structures and standards used by many organizations.

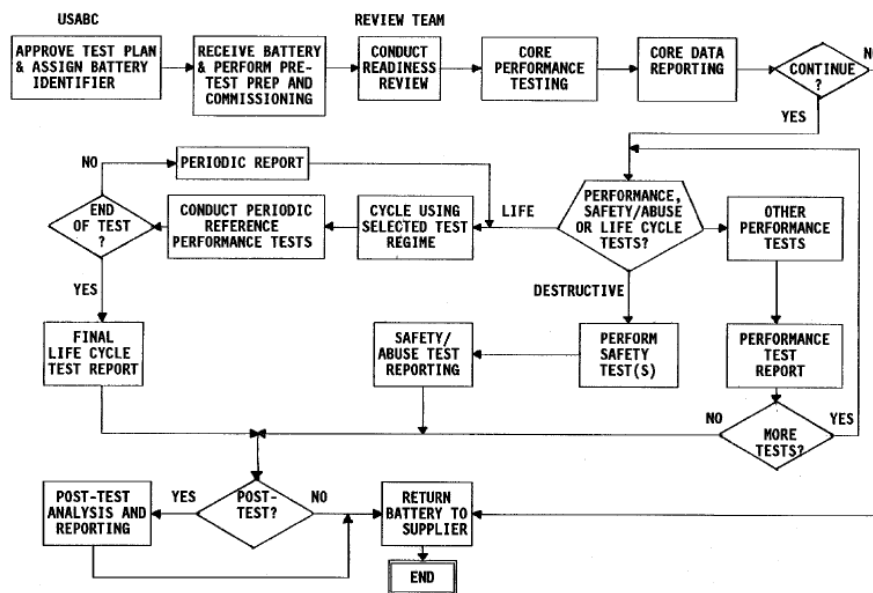


Figure 5.1: Battery test procedure following the USABC manual [103]

The general process to set-up a test campaign can be rapidly described in few steps and it's represented in the flowchart of figure 5.1:

- 1) Test plan preparation
- 2) Commissioning following the manufacturer's disposition
- 3) Electrical core performance tests
- 4) Optional performance, safety/abuse or life-cycle tests
- 5) Optional post-test analysis

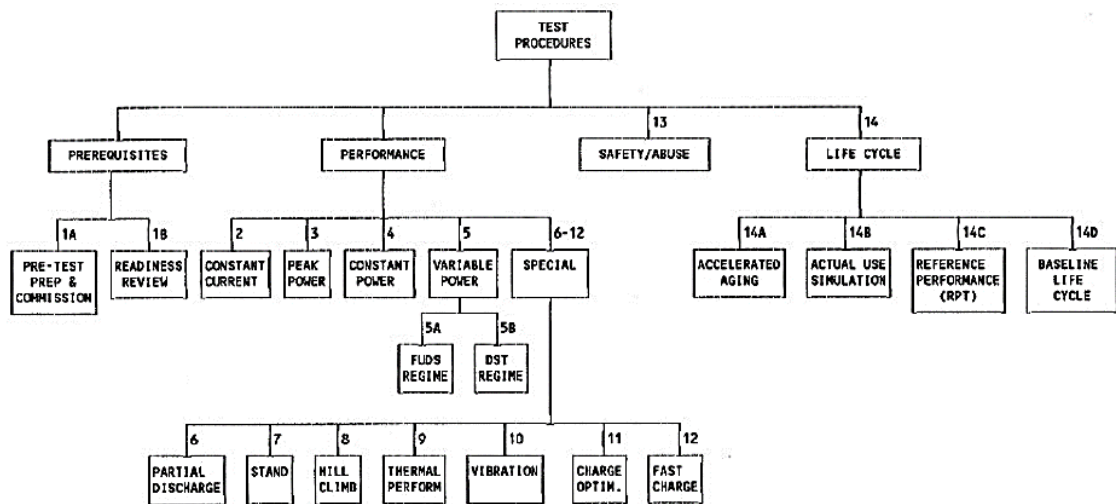


Figure 5.2: List of the main test procedures, and their variations, from USABC test manual [103]

The principal part of this manual is the compilation of individual tests starting from the base procedures described in the manual: this is particularly important to optimize and to increase the degree of flexibility, required in each specific campaign of test (in figure 5.2 there is a block diagram to list the base test procedures and the available alternatives).

5.1.2) Core Performance Testing

Constant current discharge test series

In this first test the task is to achieve very repeatable and standardized conditions to evaluate the effective capacity of the battery (pack or module). The C-rate can be varied among the tests in order to achieve an information on the effect of different discharge rates but a minimum of three C/3 tests are mandatory.

Also the charge profile should be known or should be achieved with an optimization procedure, the temperature needs to be regulated keeping the battery on open circuit condition (23 +/- 2°C). Then the procedure proceeds with sequences of discharge cycles followed by charge cycles (discharge cycles end when the rated capacity has been reached or when the cut-off voltage is reached), while, for following testing, the battery capacity is considered stable when three C/3 discharge cycles give results, in terms of measured capacity within 2%.

If a full set of tests is performed, a Puekert Plot can help to analyse the results; while, if the measured capacity is less than the rated one at a certain C-rate, it's necessary to average the value obtained in the three cycles.

Peak Power test

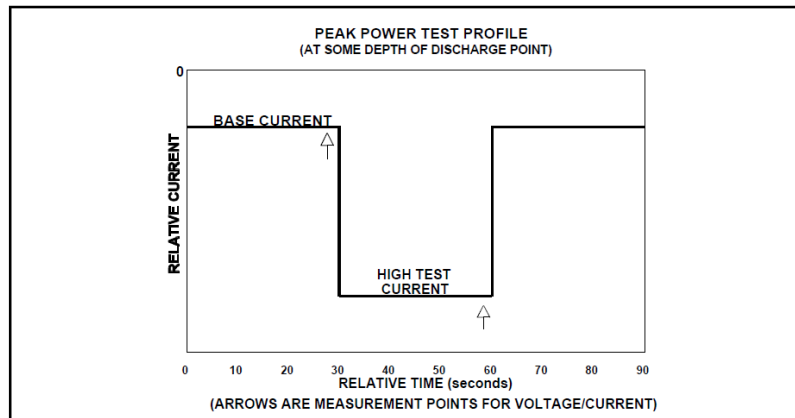


Figure 5.3: Illustration of the 30 seconds steps for a specific DoD level [103]

In this test the “sustained power capability” is measured with 30 seconds discharge of a battery at 2/3 of its Open Circuit Voltage (OCV determined with a specific test at the beginning of the life); it’s important to underline that this is not the “actual peak power of the battery”. This test can be repeated for different DoD levels: testing with DoD80 it’s particularly significative since it represents the USABC Power Goal, then this is the value used to compare different battery technologies.

Speaking about the procedure, the preparatory operation is a 30 seconds discharge at 100% SoC with the Base Discharge Rate ($I_{base_disch_rate} = [12 \cdot C_{rated} - I_{high_test_current}] / 35$) that combined with the High Test Current gives a C-rate equal to C/3. Proceeding, ten 30 seconds tests are performed starting from 0% to 90% DoD using the same High Test Current (see below) but without to go below the Discharge Voltage Limit; between two consecutive tests it’s necessary to discharge the battery at the next DoD level following the Base Discharge Rate (all the steps are represented in figure 5.3).

The High Test Current must be selected among the lower between:

- The maximum rated current for the battery
- $[0.8 \cdot \text{Rated_Peak_Power}] / [0.67 \cdot \text{OCV_at_DoD80}]$

The measured sustained power is calculated, for each test, deriving the battery resistance and the equivalent IR-free voltage from the variation in the battery voltage and current at that DoD (measured just prior to and near the end of each step).

$$\text{Battery resistance: } R = \Delta V \div \Delta I$$

$$\text{Battery IR-free Voltage: } V_{IRFree} = V - IR$$

Peak Power Capability is then the **minimum** negative value calculated from any of the following four equations:

$$\text{Peak Power Capability} = (-2/9) \cdot (V_{IRFree}^2) \div R$$

or

$$\text{Peak Power Capability} = - \text{Discharge Voltage Limit} \cdot (V_{IRFree} - \text{Discharge Voltage Limit}) \div R$$

or

$$\text{Peak Power Capability} = I_{MAX} \cdot (V_{IRFree} + R \cdot I_{MAX})$$

or

$$\text{Peak Power Capability} = \text{Actual Power at end of step (only if voltage or current limiting occurs)}$$

If the voltage limit is encountered during a discharge step, the High Test Current can be reduced to allow the other step to be completed at a constant current that allows to reach further limits, otherwise the test is

terminated. After the last step (DoD=90%) the battery is fully discharged at the Base Discharge Rate till the Discharge Voltage Limit is reached; this limit is the greater between:

- Manufacturer's Cut-Off voltage
- $[0.67 \cdot \text{OCV}_{\text{at_DoD80}}]$

The acquired data include:

- 1) Measurements of current and voltage at 1 second intervals, before during and after each step.
- 2) A plot of the Peak Power Capability versus the "actual DoD" at the end of each step.
- 3) Plots of the Battery IR-free voltage versus the "actual DoD".

Constant Power Discharge Test

Purpose of this test is the determination of the voltage versus power behaviour of a battery with respect to different DoD values, highlighting the ability to sustain discharge processes at different constant power levels (simulating the stress on the battery during a constant vehicle speed operation).

Before to start with this procedure, the battery capacity stability must be checked with a Constant Current Discharge Test then the battery must be fully recharged and the temperature has to stay within a $23 \pm 2^\circ\text{C}$ range.

A full constant power test will require different discharge phases with at least three power levels:

- The higher power level allows to discharge 75% of the energy contained in the battery in 1 hour
- The medium and low power levels can be set at 2/3 and 1/3 of the previous one.

Each phase will end when the specified target point will be achieved and will be repeated at least two times, this just if there are not critical conditions such as overheating or other dangerous phenomena that would lead to test the batteries outside the operating limits.

This time the acquired data are:

- 1) Ragone Plot (Specific Energy versus Specific Power)
- 2) Plots of Energy versus Power at different DoD
- 3) Plots of Voltage versus Current at different DoD

Variable Power Discharge Test

With this test it is possible to emulate the behaviour of the battery used in an electric vehicle including the regenerative braking.

The discharge regimes could vary very much considering different vehicles, drivers and driving cycles: in the USABC manual the reference variable power discharge profiles are:

- 1) The standard Federal Urban Driving Schedule time-velocity profile (FUDS reported in figure 5.4): considering a vehicle with a Peak Power demand of 111 W/Kg and an average Power demand of 10 W/Kg in a 1372 seconds cycle.
- 2) The Dynamic Stress Test profile: a simplified version with the same average Power demand as the FUDS profile but with a sequence of power steps with 7 different power levels in 360 seconds.

FUDS

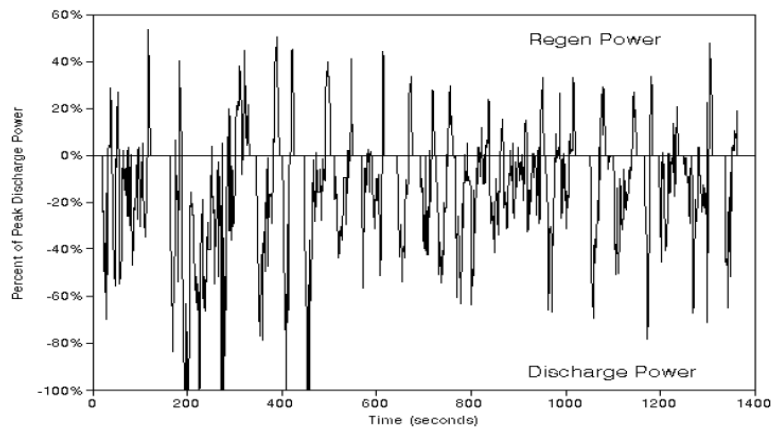


Figure 5.4: FUDS test cycle [103]

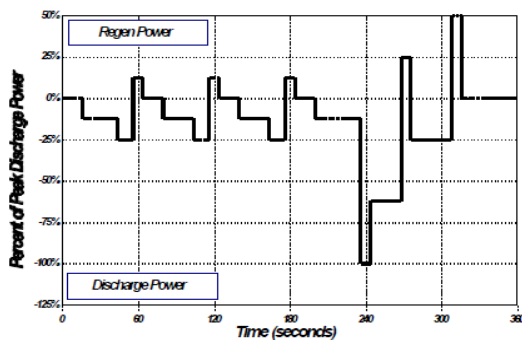
FUDS represent the best solution to simulate a “real driving cycle” because is highly demanding in terms of frequency of high and low peaks and ratio of maximum regenerative charging to discharge power (as can be seen in figure 5.4). The time-velocity profile is converted into a power-time profile for a specific vehicle (Improved Dual Shaft Electric Propulsion (IDSEP) minivan). The above picture is scaled to Percent of Peak Discharge Power and the specific power is artificially limited to 79 W/Kg instead of the 111 W/Kg described before. The procedure starts keeping the battery to a defined initial temperature (from the manufacturer recommendation or from the test-plan). Starting from 100% SoC condition, the battery is discharged through the FUDS regime applied continuously (end-to-end) without rest periods till an end-of-discharge point is reached: usually the rated capacity in Ah or the Discharge Voltage Limit as seen before.

This End-of-Discharge point is based on the net capacity, then considering the spent Ah minus the recovered energy from the brakes). The charging procedure will be scheduled considering the chosen charging mode and the constraints, in term of temperature, for the next tests. It's necessary to set safety limits, cutting the amount of energy recovered during braking and the C-rate during the discharging phases, to avoid possible unit damage.

Among the valuable results:

- 1) Value of the maximum power step.
- 2) Number of profiles completed.
- 3) Deviations from the procedure resulting in lower regeneration limits.

DST



Step No.	Duration (seconds)	Discharge Power (%)	Step No.	Duration (seconds)	Discharge Power (%)
1	16	0	11	12	-25
2	28	-12.5	12	8	+12.5
3	12	-25	13	16	0
4	8	+12.5	14	36	-12.5
5	16	0	15	8	-100
6	24	-12.5	16	24	-62.5
7	12	-25	17	8	+25
8	8	+12.5	18	32	-25
9	16	0	19	8	+50
10	24	-12.5	20	44	0

Figure 5.5: DST power profile [103]

This is a simplified version of the FUDS power-time cycle but can adequately simulate the dynamic discharging of a battery in an electric vehicle and can be easily implemented in the equipment of laboratories and researchers.

DST (figure 5.5) differs from the first cycle because it's scaled to a fraction of the maximum rated power or to 80% of the USABC power goal at DoD80 and requires higher regeneration levels.

In case the test battery cannot be operated at the required peak power, it's possible to design a scaled procedure called DST_n where "n" is the scaled peak power value in W/Kg.

Also in this case charging mode and initial temperature must be defined and the procedure starts from a 100% SoC (fully charged) condition.

DST is repeated end-to-end without rest between the 360 seconds cycles and not more than 1 second between power steps; repetitions continue till the end-of-discharge point (as seen in FUDS) or the impossibility to continue the test in the operating limits.

Then if the scheduled power value cannot be performed within the Discharge Voltage Limit or other specified battery limits, the discharge is terminated at that point.

Finally, the recharge is executed as soon as practical and in case of risk for the battery integrity, lower limits of regen power, voltage or current can be applied to the test plan.

Among the valuable results:

- 1) Value of the maximum power step.
- 2) Number of profiles completed.
- 3) Capacity of the test unit (both gross and net in Ah and kWh).
- 4) Deviations from the procedure resulting in lower regeneration limits.
- 5) Designation DST_n should be used to report the scaled peak power level.

5.1.3) Life Cycle Tests

There are several testing procedures to forecast if the expected EV lifespan (cycle and calendar life) will satisfy the USABC goals and to identify some of the most significative ageing and failure mechanisms.

It's important to fix standard operating conditions, whenever possible, to compare in the most useful way different technologies and different cells, modules or battery packs.

Availability of online data resulting from real usage conditions is, sometimes, enough to project the ageing behaviour: this is not the case of Li-Ion batteries where highly non-linear behaviour are triggered by many different degradation modes.

Then the first phase of the procedures is focused on the definition of the testing conditions together with a DoE necessary to maximize the efficiency of the test procedure considering also the number of available components:

- Verification of the manufacturer information
- Identification of stress factors and ageing parameters
- Collection and analysis of statistically significant data

After this initial experiment design, it's possible to follow several main steps (as reported in figure 5.6):

- 1) Selection or design of accelerated/actual life cycle test
- 2) Application of the ageing regime for a defined number of cycles or a time interval
- 3) Execution of a series of reference base-line cycles

4) Repetition of second and third steps till End-of Life (EoL) condition

While in the actual-use tests there are severe constraints as far as the testing time is concerned (could be necessary to test for months or years the battery pack and it would require high costs) the accelerated procedure requires a complex procedure design because it's necessary a deep knowledge of the component behaviour and of the main ageing mechanisms to select and control just the significative stress factors in order to achieve results representative of the real usage.

Thus, in general, because of the lack of time and the changing nature of the technologies, a relatively low percentage of the life-cycle testing are performed with the actual-use regime.

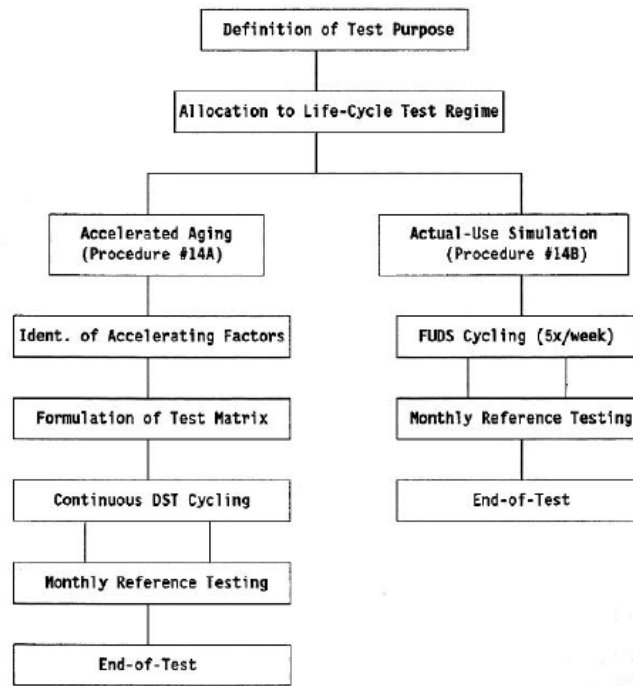


Figure 5.6: Block diagram schematizing the steps in the Life-Cycle Test procedure [103]

Reference Performance Test (RPT)

It's the fundamental test to verify the degradation level during the life of the battery: for this reason, the RPT must be repeated periodically during the cycle life and when compared with reference base-line data, allows to characterize performance, failure mechanisms and their evolution.

Usually the intervals correspond to 5-10% of the forecasted battery life (i.e. 28 days or 50 cycles) but other intervals could be set to satisfy specific requirements and the same holds for the ambient conditions that usually are nominal environment conditions but could be varied for specific purposes such as higher temperature to accelerate battery ageing.

The test must be started with a fully charged candidate and a rest period then it's possible to proceed with the sequence of steps (3 in total) considering a fully charge after the end of each phase:

- 1) Constant Current discharge at C/3 rate (only) to 100% of rated capacity
- 2) DST discharge scaled to 80% of the USABC peak power goal for the technology, to 100% of rated capacity
- 3) Peak Power discharge

The first step should be preparatory to the following ones, restoring the operating capabilities of the unit after the rest period; the second and third steps are necessary to characterize the actual status of the battery

identifying performance losses through the evaluation of the remaining capacity and of the pulse power response but it's also possible to require others results using the same Reference Performance Test.

Accelerated Aging Testing

Imposing higher values on certain stress factors it's possible to accelerate the ageing phenomena in the battery; with this method is then possible "compress" the testing time.

In case the test would represent a simulation of the operation in an electric vehicle, the test must be executed following DST procedure and the goal it's, one more time, to reach the EoL threshold (80% of the original capacity).

To assure the value of the recorded data it's necessary to make phenomenological correlations to actual-use service life, then it's necessary to perform a process based on previous experience, this allows to verify if the boundary conditions of the accelerated test give results, on the battery performance, near to the real usage.

Experience-based procedures (as in this case) can just give rise to empirical correlations but this fact it's accepted to overcome constraints in terms of cost and time.

The main steps can be summarized:

- 1) Identification of accelerating parameters (usually Temperature, DoD, C-rate etc.): it's necessary a deep knowledge of the degradation modes and of the most important failure mechanisms (related to the studied technology).
It's also necessary to distinguish among the stress factors their relative importance in accelerate the ageing (it's possible to link each parameter with a severity index) and what mechanisms are affected by the actions. Finally, the range for each stress factor (min/max) must be estimated considering that minimum stress-factor level must still represent an accelerated condition.
- 2) Test Matrix composition: DoE activities to design an efficient experimental procedure is essential to reduce the risk to forget important results and, moreover, to reduce the related cost/time.
Usually full factorial plans are preferred to analyse more than a factor at a time with all the interactions among them; often fractional factorial plans are used to reduce the necessary tests excluding some of the factors/interactions that can be considered marginal.
Also limits on the availability of the candidates can be an obstacle against the choice to build a full plan. Three elements should be included in all accelerated lifecycle testing: time compression, a dynamic discharge regime (DST modified to include the selected stress factors) and periodic reference benchmarking (RPT).
Thus, the target must be to analyse all the available results of the test obtained varying the selected stress factors.
- 3) Analysis of the performance of the test plan: test matrix defined in the previous step, could be improved with randomization of the factors' order, considering location, sequence and so on, to reduce uncontrollable effects and noise factors.

Now entering in the details of the procedure it's possible to describe some specific steps that must be followed in each test:

- DST can be applied end-to-end, without rest periods between the end of each segment, till the specified DoD level or another limit value declared by the battery manufacturer.
- At fixed intervals it's necessary to stop DST to perform RPT and then to characterize the actual status of the tested components.
- The results must contain all the cycles until EoL is reached and further cycling should be considered apart.

Obtained data contain the historical evolution of the performance (capacity, power...) with all the anomalies recorded during the procedure: among the information it's possible to analyse the number of cycles, the ageing regime adopted, energy efficiency, OCV at the end of charge/discharge phase, temperatures and so on.

In the report of a test unit it's necessary to include some characterizing information:

- A list of the tests executed before the life cycle testing (to describe the starting conditions of the battery).
- Results of all the RPTs.
- All repetitive discharge tests for which the specified capacity is achieved.

It's finally necessary to assure a correct analysis of the recorded data, for this purpose some generic steps can be suggested to build a plan:

- 1) Identification of the smallest test unit (cell or module) for which there are failure/ageing information and collect those data in a specific database with all the service-life statistics.
- 2) Individuation or development of an appropriate mathematical model to adequately describe the effects of the controlled stress factors on the lifespan finally correlating and linking each factor to establish the influence grade.
- 3) Individuation of a statistical distribution matching in a good way the recorder results and considering also the uncertainty in the service-life data.
- 4) Application of iterative mathematical methods to increase the database and then the information on each factors/interaction and their influence on the battery life (i.e. Monte Carlo method).

Ambient Temperature Influence

Within this procedure it's possible to reproduce the thermal loads that an On-Board battery could experience, and sometimes it's used to validate the accelerated procedure and the data derived from this kind of tests. The testing scheduling implies to discharge the battery applying FUDS cycles and varying the temperature range to simulate the real environment conditions (i.e. following the temperature ranges and the testing time in figure 5.7).

Temperature Range	Full Range Batteries	Hot Climates Only	Cold Climates Only
Cold $T \leq -8^{\circ}\text{C}$	10	-	10
Cool $-8^{\circ} < T < 0^{\circ}\text{C}$	15	-	15
Normal $20^{\circ} \pm 10^{\circ}\text{C}$	50	50	60
Warm $30^{\circ} < T < 38^{\circ}\text{C}$	15	40	15
Hot $T \geq 38^{\circ}\text{C}$	10	10	-

Figure 5.7: Temperature ranges and percentage of test time to simulate different climatic conditions [103]

The main steps can be summarised in:

- 1) The candidate must be cycled 5 days per week with FUDS power profiles (calibrated on the USABC goals) in a conditioned test environment to control and change the ambient temperature.
- 2) For each discharge the power profile must be applied end-to-end with no rest periods, till a DoD of 80% of the rated capacity or other manufacturer's limits.
- 3) After predetermined intervals it's necessary to perform RPTs (at normal ambient temperature) characterizing the actual status of the tested unit.
- 4) Repeat previous steps until an end-of-test condition (specified in the test plan) is reached.

It's important to notice that this test could be a viable way to analyse the efficiency and the performance of a thermal management system to assure the effectiveness of its design on the temperature control.

The complex structure of these test require a higher effort to analyse and to obtain the right interpretation of the data: it's necessary to start from an exhaustive description of the test unit structure and of the scheduled test procedure, including also the power and temperature regimes applied, then the interpretation of the results must be accompanied with failure analysis, suggested improvements in the battery design and in the thermal management system, in installation procedures and/or test variations.

5.1.4) Safety/Abuse Tests

Being the intrinsic nature of LIBs exposed to dangerous and irreversible phenomena (i.e. run-away) it's necessary a particular test procedure to identify the main critic events that can take form, the abuse conditions that must be avoided to stop these mechanisms and some ways to anticipate and interrupts such mechanisms. Then studying the so-called worst-case accidents it's possible to highlight the safety operation areas that must be respected during the service-life and identify the most important intentional/unintentional abuse conditions that would lead to destroy the system: this operation is mandatory to respect the governments regulations and to guarantee the safety requirements necessary to share a product on the market.

Conditions investigated include (at least one battery pack for each test must be considered):

- Response to vehicle crashes (mechanical abuse)
- External uncontrollable conditions (environmental exposure)
- Electrical charger malfunction (electrical abuse)

These investigations must consider not only the battery pack but also the ancillary components that are fundamental to the correct operation of the On-Board energy storage and could be damaged leading to instability of the whole system.

It's necessary to prepare the battery pack with a short number of cycles from the life-cycle test regime, then the battery completely charged can be mounted on the support frame that simulates the installation in an electric vehicle.

The specific procedure is in evolution and it's based on the Federal Motor Vehicle Safety Standards (FMVSS) for electric vehicles; requirements and target must be specified in the test plan and usually data a recorded for 2 hours (with measures at specified time intervals i.e. 1 minute) for each safety/abuse test.

Specific data acquisition for the abuse tests is to include:

- 1) Battery voltage;
- 2) Physical response (dimensional change, weight change, degree of fragmentation, existence of fire, breaching of containment);
- 3) Release of liquid and gaseous products (quantity, composition);
- 4) Thermal response on and near the battery;
- 5) Video and audio recording of the entire event;

A complete battery failure analysis is to be performed and documented with copy of the video recording of each event and finally, anomalies with the battery or the test procedure have to be noted.

5.1.5) Other Performance Tests

Three more special tests (rarely executed but that can respond to particular needs) will be reported in the next rows.

These tests are used to explore operating conditions outside from the common applications therefore it's possible to say that are infrequently in a normal testing activity:

- Partial Discharge test
- Stand (self-discharge) test
- Sustained Hill Climb test
- Thermal Performance test
- Vibration test
- Charge Optimization test
- Fast Charge test

In this work are described just three among the listed tests, for more details it's possible to use the USABC test manual in which all the alternatives are described and explained.

Partial Discharge Test

It's a procedure particularly useful to evaluate the evolution of capacity and power fade of units subjected to different DoD, then subjected to different degrees of partial discharge.

- 1) The battery is initially discharged (usually at C/3) for three consecutive cycles until 100% DoD is reached (then until cut-off voltage is achieved).
- 2) Then the recharge scheme suggested by the manufacturer is followed and the deliverable capacity (Ah) is established.
- 3) Following the test plan, partial discharge steps at C/3 are executed to explore different DoD (partial discharge and recharge will be separated by one hour).
- 4) Ten (or another specified number) partial discharge cycles are repeated.
- 5) Again a 100% DoD discharge cycle (about 3 hours at C/3) is used to measure the available capacity repeating the step for at least three times.

The battery voltage and current plots must be analysed to verify that after each partial discharge cycle the charge procedures achieved a 100% SoC status before to start with the next step (it's possible to consider end-of-charge and end-of-discharge voltages).

Among the valuable data, are relevant measures of temperature, voltage, current as a function of time: with these results it's possible to establish if the charge scheme can adequately restore the SoC of the battery at 100% after each partial discharge and, moreover, it's possible to analyse memory effects leading to capacity fade.

In addition, two plots

- End-of-charge/discharge voltages vs test cycles.
- Capacity at the end of the partial discharge cycles vs 100% DOD cycles (capacity normalized to that obtained before the partial discharge cycles).

Stand Test

This is the core test to evaluate the self-discharge rate of a battery under storage condition: this is representative of an electric vehicle parked for a long time and not connected through the charger to the grid. Self-discharge could be partially temporary (reversible phenomena) and/or permanent (irreversible phenomena).

Schematizing the steps:

- 1) The battery must be recharged following the procedure suggested by the manufacturer and then fully discharged at C/3 (in order to define the deliverable capacity at this C-rate)
- 2) Then the battery is charged and let stand, in OCV conditions and ambient/operating temperature, for a period specified in the test plan (usually 2 days for the short/mid-term and 30 days for the long-term)
- 3) At the end of the stand period it's again necessary to fully discharge the battery (C/3) in order to evaluate the "stand loss" that is equal to the difference between the capacity measured in the step 1 and the one measured after the stand period.

If there are anomalies in the measured value could be necessary to adjust the time interval and repeat the test: a measure below 5% could be not statistically distinguishable because is in the uncertainty windows of the experiment, on the other side a stand loss above 10% should be further investigated with other test at different ambient temperatures.

The specific data to be reported is to include the stand loss as a percentage of the measured capacity versus the stand time over which the test was conducted, the baseline capacity removed (Ah), and the capacity lost during the stand period (Ah).

Thermal Performance Test

It's a test that has the target to characterize the performance of the battery under different ambient temperatures with a focus on the variation of many technological factors and parameters but trying to exclude the effect of different thermal management systems. For this reason, it's not possible to generalise a test procedure that allows to investigate all the parameters but instead a specific set should be targeted and, with a correct design of the experiments would be possible to isolate these results.

Results can be used to determine the need for thermal management and/or the allowable operating temperature range for a battery but after these considerations a further analysis of the performance of the different thermal management system alternatives should be accomplished to verify the satisfaction of these requirements.

The procedure consists in a sequence of charge/discharge cycles on a battery in thermal equilibrium (then pre-conditioned to higher/lower temperatures): suggested temperatures are -30°C, 23°C (ambient) and 65°C.

Discharge regimes could be static (constant current i.e. C/3), at constant power or dynamic (i.e. FUDS and DST) depending on the features of interest.

With this procedure it's also possible to study the charge performance (i.e. charge acceptance) at high/low temperatures, for example simulating charge phases at different geographic locations).

The obtained temperature data should be reported graphically as a function of time for both the discharge and charge portions of the cycle.

5.2) Synthetization of the experiments in literature

5.2.1) Introduction

In this chapter the degradation behaviour concerning calendar and cycle ageing will be studied through the analysis and the description of the experiments found in literature: this allows to divide different phenomena affecting the performance under different storage/operating conditions. For these reasons, the results will be subdivided and the respective degradation modes will be linked to the performance variation.

The first phase is the individuation of the key stress factors and their importance acting as degradation accelerators: in [104] there is a clear description of the most important parameters affecting power and capacity fade with the explanation of the physical phenomena underneath these behaviours. It's also important to understand the root causes that lead to degradation phenomena in order to develop a set of strategies (i.e. in the BMS) to counteract and minimize such behaviours: these include accurate ageing estimation, advanced thermal management systems, focused battery design. This classification has been developed considering and comparing the results from an electro-chemical model (P2D Li-Ion battery model) and the results of experiments on different cells: numerical fitting minimised the square of error between simulated and measured voltage using a non-linear fitting algorithm. The central idea is that tracking the values of the most significative parameters, it's possible to deduce the degradation mechanisms during the battery life. Looking at the structure of the Pseudo2Dimensional model, there are 57 scalar parameters that must be considered to obtain a realistic battery model: it's then necessary to identify and select a lower number of factors under investigation. Not all these parameters influence in the same way the ageing modes, moreover, different scenarios involve a different set of stress factors.

The identification process can be schematized with two main steps (the procedure is fully summarized in figure 5.8):

- 1) Evaluation of the P2D model with a given set of parameters
- 2) Determination of the parameter set that minimises the sum of squared error between the simulation results and the experimentally measured voltage response for a given drive cycle

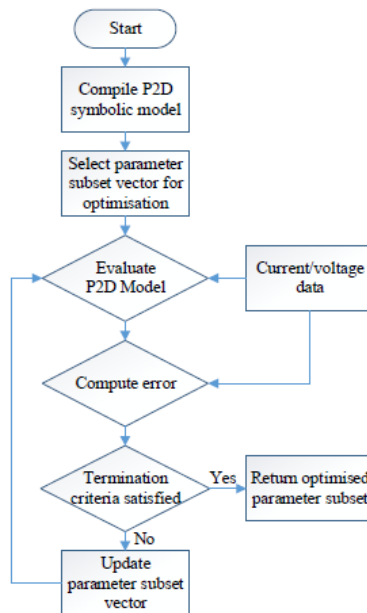


Figure 5.8: Parameters Optimization procedure from [104]

From different discharge current-voltage profiles, it's possible to get different combinations of significant stress factors minimising the quadratic error cost function where e and m are two experimental coefficients and w1 and w2 are the weights attributed:

$$\text{Minimise } F(\gamma) = w_1 \sum_{t=0}^{t_{\max}} [v_e(t) - v_m(t, \gamma)]^2 + w_2 \left[(t_e^{\text{end}} - t_m^{\text{end}}) \right]^2, \text{ subject to } \gamma_i \geq 0$$

To validate each identified set, it's necessary to compare the simulated voltage response for a drive cycle with the measured voltage.

These optimised parameters can be tracked and used to characterize and describe the degradation modes evolution:

- Number and frequency of cycling
- SoC
- Swing in State of Charge (DSOC)
- C-rates during charge and discharge
- Temperature
- Voltage exposure

The effects of these stress factors (derived from published literature) and their quantification with P2D model, can be represented with different block diagrams; it's also possible to subdivide the effects on the positive and the negative electrodes.

Calendar ageing: key stress factors

Starting from the storage scenario, maybe with a vehicle leaved parked for a certain amount of time, it's easy to understand that the only elements in the list that should be considered are the temperature at which the vehicle, and then the battery pack, are exposed and the SoC at which is the battery at the beginning of the rest period. Without to give numerical values, this will be the topic of the next chapters, the description of the most important mechanisms that lead to lower battery performance (in terms of capacity and power) will be introduced for both calendar and cycle ageing.

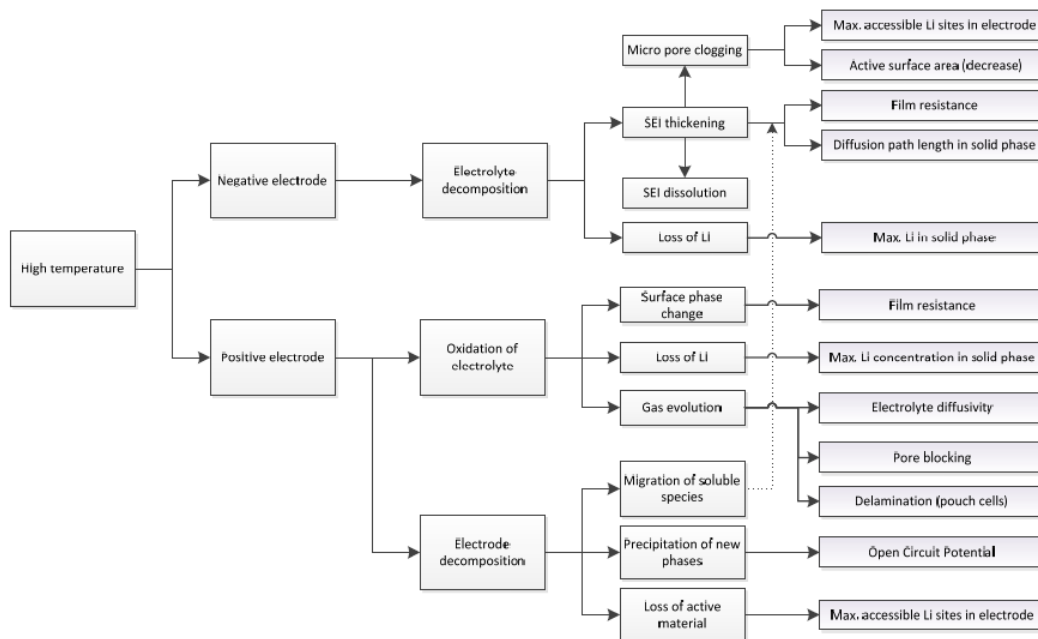


Figure 4.9: High temperature effects on both the electrodes [104]

Temperature is of course one of the obvious player affecting the evolution of the calendar ageing: both high temperature and low temperature storage conditions can lead to many effects on both anode and cathode (figures 4.9 and 4.10). In high temperature conditions the most important phenomenon is the electrolyte decomposition at the boundary between the anode (negative electrode) and the liquid electrolyte: this due to secondary reactions consuming Lithium ions and resulting in capacity fade. Solid Electrolyte Interface layer on the anode it's a further fundamental mechanism that, on one side leads to a greater internal resistance and a slower ionic diffusion, resulting in power fade, on the other side acts like a protection against the secondary reactions and the exfoliation of the anode.

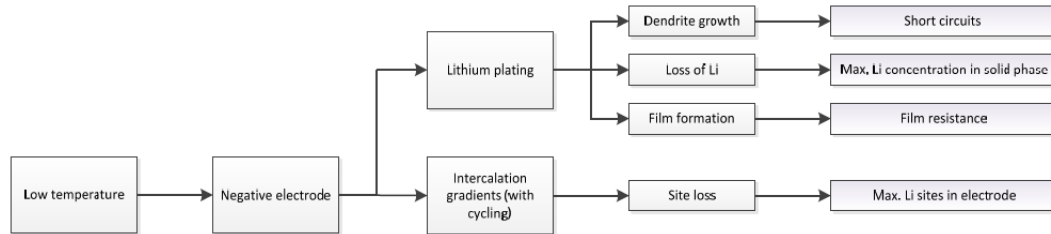


Figure 5.10: Low temperature effects on the negative electrode [104]

In case of storage in low temperature ambient, the stronger degradation mechanism is the precipitation of Lithium (solid form), from the liquid electrolyte to the negative electrode surface, this occurs when the anode potential is near to that of the Lithium deposition potential leading to losses in the available Lithium inventory.

The quantification and the relative importance of these phenomena could be used to design appropriated strategies and to manage an active thermal management system. The target should be to minimise the performance losses every time the vehicle it's parked (at home or at work), this become particularly important looking at the behaviour of the larger part of the car owners: most of the time, during the vehicle life, is spent still in rest position, then the fraction of capacity and power fade due to this condition is not negligible and should be faced to enlarge, as much as possible, the useful life of the battery.

The second individuated parameter, affecting the evolution of a battery during storage periods, is the SoC at which the battery is stored.

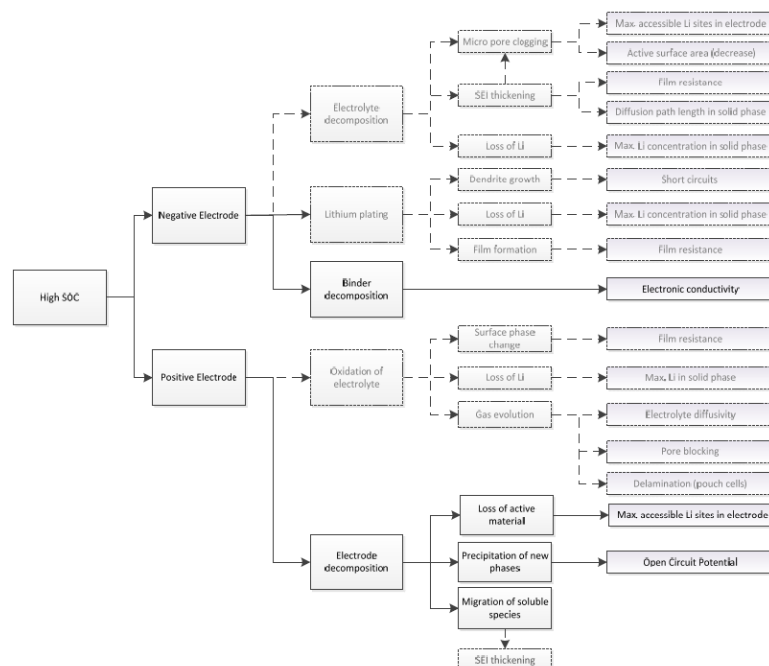


Figure 5.11: Effects of High SoC on both the electrodes [104]

High State of Charge (figure 5.11) and High temperatures are well-known worst storage conditions that accelerate the degradation modes: this can be adequately simulated exploiting the Arrhenius equation in which, to an increase in the SoC, it's related a lower activation energy (barrier for the thermal activation of the reactions) and then promoted parasitic reactions.

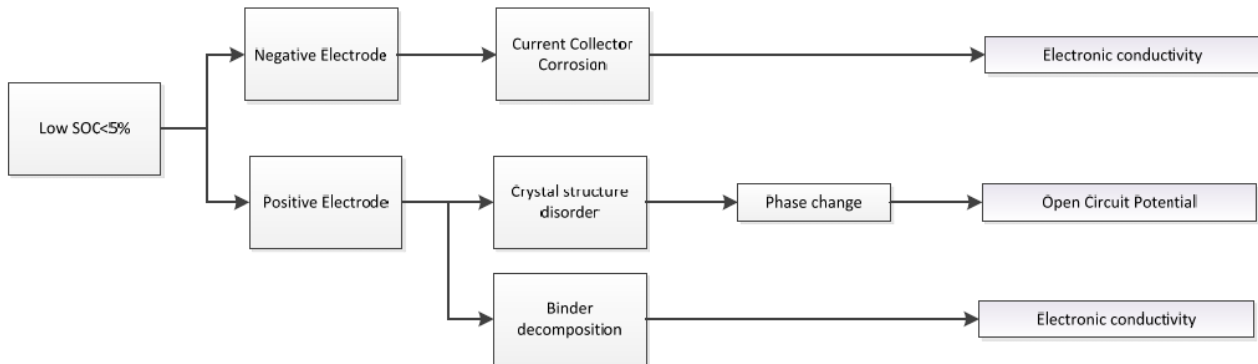


Figure 5.12: Effects of Low SoC on both the electrodes [104]

On the opposite side the storage at very low SoC could be not practical due to negative effects on the performance caused by different mechanisms, such as the current collector corrosion and the binder decomposition, resulting in worse electronic conductivity.

Cycle ageing: key stress factors

The factors considered in the previous rows and the considerations derived still hold during the cycling but now the strategies are not anymore focused on the minimisation of such effects because the main target is to achieve the best performance during the vehicle utilization without to exceed from the operational limits. For this reason, the focus will be on the remaining key stress factors starting from the current adopted during charge and discharge activities (figure 5.13).

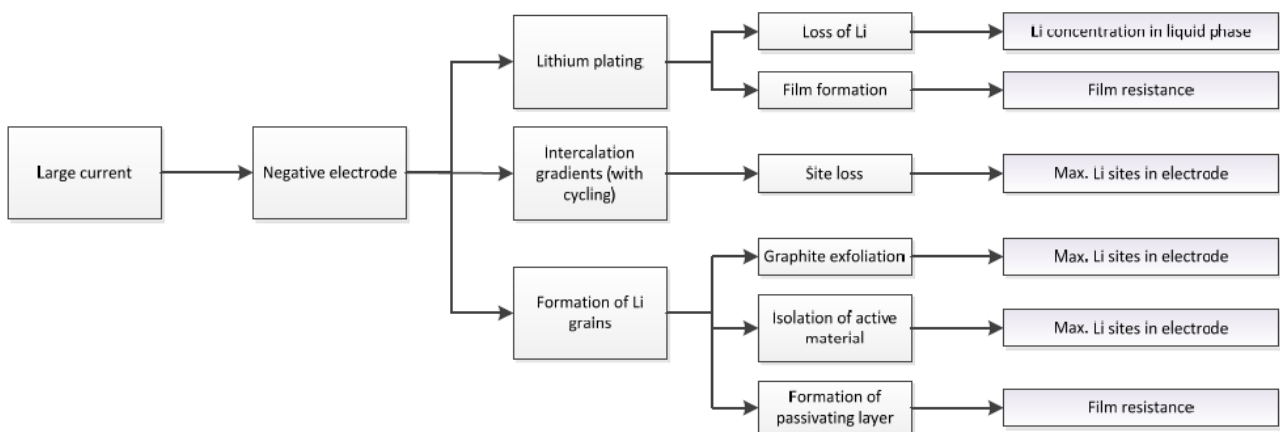


Figure 5.13: Effects of large current rates on the negative electrode [104]

This time the worst possible condition occurs with high charging/discharging rates and low operating temperatures; poor current distribution and high charging rates promote Lithium plating causing a potential drop to or below 0V relative to Li/Li⁺ (intercalation is less energetically favourable). Another phenomenon, related to high C-rates, is the appearance of Lithium grains, electrode exfoliation and loss of active material then capacity fade.

Large swings in the SoC are much important in batteries for electric vehicle applications, indeed the target range can be reached just exploiting, as much as possible and convenient, the whole SoC range (from 100% to the minimum accepted value).

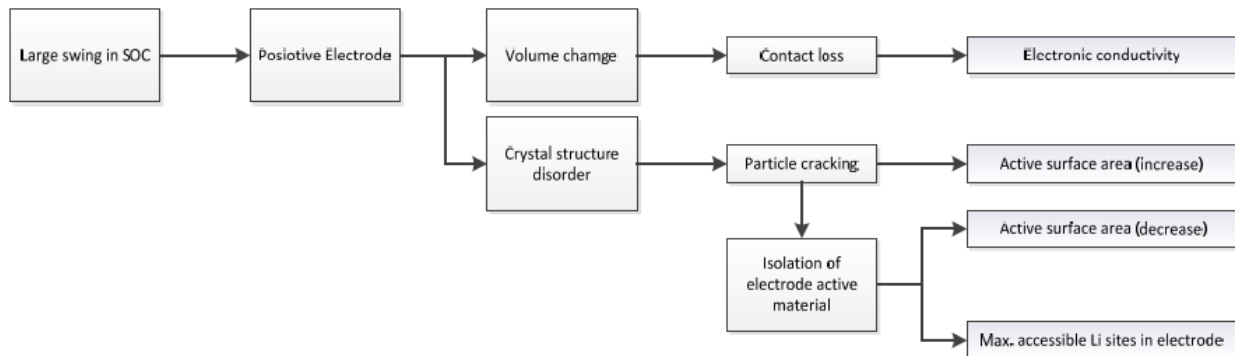


Figure 5.14: Effects of Large Swing in SoC on the positive electrode [104]

Volume changes, due to intercalation of Lithium Ions in the host matrix, and variations in the crystal structure are sources of mechanical stress on the electrodes, resulting in strain and particle cracking and affecting both the ionic conductivity and the active surface area.

The last considered factor is the number of cycles that, one more time, produces effects on both the electrodes: also this time there are related mechanical stresses similar to the previous ones.

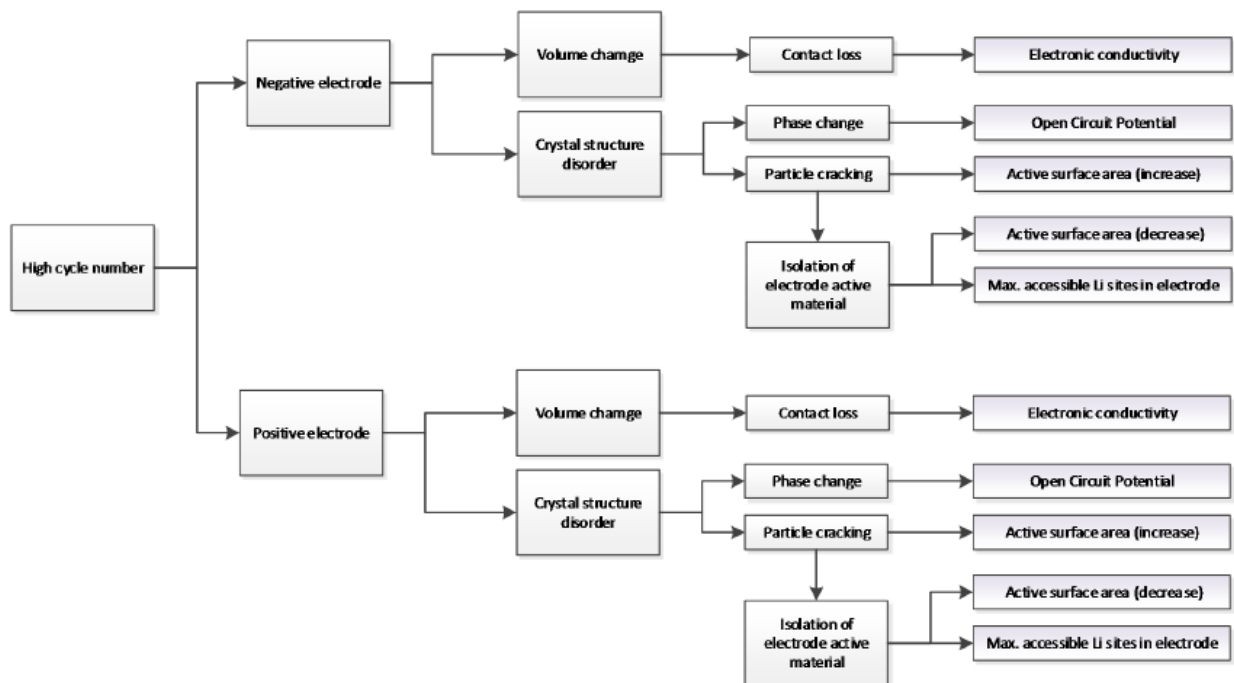


Figure 5.15: Effects of High Cycle Number on both the electrodes [104]

5.2.2) Description of the experiments

In the next examples, some different Li-Ion technologies are studied to extrapolate behaviours and trends that could help to understand and face the most evident and significative degradation mechanisms: the typologies considered are representative of the available commercial batteries, then with liquid electrolyte and graphitic carbon anodes.

The selected cathode chemistries are among the most diffused in the automotive sector and future works could explore more possible scenarios focusing the attention on solid electrolytes, Lithium metal anodes and so on.

Calendar ageing: experiments and results

Considering different SoC and Temperature conditions it's possible to characterize the behaviour of a battery cell under storage conditions; one of the most important effects, that a battery in rest for a long period experiences, is the self-discharge: this reduces the amount of energy available for the first cycle after the park period.

Moreover, is well-known that storing the battery pack at high temperatures and high SoC for long periods of time could be more detrimental than cycling [105].

Temperature	40% charge	100% charge
0°C	98% (after 1 year)	94% (after 1 year)
25°C	96% (after 1 year)	80% (after 1 year)
40°C	85% (after 1 year)	65% (after 1 year)
60°C	75% (after 1 year)	60% (after 3 months)

Figure 5.16: Recoverable capacity of a Li-Ion battery after one year of storage at different temperatures [105]

Then temperature influences, sometimes permanently, the capacity of the battery cell/pack and, as far as the calendar ageing is concerned, a lower degradation level can be reached decreasing the storage temperature, ideally toward 0°C (the phenomenon is complex and other aspects must be considered in the study).

Low temperature levels are not acceptable during the cycling, where relatively high discharge rates are common, but the possibility to control the temperature with an active thermal management system would give the opportunity to reduce as much as possible the capacity loss heating up the pack before to be utilized.

This behaviour is shared among different battery chemistries, in [107] the Lithium-Iron Phosphate chemistry is tested accelerating the ageing phenomena with different high temperature steps and different SoC levels (figure 5.17).

Ageing Case	Temperature	SOC
<i>Case 1</i>	55°C	50%
<i>Case 2</i>	47.5°C	50%
<i>Case 3</i>	40°C	50%
<i>Case 4</i>	55°C	10%
<i>Case 5</i>	55°C	90%

Figure 4.17: Ageing cases, with different temperature and SoC levels, used in [107]

In this test 15 cells (LFP/2.5 Ah/3.3 V) have been stored for 24-36 months and every 30 days a Reference Performance Test (RPT) was executed to analyse the evolution of performance parameters like the internal resistance: the results show a non-linear behaviour varying the stress levels.

Then in this case to extrapolate the storage temperature that maximize the calendar age and to interpolate the results obtaining a continuous range of values, three stress levels have been considered for both the stress parameters (T and SoC).

RPT test, already described in the previous chapter, has been performed at 25°C and measured the internal resistance, for charge and discharge operations, using different 18 seconds current pulses (4C, 2C, C, C/2 to obtain the variation of the internal resistance with different C-rates) and scheduling 15 minutes of rest after each measure (to get the thermodynamic stability as illustrated in figure 5.18).

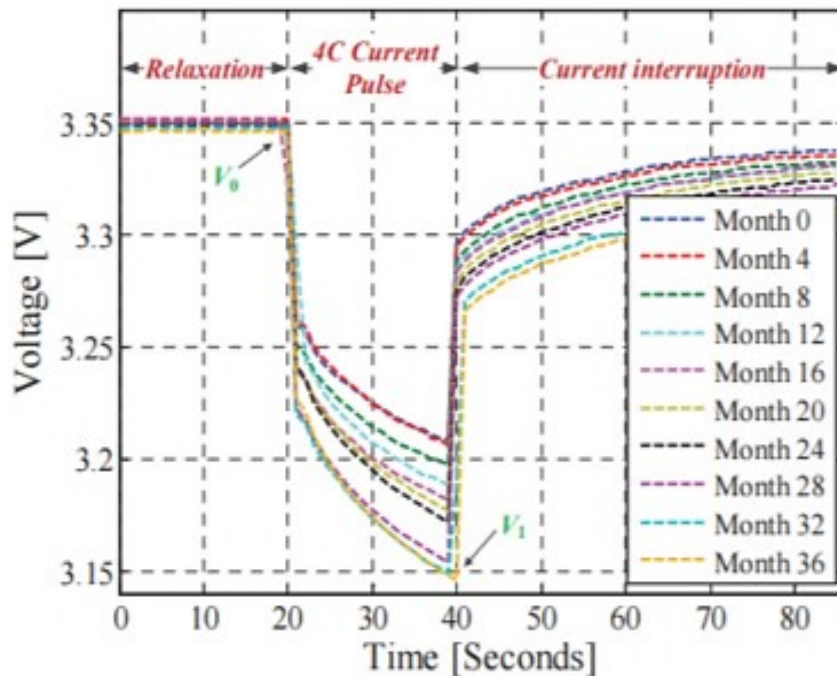


Figure 5.18: Voltage response with different degradation levels of LFP/C cells [107]

Looking at the results in figure 5.19, the previously introduced considerations on the detrimental effect of high temperatures and high SoC on the capacity performance is well represented by the internal resistance evolution with the time: case 3 (red line), in which we have the lower temperature value (40°C), results in a lower internal resistance growth rate for each of the C-rates applied.

Further considerations can derive from the results obtained varying the SoC at which the battery is stored: measured data show that in case 3 (SoC at 10%) the internal resistance grows less than the case of 50% and 90% of state of charge; while the disadvantages in storing the battery cells at very high SoC (i.e. 90%) is proved and well understood, the choice between a low and a middle State of Charge is not so clear, especially with different chemistries, so other experiments will be analysed.

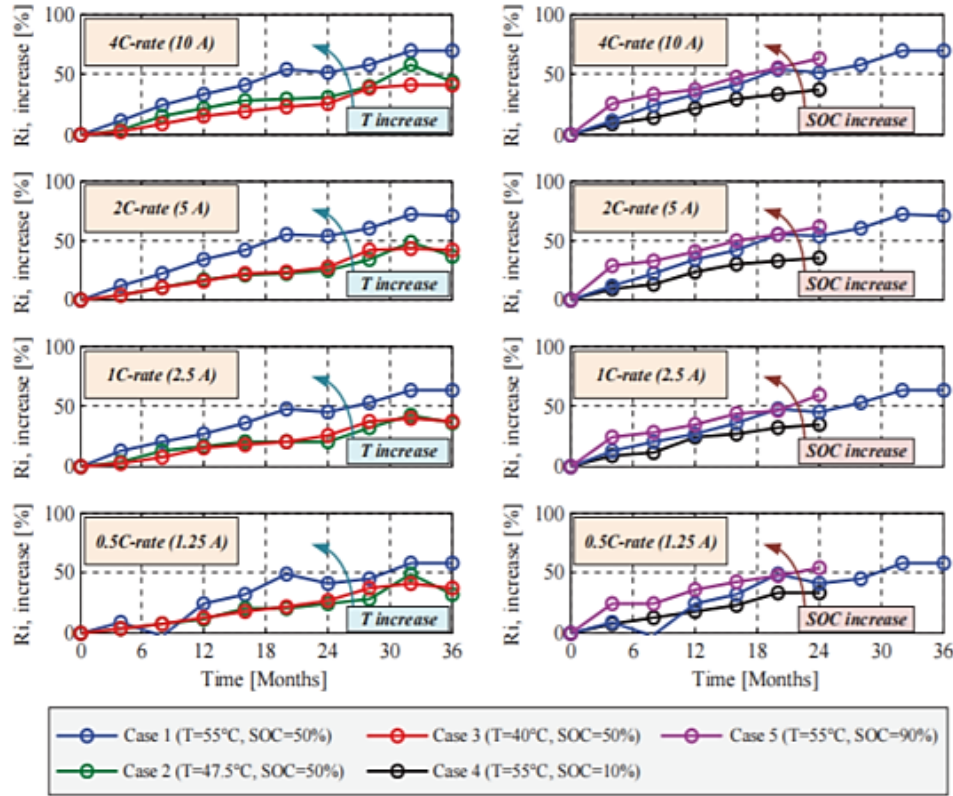


Figure 5.19: Internal resistance vs different C-rates, temperatures and SoC [107]

Continuing with the investigation on the calendar ageing phenomenon, further data come from [108] where 16 NCA cells (3.350 Ah) were tested, also this time, with different combination of temperature and SoC in order to get results in terms of average capacity fade, rate capability variation and resistance variations. The testing conditions are reported in the figure 5.20 and for each test case two cells have been used:

Case	Result	Temp	SoC
1	Capacity fade/Rate capability/Internal resistance	-27	99
2	=	-27	5
3	=	25	50
4	=	25	100
5	=	45	20
6	=	45	70
7	=	55	5
8	=	55	81,5

Figure 5.20: Results obtained and testing conditions from [108]

After 66 weeks of storage the cells capacity loss measured oscillates between -1% of case 1 and 13% of case 8 confirming the high influence of the temperature that it's the most important stress factor in these conditions and, at -27°C , seems to neutralise the effects of SoC on the degradation evolution but showing the worst performance concerning the available rate capability after the rest period (then low temperatures leads to high power fade illustrated in figure 21-b).

Analysing the cells at the same temperature and switching the SoC values, better results (less capacity loss in figure 21-a) have been achieved by cells at lower SoC: at 55°C passing from 5% to 81.5% of SoC resulted in 6.5% increment in capacity fade while at 45°C the loss between 20% and 70% of SoC led to 4% of loss: this can be synthetized saying that low SoC conditions (0-20%) are less affected by capacity fade with respect to high SoC conditions (70-100%) but remains to be understood the best solution between middle (30-60%) and low SoC values.

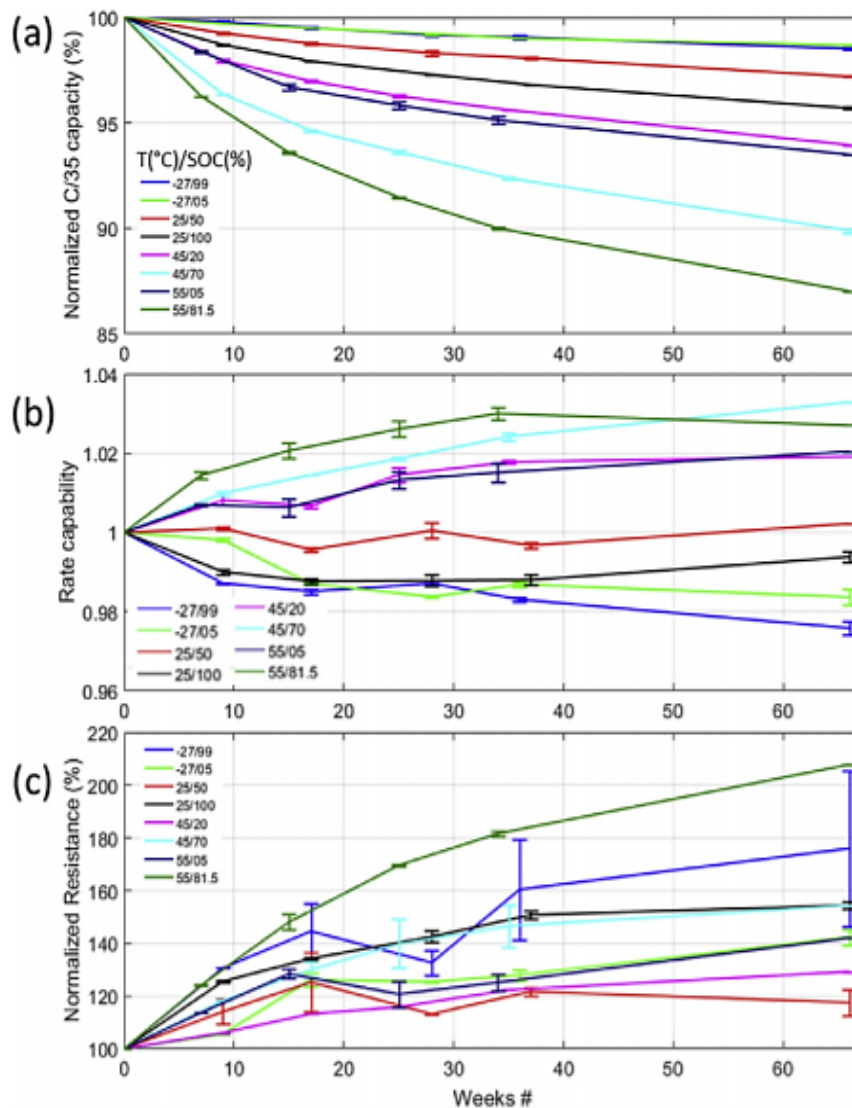


Figure 5.21: Capacity fade (a), rate capability (b) and internal resistance (c) versus eight test conditions from [108]

It's necessary to find a trade-off between the storage conditions that allow to reduce the capacity loss (i.e. cases 1-2-3-4) and the conditions that keep under control the power fade and the rate capability (i.e. cases 8-7-6-5-3) for this purpose it's necessary to analyse data that exclude the temperature effect and highlight the SoC contribution in the low-middle range (fixing T and measuring the performance at different SoC levels between 0 and 50 SoC).

For this target an important contribution comes from [109] where 27 NCA cells (3 Ah/2.5 V), after an initial characterization (following USABC procedures), were stored for approximately 385 days using three cells for each different condition (the whole set is reported in figure 5.22). Characterization procedures (i.e. RPT) were carried out every 8 weeks tracking the evolution of cell ageing in terms of power, capacity fade and internal resistance.

Test	T	SOC_{start}	ΔSoC	C_{rate}^{charge}	$C_{rate}^{discharge}$
1	10 °C	90%			
2	10 °C	50%			
3	10 °C	20%			
4	25 °C	90%			
5	25 °C	50%			
6	25 °C	20%			
7	25 °C	95%	80%	0.3C	1.2C
8	25 °C	95%	80%	0.3C	0.4C
9	25 °C	95%	30%	0.3C	1.2C
10	25 °C	95%	30%	0.3C	0.8C
11	25 °C	95%	30%	0.3C	0.4C
12	25 °C	50%	30%	0.3C	1.2C
13	45 °C	90%			
14	45 °C	50%			
15	45 °C	20%			

Figure 5.22: Testing conditions considered in [109]

The results reported are the measured values of capacity fade and resistance increase, with the relative interpolation (dotted lines), of the cells tested under three different temperatures (10-25-45 °C) and two SoC levels (50-20%); a test was also executed with a higher SoC (90%) but this condition it's clearly the worst case and there is not the necessity of further analysis.

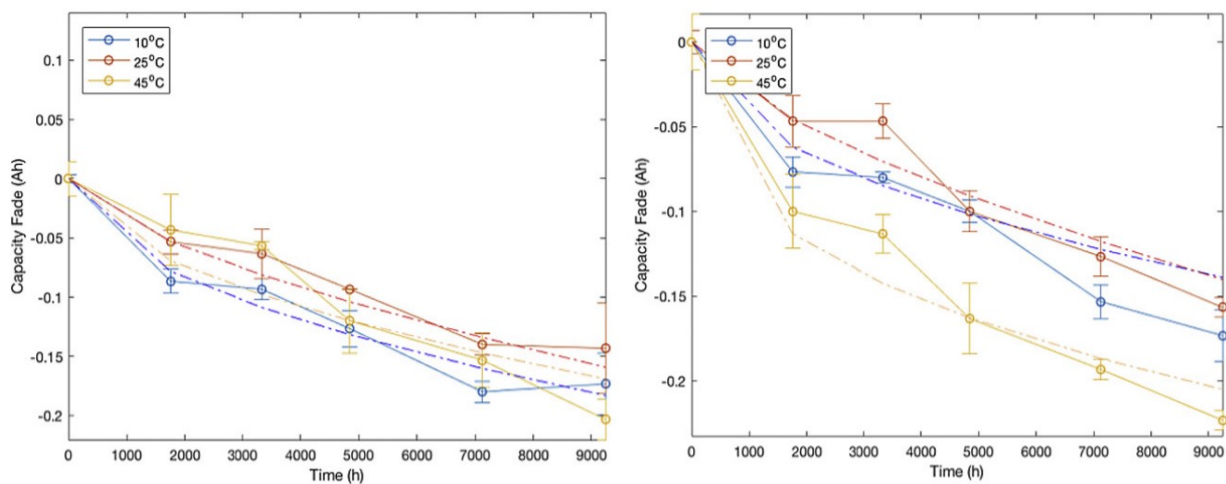


Figure 5.23: Capacity fade between cells at 20% SoC (on the left) and 50% SoC (on the right) [109]

In figure 23 there are the capacity fade plots at 50% and 20% of SoC: as expected the performance fade, in both the conditions, are negatively affected by higher storage temperatures, in concordance with the other experiments; a further consideration is that the difference between the values measured at 10°C and 25°C are within their error bounds, then it's possible to say that the phenomena are similar.

Finally, the numerical fitting, shown with the dotted lines, allows to determine a generic behaviour among the different conditions when the batteries are stored with a SoC equal to 20% instead of 50% (10 and 25°C), highlighting a decrease in the available capacity between 0.15 and 0.2 Ah in the first case and a value of less than 0.15 Ah in the second case: this behaviour should be furtherly studied, highlighting the differences between the SoC values between 20% and 50%.

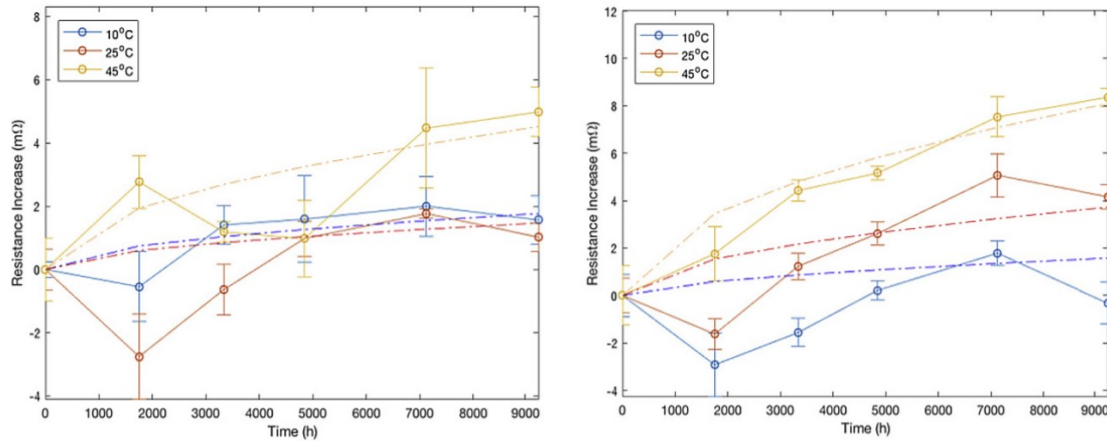


Figure 5.24: Resistance increase between cells at 20% SoC (on the left) and 50% SoC (on the right) [109]

The advantage in a SoC near to 20% is much more evident considering the variation in the internal resistance (figure 5.24), especially in combination with high temperatures (45°C) where the increase in the resistance after 9000 hours it's estimated around 8 mΩ, with SoC equal to 50%, and 4 mΩ for SoC equal to 20%.

Cycle ageing: experiments and results

During cycling conditions, the stress factors that must be considered increase to four: "Temperature", "SoC", "Swing in SoC" and "C-rates".

These are the most relevant parameters to compare different operating conditions and the resultant effects on the battery life. The experiments that will be reported, one more time, are mainly based on the USABC test procedures and for a detailed description of the steps it's possible to read the previous chapter.

Li-Ion batteries life, as a function of the operating temperature, shows a characteristic trend different from other battery typologies: there is an ideal temperature window (10-50 °C) that should be maintained during working operations to achieve the maximum cycle life.

There are of course differences between the chemistries on the market, but all share this general behaviour [110].

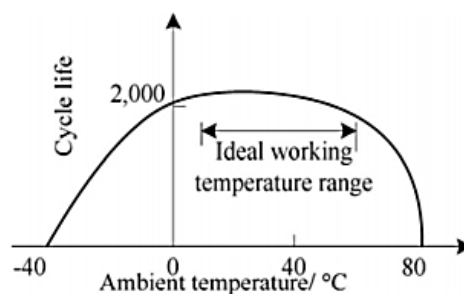


Figure 5.25: Effect of the temperature on cycle-life and ideal temperature range [111]

Going on in the investigation of the other stress factors it's interesting and useful the experiment executed in [109] looking at the cells tested to evaluate cycle ageing (tests 7-12 in figure 5.22).

After an initial characterization, the cells were cycled, under the cycling condition for approximately 400/500 Ah, equivalent to 850/2300 cycles (as before three cells for each condition were utilized).

Initial SoC is another important parameter that could determine a larger or smaller cycle ageing and in [109] the combination of different operating conditions includes also this factor: tests 9 and 12 have been executed with the same temperature (25°C), swing in SoC (30% DoD) and C-rate (1.2C) but with different initial SoC, 95% in the first case and 50% in the second one.

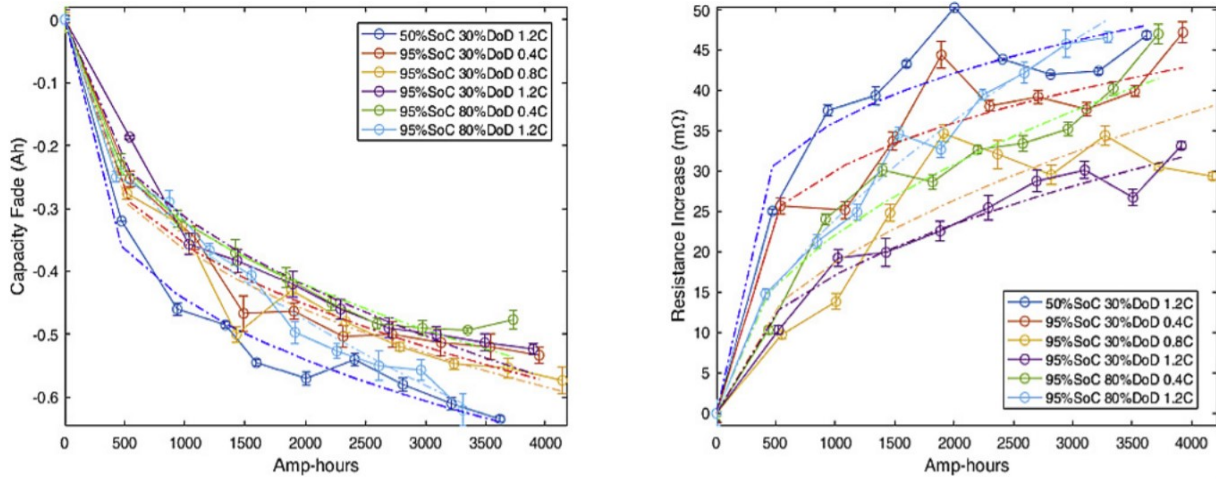


Figure 5.26: Capacity fade (left) and internal resistance increase (right) for all the testing conditions [109]

Purple and blue lines in figures 5.26 are the ones that represent the results of these two tests: in the first case, starting with 95% SoC and discharging the cells at 1.2C till 65% of SoC the capacity fade after almost 3500 Ah is about -0.5 Ah while in the second case, starting from 50% SoC and in the same conditions discharging the cells till 20% SoC, the loss after the same capacity throughput is more than -0.6 Ah.

In the same way the increase in internal resistance is evidently worsened, from the first to the second case, with an increase of almost 15 mΩ in the same test period.

Then, as a first approximation, the middle and low initial SoC must be avoided to reduce the increase in internal resistance and the capacity fade (this should not be a common condition in battery packs for EVs because the maximum available SoC should be exploited to increase the range).

Deeper analysis can consider also the effects of different swing in the SoC; from the previous plots there are significative tests that could be compared: tests 7 and 8 show the same operating conditions of tests 9 and 11 but with a larger DoD (80% vs 30%).

Tests 7 and 9 have the same discharge rate (1.2C) and the same initial SoC (95%) but are subjected to different DoD and the results clearly indicate that the deeper discharge caused higher capacity fade and higher resistance increase.

Not the same expected results are shown comparing tests 8 and 11: in this case with a C-rate of 0.4C the larger swing in SoC is not anymore evidently detrimental; it's possible to say that from the two results, the capacity fade is almost the same but a larger increase in the cell resistance is experienced in the test with a lower DoD (test 11) with a gap that oscillates around 5 mΩ in the middle of the procedure.

Further investigation is necessary to link the initial SoC, considering just values above a 60/70%, and the swing due to discharge phases.

DST cycles reported in [112] are particularly significant because representative of the operating conditions that a battery pack could experience during frequency regulation services or driving cycles (also if the real driving conditions would probably stress much more the battery system).

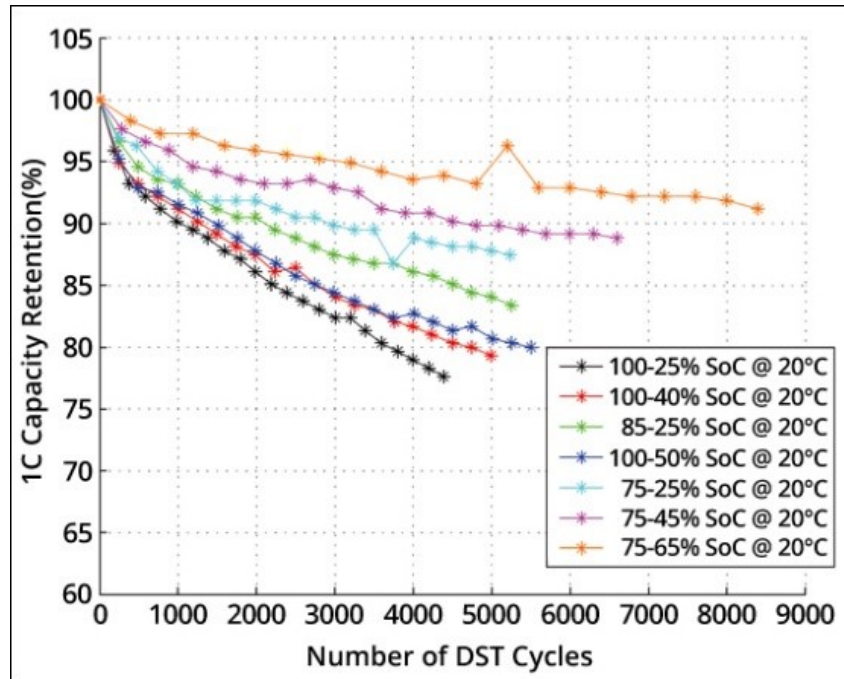


Figure 5.27: Capacity retention versus DST cycles from [112]

Results, expressed in terms of capacity retention in figure 5.27, highlight that the performance are reduced passing from initial SoC about 75% toward the full charge initial conditions.

Nevertheless, small swings are obviously less impacting on the capacity fade but in BEVs the necessity to get the longest available range leads to the choice of utilize high initial SoC and large DoD.

In other applications or services (i.e. frequency regulation) the focus on a set of advantageous conditions could allow to develop special strategies preventing excessive degradation.

The last stress factor that has to be considered is the discharge C-rate and its relationship with the internal resistance of the battery: in [113] very different cell chemistries and design are analysed and studied using different discharge currents (figure 5.28).

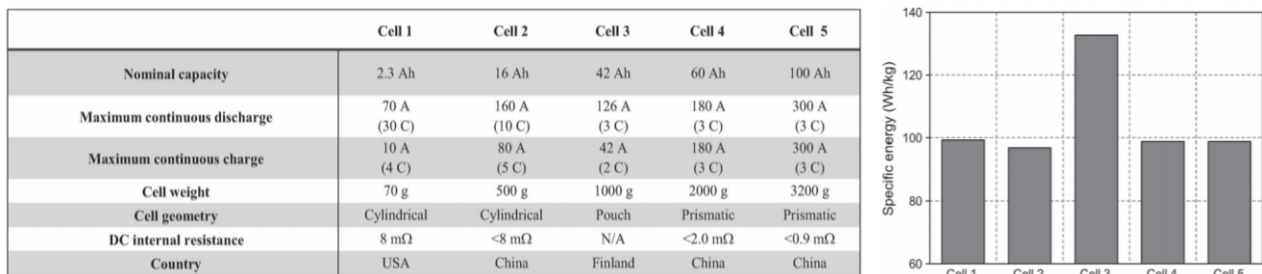


Figure 5.28: Characterization of the cells tested in [113]

A brief description of the procedure utilized in the testing process it's contained in the table below:

Step	Procedure	Description
1	commissioning	batteries were identified and weighed to calculate the specific energy (Wh/kg) and specific power (W/kg).
2	conditioning stage	tests to determine the effective capacity under various regimes and to obtain reference results when all the batteries are fresh
3	added thermodynamic tests at C/25	provides a practical capacity reference with minimal kinetic effects, close to the maximum capacity attainable
4	testing procedures	various tests to study the fastcharging capabilities, IR, and aging of the selected batteries used to characterize the degradation
5	reference tests sequence	during the life of the tested battery. Reference tests are performed at regular intervals (i.e., 300 cycles). Once the reference tests are finished, the testing procedures are resumed.

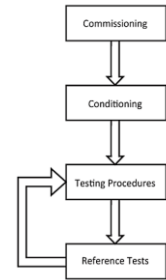


Figure 5.29: Testing procedure proposed in [113]

As anticipated the results describe the correlation between different C-rates and the increase in internal resistance: for simplicity the result, reported in figure 5.30, refers to charge and discharge performance of the cell 5.

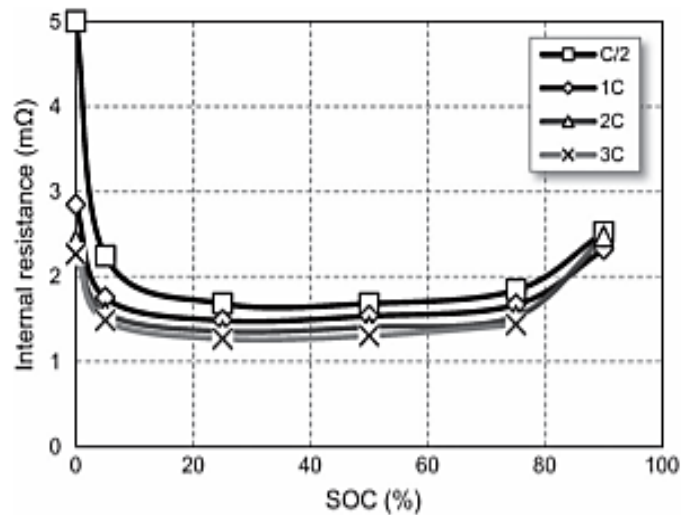


Figure 5.30: Evolution of the internal resistance measured on the cell 5 during charge [113]

Ohmic resistance increase is an ageing mechanism affecting the voltage in both charge and discharge phases: due to this phenomenon the delivered energy during discharge is lowered and an higher amount of energy it's necessary to complete the charge.

Positive and negative electrodes are not directly affected by the resistance increase (there are not direct capacity losses) but the combination of high resistance and high C-rates ($>1C$) results in an anticipated cut-off voltage then full-charge/discharge cannot be reached by all the cells.

Charging and discharging at different C-rates implies to operate with different values of internal resistance: C/2 charge and discharge phases are the reference measures and it's evident that passing to 2C and 3C there is a relevant internal resistance variation.

Especially during the charge and discharge procedures at low/high SoC a higher internal resistance can be observed, this could lead to different operating strategies and enforces the results obtained before suggesting the possibility to work at SoC lower than 75/80% to reduce thermal stresses on the battery and risk of secondary reactions.

Nevertheless fast charge/discharge implies also a higher temperature increase and if the thermal management system is not calibrated adequately, it can result in an operating temperature outside the optimal window, leading to accelerated ageing phenomena then lower cycle life (figure 5.31 on the left).

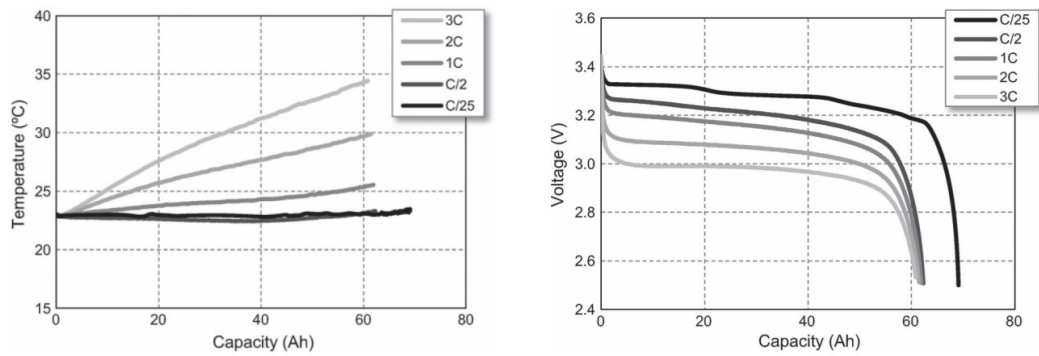


Figure 5.31: Discharge temperature and voltage curves measured on cell 4 [113]

Deliverable voltage is strongly influenced by the C-rate adopted with the higher value, in this case around 3.3 V, that can be sustained just in case of a discharge with very low rate that allows to be near to a thermodynamic equilibrium while the maximum deliverable capacity is almost unaffected (figure 31-b).

In the last experiment considered [114], the capacity fade is studied and analysed as a function of the most impacting degradation modes using the procedure described in figure 5.32:

Step	Procedure	Description
1	Test preparation	The tests began with the conditioning procedures following the USABC guidelines, with an added C/25 charge and discharge cycle.
2	Storage period	The tested cell was stored for 13 months in the thermal chamber (23 C) at 95% state of charge (SOC)
3	As the rest period was concluded, reference performance tests (RPT)	RPT consisted of standard charges (CC % 1C & CV % 3.6 V) with 1C and C/3 discharge regimes, followed by a CC C/25 charge and discharge.
4	Dynamic stress test (i.e., DST) profile as recommended in the USABC manual	testing under dynamic conditions was initiated and it consisted in performing fast charge coupled with dynamic pulse-based full discharges.
5	Data collection	Every 300 full dynamic cycles, RPTs were carried out to evaluate cell degradation. Data collection intervals were controlled by voltage variation at 5 mV per step during the RPTs, and 20 mV during dynamic cycling.

Figure 5.32: Testing procedure adopted in [114]

The obtained data derive from variable power discharge tests to simulate the demands of a BEV on the battery system.

The capacity fade follows a trend that can be described in two steps (figure 5.33) and the end-of life condition (80% of the rated capacity) under dynamic cycling is reached around 1400 DST cycles.

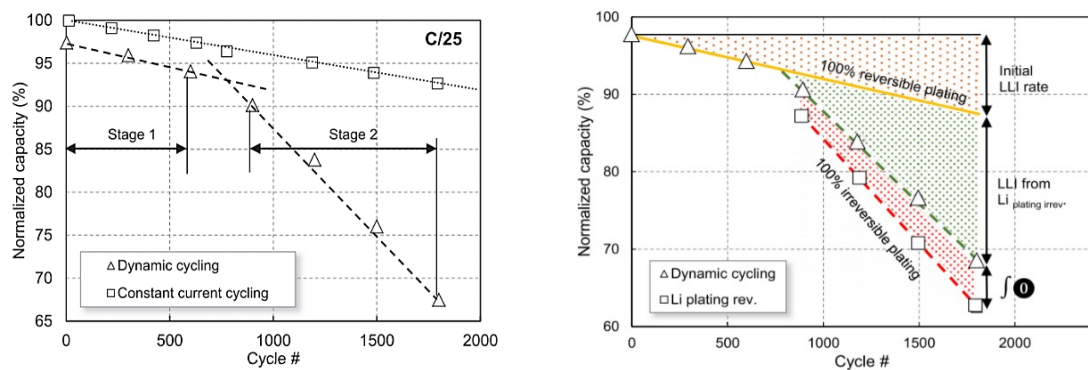


Figure 5.33: Capacity fade evolution and different contributions of reversible and irreversible plating [114]

The first stage is characterized by reversible degradation mechanism (100% reversible plating) but the end-of-life target is reached due to Loss of Lithium Inventory (LLI) explained with irreversible plating.

5.2.3) Conditions to minimize degradation during V2G operations

Storage		
Stress Factors		
Temperature	0/10°C	[105][107][108][109]
SoC	30-50%	[105][107][108][109]

Figure 5.34: Identification of the operating conditions to minimize storage ageing

Storage conditions leads to two main form of losses:

- 1) Self-discharge: usually recoverable with charging procedures before the use of the battery pack.
- 2) Irreversible losses: that cannot be recovered implying a permanent capacity loss.

From the previously described experiments, cells should be ideally stored at very low SoC but moreover at very low storage temperatures (in case of temperature below 0°C the SoC influence is neutralised).

Lithium-ion suffers from stress when exposed to high temperatures (above 30°C) and at a high charge voltage (i.e. 4.10 V/cell at high SoC). Looking at the examples in [105], a lithium-ion cell charged to 4.20V/cell typically could deliver around 300–500 cycles but, if charged to only 4.10V/cell, the cycle-life could be prolonged to 600–1,000 cycles and so on but sacrificing a fraction of the available capacity.

Nevertheless, LIBs manufacturers suggest to avoid SoC values lower than 40% when the battery is stored for a medium/long period; this is due to a behaviour that affects LIBs when self-discharge leads to have a voltage below the minimum cut-off voltage of the cells (i.e. 2.5 V/cell but it's of course dependent on the electrodes chemistry and on the cell design). LIBs batteries include protection circuits that prevent over-discharge and makes unusable the system (to prevent the battery pack from abuse) below a voltage value between 2.2 and 2.9 V/cell depending on the chemistry and the design of the cells.

When the cut-off voltage threshold is trespassed, the battery falls in the so-called sleep mode: Copper dendrites grow if the cell is stored at low voltages for more than several days and working after this event could lead to abnormal and dangerous behaviours, short-circuits, thermal instability and, in the worst case, irreversible runaway.

In case the battery was not protected against this condition, a safety strategy must be applied to restore, whenever possible, adequate operating conditions without risks for the stability of the system: the procedure consists in “wake up current” allowing to boost the SoC and the voltage to sufficient values, checking the response of the whole system, finally assuring the capability of the battery pack to continue its service life. Anyway, after abuse (deep discharges and storage at very low voltages), the restored battery would show lower performance with respect to a new one: this is particularly evident comparing the self-discharge rates of batteries with different histories in figure 5.35.

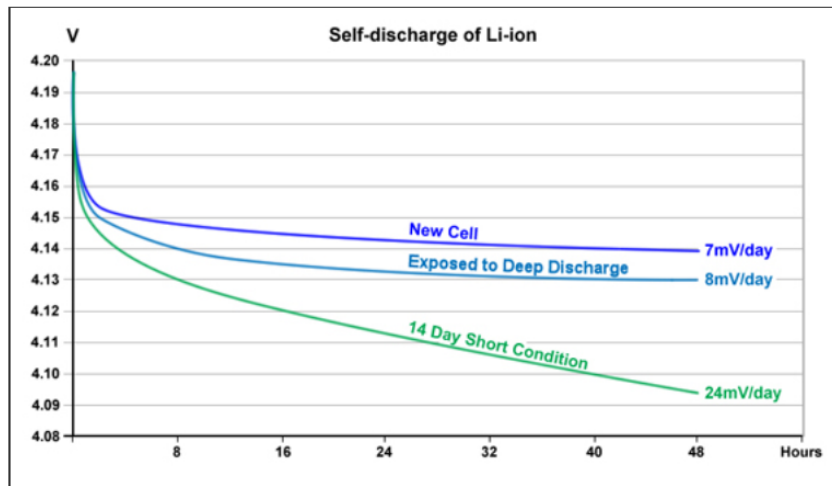


Figure 5.35: Self-discharge rates of batteries previously exposed to different discharge levels [105]

Then cut-off limit must be respected and makes tough to keep a battery pack stored at a low SoC because would be unavoidable a dangerous drop in voltage due to self-discharge phenomena. LIBs suffer a significative Loss in SoC in the first storage period (till 5% in the first 24 hours) then the loss rate is lower with values at 25°C around 4-5% in a month.

State-of-charge	0°C (32°F)	25°C (77°F)	60°C (140°F)
Full charge	6%	20%	35%
40–60% charge	2%	4%	15%

Figure 5.36: Monthly loss in capacity due to self-discharge at different temperatures and SoC [105]

As can be seen in figure 5.37, just complex and advanced management systems could try to keep SoC at very low values without exceed the minimum voltage limit: at a certain value the decrease in voltage becomes very steeply also with very low variations in SoC (below 15°C) then the risk to fall in sleep-mode is very high due to the described typical self-discharge rates.

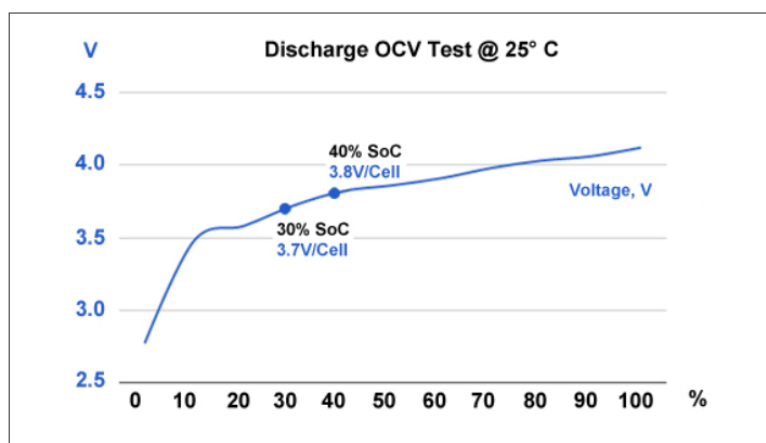


Figure 5.37: Discharge voltage as a function of SoC [105]

A clean and dry location is another essential characteristic that must assured to enable optimal storage conditions; from the experimental results the target temperature should be near to 0°C (in some experiments also sub-zero temperatures showed very good capacity retention) but of course these requirements are not easy to be accomplished and temperatures near to 10°C seems to be more realistic (it's dependent on the geographic location).

Cycling		
Stress Factors		
Temperature	15-50°C	[110][109][112][113][114]
SoC	80-70%	[110][109][112][113][114]
DeltaSoC	10-50%	[110][109][112][113][114]
C-rate	< C/2	[110][109][112][113][114]

Figure 5.38: Identification of the operating conditions to minimize cycle ageing

Now analysing experimental results in case of cycling it's possible to identify another set of values that could be used to obtain V2G services with the lowest detrimental effect on the battery lifespan.

While it's well known that a certain temperature window between 15-50°C, slightly changing with different chemistries, must be respected to minimize the degradation evolution, considerations about the initial SoC and the DoD values to achieve the same target are not so easy.

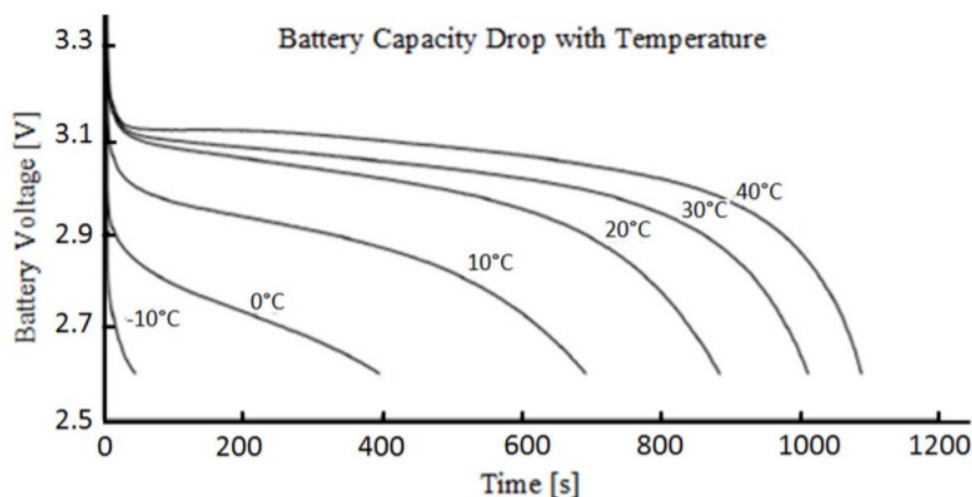


Figure 5.39: Voltage profiles as a function of different operating temperatures [84]

Temperature has also important effects on the voltage profile that can be sustained during cycling (figure 5.39): this fact has more to do with performance evolution but could result in insufficient specifications below 10-15°C.

Fully charging the battery means to work in areas with very high internal resistance and then in a very low efficient way; the same holds for the discharge where in combination with high C-rates it's easy to reach very high temperature values (figure 5.40).

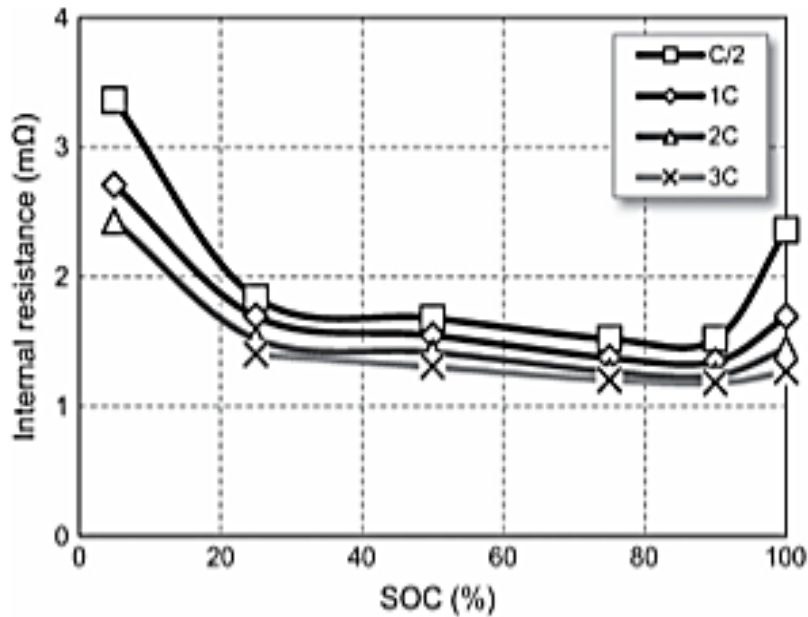


Figure 5.40: Evolution of the internal resistance measured on the cell 5 during discharge [113]

To avoid these working conditions a viable choice could be to interrupt the charge at 80/70% of SoC, this is in contrast with the target of an On-Board battery pack that has the main role to allow the maximum allowable range, but in certain conditions a smart strategy could supply profitable services to the grid if the impact on the lifespan and on the performance of the vehicle is significative reduced.

Speaking about the SoC swing, this is mostly dependent on the type of service that must be supplied (as described in the relative chapter) and more the throughput energy delivered more the capacity fade is negatively affected. Starting from the initial SoC in the range defined before, a swing should not be larger than 50%, above this indicative value the ageing mechanisms are accelerated and significative effects on the cycle life are predictable.

The last stress factor that could be studied is the discharge C-rate: while is established that high C-rates (above 1C/2C) have a strong and detrimental impact on the lifespan, it's interesting to analyse lower values that could represent a valuable trade-off between the requirements of grid support necessity and BEV performance retention.

6. Conclusion and future works

In this review have been analysed and described the development that would be necessary to integrate and implement V2G services starting from the hardware configuration that's diffused in the automotive scenario.

The first important aspect that would allow to exploit the potentialities of BEVs/PHEVs, supporting the grid, is the establishment of aggregators, directly managed by the Independent System Operators, coordinating the available vehicles, as a unique smart Electric Energy Storage, and the Energy Service Provider.

For this purpose, an advanced ITC communication system is required to exchange the status of both grid and vehicles to actively act on the network: this is a fundamental infrastructure mandatory to get effective results (each single vehicle capacity and power characteristics are uninfluential with respect to the grid requirements) and to reduce the effort of each vehicle.

These systems should be built on robust and widespread standards, to assure the coordination of many different electric vehicles, and should exchange a high amount of data due to the necessity of very short update intervals (i.e. in frequency regulation); moreover, should guarantee several constraints, for example the limits in SoC and temperature of the battery packs, switching offline the vehicles that do not satisfy the requirements.

Finally, just with extrapolation from statistic data and predictive models it's possible to design control strategies to assure the required redundancy taking into account the randomness of the EVs connected.

The choice among the alternative services it's another parameter that would strongly affect the choices in terms of hardware and control strategies of each BEV/PHEV: from the comparison of the possibilities studied and tested in the literature, the frequency regulation, one of the so-called ancillary services, seems to be the most promising choice.

In particular "Primary frequency control", a local automatic control (frequency-responsive solution that measures the local grid frequency with a resolution of several μHz and updating and adjusting the charging rate based on the deviation from the frequency target value) that modifies the generation and the consumption of sources/loads, and "Secondary frequency control", a centralized automatic control that regulates the active power production of the generating units, could exploit the intrinsic characteristics of the battery pack, deploying the full power capacity in few seconds/minutes, achieving an optimal regulation with a fast-response variation of the generated power above and below a baseline nominal value.

Speaking about the power electronic that would be required to supply the described services, it's clear from the literature that AC Level 1 (power below 1.92 kW) and AC level 3 (power above 19.2 kW) chargers are not suitable to match the requirements and the constraints: the first one would require too much time to restore the SoC necessary in case the owner would need the vehicle maximum range, while the second one, exploiting the full power, would stress too much the battery pack, would require expensive infrastructural upgrades and would not be supported by the PHEVs with their limited capacity.

Dual-stage bi-directional topologies have been identified as the best configuration to supply frequency regulation and to enhance the flexibility of V2G technology: AC/DC stage (i.e. full-bridge layout) controls the input/output currents while the DC/DC stage (usually boost or buck-boost converter) controls voltage and current in the dc-link with the battery and is used to obtain a power factor correction.

As far as the first stage is concerned, different topologies can be selected according to some characterizing parameters: number of switches, stress on switches (voltage and current), passive components size (capacitors and inductors), low harmonic contents and reachable power.

For power sizes above 5 kVA it's necessary to reduce the stress on each switch (in terms of thermal load) keeping low EMI and circuitry complexity; for these reasons two suitable layouts are represented by Bridgeless Interleaved PFC boost converters and Bridgeless Interleaved Resonant PFC converters capable to achieve:

- Low Capacitors Ripple
- Very High Efficiency

As introduced before the complexity increases also due to the necessity to “communicate” through flows of data between the grid and the Battery Management System of the vehicle: for this purpose, a complex scheme of communication channels and control devices are necessary affecting the devices’ cost.

Another appealing ancillary service is represented by the Reactive Power Injection in order to compensate voltage drops: this compensation should be provided as close as possible to the loads reducing or avoiding the penalties for excessive consumption of reactive power.

In this way would be possible to reduce the effort and the stress on the battery pack: this because, differently from the frequency, it’s not required an additional active power flow from the battery pack to the grid with the consequent negative effect on the battery lifespan.

Also in this case dual-stage bi-directional converters are mandatory to achieve a good efficiency but, differently from the previous cases, the passive components, in particular capacitors, should be oversized (+7/8% for a full-bridge converter with a nominal apparent power of 6.6 kVA) to supply the same amount of active or reactive power (to exploit all the four quadrants at the same power levels); these components are already subjected to ripples that reduce their cycle life and, being expensive and bulky components, the economic viability of this solution should be furtherly studied.

The key component that will determine the success or the failure of this technology will be the On-Board Energy Storage System: nowadays almost all the PHEVs/BEVs are equipped with Li-ion battery packs and for this reason a crucial point is to determine if V2G services would affect negatively the lifespan of such devices.

Starting from experiments in the literature has been possible to identify a set of operating conditions that would minimize the additional stress of V2G services: considering for example the frequency regulation, an uncontrolled V2G operation, with charge and discharge to match the nominal frequency value, would ideally increase the cycles of the battery pack, shortening a fraction of lifespan available for drive the vehicle.

There are many different ideas on the possibility to manage V2G in a “smart” way to reduce the capacity loss during storage periods, this is not a clear concept (different studies have opposite results) and just with complex control equipment and strategies would be possible to set up the necessary framework, but it would not be the case in the first decades of development.

Then the last part of this work tried to determine the boundary conditions that would allow to reduce the main degradation modes during both rest periods and V2G cycles.

These results would directly affect devices and equipment directly involved in the management of the storage system: this implies active thermal management systems to adequately regulate the temperature (differently from storage to cycling conditions) and advanced chargers and BMSs to determine the required SoC, delta SoC and C-rate.

During long rest periods the results show how the temperature is the dominant parameter: with very low temperature (0-10°C) the ionic conductivity is reduced and the self-discharge phenomenon is minimized, but if these temperature ranges cannot be reached, it’s then possible to slow down the self-discharge reducing as much as possible the SoC (then also the cells voltages), ideally toward 30%, but today these regions are avoided to prevent the so-called “sleep-mode” (lowest SoC regions are characterized by a rapid drop in voltage and irreversible phenomena) then dedicated circuitry and control algorithms would be necessary to exploit this condition.

Finally looking at the frequency regulation through V2G applications, the results show how would be convenient to schedule the periods in which the vehicle is V2G enabled in order to have the freedom to manage SoC and C-rate in the best way: while for normal usage a BEV has to be charged at maximum SoC to reach the higher available range in the charge depletion mode, the concept is no longer valid for V2G services.

Temperature ranges are the same that must be respected during normal drive cycles (with a range between 15-50°C that should be respected to get the maximum cycle life) but the higher SoC (above 70-80%) should be avoided because are characterized by higher cell internal resistance.

The swing in SoC should be limited with respect to the driving conditions: ideally the cycles should not discharge the battery pack below 40% SoC (i.e. charging and discharging phases around 50% SoC).

The charge-discharge rate should be limited, in a network of vehicles managed by an aggregator, and values below $C/2$ seem to reduce the thermal stress on the cells and, also if could be too conservative, should be a good starting point to start new tests and simulations (values below show all very similar results and would reduce the V2G capability of each vehicle).

With this work have been analysed devices and components starting from the power electronics between grid and vehicles, till the On-Board Energy Storage System, including the high-level controllers just as the Aggregator and the Battery Management System.

In this way have been possible to describe constraints and requirements that would lead the development of such components to support the implementation of V2G structures and applications but also a change in the way BEVs/PHEVs are considered by customers and OEMs (from simple vehicles to smart loads/sources).

In the future the efforts focused on the improvement of the battery performance could solve part of the issues related to the challenging requirements in terms of lifespan and specific energy, nowadays there are not technologies ready to be industrialised, but also the specific price (if will be lower than 100 \$/kWh) could shift the performance limits reducing some constraints.

The technological feasibility of V2G should be verified for each new cell chemistry and, not less important, the economic feasibility should be studied (considering models including the market structure and the costs of the battery pack performance reduction) to prove and show the advantages that must be perceived by customers before they decide to share their vehicles' capabilities.

List of Figures

Figure 2.1: Evolution of different forms of renewable sources [1]	3
Figure 2.2: Vehicles necessary to store a percentage of the energy produced by wind turbines [1].....	4
Figure 2.3: Role of the master aggregator in V2G concept [5].....	5
Figure 2.4: Characterization of Uni/Bi-directional V2G services, requirements and targets [6].....	6
Figure 2.5: Comparison between conventional power system layout and new paradigm [7]	6
Figure 2.6: Integration of sensitive loads and energy manager in the power grid [7].....	7
Figure 2.7: Classification of electrified vehicles [9]	9
Figure 2.8: elementary traction system building blocks.....	9
Figure 2.9: Parallel-hybrid layout and main characteristics [10]	10
Figure 2.10: Series-hybrid layout and main characteristics [10]	10
Figure 2.11: Series&Parallel-hybrid layouts [10].....	10
Figure 2.12: European market forecast from literature.....	12
Figure 2.13: Expected market share between BEVs/PHEVs from “BLUE MAP SCENARIO” [11].....	12
Figure 2.14: CO2 target values for the automotive industry and fleet values from different manufacturers	14
Figure 2.15: Different powertrains and manufacturers with the relative CO2 emissions	14
Figure 2.16: CO2 emissions reduction strategies between past and future	15
Figure 2.17: Automotive technologies: CO2 emissions reduction vs increase in cost	15
Figure 2.18: Real NOx emissions (dark grey) versus European NOx emissions limits (light grey)	16
Figure 2.19: WLTP cycle (on the left) and the technical comparison with NEDC (on the right)	16
Figure 2.20: EU – LD Emissions Testing Roadmap from FEV, ICCT and Delphi	17
Figure 2.21: Pareto plot describing the trade-off between high-power/energy designs for different storage systems.....	17
Figure 2.22: Effect of uncoordinated charging at different geographic locations [6].....	19
Figure 2.23: Power quality degradation in case of un-coordinated and coordinated charging [13].....	19
Figure 2.24: Impact of BEVs on California’s annual electrical energy (a) and peak power (b) demands [16]	20
Figure 2.25: Resulting peak power from the un-coordinated charging of 2200 BEVs [6]	20
Figure 3.1: Summary of different grid services and their technical requirements [1].....	23
Figure 3.2: MV to LV scheme representing the local power network with V2G applications [32]	23
Figure 3.3: Peak shaving and valley filling between system capacity and system load	24
Figure 3.4: Load following capacity [33]	25
Figure 3.5: Relationship between price and energy supply [39].....	26
Figure 3.6: ICT systems in V2G applications [29].....	26
Figure 3.7: Representation of the different levels of frequency regulation [30].....	27
Figure 3.8: Primary, Secondary and Tertiary frequency control with respect to the activation time [39]	28
Figure 3.9: Spinning and non-Spinning reserves and their temporal activation [40]	28
Figure 3.10: Layouts to promote the integration of photovoltaic/wind turbines with BEVs [36][37].....	29
Figure 3.11: Comparison of the different terminology of different regulation levels in different countries [34]	30
Figure 3.12: Technical comparison of Primary Frequency control parameters in different systems [34] [35]	30
Figure 3.13: Technical comparison of Secondary Frequency control parameters in different systems [34] [35]	31
Figure 3.14: Frequency oscillations around the nominal value (60 Hz) [38]	31
Figure 3.15: communication layout between grid operator, aggregator and BEVs [28]	32
Figure 3.16: Frequency regulations UP and DOWN [28].....	32
Figure 3.17: Frequency regulation performed using V2G [28].....	32
Figure 3.18: Frequency responsive capacity subdivided among different sources in WECC and SMUD markets [39].....	33
Figure 3.19: Secondary Frequency control through the analysis of ACE signal	34
Figure 3.20: Detailed description of the characteristics of regulation reserves in Germany [30]	34
Figure 3.21: Reactive power compensation concept [31]	35
Figure 3.22: Different levels of reactive power compensation [31]	36
Figure 3.23: Technical comparison of voltage control parameters in different systems [34]	37

Figure 3.24: Market characteristics for basic voltage control ancillary service [34]	37
Figure 3.25: Reactive power services deliverable with different chargers [41]	38
Figure 3.26: Possible configuration of power grid support using a BEV [41]	38
Figure 3.27: Operating region in the P-Q plane and available mode for a bidirectional charger [42]	39
Figure 3.28: Capacitor increase for 100% reactive power compensation [41]	39
Figure 3.29: Active (RED) and Reactive (BLUE) power with $V_{dc}=2.7V_g$ (left) and $V_{dc}=3.55V_g$ (right) [43]	39
Figure 3.30: Schematization of the harmonic filtering process [31]	40
Figure 3.31: Difference between input and output signals	41
Figure 3.32: Deviation from the sine wave due to harmonic distortion and evidence in the spectrum analysis	41
Figure 3.33: grid active filtering through the connection of BEVs with bi-directional converters [44]	42
Figure 3.34: power flow between grid, vehicle and home [45]	42
Figure 3.35: Current harmonic spectrum after the filtering process [45]	43
Figure 3.36: DC link voltage during active filtering [45]	43
Figure 3.37: List of the most significative grid support services and their suitability with V2G [46]	44
Figure 3.38: Four-quadrant Full-Bridge single/three-phase converters	46
Figure 3.39: Bridgeless PFC boost converter [48][49][50]	46
Figure 3.40: Bridge-less interleaved PFC boost converter and its efficiency with different input voltages [48] [49] [50]	47
Figure 3.41: Topologies comparison [48]	48
Figure 3.42: conventional Power Factor Correction boost converter [48]	49
Figure 3.43: Interleaved layout	49
Figure 3.44: Resonant layout	49
Figure 3.45: ZSC layout	50
Figure 3.46: ZVS layout [54]	50
Figure 3.47: Bidirectional Full-bridge + Buck-Boost converter [51]	51
Figure 3.48: Bidirectional Full-bridge + DAB converter [51]	51
Figure 3.49: Bidirectional Direct/Indirect matrix converters [54]	51
Figure 3.50: On-Board vs Off-Board layouts [55]	52
Figure 3.51: Power size of On-Board charger mounted in different BEVs	53
Figure 3.52: Performance evolution trends for different power converter applications [54]	53
Figure 3.53: Pareto plots for different converter topologies [54]	54
Figure 3.54: Evolution of the power density in the next years [54]	54
Figure 3.55: Generic structure of an off-board charger (LF isolation on the left and HF isolation on the right [56])	55
Figure 3.56: EVSE system block diagram	55
Figure 3.57: Output power and operating current of several Off-Board chargers available in the market	56
Figure 3.58: AC/DC levels and suitable charging connectors	57
Figure 3.59: SAE J1772 connector	58
Figure 3.60: IEC 62196 connector	58
Figure 3.61: SAE J1772 combo connector	59
Figure 3.62: CHAdeMO connector	60
Figure 3.63: Base layout of an integrated charger [47]	61
Figure 3.64: Representation of stator/rotor windings from [59]	62
Figure 3.65: WRAM layout [59]	62
Figure 3.66: PMSM layout [59]	63
Figure 3.67: Integrated charger with two inverters and two motors [47]	63
Figure 3.68: PM non-isolated integrated charger with connection through multiple points [47]	64
Figure 3.69: SMR integrated charger layout [47]	64
Figure 3.70: Charging flow in a vehicle equipped with integrated SMR charger	65
Figure 3.71: Stationary WTP (external view on the left and hardware layout on the right [47])	66
Figure 3.72: Inductive coupling roadbed (external view on the left and hardware layout on the right [47])	67
Figure 3.73: Main compensation topologies [47]	67
Figure 3.74: technical comparison of the most promising wireless charging architectures [64]	67

Figure 4.1: Specific energy vs specific power of different battery typologies (Johnson control -SAFT 2005/2007).....	69
Figure 4.2: Basic scheme and components of a conventional battery cell [69]	70
Figure 4.3: SoC variation due to different temperature conditions.....	72
Figure 4.4: influence between Specific power and DoD.....	73
Figure 4.5: List of available battery technologies and their technical specifications [69].....	73
Figure 4.6: List of experts participating in [70]	74
Figure 4.7: Technology path and state of development of some alternatives from [70]	75
Figure 4.8: Classification of the experts following their level of expertise for each technological alternative [70].....	75
Figure 4.9: Suggested allocation of the RD&D budget for the period 2020-2030 [70].....	76
Figure 4.10: Suggested subdivision of the available RD&D budget among different development phases [70]	76
Figure 4.11: Scheme of a Li-Air battery and comparison of the working principle with the Li-Ion technology	77
Figure 4.12: potential vs capacity curve (1st cycle) for a non-aqueous Li-O ₂ battery [75].....	79
Figure 4.13: Scheme of a Li-S cell.....	80
Figure 4.14: Theoretical/Practical specific energy of many battery technologies [76]	82
Figure 4.15: Lithium battery systems classified considering anode and electrolyte characteristics [77]	84
Figure 4.16: Intercalation and de-intercalation mechanisms.....	85
Figure 4.17: Charge and discharge phases.....	85
Figure 4.18: Lithium-ion battery vs Solid-state Lithium battery layouts	86
Figure 4.19: Intercalation in the graphitic anode layers with voltage evaluation in different stages [72][73]	87
Figure 4.20: Lithium Titanite Oxide crystalline structure [78]	88
Figure 4.21: (a) layered, (b) spinel, (c) olivine, and (d) tavorite [78]	89
Figure 4.22: Technical comparison among many electrodes' chemistries	91
Figure 4.23: Graphical characterization of the features of interest among different Li-Ion chemistries [80]	91
Figure 4.24: Requirements of the battery pack for different electrification levels [77]	92
Figure 4.25: Distribution of the main electrical specifications among different electrification levels	93
Figure 4.26: Energy storage requirements to supply different grid-support services (on the left) and feasibility analysis of different Li-Ion chemistries to satisfy stationary/automotive targets (on the right) from [77]	93
Figure 4.27: Review on the aging mechanisms in Li-ion batteries for electric vehicles based on the FMEA method [81] ..	94
Figure 4.28: SEI layer growth and corresponding evolution in potential vs capacity plot [90].....	95
Figure 4.29: representation of the SEI formation in early steps [73]	96
Figure 4.30: representation of the SEI formation in final steps [73]	96
Figure 4.31: Interconnections between stress factors, degradation mechanisms, degradation modes and effects.....	97
Figure 4.32: AC and DC charging systems power flows.....	98
Figure 4.33: List of some EVSE on the market and relative values of output power and current	98
Figure 4.34: features and processes running inside a BMS.....	99
Figure 4.35: Safety operating window for Li-Ion batteries [84]	100
Figure 4.36: Building blocks of a BMS (on the left [83]) and list of the main hardware/software sub-systems [86].....	100
Figure 4.37: Bypass Cell Balancing FETs Used to Slow the Charge Rate of a Cell During the Charging [83]	102
Figure 4.38: Active Balancing During the Discharge Cycle [83]	102
Figure 4.39: Comparison among different SoC methods from literature [84].....	104
Figure 4.40: Relationship between cycle life and operating temperature for different C-rates [85]	104
Figure 4.41: Serial and parallel cooling system layouts [87].....	105
Figure 4.42: Heat-pipe battery cooling system [87].....	106
Figure 4.43: Adaptive control strategies.....	107
Figure 4.44: Advantages and disadvantages comparison between EIS and IC-DV techniques [89]	108
Figure 4.45: Features of interest individuated on the IC curve [88]	108
Figure 4.46: IC-DV, calculation of the incremental capacity curve for equally spaced capacity intervals [90]	109
Figure 4.47: IC curve [89]	110
Figure 4.48: DV curve [89].....	110
Figure 4.49: cathode and anode contributions [92]	111
Figure 4.50: Charge/discharge curves (on the left) and relative IC curve (on the right) [90]	111

Figure 4.51: Relationship between IC-DV curves and the main degradation modes [89]	112
Figure 4.52: Graphical representation of the evolution of the main degradation modes in IC and DV curves [89].....	112
Figure 4.53: Value-chain of a battery pack for EVs/PHEVs [80]	113
Figure 4.54: Run-away process resulting in flames.....	114
Figure 4.55: EVs on the market ordered for decreasing efficiency (from the top to the bottom)	115
Figure 4.56: NEDC.....	116
Figure 4.57: Difference between data from real driving conditions and data from NEDC	116
Figure 4.58: Layered cathode (a) and graphite anode (b) structures from [71].....	117
Figure 4.59: BEV and ICE prices (pre-taxes) in U.S.A. in thousands of \$ (source: Bloomberg New Energy Finance)	118
Figure 4.60: historical data of the evolution of battery specific cost between 2013 and 2016.....	118
Figure 4.61: battery typologies studied in [96]	119
Figure 4.62: prediction of the battery cost, in the next decade, starting from the record from 2010 [97].....	119
Figure 4.63: Process-based cost modelling from [96]	119
Figure 4.64: Cell manufacturing process including input/output material flows [96]	120
Figure 4.65: Sales price of battery I (on the left) and battery II (on the right) [96].....	121
Figure 4.66: Periodic table with identification of the main elements for anodes and cathodes in Li-Ion batteries [78].....	121
Figure 4.67: Price ranges of the main raw materials utilized in Li-Ion batteries [98]	122
Figure 4.68: Estimations of Lithium carbonate usage per kWh found in literature [100]	124
Figure 4.69: Estimations of the Lithium amount for different vehicles batteries from the literature [101]	125
Figure 4.70: Vehicle sales, in millions of units, for 2050 [100]	125
Figure 4.71: Lithium production scenarios and uncertainties from historical data to 2050 [100].....	125
Figure 4.72: Sources of Lithium in nature and main applications [100].....	126
Figure 4.73: Distribution of Lithium reserves in 2011 [100].....	127
Figure 4.74: Lithium production prediction, subdivided among brine, spodumene and new reserves [100].....	128
Figure 4.75: Maximum production in kilo-tonnes predicted through different models [101].....	129
Figure 4.76: Medium-Long term projected future Lithium production [101]	129
Figure 4.77: Comparison of the most important studies in literature about the possible Lithium constraints [100]	129
Figure 4.78: Estimated number of discarded batteries from BEVs [98]	130
Figure 4.79: Flowchart of one among the available processes to recover raw materials from the spent LIBs [78]	131
Figure 4.80: Materials weight percentages for three cell's chemistries [98].....	132
Figure 4.81: Time in hours required to conclude each of the operations involved in the reuse process [98].....	132
Figure 4.82: Predicted recycle rates in different studies and different time-scales	133
Figure 4.83: Alternative recycling processes [102].....	133
Figure 5.1: Battery test procedure following the USABC manual [103].....	134
Figure 5.2: List of the main test procedures, and their variations, from USABC test manual [103]	135
Figure 5.3: Illustration of the 30 seconds steps for a specific DoD level [103].....	136
Figure 5.4: FUDS test cycle [103].....	138
Figure 5.5: DST power profile [103]	138
Figure 5.6: Block diagram schematizing the steps in the Life-Cycle Test procedure [103].....	140
Figure 5.7: Temperature ranges and percentage of test time to simulate different climatic conditions [103]	142
Figure 5.8: Parameters Optimization procedure from [104].....	146
Figure 4.9: High temperature effects on both the electrodes [104]	147
Figure 5.10: Low temperature effects on the negative electrode [104]	148
Figure 5.11: Effects of High SoC on both the electrodes [104].....	148
Figure 5.12: Effects of Low SoC on both the electrodes [104].....	149
Figure 5.13: Effects of large current rates on the negative electrode [104]	149
Figure 5.14: Effects of Large Swing in SoC on the positive electrode [104]	150
Figure 5.15: Effects of High Cycle Number on both the electrodes [104].....	150
Figure 5.16: Recoverable capacity of a Li-Ion battery after one year of storage at different temperatures [105].....	151
Figure 4.17: Ageing cases, with different temperature and SoC levels, used in [107]	152
Figure 5.18: Voltage response with different degradation levels of LFP/C cells [107]	152

Figure 5.19: Internal resistance vs different C-rates, temperatures and SoC [107].....	153
Figure 5.20: Results obtained and testing conditions from [108]	153
Figure 5.21: Capacity fade (a), rate capability (b) and internal resistance (c) versus eight test conditions from [108].....	154
Figure 5.22: Testing conditions considered in [109]	155
Figure 5.23: Capacity fade between cells at 20% SoC (on the left) and 50% SoC (on the right) [109].....	155
Figure 5.24: Resistance increase between cells at 20% SoC (on the left) and 50% SoC (on the right) [109]	156
Figure 5.25: Effect of the temperature on cycle-life and ideal temperature range [111].....	156
Figure 5.26: Capacity fade (left) and internal resistance increase (right) for all the testing conditions [109].....	157
Figure 5.27: Capacity retention versus DST cycles from [112]	158
Figure 5.28: Characterization of the cells tested in [113]	158
Figure 5.29: Testing procedure proposed in [113]	159
Figure 5.30: Evolution of the internal resistance measured on the cell 5 during charge [113].....	159
Figure 5.31: Discharge temperature and voltage curves measured on cell 4 [113]	160
Figure 5.32: Testing procedure adopted in [114]	160
Figure 5.33: Capacity fade evolution and different contributions of reversible and irreversible plating [114].....	160
Figure 5.34: Identification of the operating conditions to minimize storage ageing.....	161
Figure 5.35: Self-discharge rates of batteries previously exposed to different discharge levels [105].....	162
Figure 5.36: Monthly loss in capacity due to self-discharge at different temperatures and SoC [105].....	162
Figure 5.37: Discharge voltage as a function of SoC [105]	162
Figure 5.38: Identification of the operating conditions to minimize cycle ageing.....	163
Figure 5.39: Voltage profiles as a function of different operating temperatures [84]	163
Figure 5.40: Evolution of the internal resistance measured on the cell 5 during discharge [113]	164

References

- [1] P. L. Przemyslaw Komarnicki, Zbigniew Styczynski, "International Development Trends in Power Systems," in *Electric Energy Storage Systems*: Springer, 2017, pp. XV, 211.
- [2] P. D. F. Ferreira, P. M. S. Carvalho, L. A. F. M. Ferreira, and M. D. Ilic, "Distributed Energy Resources Integration Challenges in Low-Voltage Networks: Voltage Control Limitations and Risk of Cascading," *IEEE Transactions on Sustainable Energy*, vol. 4, no. 1, pp. 82-88, 2013.
- [3] H. Lund and W. Kempton, "Integration of renewable energy into the transport and electricity sectors through V2G," *Energy Policy*, vol. 36, no. 9, pp. 3578-3587, 2008/09/01/ 2008.
- [4] I. S. Bayram, G. Michailidis, M. Devetsikiotis, F. Granelli, and S. Bhattacharya, "Smart Vehicles in the Smart Grid: Challenges, Trends, and Application to the Design of Charging Stations," in *Control and Optimization Methods for Electric Smart Grids*, A. Chakraborty and M. D. Ilic, Eds. New York, NY: Springer New York, 2012, pp. 133-145.
- [5] C. Guille and G. Gross, "A conceptual framework for the vehicle-to-grid (V2G) implementation," *Energy Policy*, vol. 37, no. 11, pp. 4379-4390, 2009/11/01/ 2009.
- [6] M. Yilmaz and P. T. Krein, "Review of the Impact of Vehicle-to-Grid Technologies on Distribution Systems and Utility Interfaces," *IEEE Transactions on Power Electronics*, vol. 28, no. 12, pp. 5673-5689, 2013.
- [7] P. M. P. d. R. Almeida, "IMPACT OF VEHICLE TO GRID IN THE POWER SYSTEM DYNAMIC BEHAVIOUR," Department of Electrical and Computer Engineering, Faculty of Engineering, University of Porto, November 2011.
- [8] W. Kempton and J. Tomić, "Vehicle-to-grid power fundamentals: Calculating capacity and net revenue," *Journal of Power Sources*, vol. 144, no. 1, pp. 268-279, 2005/06/01/ 2005.
- [9] J. Beretta, *Automotive Electricity - Electric Drives*. ISTE Ltd and John Wiley & Sons, Inc., 2009, p. 324.
- [10] D. Leskarac, C. Panchal, S. Stegen, and J. Lu, *PEV charging technologies and V2G on distributed systems and utility interfaces*. 2015, pp. 157-221.
- [11] "Technology Roadmap Electric and plug-in hybrid electric vehicles," INTERNATIONAL ENERGY AGENCY 2011, Available: https://www.iea.org/publications/freepublications/publication/EV_PHEV_Roadmap.pdf.
- [12] D. D. Mohr *et al.*, "The road to 2020 and beyond: What's driving the global automotive industry?," McKinsey & Company, Inc. August 2013
- [13] S. Habib, M. Kamran, and U. Rashid, *Impact analysis of vehicle-to-grid technology and charging strategies of electric vehicles on distribution networks - A review*. 2015.
- [14] R. Garcia-Valle and J. A. P. Lopes, *Electric Vehicle Integration into Modern Power Networks* Springer-Verlag New York, 2013, pp. XI, 325.
- [15] S. L. Andersson *et al.*, "Plug-in hybrid electric vehicles as regulating power providers: Case studies of Sweden and Germany," *Energy Policy*, vol. 38, no. 6, pp. 2751-2762, 2010/06/01/ 2010.
- [16] S. J. Gunter, K. K. Afridi, and D. J. Perreault, "Optimal design of grid-interfaced EV chargers with integrated generation," in *2012 IEEE PES Innovative Smart Grid Technologies (ISGT)*, 2012, pp. 1-8.
- [17] M. Ehsani, M. Falahi, and S. Lotfifard, *Vehicle to Grid Services: Potential and Applications*. 2012, pp. 4076-4090.
- [18] T. Markel, M. Kuss, and P. Denholm, "Communication and control of electric drive vehicles supporting renewables," in *2009 IEEE Vehicle Power and Propulsion Conference*, 2009, pp. 27-34.
- [19] C.-S. Norman Shiau, C. Samaras, R. Hauffe, and J. Michalek, *Impact of battery weight and charging patterns on the economic and environmental benefits of plug-in hybrid vehicles*. 2009, pp. 2653-2663.
- [20] J. A. Lopes, F. Soares, P. Almeida, and M. Moreira da Silva, *Smart Charging Strategies for Electric Vehicles: Enhancing Grid Performance and Maximizing the Use of Variable Renewable Energy Resources*. 2009.
- [21] J. A. Lopes, F. Soares, and P. Almeida, *Identifying management procedures to deal with connection of Electric Vehicles in the grid*. 2009, pp. 1-8.
- [22] M. Galus, M. Zima, and G. Andersson, *On integration of plug-in hybrid electric vehicles into existing power system structures*. 2010, pp. 6736-6745.
- [23] K. Clement-Nyns, E. Haesen, and J. Driesen, "The Impact of Charging Plug-In Hybrid Electric Vehicles on a Residential Distribution Grid," *IEEE Transactions on Power Systems*, vol. 25, no. 1, pp. 371-380, 2010.
- [24] K. Qian, C. Zhou, M. Allan, and Y. Yuan, *Modeling of Load Demand Due to EV Battery Charging in Distribution Systems*. 2011, pp. 802-810.
- [25] C. Weiller, "Plug-in hybrid electric vehicle impacts on hourly electricity demand in the United States," *Energy Policy*, vol. 39, no. 6, pp. 3766-3778, 2011/06/01/ 2011.

- [26] A. De Los Rios, J. Goentzel, K. E. Nordstrom, and C. W. Sievert, *Economic analysis of vehicle-to-grid (V2G)-enabled fleets Participating in the regulation service market*. 2012.
- [27] P. J. Haddick and R. Egunjobi, "Level I and level III Electric Vehicle inverter penetrance on municipally operated residential-commercial distribution circuits: Analysis of phase to phase load imbalance compensation potential, ancillary voltage regulation services, and economic due diligence regarding V2G implementation," in *2015 North American Power Symposium (NAPS)*, 2015, pp. 1-5.
- [28] A. N. Brooks, "Vehicle-to-Grid Demonstration Project: Grid Regulation Ancillary Service with a Battery Electric Vehicle," AC Propulsion, Inc. 2002, Available: <https://www.arb.ca.gov/research/apr/past/01-313.pdf>.
- [29] Z. Wang and S. Wang, "Grid Power Peak Shaving and Valley Filling Using Vehicle-to-Grid Systems," *IEEE Transactions on Power Delivery*, vol. 28, no. 3, pp. 1822-1829, 2013.
- [30] C. GmbH, "Description of load-frequency control concept and market for control reserves," German TSOs 27 February 2014.
- [31] J. Matias, "Reactive Power Compensation," © ABB High Voltage Products 05-June-2013.
- [32] K. Mahmud, S. Morsalin, Y. Kafle, and G. Town, *Improved peak shaving in grid-connected domestic power systems combining photovoltaic generation, battery storage, and V2G-capable electric vehicle*. 2016, pp. 1-4.
- [33] J. Mindaugas, S. B. Marta, K. Konstantinos, P. D. R. Ronald, G. M. Carmen, and C. Johan, "Best practices and informal guidance on how to implement the Comprehensive Assessment at Member State level," EUR - Scientific and Technical Research Reports 2015.
- [34] Y. Rebours, D. s. Kirschen, M. Trotignon, and S. Rossignol, *A Survey of Frequency and Voltage Control Ancillary Services—Part I & II*.
- [35] Y. Rebours and D. Kirschen, "What is spinning reserve."
- [36] P. Goli and W. Shireen, "Smart scheduling of PHEVs in PV integrated charging facilities based on DC link voltage sensing," in *2015 IEEE Transportation Electrification Conference and Expo (ITEC)*, 2015, pp. 1-6.
- [37] P. Goli and W. Shireen, "Control of PHEV charging facilities integrated with small scale wind turbine," in *2015 IEEE Transportation Electrification Conference and Expo (ITEC)*, 2015, pp. 1-6.
- [38] A. N. Brooks, "Vehicle charging as a source of grid frequency regulation," in *2013 World Electric Vehicle Symposium and Exhibition (EVS27)*, 2013, pp. 1-6.
- [39] D. Aswani and B. Boyce, "Autonomous grid services through Electric Vehicles," in *2015 IEEE Power & Energy Society General Meeting*, 2015, pp. 1-5.
- [40] O. R. N. Laboratory, U. S. D. o. E. O. o. Scientific, and T. Information, *Spinning Reserve from Responsive Load*. Oak Ridge National Laboratory., 2009.
- [41] M. C. Kisacikoglu, B. Ozpineci, and L. M. Tolbert, "EV/PHEV Bidirectional Charger Assessment for V2G Reactive Power Operation," *IEEE Transactions on Power Electronics*, vol. 28, no. 12, pp. 5717-5727, 2013.
- [42] M. Kisacikoglu, B. Ozpineci, and L. M. Tolbert, *Effects of V2G reactive power compensation on the component selection in an EV or PHEV bidirectional charger*. 2010, pp. 870-876.
- [43] G. Buja, M. Bertoluzzo, and C. Fontana, *Reactive Power Compensation Capabilities of V2G-Enabled Electric Vehicles*. 2017, pp. 1-1.
- [44] F. Islam, H. Pota, and A. B. M. Nasiruzzaman, *PHEV's park as a virtual active filter for HVDC networks*. 2012.
- [45] R. Zgheib, K. Al-Haddad, and I. Kamwa, *V2G, G2V and Active Filter Operation of a Bidirectional Battery Charger for Electric Vehicles*. 2016.
- [46] S. Cundeva and A. Dimovski, "Vehicle-to-grid system used to regulate the frequency of a microgrid," in *IEEE EUROCON 2017 -17th International Conference on Smart Technologies*, 2017, pp. 456-460.
- [47] M. Yilmaz and P. T. Krein, *Review of Battery Charger Topologies, Charging Power Levels, and Infrastructure for Plug-In Electric and Hybrid Vehicles*. 2013, pp. 2151-2169.
- [48] F. Musavi, M. Edington, W. Eberle, and W. G. Dunford, *Evaluation and Efficiency Comparison of Front End AC-DC Plug-in Hybrid Charger Topologies*. 2012, pp. 413-421.
- [49] F. Musavi, W. Eberle, and W. G. Dunford, "A High-Performance Single-Phase Bridgeless Interleaved PFC Converter for Plug-in Hybrid Electric Vehicle Battery Chargers," *IEEE Transactions on Industry Applications*, vol. 47, no. 4, pp. 1833-1843, 2011.
- [50] S. S. Williamson, A. K. Rathore, and F. Musavi, "Industrial Electronics for Electric Transportation: Current State-of-the-Art and Future Challenges," *IEEE Transactions on Industrial Electronics*, vol. 62, no. 5, pp. 3021-3032, 2015.
- [51] N. Wong and M. Kazerani, *A review of bidirectional on-board charger topologies for plugin vehicles*. 2012, pp. 1-6.
- [52] F. Musavi, M. Edington, W. Eberle, and W. G. Dunford, *Energy efficiency in plug-in hybrid electric vehicle chargers: Evaluation and comparison of front end AC-DC topologies*. 2011, pp. 273-280.

- [53] M. C. Kisacikoglu, M. Kesler, and L. M. Tolbert, "Single-Phase On-Board Bidirectional PEV Charger for V2G Reactive Power Operation," *IEEE Transactions on Smart Grid*, vol. 6, no. 2, pp. 767-775, 2015.
- [54] J. Kolar, J. Biela, S. Waffler, T. Friedli, and U. Badstuebner, *Performance trends and limitations of power electronic systems*. 2010, pp. 1-20.
- [55] J. Wirtz, "On-Board Vs. Off Board Charging," Eaton Corporation 2011.
- [56] C. Capasso, S. Riviera, S. Kouro, and O. Veneri, "Charging Architectures Integrated with Distributed Energy Resources for Sustainable Mobility," *Energy Procedia*, vol. 105, pp. 2317-2322, 2017/05/01/ 2017.
- [57] S. Ahmed *et al.*, "Enabling fast charging – A battery technology gap assessment," *Journal of Power Sources*, vol. 367, pp. 250-262, 2017/11/01/ 2017.
- [58] C. Shi, Y. Tang, and A. Khaligh, "A Single-Phase Integrated Onboard Battery Charger Using Propulsion System for Plug-in Electric Vehicles," *IEEE Transactions on Vehicular Technology*, vol. 66, no. 12, pp. 10899-10910, 2017.
- [59] H. Turker, "Review of electric motors for grid connected integrated battery chargers in electric vehicle applications," in *2016 IEEE International Conference on Renewable Energy Research and Applications (ICRERA)*, 2016, pp. 1029-1033.
- [60] D.-G. Woo, G.-Y. Choe, J.-S. Kim, B.-K. Lee, J. Hur, and G.-B. Kang, *Comparison of integrated battery chargers for plug-in hybrid electric vehicles: Topology and control*. 2011, pp. 1294-1299.
- [61] S. Lacroix, E. Labouré, and M. Hilairet, *An Integrated Fast Battery Charger for Electric Vehicle*. 2010, pp. 1-6.
- [62] H.-C. Chang and C.-M. Liaw, *Development of a Compact Switched-Reluctance Motor Drive for EV Propulsion With Voltage-Boosting and PFC Charging Capabilities*. 2009, pp. 3198-3215.
- [63] D. Vilathgamuwa and J. Sampath, "Wireless power transfer (WPT) for electric vehicles (EVS) – Present and future trends," in *Plug in electric vehicles in smart grids*: Springer, 2015, pp. 33-60.
- [64] F. Musavi, M. Edington, and W. Eberle, *Wireless power transfer: A survey of EV battery charging technologies*. 2012, pp. 1804-1810.
- [65] J. S. Johansen, "Fast-Charging Electric Vehicles using AC," Master's Thesis, Department of Electrical Engineering Centre for Electric Technology (CET), Technical University of Denmark, September 2013.
- [66] V. Monteiro, J. C. Ferreira, A. A. N. Meléndez, C. Couto, and J. L. Afonso, "Experimental Validation of a Novel Architecture Based on a Dual-Stage Converter for Off-Board Fast Battery Chargers of Electric Vehicles," *IEEE Transactions on Vehicular Technology*, vol. 67, no. 2, pp. 1000-1011, 2018.
- [67] I. Husain, *Electric and Hybrid Vehicles: Design Fundamentals*, Second Edition. 2010, p. 524.
- [68] M. E. V. Team, "A Guide to Understanding Battery Specifications," ed, 2008.
- [69] D. Linden and T. B Reddy, *Handbook of Batteries*, 3rd Edition. 2001.
- [70] M. Catenacci, E. Verdolini, V. Bosetti, and G. Fiorese, *Going Electric: Expert Survey on the Future of Battery Technologies for Electric Vehicles*. 2013, pp. 403-413.
- [71] M. Alamgir, "Lithium Has Transformed Vehicle Technology: How trends in Li-ion battery technology have developed for vehicle electrification," *IEEE Electrification Magazine*, vol. 5, no. 1, pp. 43-52, 2017.
- [72] J. Świątowska and P. Barboux, "Chapter 4 - Lithium Battery Technologies: From the Electrodes to the Batteries," in *Lithium Process Chemistry* Amsterdam: Elsevier, 2015, pp. 125-166.
- [73] A. Chagnes, "Chapter 5 - Lithium Battery Technologies: Electrolytes," in *Lithium Process Chemistry* Amsterdam: Elsevier, 2015, pp. 167-189.
- [74] A. Chagnes, "Chapter 2 - Fundamentals in Electrochemistry and Hydrometallurgy," in *Lithium Process Chemistry* Amsterdam: Elsevier, 2015, pp. 41-80.
- [75] P. Poizot, F. Dolhem, J. Gaubicher, and S. Renault, "Chapter 6 - Perspectives in Lithium Batteries A2 - Chagnes, Alexandre," in *Lithium Process Chemistry*, J. Świątowska, Ed. Amsterdam: Elsevier, 2015, pp. 191-232.
- [76] J.-s. Lee *et al.*, *Metal–Air Batteries with High Energy Density: Li–Air versus Zn–Air*. 2011, pp. 34-50.
- [77] A. I. Stan, M. Świerczyński, D. I. Stroe, R. Teodorescu, and S. J. Andreasen, "Lithium ion battery chemistries from renewable energy storage to automotive and back-up power applications — An overview," in *2014 International Conference on Optimization of Electrical and Electronic Equipment (OPTIM)*, 2014, pp. 713-720.
- [78] N. Nitta, F. Wu, J. T. Lee, and G. Yushin, "Li-ion battery materials: present and future," *Materials Today*, vol. 18, no. 5, pp. 252-264, 2015/06/01/ 2015.
- [79] A. Vu, L. K. Walker, J. Bareño, A. K. Burrell, and I. Bloom, "Effects of cycling temperatures on the voltage fade phenomenon in 0.5Li₂MnO₃-0.5LiNi_{0.375}Mn_{0.375}Co_{0.25}O₂ cathodes," *Journal of Power Sources*, vol. 280, pp. 155-158, 2015/04/15/ 2015.

- [80] A. Dinger *et al.*, "Batteries for electric cars: challenges, opportunities and the outlook to 2020," The Boston Consulting Group 2010, Available: <https://www.bcg.com/documents/file36615.pdf>.
- [81] C. Schlasza, P. Ostertag, D. Chrenko, R. Kriesten, and D. Bouquain, *Review on the aging mechanisms in Li-ion batteries for electric vehicles based on the FMEA method*. 2014, pp. 1-6.
- [82] B. Basille and J. Rangaraju, "Which new semiconductor technologies will speed electric vehicle charging adoption?," Texas Instruments Incorporated September 2017.
- [83] Available: <http://www.electronicdesign.com/power/look-inside-battery-management-systems>
- [84] L. Lu, X. Han, L. Jianqiu, J. Hua, and M. Ouyang, *A review on the key issues for lithium-ion battery management in electric vehicles*. 2013, pp. 272-288.
- [85] M. A. Hannan, M. S. H. Lipu, A. Hussain, and A. Mohamed, "A review of lithium-ion battery state of charge estimation and management system in electric vehicle applications: Challenges and recommendations," *Renewable and Sustainable Energy Reviews*, vol. 78, pp. 834-854, 2017/10/01/ 2017.
- [86] Y. Xing, E. W M Ma, K.-L. Tsui, and M. Pecht, *Battery Management Systems in Electric and Hybrid Vehicles*. 2011.
- [87] J. Jaguemont, L. Boulon, and Y. Dubé, "A comprehensive review of lithium-ion batteries used in hybrid and electric vehicles at cold temperatures," *Applied Energy*, vol. 164, pp. 99-114, 2016/02/15/ 2016.
- [88] M. Dubarry, M. Bercebar, A. Devie, D. Anseán, N. Omar, and I. Villarreal, "State of health battery estimator enabling degradation diagnosis: Model and algorithm description," *Journal of Power Sources*, vol. 360, pp. 59-69, 2017/08/31/ 2017.
- [89] C. Pastor-Fernández, K. Uddin, G. H. Chouchelamane, W. D. Widanage, and J. Marco, "A Comparison between Electrochemical Impedance Spectroscopy and Incremental Capacity-Differential Voltage as Li-ion Diagnostic Techniques to Identify and Quantify the Effects of Degradation Modes within Battery Management Systems," *Journal of Power Sources*, vol. 360, pp. 301-318, 2017/08/31/ 2017.
- [90] D. Anseán González, "High power li-Ion battery performance: a mechanistic analysis of aging," 2015.
- [91] M. Dubarry, C. Truchot, and B. Y. Liaw, *Synthesize battery degradation modes via a diagnostic and prognostic model*. 2012, pp. 204-216.
- [92] I. Bloom *et al.*, "Differential voltage analyses of high-power, lithium-ion cells: 1. Technique and application," *Journal of Power Sources*, vol. 139, no. 1, pp. 295-303, 2005/01/04/ 2005.
- [93] I. Bloom, J. Christophersen, and K. Gering, "Differential voltage analyses of high-power lithium-ion cells: 2. Applications," *Journal of Power Sources*, vol. 139, no. 1, pp. 304-313, 2005/01/04/ 2005.
- [94] (June 17, 2014). *Overview and Progress of the Battery Testing, Design, and Analysis Activity*.
- [95] Available: <https://www.gruppoacquistoauto.it/approfondimenti/consumi-auto-elettriche-aggiornamento/>
- [96] G. Berckmans, M. Messagie, J. Smekens, N. Omar, L. Vanhaverbeke, and J. Van Mierlo, "Cost Projection of State of the Art Lithium-Ion Batteries for Electric Vehicles Up to 2030," *Energies*, vol. 10, no. 9, p. 1314, 2017.
- [97] C. Curry, "Lithium-ion Battery Costs and Market," Bloomberg New Energy Finance 2017, Available: <https://data.bloomberglp.com/bnef/sites/14/2017/07/BNEF-Lithium-ion-battery-costs-and-market.pdf>.
- [98] S. Rohr, S. Wagner, M. Baumann, S. Müller, and M. Lienkamp, *A techno-economic analysis of end of life value chains for lithium-ion batteries from electric vehicles*. 2017, pp. 1-14.
- [99] Y.-p. Cheng, Y. Li, S. Jiang, and H.-q. Xie, "The recovery of lithium cobalt oxides from spent Li-ion batteries and its electrochemical performances," in *2016 IEEE International Conference on Power and Renewable Energy (ICPRE)*, 2016, pp. 204-208.
- [100] J. Speirs, M. Contestabile, Y. Houari, and R. Gross, *The future of lithium availability for electric vehicle batteries*. 2014, pp. 183-193.
- [101] H. Vikström, S. Davidsson, and M. Höök, *Lithium Availability and Future Production Outlooks*. 2013, pp. 252-266.
- [102] B. Swain, "Recovery and recycling of lithium: A review," *Separation and Purification Technology*, vol. 172, pp. 388-403, 2017/01/01/ 2017.
- [103] "USABC electric vehicle Battery Test Procedures Manual. Revision 2," UNT Libraries Government Documents Department. 1996, Available: <https://digital.library.unt.edu/ark:/67531/metadc666152/>.
- [104] K. Uddin, S. Perera, W. Widanage, L. Somerville, and J. Marco, "Characterising Lithium-Ion Battery Degradation through the Identification and Tracking of Electrochemical Battery Model Parameters," *Batteries*, vol. 2, no. 2, p. 13, 2016.
- [105] I. Buchmann. (2003). *Battery University*. Available: <http://batteryuniversity.com/>

- [106] B. Shabani and M. Biju, "Theoretical Modelling Methods for Thermal Management of Batteries," *Energies*, vol. 8, no. 9, 2015.
- [107] D.-I. Stroe, M. Swierczynski, S. Knudsen Kar, and R. Teodorescu, *A comprehensive study on the degradation of lithium-ion batteries during calendar ageing: The internal resistance increase*. 2016, pp. 1-7.
- [108] M. Dubarry, A. Devie, and K. McKenzie, *Durability and reliability of electric vehicle batteries under electric utility grid operations: Bidirectional charging impact analysis*. 2017, pp. 39-49.
- [109] K. Uddin, T. Jackson, W. D. Widanage, G. Chouchelamane, P. A. Jennings, and J. Marco, "On the possibility of extending the lifetime of lithium-ion batteries through optimal V2G facilitated by an integrated vehicle and smart-grid system," *Energy*, vol. 133, pp. 710-722, 2017/08/15/ 2017.
- [110] Q. Li, J. Zou, and L. Li, "Optimum operation on electric vehicles considering battery degradation in V2G system," in *2017 36th Chinese Control Conference (CCC)*, 2017, pp. 2835-2840.
- [111] C. Zhou, K. Qian, M. Allan, and W. Zhou, "Modeling of the Cost of EV Battery Wear Due to V2G Application in Power Systems," *IEEE Transactions on Energy Conversion*, vol. 26, no. 4, pp. 1041-1050, 2011.
- [112] B. Xu, A. Oudalov, A. Ulbig, G. Andersson, and D. Kirschen, "Modeling of lithium-ion battery degradation for cell life assessment," *IEEE Transactions on Smart Grid*, 2016.
- [113] D. Anseán, M. Gonzalez, J. Viera, J. C. Antón, C. Blanco, and V. Manuel Garcia, *Evaluation of LiFePO₄ batteries for Electric Vehicle applications*. 2013, pp. 1-8.
- [114] D. Anseán *et al.*, "Operando lithium plating quantification and early detection of a commercial LiFePO₄ cell cycled under dynamic driving schedule," *Journal of Power Sources*, vol. 356, pp. 36-46, 2017/07/15/ 2017.